



**Universidade do Minho**  
Escola de Medicina

Ana Carla David Pereira

**Remodeling of medial prefrontal cortex (mPFC)  
glutamatergic pathways in experimental  
monoarthritis: role of the ventral mPFC in  
descending nociceptive modulation**

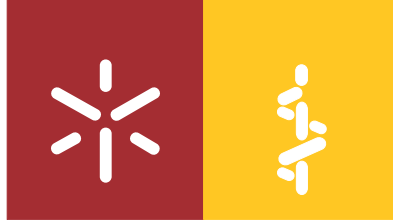
**FCT**  
Fundação para a Ciência e a Tecnologia  
MINISTÉRIO DA EDUCAÇÃO E CIÊNCIA



Ana Carla David Pereira **Remodeling of medial prefrontal cortex (mPFC) glutamatergic pathways in experimental monoarthritis: role of the ventral mPFC in descending nociceptive modulation**

UMinho | 2017

março de 2017



**Universidade do Minho**  
Escola de Medicina

Ana Carla David Pereira

**Remodeling of medial prefrontal cortex (mPFC)  
glutamatergic pathways in experimental  
monoarthritis: role of the ventral mPFC in  
descending nociceptive modulation**

Tese de Doutoramento em Ciências da Saúde

Trabalho efetuado sob a orientação da  
**Professora Doutora Filipa Pinto-Ribeiro**  
e do  
**Professor Doutor Armando Almeida**

março de 2017

## DECLARAÇÃO DE INTEGRIDADE

Declaro ter atuado com integridade na elaboração da presente tese. Confirmando que em todo o trabalho conducente à sua elaboração não recorri à prática de plágio ou a qualquer forma de falsificação de resultados.

Mais declaro que tomei conhecimento integral do Código de Conduta Ética da Universidade do Minho.

Universidade do Minho, 29 de Março de 2017

Nome completo: Ana Carla David Pereira

Assinatura: Ana Carla David Pereira



*"Science has not yet taught us if madness is or is not the sublimity of the intelligence."*

Edgar Allan Poe



## **Agradecimentos/Acknowledgements**

No fim desta etapa, cabe-me agradecer a todos aqueles que direta ou indiretamente me ajudaram a ultrapassar esta meta.

O primeiro lugar pertence à minha mãe. Sem ela eu nunca teria conseguido chegar tão longe: obrigada pelos conselhos, pelo ombro amigo e pelos sacrifícios que fizeste e fazes para que nós consigamos realizar os nossos sonhos.

Ao Professor Armando Almeida, pela oportunidade, apoio e orientação, pelos conhecimentos que partilhou e pela amizade durante todos estes anos.

À Professora Filipa Pinto-Ribeiro, pelo apoio, orientação, paciência e confiança inabalável nas minhas capacidades. Sempre me incentivaste a dar o melhor de mim e, sem ti, não teria aqui chegado. Obrigada pelos conselhos, pelas gargalhadas e pela amizade.

To Professor Antti Pertovaara, thank you for your kindness and willingness to receive me in Helsinki, and for all the knowledge you shared with me.

À Diana Amorim, por toda a ajuda nos trabalhos que estão nesta tese, mas também por todos os momentos de amizade.

À Sara Gonçalves, Filipa Pinheiro, Octávia Costa, Catrine Dahlstedt, Sara Nunes, Antónia Palhares e aos restantes pupilos por partilharem comigo trabalho e histórias e por me ensinarem a ser paciente.

À Sónia Puga e à Stephanie Oliveira, por todos os jantares, lanchinhos e passeios, mas sobretudo, obrigado por estarem lá sempre para me ouvir rezingar.

À Bárbara, Eliana, Carina, Joana, Sara e Andreia, pelos jantares, conversas e alegria.

Ao Pedro, por seres o irmão chato que eu queria.

À minha família.

A todos os colegas no ICVS, em particular aos NeRDs, e no departamento de Fisiologia do Biomedicum, Helsínquia.

This work was supported by a grant from Fundação para a Ciência e a Tecnologia:

SFRH/BD/90374/2012

**FCT**  
Fundação para a Ciência e a Tecnologia  
MINISTÉRIO DA EDUCAÇÃO E CIÊNCIA





**Remodeling of medial prefrontal cortex (mPFC) glutamatergic pathways in experimental monoarthritis: role of the ventral mPFC in descending nociceptive modulation**

**Abstract**

The understanding of pain mechanisms and the development of novel therapies relies mostly on our knowledge of neurotransmitter pharmacology in nociceptive processing. These neurotransmitter pathways have been extensively characterized at the peripheral nervous system, spinal cord and brainstem levels; however, our knowledge is less comprehensive regarding frontal brain regions. The beginning of the XXI century brought the conventionalization of brain imaging technologies and the uncovering of the major involvement of cortico-limbic structures in pain phenomena. Imaging studies showed that continuous noxious peripheral inputs elicit profound morphological and functional changes in areas such as the prefrontal cortex (PFC), contributing to the emotional and cognitive imbalances occurring in chronic pain. However, contrary to well-studied brainstem pain modulatory areas, such as the rostral ventromedial medulla (RVM) or the dorsal reticular nucleus (DRt), the molecular mechanisms in frontal regions of the brain remain understudied. Hence, we propose to clarify the role of two medial PFC (mPFC) areas, the prelimbic and infralimbic cortices (PL and IL, respectively) towards nociceptive modulation in normal conditions, as well as in prolonged inflammatory pain.

The long-term effects of intra-articular injection of kaolin and carrageenan (K/C; four weeks after induction) upon nociceptive behavior and knee joint structure consisted of the development of severe lesions in the articular joint concomitantly to sustained primary hyperalgesia and altered gait. Using a behavioral approach, the tonic and phasic actions of the PL and IL were evaluated in healthy (SHAM, saline intra-articular injection) animals by locally microinjecting lidocaine and glutamate, respectively. This approach uncovered the opposing effects of glutamate in the PL and IL: fast antinociception resulted from PL activation, while slow pronociception resulted from IL activation. The use of metabotropic glutamate receptor (mGluR) agonists and antagonists allowed to dissect the slow effect of glutamate in the IL and to conclude that it acts preferentially upon mGluR5 to facilitate nociception in both SHAM and K/C animals. Interestingly, mGluR5 has no tonic nociceptive input in healthy animals, as observed by the lack of effect of an mGluR5 antagonist. After four weeks of K/C, however, mGluR5 antagonist exerted antinociception, an effect

dependent on intact astrocyte function, as shown by the loss of mGluR5 antagonist effect after astrocyte ablation with a specific gliotoxin, L- $\alpha$ -aminoadipate.

The contribution of mGluR5 to IL-mediated pronociception was also evaluated by performing electrophysiological recordings of the nociceptive modulatory cells of the RVM and the DRt, as well as in the nociceptive neurons of the spinal dorsal horn. Pronociception from the IL was relayed through the DRt in healthy animals; however, the relay shifted to the RVM after prolonged inflammatory pain. In the dorsal horn, the heat-evoked responses of both wide-dynamic range (WDR) and nociceptive specific (NS) neurons were exacerbated by IL application of mGluR5 agonist in SHAM and K/C animals. Finally, there is also evidence that spinal TRPV1 are possible mediators of IL-induced pronociception.

In conclusion, mGluR5 in the IL exacerbates nociceptive behavior, as well as the electrophysiological responses of DRt and spinal nociceptive neurons to peripheral noxious stimulation in rodents. Long-term exposure to inflammatory pain leads to plastic changes in the IL, which promote astrocytic dependent nociceptive modulation and the remodeling of IL-mediated pronociceptive descending pathways from a DRt to a RVM-dependent pathway. Further studies should focus on modulation of the motivational/affective aspects of pain modulation by the IL, for a better understanding of the mechanisms that underlie the development of chronic pain and its associated comorbidities.

**Reorganização das vias glutamatérgicas do córtex pré-frontal medial (mPFC) em monoartrite experimental: o papel do mPFC ventral na modulação descendente da nociceção**

**Resumo**

A compreensão dos mecanismos de dor e o desenvolvimento de novas terapias para o seu tratamento depende principalmente do nosso conhecimento da farmacologia dos neurotransmissores implicados no processamento nociceptivo. Estas vias de neurotransmissores estão extensamente caracterizadas ao nível do sistema nervoso periférico, da medula espinhal e do tronco cerebral; em relação às áreas frontais do cérebro, no entanto, o nosso conhecimento é menos abrangente. No início do século XXI o uso de tecnologias de imagiologia cerebral tornou-se mais corrente e levou à descoberta do enorme envolvimento de estruturas cortico-límbicas em fenómenos de dor. Estudos de imagiologia mostraram que estímulos periféricos nóxicos contínuos provocam alterações morfológicas e funcionais profundas em áreas como o córtex pré-frontal (PFC) e contribuem para o desenvolvimento de distúrbios emocionais e cognitivos em dor crónica. No entanto, ao contrário de áreas moduladoras da dor bem caracterizadas como o bolbo rostral ventromedial (RVM) ou o núcleo reticular dorsal (DRt), os mecanismos moleculares das áreas frontais do cérebro permanecem pouco estudados. Consequentemente, propusemo-nos a clarificar o papel de duas áreas do PFC medial (mPFC), os córtices pré-límbico e infralímbico (PL e IL, respetivamente), na modulação da nociceção em condições normais, bem como em dor inflamatória prolongada.

Os efeitos a longo prazo da injeção intra-articular de caulino e carragenina (K/C; quatro semanas depois da indução) no comportamento nociceptivo e na estrutura articular do joelho consistiram no desenvolvimento de lesões severas na articulação concomitantemente com hiperalgesia primária persistente e alterações na marcha. Através do uso de uma abordagem comportamental e da microinjeção local de lidocaína e de glutamato, avaliaram-se os efeitos nociceptivos tónicos e fásicos, respetivamente, do PL e do IL em animais normais (SHAM, injeção intra-articular de solução salina). Esta abordagem revelou os efeitos opostos exercidos pelo glutamato no PL e no IL: a ativação do PL promoveu um efeito antinociceptivo rápido, enquanto a ativação do IL resultou num efeito pronociceptivo lento. Para examinar o efeito comportamental lento do glutamato no IL usaram-se agonistas e antagonistas de recetores metabotrópicos de glutamato (mGluR),

concluindo-se que o glutamato atua preferencialmente nos recetores mGluR5 do IL para facilitar a nociceção em animais SHAM e K/C. Curiosamente, os mGluR5 não exercem uma ação tónica em animais normais, tal como pôde ser observado pela falta de alterações comportamentais após a injeção de um antagonista de mGluR5. Pelo contrário, após quatro semanas de dor inflamatória o antagonista do mGluR5 promoveu um efeito antinociceptivo. Este efeito é dependente do funcionamento normal dos astrócitos, já que o antagonista de mGluR5 perdeu o efeito após a ablação dos astrócitos com uma gliotoxina específica, o L- $\alpha$ -aminoadipato, injetada no IL.

A contribuição dos mGluR5 para o efeito pronociceptivo mediado pelo IL foi também estudado através da avaliação eletrofisiológica de alterações na atividade das células moduladoras da nociceção do RVM e do DRt, bem como dos neurónios nociceptivos do corno dorsal da medula espinhal. Em animais normais, a pronociceção desencadeada pelo IL foi mediada através do DRt, mas em animais com dor inflamatória esta mediação descendente passou a ser feita através do RVM. No corno dorsal, as respostas evocadas por estímulos quentes nócicos em neurónios *wide-dynamic range* (WDR) ou *nociceptive specific* (NS) foram exacerbadas pela aplicação de um agonista do mGluR5 no IL quer em animais SHAM, quer em animais K/C. Finalmente, existem também indícios de que os recetores TRPV1 da medula espinhal podem ser mediadores do efeito pronociceptivo do IL.

Em conclusão, os mGluR5 no IL promovem a facilitação do comportamento nociceptivo, assim como das respostas eletrofisiológicas do DRt e de neurónios nociceptivos da medula espinhal a estímulos periféricos nócicos em roedores. A exposição prolongada a dor inflamatória causou alterações plásticas no IL, promovendo a modulação da nociceção por parte dos astrócitos, e levando à reorganização das vias descendentes do IL de uma via mediada pelo DRt para uma via mediada pelo RVM. Em trabalhos futuros, deverá ser explorada a modulação por parte do IL dos aspetos motivacionais e afetivos da dor, de modo a promover um melhor entendimento dos mecanismos subjacentes ao desenvolvimento de dor crónica e das comorbidades a ela associadas.

## **Table of contents**

<b>Chapter 1: Introduction</b>	1
1.1 – The definition of pain	3
1.2 – Nociceptive transmission	3
1.2.1 – Nociceptors and spinal cord	3
1.2.1.1 – Transient receptor potential cation channel subfamily V member 1 (TRPV1)	4
1.2.2 – Ascending pathways	6
1.2.3 – Supraspinal processing	6
1.2.4 – Descending modulation	8
1.3 – Chronic pain	9
1.3.1 – Osteoarthritis	10
1.3.1.1 – Animal models of inflammatory pain	11
1.3.2 – Mechanisms of chronic inflammatory pain: peripheral and central sensitization	13
1.3.2.1 – The prefrontal cortex during chronic pain	15
1.3.2.2 – Descending modulation during chronic pain	18
1.3.3 – Pain modulation by metabotropic glutamate receptors	21
1.4 – Pain modulation by non-neuronal cells	24
1.4.1 – Microglia	25
1.4.2 – Astrocytes	27
1.4.2.1 – Pain modulation by astrocytic glutamatergic signaling	29
1.5 – Aims	31
1.6 – References	32
<b>Chapter 2: Experimental work</b>	61
2.1 – Injection of kaolin/carrageenan in the rat knee joint induces progressive experimental knee osteoarthritis.	63
2.2 – Metabotropic glutamate 5 receptor in the infralimbic cortex contributes to descending pain facilitation in healthy and arthritic animals	95

2.3 – Astrocytic mGluR5 in the infralimbic cortex are engaged in descending nociceptive modulation in experimental monoarthritis	109
2.4 – The medullary dorsal reticular nucleus as a relay for descending pronociception induced by the mGluR5 in the rat infralimbic cortex	133
2.5 – The rostral ventromedial medulla relays descending pronociception induced by infralimbic cortex mGluR5 in monoarthritic, but not healthy, rats	149
<b>Chapter 3: Discussion</b>	155
3.1 – Technical considerations	158
3.1.1 – Behavioral assessment of nociception	158
3.1.1.1 – Thermal hyperalgesia	159
3.1.1.2 – Mechanical hyperalgesia	160
3.1.1.3 – Indirect measures: gait analysis	160
3.1.2 – Behavioral assessment of anxiety and depressive-like behaviors	161
3.1.3 – Functional interventions	163
3.1.3.1 – Pharmacological and electrical modulation	163
3.1.3.2 – L- $\alpha$ -aminoadipate (L $\alpha$ AA)	164
3.1.4 – Anesthesia and electrophysiological recordings	165
3.1.4.1 – Ketamine and medetomidine	165
3.1.4.2 – Sodium pentobarbital	166
3.1.4.3 – Type of electrophysiological recordings	167
3.2 – Suitability of the K/C model to study OA	167
3.3 – Pain modulation by the mPFC	169
3.3.1 – Dissociation of PL and IL functions	169
3.3.2 – Modulation of nociception by the IL	171
3.3.3 – Descending relays for IL-mediated pronociception	174
3.3.3.1 – Spinal pathways	174
3.3.3.2 – Influence of IL mGluR5-mediated pronociception on dorsal horn activity	175
3.3.3.3 – TRPV1	176
3.4 – References	177
<b>Chapter 4: Conclusions and future perspectives</b>	191

## **Abbreviations**

ACC – anterior cingulate cortex

AMPA –  $\alpha$ -amino-3-hydroxy-5-methyl-4-isoxazolepropionic acid

AMY – amygdala

BDNF – brain-derived neurotrophic factor

BLA – basolateral nucleus of the amygdala

cAMP – cyclic adenosine monophosphate

CB1 – endocannabinoid receptor 1

CeA – central nucleus of the amygdala

CFA – complete Freund's adjuvant

CGRP – calcitonin gene-related peptide

CNS – central nervous system

Cx43 – connexin 43

DLPFC – dorsal lateral prefrontal cortex

DNIC – diffuse noxious inhibitory control

DRt – dorsal reticular nucleus

ERK – extracellular signal-regulated kinase

FST – forced swimming test

GABA –  $\gamma$ -Aminobutyric acid

GFAP – glial fibrillary acidic protein

GLAST – glutamate and aspartic acid transporter

GLT-1 – glutamate transporter-1

Iba1 – ionized calcium-binding adapter molecule

IC – insular cortex

IL – infralimbic cortex

IL-1 $\beta$  – interleukin-1 $\beta$

IP<sub>3</sub> – inositol triphosphate

IP<sub>3</sub>R2 – type 2 inositol triphosphate receptors

JNK - c-Jun N-terminal kinases

K/C – animals with kaolin/carrageenan intra-articular injection

LTD – long term depression  
L $\alpha$ AA – L- $\alpha$ -aminoadipate  
MAPK – mitogen-activated protein kinase  
mGluR – metabotropic glutamate receptors  
MIA – sodium monoiodoacetate  
mPFC – medial prefrontal cortex  
NMDA – N-methyl-D-aspartate  
NO – nitric oxide  
NRG-1 – neuregulin 1  
NRM – nucleus raphe magnus  
NS – nociceptive specific  
OA – osteoarthritis  
OF – open field test  
PAG – periaqueductal gray matter  
PAM – pressure application measurement  
PFC – prefrontal cortex  
PI3 – phosphatidylinositol-3-kinase  
PL – prelimbic cortex  
RVM – rostral ventromedial medulla  
S1 – primary somatosensory cortex  
S2 – secondary somatosensory cortex  
SHAM – animals with saline intra-articular injection  
SPT – sucrose preference test  
STT – spinothalamic tract  
TGF- $\beta$  – transforming growth factor- $\beta$   
TNF- $\alpha$  – tumor necrosis factor- $\alpha$   
TrkB – tyrosine receptor kinase B  
TRPV1 – transient receptor potential cation channel subfamily V member 1  
WDR – wide dynamic range







## 1. Introduction

### 1.1 The definition of pain

The International Association for the Study of Pain (IASP) has defined pain as “*an unpleasant sensory and emotional experience associated with actual or potential damage, or described in terms of such damage*”<sup>1</sup>. Traditionally, the pain experience was segregated in two main dimensions reflected in IASP’s definition – sensation and emotion – associated to anatomically distinct pathways, the medial and the lateral spinothalamic tracts (STT), respectively<sup>2</sup>. Consequently, the role of cortical structures in pain modulation remained controversial until the advent of non-invasive brain imaging. It then became clear that circuits involved in cognitive processes, such as memory, learning and reward, are important contributors to the processing of nociceptive information<sup>3,4</sup> and explaining why pain and stimulus intensities are not proportional. The pain neuromatrix model was therefore proposed: pain is a conscious experience that results from an individualized perception of a damaging stimulus, influenced by our memories and emotions, as well as by genetic, cognitive and pathological factors<sup>3,5</sup>.

### 1.2 Nociceptive transmission

#### 1.2.1 Nociceptors and spinal cord

Nociception refers to the information triggered by a noxious (damaging) stimulus to the organism and is integrated in the pain experience after being processed with the emotional and cognitive components of pain. Peripheral stimulation initiates the sensory experience by activating three main types of primary afferent fibers: A $\beta$ , A $\delta$  and C-fibers. Each type of fiber is able to discriminate different stimuli based on their characteristics. A $\beta$ -fibers (4-8 $\mu$ m in diameter) transmit action potentials fast due to their high axonal myelination and have low activation thresholds<sup>6-8</sup>. In normal conditions, they respond solely to innocuous tactile stimulation, but can be recruited in chronic pain conditions<sup>9</sup>. Usually, only A $\delta$  and C-fibers respond to nociceptive stimulation and are therefore termed nociceptors. A $\delta$ -fibers are medium sized (2-6 $\mu$ m in diameter) myelinated afferents, with higher activation thresholds than A $\beta$ -fibers. They mediate the acute and well-localized “first” pain and can be further sub-divided into two classes: type I, with low activation threshold for mechanical and chemical stimuli but high for heat stimuli; and type II, with low threshold for heat stimuli, but

high for mechanical stimuli<sup>6-8,10</sup>. Unmyelinated C-fibers are the smallest type of afferents (0.4-1.2 $\mu$ m in diameter) and consequently display slow conduction velocity. They have high activation thresholds and convey a roughly localized “second” pain<sup>6-8,10</sup>. Like A $\delta$ , there are also different populations of C-fibers. Polymodal C-fibers are responsive to both mechanical and thermal stimulation<sup>11</sup>, and a subset denominated “silent” nociceptors responds only to heat and chemical stimuli and is mechanically insensitive<sup>12</sup>. These last are thought to be involved in altered pain perception in inflammatory pain conditions<sup>6</sup>.

The cell bodies of nociceptors are located in the dorsal root ganglia, from which a small central branch and a long peripheral branch emerge, allowing them to function as a bidirectional signaling mechanism<sup>6</sup>. In the spinal cord, primary afferents synapse in second-order neurons of the dorsal horn. The dorsal horn consists of anatomically organized laminae, to where each type of peripheral fiber projects: A $\delta$ -fibers project to laminae I and V, C-fibers project to superficial laminae I and II and indirectly to lamina V, and A $\beta$ -fibers project to deep laminae III-VI<sup>6,7</sup>. Due to this distribution, dorsal horn neurons can be classified into three subtypes: superficial laminae neurons that respond to noxious stimuli and are classified as nociceptive-specific (NS); deep-laminae III and IV neurons that respond to innocuous stimuli and are denominated proprioceptive or non-nociceptive; and deep-lamina V neurons that respond to innocuous and noxious inputs and are classified as wide dynamic range (WDR) neurons<sup>6,13</sup>. Neurons belonging to this last category display a response magnitude proportional to the stimulus intensity and are therefore considered to encode and relay information on stimulus intensity<sup>13</sup>.

Neurons in the spinal cord can also be classified according to their output target as projecting neurons and local interneurons<sup>13</sup>. Projection neurons relay information to supraspinal regions. Local interneurons play an integrative role in communicating between spinal cord segments and within dorsal horn laminae. Additionally, spinal interneurons can also be involved in descending mechanisms of pain modulation originating in the dorsal horn<sup>13</sup>.

#### *1.2.1.1 Transient receptor potential cation channel subfamily V member 1 (TRPV1)*

TRPV1 is a non-selective, ligand-gated ion channel expressed in the soma, peripheral and central axonal branches of primary afferent fibers, that processes nociceptive stimuli<sup>14,15</sup>. It has been recognized as a polymodal transducer that can respond to a wide variety of stimuli, including

noxious heat (>43°C), low pH and, more notably, chemical compounds such as capsaicin<sup>16</sup>. Interestingly, capsaicin, but not noxious heat, desensitizes TRPV1 channels and topical application of this compound has been used to alleviate inflammatory pain<sup>17</sup>. Expression of this receptor is found in C-fiber polymodal afferents and in type II A $\delta$ -fibres, where it induces the release of calcitonin gene-related peptide (CGRP) and substance P in laminae I and II of the dorsal horn<sup>18,19</sup>. This receptor can also be activated by numerous endogenous ligands, such as the endocannabinoid anandamide, arachidonic acid metabolites and other lipids<sup>20</sup>.

Although for some time TRPV1 was thought to be the main transducer of acute heat sensation, deletion of the *VR1* gene in mice dorsal root ganglia did not abolish heat-evoked responses<sup>21</sup>, although there was some degree of impairment and considerable disruption of primary afferent responses both in the periphery and in the spinal cord<sup>15</sup>, indicating the existence of other acute heat pain transducers. Since these knockout mice still desensitized with capsaicin application, it is thought that TRPV2, 3 and/or 4 are also transducers of heat sensation<sup>6,18</sup>. The main role of TRPV1 seems to be in the development of pain hypersensitivity due to peripheral sensitization by inflammation, a phenomenon known as primary hyperalgesia<sup>7,15</sup>. In fact, TRPV1 knockout animals display no alterations in heat-evoked behaviors after induction of peripheral inflammation<sup>15</sup>.

Interestingly, intrathecal delivery of TRPV1 antagonists effectively reduces mechanical allodynia in neuropathic pain models<sup>22</sup>, despite the inability of TRPV1-expressing primary afferents to convey mechanical pain<sup>23</sup>. This phenomenon was linked to the expression of TRPV1 in dendrites and soma of dorsal horn lamina II interneurons<sup>24-26</sup>, which seem to be exclusively GABAergic<sup>25</sup>. When activated, TRPV1 can lead to long-term depression (LTD) of GABAergic transmission in the spinal cord and consequently to increased dorsal horn excitability<sup>26</sup>.

Finally, TRPV1 is also widely expressed in supraspinal brain regions, although at lower concentrations than in primary afferents. It is found in several structures, including key regulators of descending nociceptive modulation like periaqueductal gray matter (PAG) and the rostral ventromedial medulla (RVM). These receptors are also associated to pain, anxiety, depression and schizophrenia, among others<sup>27</sup>.

### *1.2.2 Ascending pathways*

Nociceptive information is conveyed to the brain through spinal projection neurons organized in ascending tracts. The STT is classically the most important for transmission of pain related information. It originates mainly in layers I and V of the dorsal horn and is organized in two main tracts, the lateral and anterior STTs. The lateral STT mainly projects to the posterior part of the ventral medial nucleus of the thalamus, which relays sensory-discriminative information of pain. The medial STT projects to the medial thalamus and relays information concerning the motivational-affective aspects of pain<sup>10,28,29</sup>. Other ascending pathways have been described as transmitting relevant nociceptive inputs, such as the spinoreticular tract, which projects to the medial thalamus, as well as to descending modulatory regions such as the medullary dorsal reticular nucleus (DRT)<sup>28,30,31</sup>; the spinomesencephalic tract, which terminates mainly in midbrain regions such as the PAG, in the parabrachial nucleus and to a lesser extent in the lateral thalamus<sup>28</sup>; and the spino-limbic tract, which relays mono and polysynaptic inputs to the medial thalamus, hypothalamus, and limbic structures such as the amygdala (AMY) and prefrontal cortex (PFC)<sup>28</sup>. Altogether, directly or indirectly, these ascending pathways distribute pain related information to a matrix of regions ranging from brainstem nuclei, involved in autonomic responses of pain, to high level circuits which process the emotional and cognitive dimensions of pain<sup>32</sup>.

### *1.2.3 Supraspinal processing*

An integral part of the behavioral response to pain consists of the motivational-affective and autonomic responses, exemplified by increases in heart rate and blood pressure, endocrine changes, increased attention, anxiety and suffering. The supraspinal pathways mediating these changes comprise areas relaying information about somatic pain, as well as additional structures of the limbic system. Most evidence of the involvement of these additional structures comes from studying brain responses to acute stimulation or in clinical pain conditions through non-invasive brain imaging techniques in human subjects<sup>33,34</sup>. Brain imaging studies in normal subjects consistently show activation of multiple cortical and sub-cortical regions during short-duration painful stimulation<sup>33</sup>. The regions most commonly reported as activated by acute noxious stimulation are the primary and secondary somatosensory cortices (S1 and S2), the anterior cingulate cortex (ACC), the insular cortex (IC), the PFC, thalamus and cerebellum<sup>33,34</sup>.

Evidence suggests that the S1 and S2 are important for the perception of the sensory characteristics of pain, such as the location and duration of the stimulus<sup>35,36</sup>. Patients with lesions in the S1 and/or S2 are incapable of localizing or describing the nature of the painful stimulation, reporting only an unpleasant feeling<sup>37</sup>. However, S1 and S2 seem to be differently activated by acute noxious stimulation. Electroencephalogram/magnetoencephalography (EEG/MEG) studies of temporal activation patterns can distinguish two sequential brain activations in S1 and S2, reflecting the “first” and “second” pain elicited by A $\delta$  and C-fiber activation<sup>38</sup>. Other studies, however, point the S2, along with the IC, as primary nociceptive input receiving areas, but not the S1, a hypothesis supported by observation that activation of these two regions occurs prior to that of S1<sup>37</sup>. Activation of the IC was also implicated in the affective processing of pain<sup>33,39,40</sup>. The dual role of the IC in pain processing is due to its heterogeneity: its posterior section is thought to be more related to the sensory aspects of pain, while the anterior section may be more important in the emotional, cognitive and memory related aspects of pain perception<sup>33,41</sup>. Patients with lesions in the IC can show pain asymbolia (pain sensation is normal but noxious stimulation responses are exaggerated)<sup>42</sup> or higher pain ratings when thermal acute stimuli were applied<sup>43</sup>, and electrical stimulation of the posterior IC can elicit painful sensations<sup>44</sup>.

The ACC seems to be the most consistently activated cortical region in response to acute peripheral stimulation<sup>33,34</sup>. ACC activity is linked to the cognitive-evaluative processing of pain. In fact, the intensity of signals measured in the ACC of normal subjects correlates with ratings of perceived pain but not with its actual intensity<sup>45</sup>. Several studies report that altering the perception of pain by suggesting to subjects that pain unpleasantness was changed<sup>40</sup>, by using distraction, negative emotional states or altering pain expectation<sup>33,34</sup> can selectively modulate ACC activity. Using animal models, the opposite could also be observed, as activating or blocking the ACC affects aversive learning in rats<sup>46</sup>.

PFC activation after acute noxious stimulation is also described by brain imaging studies, however, it is reported less systematically than the previously discussed areas and does not correlate with stimulus intensity. Instead, peak activity seems to correlate with the identification of a stimulus as painful<sup>36</sup>. Increased activity of the PFC was also reported in subjects distracted from pain<sup>33</sup>, or anticipating or expecting pain<sup>47</sup>. Additionally, when analyzing different subregions of the PFC, it was observed that they can display opposing responses to the same stimulus; for example, the activity of the dorsal frontal cortex decreases while the orbitofrontal increases<sup>48</sup>. The authors proposed that

the orbitofrontal cortex is involved in the affective dimension of pain perception, while the dorsal lateral PFC (DLPFC) is more involved in top-down modulation of pain and in limiting the extent of suffering, indicating that this area should not be studied as a whole.

#### *1.2.4 Descending modulation*

The processing of pain characteristics, as well as their integration with other cognitive and affective processes such as attention, context, emotions and mood, ultimately results in the modulation of spinal transmission of nociceptive inputs by descending pathways commonly known as descending modulation of pain. As a result, nociceptive transmission can be exacerbated (pronociception) or attenuated (antinociception)<sup>9</sup>. Pain control results from a balance between inhibitory and facilitatory descending inputs upon spinal nociceptive transmission.

Most of the knowledge regarding the mechanisms of pain modulation comes from preclinical studies. Several interconnected circuits are described to modulate pain at different levels, such as the PAG-RVM circuit<sup>9,49,50</sup>, the spino-bulbo-spino loops through the medullary DRt<sup>51</sup> and the caudal lateral ventrolateral medulla<sup>52</sup>, spinal interneurons, and the frontal-cortical-brainstem circuit<sup>53,54</sup>.

The most comprehensively studied is the PAG-RVM circuit. The PAG is a crucial player in a circuit that controls nociceptive transmission at the dorsal horn level via a relay in the RVM<sup>55</sup>. Activation of either of these areas is sufficient to block noxious stimuli-evoked reflexes in rodents<sup>56</sup> and in human subjects<sup>57</sup>. The PAG is extensively interconnected with upstream pain processing regions, such as the PFC, the ACC, the IC, the AMY and several thalamic and hypothalamic subregions<sup>58-60</sup>; as well as with brainstem regions involved in the descending modulation of pain, such as the pontomedullary reticular formation, the locus coeruleus, the RVM and the DRt<sup>55,61,62</sup>. Through this extensive network, the PAG can integrate inputs from all the dimensions of pain and modulate dorsal horn activity<sup>50</sup>. However, since the PAG has only minimal projections to the dorsal horn, it relays the information through the RVM<sup>49,50</sup>, which is considered to be the effector nucleus of supraspinal descending pain modulation. The RVM can exert bidirectional control over dorsal horn nociceptive neuronal activity; in other words, it can exert both inhibitory and facilitatory actions. This is achieved through the activity of two functionally distinct cell types: OFF-cells and ON-cells. OFF-cells are considered to inhibit pain perception, as they have a stable firing activity that is abolished immediately before the behavioral evasive response to a peripheral noxious stimulus;



moreover, their activity is increased by opioids. ON-cells are thought to facilitate pain perception, as they show increased firing activity immediately before a behavioral evasive response to peripheral noxious stimulation. Additionally, since they have  $\mu$ -opioid receptors, their activity is directly inhibited by opioids<sup>49,50,55</sup>. A third type of cells can be identified in the RVM which are non-responsive to peripheral noxious stimulation and therefore known as NEUTRAL-cells. Despite the lack of response to acute noxious stimulation, based on their distinct neurochemical profile (for example, a subset of NEUTRAL-cells is serotonergic<sup>63</sup>), it is thought that NEUTRAL-cells participate in descending pain modulation, particularly in chronic pain conditions<sup>49,50</sup>.

The medullary DRt<sup>61</sup> is reciprocally connected to neurons in superficial and deep layers of the dorsal horn<sup>30,31,64,65</sup>, constituting a reverberating dorsal horn-DRt-dorsal horn loop. Similarly to the PAG, the DRt receives projections from several supraspinal pain modulatory areas, including the PFC, somatosensory cortices, hypothalamus, thalamus, the PAG and the RVM<sup>66</sup>. This circuit is involved in the facilitation of nociception, as activation of the DRt leads to hyperalgesic behavior<sup>30,67,68</sup> and facilitatory inputs from upstream brain regions are relayed through this brain region<sup>69,70</sup>. Interestingly, the DRt is the effector nucleus of the diffuse noxious inhibitory control (DNIC)<sup>71</sup>. Commonly known as “pain inhibits pain”, DNIC occurs when a response to a noxious stimulus, and the corresponding WDR neuronal response, are inhibited by another spatially distant noxious stimulus<sup>72,73</sup>. This effect is proposed to promote nociceptive facilitation by augmenting the contrast between noxious-evoked neuronal activation and spinal background activity<sup>74</sup>.

### **1.3 Chronic pain**

Acute pain, or nociceptive pain, serves a biological purpose as a defense and alert aimed at perceiving and avoiding a potentially perilous situation. It is subject to a fine-tuned balance of inhibitory and facilitatory systems that allow us to adapt to environmental and physiological situations. Therefore, in a life threatening situation, an increased antinociceptive input allows to prioritize the most immediate danger and engage in the “fight-or-flight” response. Later, when the threat disappears, pronociceptive inputs promote protective behaviors towards the damaged area. However, in some instances pain can persist beyond its physiological value and healing time, lose its warning function and become chronic<sup>75</sup>. Pain is considered to become chronic when it lasts or recurs for more than 3 to 6 months<sup>76</sup>. The fine-tuned regulation of inhibitory and facilitatory systems

becomes deregulated, either by decreasing inhibitory inputs and/or increasing facilitatory ones, leading to an exaggerated perception of a noxious stimulus (hyperalgesia), perception of a previously innocuous stimulus as painful (allodynia) or even the emergence of spontaneous pain<sup>1</sup>.

Recent reports estimate chronic pain affects approximately 20% of the worldwide population<sup>77</sup>. While acute pain mechanisms are well defined and treatment is easily achieved with classic analgesics<sup>78</sup>, many chronic pain cases are of unclear etiology limiting the ability to treat it. Often the development of mood and cognitive comorbidities further complicates clinical prognosis<sup>79-81</sup>. In such cases, the treatment of painful symptoms alone can be insufficient, and a multidisciplinary approach, with recourse to antidepressants and anticonvulsants is required<sup>79,80,82</sup>.

Overall, chronic pain can originate from increased stimulation of primary nerve afferent due to tissue injury or inflammation – pathophysiological nociceptive pain – or from neuronal damage in peripheral or central nervous system (CNS) – neuropathic pain<sup>83</sup>. Moreover, some pathologies can present both components, such as fibromyalgia<sup>84</sup>. In addition to the source of pain, the perceived location and etiology of pain are also taken into account. Based on these categories, a total of seven groups can be defined: chronic primary pain, chronic cancer pain, chronic posttraumatic and postsurgical pain, chronic neuropathic pain, chronic headache and orofacial pain, chronic visceral pain and chronic musculoskeletal pain<sup>84</sup>.

The chronic musculoskeletal pain category includes pain that arises from persistent inflammation, such as rheumatoid arthritis, and pain arising from structural changes affecting bones, joints, tendons or muscles, such as osteoarthritis (OA)<sup>84</sup>.

### *1.3.1 Osteoarthritis*

OA is one of the oldest known diseases on the planet. The oldest evidence of its presence is found in 70 million years old dinosaur skeletons<sup>85</sup>, and it is traceable throughout nearly every period and civilization. Nowadays, OA is one of the most prevalent forms of arthritis, ranking 11<sup>th</sup> in the list of contributors to global disability. Predictions point out to an increase in the number of people suffering from OA due to increasing aging and obesity<sup>86,87</sup>.

Interestingly, OA pathology has remained mostly unchanged for the last 100 million years<sup>85</sup>. This degenerative disease usually affects weight bearing joints, such as knees and hips, and is

characterized by degradation of the articular cartilage, thickened subchondral bone, excess of marginal bone (osteophyte formation), synovitis and capsular thickening<sup>88,89</sup>. Therapeutic approaches focus mainly on treatment of symptoms, especially for pain management. Despite being one of the main complaints, OA-associated pain is still sub-optimally treated. Recent studies highlighted the existence of heterogeneous phenotypes based on different disease pathogenesis, despite patients presenting the same symptoms. Therefore, gene related OA and OA originating from trauma, obesity or ageing present different phenotypes that should be taken into account when prescribing treatment<sup>90</sup>. Furthermore, many failed clinical trials point phenotype heterogeneity in their cohorts as a possible cause for lack of significant results<sup>91</sup>. The lack of in-depth knowledge of pathogenesis mechanisms hinders the establishment of reliable biomarkers. For instance, until the 1990's the pathophysiology of OA was thought to be cartilage-driven; however, the role of synovial inflammation is now receiving more attention, and an integrated role for bone and synovial tissue is proposed to lead to the perpetuation of the disease<sup>90,91</sup>. In the first stages of the disease, OA pain is mostly elicited by movement or loading of the joint. However, as the disease progresses an inflammatory profile develops, with increased cytokine production and infiltration of inflammatory cells into the joints<sup>92</sup>, and at this late stage, pain can also occur at rest. Additionally, the prevalence of comorbidities such as anxiety, depression and sleep disorders in OA patients is very high. Research on the mechanisms underlying pain and mood interactions is scarce and so their contribution to OA-associated pain remains mostly unknown. Consequently, recognition of comorbidity symptoms in primary care settings is usually low and they frequently go untreated<sup>90,93,94</sup>.

### *1.3.1.1 Animal models of inflammatory pain*

Animal models are important tools to study the pathogenesis and the development of therapeutic interventions for disease. They provide information on the mechanisms that lead to the development of pathological conditions and are a basis for drug discovery with clinically translatable potential<sup>13,95-97</sup>. A good model of OA should allow to define the type and severity of the injury, the time of onset and the progression of the disease, and to relate these events to biomarkers of disease activity<sup>98</sup>. Preclinical research in this disease is based in animal models of joint injury and repair but, to date, there is no ideal animal model for the study of OA. Naturally occurring OA models are the most similar to human OA from a pathophysiological perspective, as they occur without any intervention and present different manifestations of the disease. They include

spontaneous models, such as the Dunkin-Hartley guinea pigs<sup>99</sup>, and genetic models, like mice with mutation of collagen type II gene<sup>100</sup>. However, these models present slow disease progression, which makes them very time consuming and, consequently, associated to higher costs<sup>98,95</sup>.

Induced models of OA are the most commonly used to study this disease. OA can be induced surgically or chemically. Surgically induced models alter the stability and load bearing of the joint, leading to the rapid development of OA; therefore, they are good tools to study late stages of OA degeneration, as they develop quickly and are highly reproducible and consistent. However, they are unsuitable to study the protective role of drug treatments, the earlier stages of OA or the pathogenic mechanisms that lead to the development of spontaneous OA<sup>98,95,101</sup>.

Chemically induced OA models are the more widely used models to assess drug therapeutic efficacy in OA-evoked pain. Chemical models consist of an intra-articular injection of substances that have deleterious effects on joint physiology – inhibition of chondrocyte metabolism (sodium monoiodoacetate (MIA)<sup>102,103</sup> or papain<sup>102</sup>) or damage of ligaments and tendons (collagenase<sup>104</sup>). Chemically induced OA models are highly reproducible, easy to implement and allow to study different stages of the disease. The MIA model is a particularly effective model to study pain and analgesic drug effects, as it produces chondrocyte death that leads to histological and morphological changes similar to those observed in human pathology, as well as osteophyte formation<sup>95</sup>. Rats that were submitted to this model present primary afferent nerve sensitization, spontaneous pain, mechanical and thermal hyperalgesia and allodynia and altered gait<sup>105</sup>. The most important limitation of chemically induced models of OA is the absence of correlation with the pathogenesis of human OA<sup>95</sup>.

Within the chemically induced models of OA, there is a subset of models of acute monoarthritis, which mimic the recurrent acute inflammatory episodes common in human OA<sup>88</sup>. Monoarthritis models rely on the induction of an immune response through the administration of a suspension of heat-killed *Mycobacterium butyricum* or *tuberculosis* (complete Freund's adjuvant – CFA<sup>106</sup>) or on the induction of an inflammatory response through the administration of an irritant substance (carrageenan, kaolin/carrageenan<sup>106,107</sup> (K/C) or zymosan<sup>88</sup>). The CFA model is characterized by joint inflammation and cartilage and bone damage, associated to nociceptive behavior and comorbid anxiety and depressive-like behavior that can last for several weeks in rats<sup>88,108</sup>. A similar pattern is observed after K/C administration, where animals develop use-dependent monoarthritis with cartilage damage, synovitis and synovial fluid exudate<sup>88</sup>. Rats present altered mechanical

hyperalgesia thresholds within hours of injection, which can persist for weeks<sup>107,109</sup>, and develop depressive and anxiety-like behaviors four weeks after induction<sup>80</sup>. Single administration of carrageenan produces shorter lasting symptoms, lasting only a few days and with less pronounced damage to cartilage than if given in combination with kaolin<sup>88</sup>. Additionally, CFA and carrageenan can be administered subcutaneously (usually in the paw) to produce inflammation and hypersensitivity<sup>110</sup>.

Similarly to these variations of monoarthritis models, the formalin test is commonly used as a fast inflammatory pain model. Subcutaneous injection of formalin produces a clear biphasic nociceptive response: an early phase, lasting up to 10 minutes, and a second phase, lasting from 20 to 60 minutes. In the two phases, rodents present licking and flinching behavior, as well favoring the affected paw. An interesting feature of this model is that while both phases are driven by primary afferent stimulation, the second phase is significantly modulated by central structures<sup>110</sup>, making it a suitable model to explore mechanisms of central sensitization.

### *1.3.2 Mechanisms of chronic inflammatory pain: peripheral and central sensitization*

The classic symptoms of inflammatory joint pathology are hyperalgesia (noxious stimuli cause stronger pain than in normal conditions), allodynia (mechanical threshold for mechanical noxious stimulation is decreased) and persistent pain at rest<sup>111</sup>. Several events were identified that contribute to the development and maintenance of these symptoms both in peripheral and central nervous system structures, corresponding to the well described chronic pain phenomena of peripheral and central sensitization<sup>1</sup>.

Inflammation elicits the production of classical inflammatory mediators such as bradykinin, prostaglandins and serotonin, and of pro-inflammatory cytokines, including tumor necrosis factor- $\alpha$  (TNF- $\alpha$ ), interleukin-1 $\beta$  (IL-1 $\beta$ ) and IL-6, which contribute to the sensitization of peripheral afferent nerves within a few minutes of their release<sup>83,112,113</sup>. If the situation persists, the expression of ion channels, receptors and mediators (TRP receptors, voltage-gated ion channels, acid-sensing ion channels, receptors for inflammatory mediators and neuropeptides) changes, further contributing to the maintenance of pain<sup>83,112</sup>. Joint inflammation causes primary afferent nerves to become sensitized to mechanical stimulation, leading to increased responses to innocuous stimuli (observed in A $\beta$ -fibers and in low-threshold C and A $\delta$ -fibers), lowering of the excitation threshold

(high threshold C and A $\delta$ -fibers respond to innocuous stimuli and silent nociceptors become responsive to mechanical stimulation), or even the development of spontaneous discharges during resting position<sup>114-116</sup>. Cutaneous nociceptors are particularly sensitized to thermal stimuli<sup>83,117</sup>. This increased responsiveness of primary afferent nerves to stimulation applied directly to the injured site is known as primary hypersensitivity<sup>118</sup>.

Another consequence of prolonged inflammation is that spinal cord neurons receiving joint input become hyperexcitable, a phenomenon known as central sensitization<sup>119</sup>. In parallel with alterations observed in primary afferent neurons, spinal WDR and NS neurons present increased responses to noxious stimulation, and the excitation threshold of NS neurons lowers. Additionally, there is also expansion of neuronal receptive fields, and consequently spinal neurons also display increased responses to stimuli applied to non-inflamed tissues<sup>120,121</sup>. Receptive field expansion is also observed behaviorally: rodents can present enhanced responses to noxious stimulation of the paw following inflammation of the knee joint<sup>122</sup>. This phenomenon is known as secondary hyperalgesia<sup>118</sup>.

Spinal cord sensitization arises from complex interactions between metabolite release and receptor expression at pre- and post-synaptic levels<sup>83,113,119</sup>. Stimulated by inflammatory metabolites on the peripheral axons, primary afferent nerves enhance their release of glutamate, substance P, neurokinin A and CGRP in the spinal cord<sup>123-126</sup>. In turn, these mediators activate their spinal receptors, including NMDA, metabotropic glutamate receptors (mGluR), neurokinin 1 and CGRP receptors<sup>127</sup>, triggering a cascade of events<sup>119,127</sup> that leads to the up-regulation of the expression (AMPA and NMDA) and phosphorylation of glutamate receptor (NMDA) subunits, resulting in increased excitatory glutamatergic transmission<sup>128</sup>. Release of other mediators such as prostaglandins and cytokines also occurs and contributes to further increase neuronal excitability by eliciting transmitter release, decreasing inhibitory input and promoting direct neuronal depolarization<sup>129</sup>.

Central sensitization was described not only at spinal cord level, but also supraspinally in the thalamus, the AMY, the ACC, the PFC and in several descending modulatory brain regions such as the PAG, the RVM and the DRt<sup>33,61,113</sup>. Interestingly, the pattern of activated brain regions in patients with chronic pain overlaps with those activated by acute stimulation, but there are some significant alterations in their involvement<sup>33,113</sup>. For instance, the activation of the sensory discriminative S1 and S2 cortices is less consistently registered in patients with chronic pain, pointing to a devaluation of the discrimination of the stimuli in patients with ongoing pain<sup>33,130</sup>, and, in the thalamus, baseline

and stimulus-evoked activity was found to be decreased in patients with chronic pain<sup>131</sup>. Additionally, the correlation between ACC activity with perceived pain intensity observed in normal subjects is abolished in patients suffering from chronic pain<sup>48</sup>. On the other hand, the PFC was found to be more consistently involved in chronic pain conditions<sup>33</sup>, and the AMY also exhibited increased activation<sup>132</sup>, implying that chronic pain alters cognitive and emotional perception of everyday experiences. This is consistent with clinical data indicating chronic pain patients usually suffer from comorbid anxiety, depression and overall decreased quality of life<sup>133</sup>.

#### *1.3.2.1 The prefrontal cortex during chronic pain*

Most of the data available concerning the involvement of PFC structures in pain processing comes from brain imaging studies in human subjects. A cortico-limbic brain circuit including the PFC and the AMY was shown to be significantly engaged during chronic pain<sup>134,135</sup>. The activity from the medial PFC (mPFC), an area associated with the intensity of emotional suffering<sup>136</sup>, shows the best correlation with high intensity spontaneous pain<sup>137</sup>. Interestingly, in chronic pain patients, the mPFC presents high connectivity with the nucleus accumbens, as opposed to an IC-accumbens connection observed in healthy subjects. This change in connectivity underlies impairments in reward prediction for acute pain analgesia observed in chronic pain patients<sup>138</sup>. The persistent mPFC activity can occur due to enhanced spinal-prefrontal projections (indirect or directly<sup>139,140</sup>) and/or be driven by gray matter atrophy in the DLPFC<sup>137,141</sup>.

The DLPFC is involved in working memory<sup>142</sup>. Acute pain can activate the DLPFC, but its activity does not correlate with stimulus intensity<sup>36</sup>. Instead, it is hypothesized that it exerts “top-down” inhibition upon orbitofrontal activity, limiting the perceived pain level<sup>143</sup>. In chronic pain patients, there is a disruption of orbitofrontal cortex activity, resulting in increased perception of negative affect<sup>144</sup>. The disruption seems to be driven by decreased gray matter density in the DLPFC<sup>141</sup>, as well as from decreased N-acetyl-aspartate and glucose content<sup>145</sup>. The cause of atrophy of the DLPFC is not known; however, it was suggested that it can be due to neurodegeneration, since decreased levels of N-methyl-aspartate are present in most neurodegenerative conditions<sup>141</sup>. Low glucose content can also be linked to decreased neuronal activity, as glucose is the main substrate of glutamatergic neurons<sup>145</sup>.

Interestingly, DLPFC activity correlates negatively with perceived intensity and unpleasantness of pain<sup>143</sup>. In addition to the connection with orbitofrontal cortex, the DLPFC and mPFC activity are inversely correlated<sup>48</sup>. Therefore, increased mPFC activity in chronic pain patients, and thus increased intensity of emotional suffering, is proposed to be driven by DLPFC atrophy. Interestingly, a role for the mPFC in endogenous descending hyperalgesia modulation was proposed by Seifert and colleagues, as they observed a direct correlation between mPFC activity and the capacity for endogenous modulation<sup>146</sup>. An interesting observation is that the above described pathways heavily overlap with circuits involved in cognitive performance. In particular, the orbitofrontal cortex is important for risk-assessment during decision making<sup>147</sup>. Thus, it is not surprising that chronic pain patients also present impairments in emotional-decision making tasks when compared with healthy subjects<sup>148</sup>.

Behavioral, anatomical and electrophysiological studies support the premise that PFC regions play an important role in nociceptive modulation and in the affective component of pain and a specific pathway involving the rodent midbrain, medial thalamus and PFC was suggested<sup>149</sup>. Importantly, homologies between rodent and primate PFC remain controversial. Anatomically, the part of the primate PFC known as granular cortex (due to the existence of a well-defined layer 4) does not have homologous regions in other species and rodents' PFC presents only similarities to the agranular primate PFC<sup>150</sup>. Due to this evidence, some researchers defend that regions such as the DLPFC and the mPFC are only present in primates<sup>150,151</sup> while others defend the opposite and that such regions do have similar representatives in the rodent brain<sup>152,153</sup>. Functionally, it was shown that lesions of proposed homologous rodent PFC areas produce similar deficits as those observed in primates<sup>152</sup>. Of note, lesions in the ACC of primates produce reduced pain responses<sup>154</sup>, while activation of the homologous area in rats promotes facilitation of withdrawal reflexes<sup>155</sup>. The same can be observed for other areas: mPFC inactivation in rodents produces deficits in working memory<sup>156</sup> and attention tasks<sup>157</sup>, similarly to the deficits observed in primates with lesions in the DLPFC<sup>158</sup>, indicating functional similarities between regions in the two different species<sup>152,159</sup>. Vertes<sup>160,161</sup> went even further and analyzed the function and anatomical distribution of the rat ventral mPFC subregions, the prelimbic and infralimbic cortices (PL and IL, respectively). He proposed that the PL, due to its role in cognition, decision-making and planning and in the affective dimension of those behaviors, is functionally homologous to the primate DLPFC; and that the IL, due to its role in visceromotor control and emotional behavior, is functionally homologous to the primate



mPFC. Together, these regions are proposed to integrate visceral and cognitive aspects to form complex goal-directed behaviors<sup>161</sup>.

The study of the PFC role in pain is more advanced in human subjects than in preclinical research models. However, the need to study in detail the molecular mechanisms underlying the activity states reported by imaging studies has recently led to an increase in PFC studies in animal models of pain. Most studies focused on the ACC, due to its salience in human brain imaging studies. It is now known that the ACC encodes mechanical stimulus intensity through neuronal response durations during peripheral noxious stimulation. This information is translated into temporal patterns and forwarded to pain modulatory regions<sup>162</sup>. Additionally, the ACC also responds to colorectal distension<sup>163</sup>. ACC activation has a facilitatory effect upon rat nociceptive behavior<sup>70,155</sup>, an effect relayed by the RVM<sup>155</sup> and the DRt<sup>70</sup>, and elicited by glutamate receptor activation<sup>70,155</sup>. Synaptic potentiation is increased in the ACC of neuropathic mice, maintaining pain-induced persistent changes, which can be reversed by blocking LTP in the ACC of these animals<sup>164</sup>. The ACC has also been implicated in the establishment of pain-related fear behavior<sup>165,166</sup>. In parallel with observations in human patients<sup>141</sup>, rats with neuropathic pain present decreased volumes in bilateral ACC associated with increased hyperalgesia<sup>167</sup>.

The pain modulatory role of the ventral mPFC subregions PL and IL<sup>161</sup> has also been addressed, although to a lesser extent. These areas are mainly associated to the attentional and cognitive processing of pain<sup>135</sup>. In this context, rats with persistent inflammatory and neuropathic pain presented impaired decision-making when compared to controls<sup>168</sup>. Such an effect was also observed in rats with impaired mPFC-AMY functioning<sup>169</sup>. Like the ACC, both PL and IL have neurons responsive to mechanical and heat noxious stimulation<sup>162</sup> and electrical stimulation of the ventral mPFC results in analgesia in rats<sup>170,171</sup>. In neuropathic pain conditions, pyramidal neuron morphology is altered and there is increased NMDA/AMPA receptors ratio<sup>172</sup>. These alterations result in an imbalance in GABAergic transmission that contributes to neuronal inhibition<sup>173</sup>. Decreased neuronal activity has also been described in rats with inflammatory pain, although it is driven by a feedback loop generated by AMY hyperactivity and mediated by metabotropic glutamate receptors (mGluR)<sup>174-176</sup>. By modulating mPFC activity either optogenetic or pharmacologically, behavioral hyperalgesia associated with both neuropathic and inflammatory pain can be reversed or enhanced<sup>173,176,177</sup>. Additionally, reversing ventral mPFC pain-driven neuronal inhibition also reverses pain-associated aversive behavior and decision-making impairments<sup>173,176</sup>. In line with

Vertes proposal for differential roles of the PL and IL<sup>161</sup>, studies that discriminate each subregion found they have specific functions in pain-related behaviors: blocking the PL, but not the IL, impairs acquisition and expression of formalin-induced place avoidance<sup>178</sup>; in addition, antinociception was elicited in neuropathic rats when NMDA receptors were activated in the PL but not in the ACC or the IL<sup>179</sup>.

### *1.3.2.2 Descending modulation during chronic pain*

As previously discussed, the balance between supraspinal descending inhibition and facilitation of spinal nociceptive transmission greatly influences the final behavioral outcome, allowing a rapid adaptation to the environmental circumstances. Long-term noxious stimulation leads to recruitment and reinforcement of an inhibitory tone in descending pain pathways, which counterbalances the excessive nociceptive input. The goal of this increased inhibition is to mitigate pain and allow the organism to seek protection<sup>180</sup> or to return to its normal activities<sup>9</sup>. During chronic pain, however, these adaptive systems can be overrun; instead, there is a marked enhancement in excitability that can result from dysregulation of descending inhibition, increased facilitation, or a combination of both<sup>9,181</sup>. A good example of these dual mechanisms comes from patients with pancreatic cancer, which only display pain behavior when the tumor is in an advanced stage and has metastasized to vital organs. Using a mouse model, it was shown that in the early stages of the disease supraspinal descending inhibition of pain is responsible for the lack of painful symptoms, as opioid antagonists with good CNS penetration, but not a non-CNS penetrant antagonist, could expose the existence of visceral spontaneous pain in the early non-symptomatic stages of pancreatic cancer<sup>182</sup>. Thus, there is increased supraspinal inhibition in an attempt to adapt to the tumor in its early stages, but that at a certain point becomes impaired or is no longer sufficient to mask the enhanced facilitation (either from increased peripheral inputs or descending facilitation) when the disease progresses. This phenotype can be paralleled in other degenerative diseases such as OA, in which the early stages of the disease are not frequently symptomatic, but which can at some point become painful<sup>90</sup>.

A great contribution for the descending inhibitory/facilitatory balance comes from the PAG-RVM circuit<sup>9,49,50</sup>. Studies both in human patients<sup>183,184</sup> and animal models<sup>185,186</sup>, have clearly demonstrated that altered activity in the PAG and the RVM play a key role in the generation and maintenance of

central sensitization and hyperalgesia. The RVM, particularly, has been shown to exert a dual inhibitory/facilitatory modulation upon spinal cord nociceptive neuronal activity and nociceptive behavior. In chronic inflammatory pain the RVM exerts both actions differentially in primary and secondary hypersensitivity behaviors<sup>118</sup>. Several studies using animal models of inflammatory pain reported enhanced descending inhibition of spinal cord neurons receiving inputs from the inflamed site<sup>187,188</sup> (primary hyperalgesia), which could be traced to the RVM. By pharmacologically inhibiting or lesioning this brain region, spinal cord neuronal activity and c-fos staining increased in animals with peripheral inflammation<sup>187,189</sup>. Interestingly, the pathway originating from the serotonin-rich nucleus raphe magnus (NRM – a subregion of the RVM) can suppress the responses of deep dorsal horn spinal neurons<sup>190</sup>. Similarly, the locus coeruleus also provides increased descending inhibition in inflammatory pain, since its lesion enhances thermal hyperalgesia<sup>191</sup>. The locus coeruleus is the main supraspinal source of noradrenergic inputs to the spinal cord, which modulates nociceptive responses of superficial dorsal horn neurons<sup>190</sup>; thus both serotonergic and noradrenergic pathways are major sources of descending inhibition during inflammation, although acting through independent pathways<sup>190</sup>.

Conversely, there is evidence that RVM-mediated descending facilitation is a major contributor to central sensitization and the development of secondary hyperalgesia behavior. In fact, inhibition or lesion of the RVM blocked secondary hyperalgesia elicited by deep tissue and cutaneous inflammation<sup>192-194</sup>, and reversed increased *c-fos* expression in the spinal cord after inflammation<sup>189</sup>. RVM-mediated facilitation arises, at least partially, from NMDA receptor activation during inflammation<sup>195</sup>. Some studies show that changes in the expression of glutamatergic NMDA and AMPA receptors follow a time dependent course: expression of both receptors is low three hours after induction of inflammatory pain, but 24 hours later it is greatly increased<sup>196,197</sup>.

Similarly, the activity pattern of RVM ON- and OFF-cells varies with time after inflammation onset. Electrophysiological studies show that in the first stages of inflammation, there is prolonged activation of ON- and suppression of OFF-cell firing<sup>198</sup>. However, in animals with chronic experimental arthritis both OFF- and ON-cell spontaneous and noxious-evoked activity are increased<sup>199</sup>. Despite being initially suggested to not participate in nociceptive modulation, a study reported that the activity of NEUTRAL-cells is altered over the course of hours during prolonged inflammation<sup>196</sup>. Additionally, and as previously discussed, the fact that a subset of these cells is serotonergic further supports their involvement in pain modulation<sup>53,200</sup>.

Parallel modulation primarily dedicated to pain facilitation can also come from circuits such as the spinal-DRT-spinal nociceptive loop. Enhanced DRT activity drives, at least partially, the establishment and development of chronic pain behaviors. Prolonged inflammatory pain leads to increased metabolic activity<sup>201</sup> and *c-fos* expression in the DRT<sup>202</sup>. Additionally, DRT stimulation with glutamate increases the responses of WDR neurons to sciatic nerve noxious stimulation<sup>203</sup>, implicating DRT activity dysregulation in neuropathic pain as well. By inhibiting DRT activity through electrolytic lesion or chemical blockade, pain behavior in the formalin test<sup>68</sup> is decreased and a reduction of *c-fos* expression in both superficial and deep dorsal horn laminae is observed<sup>68</sup>. Additionally, increased WDR activity in the spinal cord of rats with neuropathic pain is also reversed after DRT blockade<sup>204</sup>.

Underlying such alterations in DRT activity in chronic pain conditions are changes in glutamatergic<sup>205</sup>, noradrenergic<sup>206,207</sup>, opioidergic<sup>208,209</sup> and GABAergic transmission<sup>208,210</sup>. By selectively blocking NMDA, AMPA/kainate or mGluR receptors in the DRT, formalin-elicited nociceptive behavior and increased *c-fos* expression can be prevented or reduced<sup>205</sup>. Additionally, the development of secondary mechanical allodynia and secondary thermal hyperalgesia can be prevented by the same treatment<sup>205</sup>. These results point to increased DRT glutamatergic signaling to nociceptive dorsal horn neurons. Similarly, noradrenergic transmission also appears to be increased in the DRT in both chronic inflammatory<sup>206</sup> and neuropathic pain<sup>207</sup>, as the local pharmacological blockade of noradrenergic receptors leads to a reduction in nociceptive behavior in both pain types.

Finally, GABAergic transmission in the DRT, particularly by metabotropic GABA receptors, is increased in an animal model of chronic inflammatory pain and its pharmacological modulation can reduce inflammation related nociceptive behavior<sup>210</sup>. GABAergic transmission in the DRT has been linked to decreased  $\delta$  and  $\mu$ -opioid receptor expression during chronic inflammatory pain<sup>208,209</sup>, which leads to enhanced descending facilitation and/or reduced opioid-mediated analgesia, ultimately contributing to the development and maintenance of hyperalgesia and allodynia in monoarthritic animals<sup>209</sup>.

### *1.3.3 Pain modulation by metabotropic glutamate receptors*

Glutamate, the major excitatory neurotransmitter in the CNS, mediates not only fast synaptic events by activating voltage-gated ionotropic receptors (NMDA, AMPA and kainate receptors), but also long-lasting intracellular processes and metabolic changes that mediate synaptic plasticity through activation of mGluRs<sup>211</sup>. The long-term synaptic plasticity associated with central sensitization during prolonged pain is considered to be primarily associated to altered phosphorylation of ionotropic glutamate receptors, and thus altered excitability<sup>212</sup>. The NMDA receptor, especially, plays a key role in activity-dependent central sensitization, as pharmacological inhibition and conditional knockout of a NMDA receptor subunit results in eradication of NMDA-sensitive synaptic currents and injury-induced pain<sup>213</sup>. Using antagonists to pharmacologically block this receptor, however, causes a number of mild to severe side effects, such as sedation, confusion, and motor incoordination, which render them unsuitable for clinical use<sup>214</sup>. The focus is now on blocking specific NMDA function by targeting modulatory sites for known NMDA modulators such as glycine<sup>215</sup>. Although the efficacy of this strategy has not been clinically confirmed in pain yet<sup>214</sup>, a phase II clinical trial for treatment-resistant depression reported modulating the glycine binding site of NMDA receptors improved antidepressant effects<sup>216</sup>.

Another strategy is to modulate mGluR activity. mGluRs are a family of eight G-protein coupled receptors that can be divided into three groups based on similarities between coupling mechanisms, molecular structure and receptor pharmacology<sup>217,218</sup>. Activation of group I mGluRs, which include receptors 1 and 5 (mGluR1 and 5), results in increased phosphoinositide turnover, increasing intracellular Ca<sup>2+</sup> release and therefore potentiating cell excitability<sup>219</sup>. Group I mGluRs are abundantly expressed throughout the CNS. Interestingly, in general mGluR1 and mGluR5 do not overlap in their expression patterns: mGluR1 is highly expressed in the cerebellum, has some expression in the hippocampus and very little in the PFC; mGluR5, on the other hand, is highly expressed in the PFC and in the hippocampus, but has very little expression in the cerebellum<sup>220,221</sup>. These receptors are predominantly localized in postsynaptic membranes, appearing to be concentrated in perisynaptic and extrasynaptic areas. Thus, mGluR receptors require high concentrations of glutamate that escape clearance mechanisms and spread beyond the synaptic cleft to become activated<sup>222,223</sup>. Importantly, mGluR5 can also be found on presynaptic membranes<sup>224</sup>, in nuclear membranes<sup>225</sup> and is the main subtype of mGluR (along with mGluR3<sup>226</sup>) in glial cells<sup>227,228</sup>, pointing to distinct functions between mGluR1 and mGluR5.

Group I mGluRs interact with a vast number of intracellular mechanisms, allowing them to modulate acute and long term synaptic transmission processes such as long-term potentiation (LTP) and LTD. Some of these mechanisms include second messenger pathways, the mitogen-activated protein kinase/extracellular signal-regulated kinase (MAPK/ERK) pathway, cyclic adenosine monophosphate (cAMP) and other receptors, including voltage- and ligand-gated channels, such as NMDA and AMPA receptors, Ca<sup>2+</sup> channels and K<sup>+</sup> channels<sup>219</sup>. The interaction with NMDA receptors is particularly important, as it is known that through NMDA activity potentiation, mGluRs up-regulate neuronal excitability and regulate neuronal currents<sup>223</sup>.

Activation of groups II (mGluR2 and 3) and III (mGluR4, 6, 7 and 8), on the other hand, results in inhibition of cAMP formation<sup>217,218</sup>, leading to inhibition of voltage-gated Ca<sup>2+</sup> channels and decreased synaptic transmission<sup>229</sup>.

Group II mGluRs are predominantly located in presynaptic membranes and inhibit neurotransmitter release<sup>229</sup>. These receptors are usually located at some distance from the synaptic cleft and their function, especially for mGluR2, is proposed to be the monitoring of glutamate that has diffused from the synaptic space following high frequency stimulation. Additionally, it has also been proposed group II mGluRs can modulate glutamate uptake by glial or neuronal transporters. Thus, group II mGluRs constitute a negative feedback mechanism that prevents excessive glutamate release which might lead to pathological conditions otherwise<sup>229</sup>. Still, the role of group II mGluRs is not as well explored as that of group I, and future work might unveil other important functions for these receptors.

Group III mGluRs are a more heterogeneous group of receptors regarding their location both in the nervous system and in the synapse. Regarding their distribution in the CNS, mGluR6 has the most restrict expression pattern, being detected exclusively in the postsynaptic membrane of retina cells<sup>223,230</sup>. Of the remaining three group III mGluRs, all have expression throughout several brain regions, but mGluR8 has a more restricted expression, mGluR4 is intermediately expressed and mGluR7 is the most widely expressed<sup>231</sup>. mGluR4, 7 and 8 are presynaptic receptors but receptors 4 and 8 are detected perisynaptically, while receptor 7 is detected in the active zone<sup>232</sup>. There is some evidence also that both mGluR4 and 7 can be detected in post-synaptic membranes in some neurons<sup>233,234</sup>.

Although group III mGluRs inhibit cAMP formation, this is not their exclusive signaling mechanism. Instead, they can also couple to MAPK or phosphatidylinositol-3-kinase (PI3) pathways<sup>235</sup>. Through these mechanisms they can block Ca<sup>2+</sup> or activate K<sup>+</sup> channels, and suppress neuronal activity. Group III mGluRs are found in glutamatergic and GABAergic neurons<sup>218</sup>, meaning they can suppress excitatory or inhibitory transmission and that therefore, the main effect of activating group III mGluRs is a balance between transmission facilitation and inhibition<sup>231</sup>.

All mGluR subtypes, except mGluR6, are distributed throughout the pain neuroaxis and can be found from peripheral afferent nerves to supraspinal regions such as the thalamus, the PFC, the AMY and the PAG, where they can modulate the induction and/or maintenance of peripheral and central sensitization<sup>212</sup>. Their activity has been implicated in the induction, expression, and maintenance of chronic pain<sup>223,236</sup>, with the majority of studies emphasizing group I mGluR effects.

In peripheral afferent neurons, group I mGluR expression is found mainly in unmyelinated C-fibers, suggesting an important role in nociception. When agonists and antagonists for these receptors were tested, it was found that activation of peripheral group I mGluRs increased thermal hyperalgesia<sup>237</sup>. Inhibition of group I mGluR prevents the development of inflammatory pain<sup>237</sup> and attenuates established inflammatory and neuropathic pain<sup>237,238</sup>. Interestingly, pain facilitation in these conditions seems to arise through an mGluR-mediated enhancement of TRPV1 function<sup>239,240</sup>.

At the spinal cord level, activation of group I mGluRs in the dorsal horn facilitates nociception<sup>236</sup> and in persistent inflammatory pain, the expression of mGluR1 and mGluR5 in neurons and glial cells is increased. mGluR5 activates ERK signaling, leading to decreased K<sup>+</sup> currents and results in increased neuronal excitability in the dorsal horn<sup>241,242</sup>. Interestingly, systemic application of mGluR5 antagonists or negative allosteric modulators is effective in reversing not only chronic pain, but also in inducing analgesic conditioned place preference, indicating that mGluR5 activation in the spinal cord is responsible, at least partially, for spontaneous pain in neuropathic mice<sup>243</sup>.

mGluR1 and 5 can modulate nociceptive processing at the level of the AMY, the PAG and the thalamus. The nociceptive circuitry in the thalamus is mainly mediated by NMDA and group I mGluR<sup>244,245</sup> and mGluR1 is the main subtype modulating the function of nociceptive-responsive neurons<sup>246</sup>. In the AMY, activation of group I mGluRs is pronociceptive<sup>247,248</sup>, and there is an upregulation of functional mGluR1 in a model of persistent inflammatory pain<sup>249</sup>. Group I mGluRs are also important in the signaling between the AMY and the PFC, which has high expression of

group I mGluRs, particularly of mGluR5<sup>220</sup>, suggesting an important modulatory role of these receptors in the affective and cognitive dimensions of pain<sup>175,176,250</sup>. In the PAG, activation of all mGluR subtypes results in descending antinociception, independent of the general opposing effects of group I and groups II and III. It is proposed that group I mGluRs inhibit presynaptic GABA release through modulation of retrograde endocannabinoid signaling<sup>251-253</sup>, resulting in the disinhibition of the PAG descending antinociceptive pathway.

There is evidence that both groups II and III also modulate nociception at several levels of the pain neuroaxis. Contrary to group I, group II mGluR activation in peripheral tissues has an antinociceptive effect<sup>254</sup>, exerted through regulation of TRPV1 activity and tetrodotoxin-resistant Na<sup>+</sup> channels<sup>255,256</sup>. One important role of group II receptors is that they inhibit pain transmission at the synapses between primary afferent and second-order neurons in the spinal dorsal horn<sup>257</sup>. From group III, only mGluR4 and mGluR7 have been detected at the spinal cord level<sup>258</sup>. They seem to have specific roles in specific types of pain, as mGluR4 activation relieves neuropathic pain symptoms, but not inflammatory pain<sup>259</sup>, and mGluR7 activation relieves inflammatory pain but not neuropathic pain behavior<sup>260</sup>.

In the PAG, group II and III mGluRs have opposite actions: while group II receptors positively modulate the descending antinociceptive pathways, group III receptors modulate it negatively<sup>252</sup>. Kiritoshi and Neugebauer (2015) showed group II mGluR agonists can decrease glutamatergic activity in the mPFC under normal and chronic inflammatory pain conditions, and that their activity is not altered by chronic pain<sup>261</sup>. In the AMY, on the other hand, a group II antagonist had pronociceptive effects but only in chronic pain conditions<sup>262</sup>. mGluR7 and mGluR8 are often reported to have opposite actions. In the AMY, PAG and RVM, mGluR7 activation results in pronociception<sup>263-</sup><sup>265</sup> while mGluR8 activation reduced pain associated to chronic inflammation or neuropathy<sup>264-266</sup>.

#### **1.4 Pain modulation by non-neuronal cells**

For many years, pain, as well as many other pathologies, was considered to depend solely on neuronal networks and mechanisms triggered by a noxious stimulus, inflammation or damage. While this is true for acute pain, the involvement of non-neuronal cell types, like glial and immune cells, in driving the establishment and maintenance of chronic pain states has been repeatedly



confirmed<sup>267,268</sup>. In the CNS there are two main types of glia – microglia and macroglia, which includes oligodendrocytes and astrocytes.

#### 1.4.1 Microglia

Microglia are the resident immunocompetent phagocytic cells in the CNS. They constitute about 5-12% of the total glial cell population<sup>269</sup> and are present in three forms in the adult CNS, (i) the ameboid, (ii) the ramified and (iii) the reactive form<sup>270</sup>. Ameboid microglia are more common in the developing stages of the brain, when there are large amounts of extracellular debris and apoptotic cells to remove<sup>270</sup>. The ramified form constitutes the quiescent permanent population in the CNS, which when activated by outside stimuli and pathological conditions becomes reactive<sup>271</sup>. *In vitro* studies show that microglia are extremely sensitive to physiological conditions and can switch from one form to the other very rapidly<sup>272</sup>. This switch implies functional and morphological changes that allow the cells to rapidly respond to CNS injury or threats, making them the first responders to damaging situations.

Reactive microglia are able to express various cytokines and growth factors<sup>273,274</sup> and capable of releasing several cytotoxic factors<sup>275</sup>. Depending on the profile of factors being secreted, microglia in their reactive state can be classified in two heterogeneous states, M1 and M2. The M1 profile is cytotoxic and leads to a pro-inflammatory response with release of TNF- $\alpha$ , IL-1 $\beta$ , superoxide, nitric oxide (NO) and proteases, which promote cell loss and dysfunction<sup>276-278</sup>. The secretion of cytotoxic factors is aimed at destroying infected or damaged neural cells, virus and bacteria. However, it can also lead to collateral neuronal damage<sup>279</sup>. The M2 profile is neuroprotective and promotes neuronal regeneration, extracellular matrix reconstruction and anti-inflammation. Some of the factors produced in this profile include IL-4, IL-10, IL-13 and transforming growth factor- $\beta$  (TGF- $\beta$ )<sup>276,280</sup>. In normal conditions the activation of each profile is under tight control and the alternate activation of M1 and M2 prevents the accumulation of damage. In pathological conditions, as immune responses become less controlled, the activation of M1 microglia can become persistent, in a process known as neuroinflammation<sup>281,282</sup>.

In response to peripheral injury, glial activation occurs in multiple pain processing pathways, but special emphasis has been given to glia in the spinal cord. Increased expression of the microglial markers ionized calcium-binding adapter molecule (Iba1) and/or CD11b was found in several

models of inflammatory pain such as the formalin<sup>283,284</sup>, zymosan<sup>284,285</sup> and carrageenan models<sup>286</sup>, and in models of neuropathic pain<sup>287-290</sup> and chronic opioid exposure<sup>291</sup>. Interestingly, only deep-tissue damage seems to induce microglial activation; for instance, intra-articular, but not intraplantar, injection of CFA leads to increased spinal cord expression of microglial markers<sup>292</sup>, and acute tissue injury elicited by cutaneous application of mustard oil also fails to increase microglial activation<sup>293</sup>. These observations suggest that deep tissue injury has a more severe impact upon spinal microglial activation, possibly depending on the existence of axonal injury or not<sup>293,294</sup>. In line with this hypothesis, several studies show glial activation in the spinal cord depends on peripheral input; for example, electrical stimulation of the rat sciatic nerve or dorsal root at a noxious intensity increases Iba1 immunoreactivity in the spinal dorsal horn and pain sensitivity<sup>295</sup>.

The pathways involved in microglia activation after peripheral injury are extensively characterized. Upon peripheral injury, primary afferents release a number of metabolites in the spinal cord<sup>296</sup>, including neurotransmitters (glutamate, substance P, CGRP, ATP, brain-derived neurotrophic factor (BDNF)), cytokines, and growth factors, such as neuroregulin-1 (NRG-1)<sup>297</sup>. The release of this plethora of metabolites can simultaneously activate several receptors in both neurons and microglia, including the purinergic receptors P2X4<sup>298</sup> and P2X7<sup>299</sup>, neuronal neuregulin 1 (NRG-1), and CX3CL1 (also known as fractalkine)<sup>300</sup>, which culminate in the phosphorylation of p38 MAPK<sup>301,302</sup> in microglia and the release of IL-1 $\beta$ <sup>299,303</sup>. Microglia can also release BDNF<sup>298</sup>, which can shift the neuronal membrane potential by binding to tyrosine receptor kinase B (TrkB) receptors, resulting in GABA<sub>A</sub> receptor-mediated depolarization of dorsal horn neurons and contributing to the establishment of nociceptive neuronal hyperexcitation in the spinal cord<sup>304,305</sup>.

Microglial proliferation is very marked in the onset stages of chronic pain<sup>306</sup> and intrathecal administration of minocycline, a nonselective inhibitor of M1 reactive microglia, at early stages of chronic pain reduces neuropathic<sup>307</sup> and inflammatory pain behaviors<sup>286</sup>. However, blocking microglia in late-phase stages of neuropathic pain does not significantly reduce nociceptive behavior<sup>307,308</sup>. This is in line with the function of microglia as the early responders to injury in the CNS. Chemical signals from damaged/activated neurons stimulate microglial release of pro-inflammatory cytokines and pronociceptive transmitters that aggravate the initial injury. Astrocytes in turn act as second wave responders. They are activated in later stages by the release of microglial gliotransmitters, when glutamatergic transmission becomes impaired, and maintain the long-term pathological states<sup>294,307,308</sup>. Supporting this hypothesis of interaction between microglia and

astrocytes, in nerve injury there is increased expression of IL-18, TNF $\alpha$  and CCL2 by microglia and of the respective receptors in astrocytes<sup>309-311</sup>. Additionally, in a knockout model of matrix metalloproteinase 9, which is expressed only in microglia, neuropathic pain was attenuated in early stages but was fully established in later stages<sup>312</sup>. The opposite has also been described, and mice deficient in GFAP develop short lasting mechanical allodynia<sup>313</sup>. Therefore, the microglial and astrocytic distinct temporal patterns of activation mirror the early-onset and long term duration of chronic pain responses.

#### *1.4.2 Astrocytes*

Astrocytes, or astroglia, are the most abundant cells in the CNS, with variable proportion depending on the brain region and ranging from 20 to 40% of all CNS cells<sup>272</sup>. Astrocytes are star-shaped cells with processes that envelop synapses. They can be classified in three main subtypes, based on their distribution: the fibrous, radial and protoplasmic astrocytes. Fibrous cells are found in white matter and have long cellular processes that are connected to the exterior wall of capillary vessels. These unbranched processes have also been found to envelop nodes of Ranvier. Radial glia exist in planes perpendicular to ventricular axes. These cells are present in developmental stages, where they assist in neuronal migration. In the adult brain they exist in the retina (Müller cells) and in the cerebellar cortex (Bergmann glia)<sup>272,314,315</sup>. Protoplasmic astrocytes are the most common form of astroglia and exist in grey matter. They have highly branched processes that envelop synapses<sup>316</sup>. One important feature of astrocytes is that they have well-defined territories and their edges have minimal overlap with each other<sup>317</sup>. It is estimated that, in the rodent cortex, one astrocyte contacts 4–8 neurons, surrounds about 300–600 neuronal dendrites and regulates up to 20,000–120,000 synapses<sup>317,318</sup>. Astrocytes are physically connected to other astrocytes by gap junctions formed by connexin 43 (Cx43) and/or Cx30<sup>272</sup>, forming networks through which intercellular transmission occurs<sup>319</sup>. In pathological conditions, astrocytes radically change their morphology, the number of synapses contained in individual astrocyte territories and the proximity of astrocyte processes to synapses<sup>320</sup>.

Astrocytes express the same variety of receptors as neurons, which allows them to sense the neurotransmitters released during synaptic transmission. Interestingly, astrocytes usually express the same type of receptors as their neighboring neurons<sup>321,322</sup>. Some relevant receptor types

expressed by astrocytes include glutamatergic, purinergic and GABAergic receptors, among others, as well as cytokine and chemokine receptors and several types of membrane transporters<sup>272</sup>. Contrary to neurons, astrocytes are non-electrically excitable cells. Instead, they use Ca<sup>2+</sup> signaling as a substrate for their excitability<sup>272</sup>. Several mechanisms have been described in the generation of Ca<sup>2+</sup> signaling. Release of intracellular Ca<sup>2+</sup> from the endoplasmic reticulum involves the activation of receptors in the membrane of astrocytes, particularly metabotropic glutamate (mGluR1, mGluR3 and mGluR5) and GABA (GABA<sub>B</sub>) receptors, or ionotropic glutamate (NMDA or AMPA) and purinergic (P2X7) receptors<sup>323,324</sup>, which in turn will lead to the activation of inositol triphosphate (IP<sub>3</sub>) receptors. The type 2 IP<sub>3</sub> receptors (IP<sub>3</sub>R2) are enriched in astrocytes and mediate spontaneous and G-protein-coupled receptor-mediated Ca<sup>2+</sup> signals<sup>325,326</sup>. However, an IP<sub>3</sub>R2-independent signaling also occurs, as a knockout of this receptor in mice does not impair Ca<sup>2+</sup> signaling at the level of astrocytic processes<sup>325</sup>. There is a high proportion of Ca<sup>2+</sup> channels such as TRPA1 or Ca<sup>2+</sup>-permeable ion channels in astrocytic processes<sup>327,328</sup>. In fact, the development of novel and more specific tools for imaging of Ca<sup>2+</sup> currents has highlighted that, contrary to what was hypothesized until a decade ago, astrocytes, like neurons, should be viewed as having different compartments within the cell<sup>323,324</sup> and that intracellular Ca<sup>2+</sup> transients in the soma can differ from those occurring at the more distal and finer branches of astrocytes<sup>329,330</sup>. In this manner, Ca<sup>2+</sup> signaling can occur in two different ways: intercellular Ca<sup>2+</sup> waves that propagate between astrocytic gap junctions and that provide astrocytes with the means for long-distance communication; and intracellular Ca<sup>2+</sup> waves, that can occur within the whole cell or be compartmentalized in specific areas called microdomains<sup>272,323,324</sup>. Although the functional role of these two distinct ways of Ca<sup>2+</sup> propagation is not known, it is possible that increased Ca<sup>2+</sup> in microdomains can modulate local neuronal signaling, while intercellular Ca<sup>2+</sup> waves regulate neuronal network synchronization<sup>320,323</sup>.

One of the end products of Ca<sup>2+</sup> signaling in astrocytes is the release of gliotransmitters. Astrocytes release several classical neurotransmitters and neuromodulators, such as glutamate, ATP, GABA and D-serine. Three main mechanisms have been described for the release of gliotransmitters: exocytotic release, diffusional release through plasmalemmal pores, or transporter mediated release<sup>272</sup>. The physiological role of gliotransmitter release is still under debate. This arises from the multiple functions that have been attributed to astrocytes. Unlike microglia and oligodendrocytes, astrocytes do not have one defined physiological function: they are connected to every housekeeping and homeostatic function in the CNS, including structural support, CNS development, homeostatic functions, regulation of blood flow through the control of blood vessels'

diameter, metabolic support, higher brain functions such as memory and sleeping and also brain defense and formation of the glial scar after nerve injury<sup>272</sup>. Additionally, in the last decade, it was shown astrocytes actively participate in the regulation of synaptic transmission alongside neurons. Due to the morphological proximity of astrocytic processes and synapses, astrocytes can sense neurotransmitter release and in turn contribute themselves with local Ca<sup>2+</sup>-induced gliotransmitter release, leading to post- and pre-synaptic modulation, a concept known as tripartite synapse<sup>272,318</sup>. Additionally, Ca<sup>2+</sup> waves that propagate through the astrocyte network can ultimately affect other neurons connected to the astrocyte or even distant structures.

It is not surprising that given the multitude of functions attributed to astrocytes, dysfunction of these cells was connected to multiple pathologies, including development and maintenance of chronic pain. Garrison and colleagues were among the first to describe that the increased reactive astrogliosis (measured by GFAP expression) in the spinal cord of rats with neuropathic pain could be blocked by inhibiting spinal NMDA receptors<sup>331,332</sup>. The administration of pharmacological astrocyte inhibitors fluorocitrate, fluoroacetate and L- $\alpha$ -amino adipate (L $\alpha$ AA) blocked nociceptive behaviors in models of acute and chronic inflammatory<sup>333,334</sup> and neuropathic pain<sup>335,336</sup>. On the other hand, direct delivery of reactive astrocytes in the spinal cord decreased the paw withdrawal threshold of rats<sup>337</sup>. In mice with augmented astrocyte activity, CFA-induced edema and thermal hyperalgesia were significantly enhanced<sup>338</sup>. Together, these findings suggest a role for astroglial activation in exacerbated pain states. One important finding is that the inhibition of astrocytes (and microglia) does not affect normal pain processing, which highlights the role of glial cells in pathological pain states<sup>267</sup>.

#### *1.4.2.1 Pain modulation by astrocytic glutamatergic signaling*

Glutamatergic input plays a considerable role in sensory and motor-driven astrocyte responses<sup>320</sup>. Accordingly, one of the more noticeable pathways through which astrocytes can contribute to maintenance of chronic pain involves the dysregulation of glutamate transporter-1 (GLT-1) and glutamate and aspartic acid transporter (GLAST). In physiological conditions, these transporters regulate the clearance of glutamate from the synaptic cleft, maintaining glutamate at non-excitotoxic concentrations<sup>339</sup>. In late stages of neuropathic and chronic opioid exposure pain models, both GLT-1 and GLAST protein levels are decreased in the spinal cord<sup>340-342</sup>, with a concomitant

increase in spinal extracellular glutamate and spontaneous pain<sup>343</sup>. In chronic inflammatory pain, the phosphorylation of c-Jun N-terminal kinases (JNK) in spinal astrocytes seems to be important for the maintenance of mechanical allodynia<sup>310,344</sup>, proportionally to the release of TNF $\alpha$  in the spinal cord<sup>344</sup>. Incidentally, TNF $\alpha$  also evokes astrocytic glutamate release<sup>296</sup>, which further contributes to an overall increase in excitatory synaptic transmission<sup>342,345,346</sup>. Another glutamate receptor that seems to contribute to chronic pain maintenance is mGluR5. In astrocytes, mGluR5 is important for the detection of glutamate release during synaptic glutamate<sup>228</sup>. In a model of bone cancer pain, spinal expression of mGluR5 was increased. mGluR5 inhibition attenuated GFAP expression, spontaneous pain, mechanical allodynia and thermal hyperalgesia<sup>347</sup>. Overall, these glutamatergic mechanisms contribute to neurotransmitter imbalance and increased synaptic transmission, one of the hallmarks of chronic pain<sup>127</sup>.

Most studies focus on the role of glial cells in pain modulation at the spinal level. However, rats with neuropathic pain present prolonged activation of astrocytes in the RVM<sup>348</sup>, indicating that glial-neuronal interactions can also contribute to the descending modulation of pain at the supraspinal level. Additionally, a recent study found increased expression of astrocytic mGluR5 in the SI of rats with neuropathic pain, which, when blocked, suppressed mechanical allodynia<sup>349</sup>. Finally, in the CFA model of inflammatory pain there is increased GFAP expression in the ACC. Ablation of astrocytes in this area did not reverse mechanical hyperalgesia, but inhibited the increased escape/avoidance behavior in animals with inflammatory pain, indicating that astrocytes in the ACC can contribute for the modulation of the affective components of pain<sup>350</sup>.

## 1.5 Aims

The advent of brain imaging techniques has unequivocally highlighted the contribution of the cortico-limbic systems in pain modulation. However, brain imaging only reports overall changes in activity, without addressing the specific accompanying mechanisms. Preclinical investigation of those mechanisms has already asserted the involvement of some areas such as the ACC and the importance they hold in our perception of pain, as well as in the development of affective and cognitive impairments driven by chronic pain. Other areas and their roles remain unexplored. Therefore, in this thesis we focused on studying the mPFC as a potential pain modulatory area, the contribution of its different neural populations towards nociception and the pain modulatory circuits it integrates, as well as the effect of chronic inflammatory pain upon mPFC functions. More specifically, we aimed at:

- (i) Evaluating the long-term impact of the K/C model of experimental monoarthritis upon the nociceptive behavior of rodents, as well as the histopathological and radiological changes observed in the affected knee joint during that period (**Chapter 2.1**);
- (ii) Assessing the main contributions of the PL and the IL to nociceptive behavior (**Chapter 2.2**);
- (iii) Studying the role of IL astrocytes towards mGluR5-mediated nociceptive modulation in healthy and monoarthritic animals (**Chapter 2.3**);
- (iv) Studying the role of the DRt and the RVM as mediators of the IL mGluR5 descending pronociceptive effect in healthy and monoarthritic animals (**Chapters 2.4 and 2.5**);
- (v) Analyzing the effect of mGluR5 activation in the IL upon the activity of spinal dorsal horn nociceptive neurons of healthy and monoarthritic animals (**Chapter 2.4**);
- (vi) Evaluating the role of spinal TRPV1 as a spinal target of IL mGluR5-mediated pronociception in healthy and monoarthritic animals (**Chapter 2.4**).

## 1.6 References

1. Loeser, JD, Treede, RD (2008) The Kyoto protocol of IASP Basic Pain Terminology. *Pain* 137, 473–7.
2. Hodge, CJ, Apkarian, A V (1990) The spinothalamic tract. *Crit. Rev. Neurobiol.* 5, 363–97.
3. Tracey, I, Mantyh, PW (2007) The cerebral signature for pain perception and its modulation. *Neuron* 55, 377–91.
4. Apkarian, AV (2008) Pain perception in relation to emotional learning. *Curr. Opin. Neurobiol.* 18, 464–8.
5. Melzack, R (2001) Pain and the neuromatrix in the brain. *J. Dent. Educ.* 65, 1378–82.
6. Basbaum, AI, Bautista, DM, Scherrer, G, Julius, D (2009) Cellular and molecular mechanisms of pain. *Cell* 139, 267–284.
7. D’Mello, R, Dickenson, AH (2008) Spinal cord mechanisms of pain. *Br. J. Anaesth.* 101, 8–16.
8. Julius, D, Basbaum, AI (2001) Molecular mechanisms of nociception. *Nature* 413, 203–10.
9. Millan, MJ (2002) Descending control of pain. *Prog. Neurobiol.* 66, 355–474.
10. Craig, ADB (2003) Pain mechanisms: labeled lines versus convergence in central processing. *Annu. Rev. Neurosci.* 26, 1–30.
11. Perl, ER (2007) Ideas about pain, a historical view. *Nat. Rev. Neurosci.* 8, 71–80.
12. Schmidt, R, Schmelz, M, Forster, C, Ringkamp, M, Torebjörk, E, Handwerker, H (1995) Novel classes of responsive and unresponsive C nociceptors in human skin. *J. Neurosci.* 15, 333–41.
13. Millan, MJ (1999) The induction of pain: an integrative review. *Prog. Neurobiol.* 57, 1–164.
14. Caterina, MJ, Schumacher, M a, Tominaga, M, Rosen, T a, Levine, JD, Julius, D (1997) The capsaicin receptor: a heat-activated ion channel in the pain pathway. *Nature* 389, 816–824.
15. Caterina, MJ, Leffler, A, Malmberg, AB, Martin, WJ, Trafton, J, Petersen-Zeitz, KR, Koltzenburg, M, Basbaum, AI, Julius, D (2000) Impaired nociception and pain sensation in mice lacking the capsaicin receptor. *Science* 288, 306–13.
16. Tominaga, M, Caterina, MJ, Malmberg, AB, Rosen, TA, Gilbert, H, Skinner, K, Raumann, BE, Basbaum, AI, Julius, D (1998) The cloned capsaicin receptor integrates multiple pain-



- producing stimuli. *Neuron* 21, 531–543.
17. Holzer, P (1991) Capsaicin: cellular targets, mechanisms of action, and selectivity for thin sensory neurons. *Pharmacol. Rev.* 43, 143–201.
  18. Dubin, AE, Patapoutian, A (2010) Nociceptors: the sensors of the pain pathway. *J. Clin. Invest.* 120, 3760–72.
  19. Price, TJ, Louria, MD, Candelario-Soto, D, Dussor, GO, Jeske, NA, Patwardhan, AM, Diogenes, A, Trott, AA, Hargreaves, KM, Flores, CM (2005) Treatment of trigeminal ganglion neurons in vitro with NGF, GDNF or BDNF: effects on neuronal survival, neurochemical properties and TRPV1-mediated neuropeptide secretion. *BMC Neurosci.* 6, 4.
  20. Immke, DC, Gava, NR (2006) The TRPV1 receptor and nociception. *Semin. Cell Dev. Biol.* 17, 582–591.
  21. Woodbury, CJ, Zwick, M, Wang, S, Lawson, JJ, Caterina, MJ, Koltzenburg, M, Albers, KM, Koerber, HR, Davis, BM (2004) Nociceptors lacking TRPV1 and TRPV2 have normal heat responses. *J. Neurosci.* 24, 6410–5.
  22. Cui, M, Honore, P, Zhong, C, Gauvin, D, Mikusa, J, Hernandez, G, Chandran, P, Gomtsyan, A, Brown, B, Bayburt, EK, Marsh, K, Bianchi, B, McDonald, H, Niforatos, W, Neelands, TR, Moreland, RB, Decker, MW, Lee, C-H, Sullivan, JP, Faltynek, CR (2006) TRPV1 receptors in the CNS play a key role in broad-spectrum analgesia of TRPV1 antagonists. *J. Neurosci.* 26, 9385–93.
  23. Cavanaugh, DJ, Lee, H, Lo, L, Shields, SD, Zylka, MJ, Basbaum, AI, Anderson, DJ (2009) Distinct subsets of unmyelinated primary sensory fibers mediate behavioral responses to noxious thermal and mechanical stimuli. *Proc. Natl. Acad. Sci. U. S. A.* 106, 9075–80.
  24. Valtschanoff, JG, Rustioni, A, Guo, A, Hwang, SJ (2001) Vanilloid receptor VR1 is both presynaptic and postsynaptic in the superficial laminae of the rat dorsal horn. *J. Comp. Neurol.* 436, 225–35.
  25. Ferrini, F, Salio, C, Lossi, L, Gambino, G, Merighi, A (2010) Modulation of inhibitory neurotransmission by the vanilloid receptor type 1 (TRPV1) in organotypically cultured mouse substantia gelatinosa neurons. *Pain* 150, 128–40.
  26. Kim, YH, Back, SK, Davies, AJ, Jeong, H, Jo, HJ, Chung, G, Na, HS, Bae, YC, Kim, SJ, Kim, JS, Jung, SJ, Oh, SB (2012) TRPV1 in GABAergic interneurons mediates neuropathic mechanical allodynia and disinhibition of the nociceptive circuitry in the spinal cord. *Neuron* 74, 640–7.

27. Madasu, MK, Roche, M, Finn, DP (2015) Supraspinal transient receptor potential subfamily V member 1 (TRPV1) in pain and psychiatric disorders. *Mod. Trends Pharmacopsychiatry* 30, 80–93.
28. Willis, WD, Westlund, KN (1997) Neuroanatomy of the pain system and of the pathways that modulate pain. *J. Clin. Neurophysiol.* 14, 2–31.
29. Dostrovsky, JO, Craig, AD (Bud) (Elsevier/Churchill Livingstone, 2013). in *Wall and Melzack's Textbook of Pain* (eds. Wall, P. D., McMahon, S. B. & Koltzenburg, M.) 182–197.
30. Almeida, A, Tavares, I, Lima, D, Coimbra, A (1993) Descending projections from the medullary dorsal reticular nucleus make synaptic contacts with spinal cord lamina I cells projecting to that nucleus: An electron microscopic tracer study in the rat. *Neuroscience* 55, 1093–1106.
31. Almeida, A, Tavares, I, Lima, D (1995) Projection sites of deep dorsal horn in the dorsal reticular nucleus. *Neuro Report* 6, 1245–1248.
32. Melzack, R (1999) From the gate to the neuromatrix. *Pain Suppl* 6, S121-6.
33. Apkarian, AV, Bushnell, MC, Treede, R-D, Zubieta, J-K (2005) Human brain mechanisms of pain perception and regulation in health and disease. *Eur. J. Pain* 9, 463–463.
34. Apkarian, AV, Bushnell, MC, Schweinhardt, P (Elsevier/Churchill Livingstone, 2013). in *Wall and Melzack's Textbook of Pain* (eds. Wall, P. D., McMahon, S. B. & Koltzenburg, M.) 111–128.
35. Peyron, R, García-Larrea, L, Grégoire, MC, Costes, N, Convers, P, Lavenne, F, Mauguière, F, Michel, D, Laurent, B (1999) Haemodynamic brain responses to acute pain in humans: sensory and attentional networks. *Brain* 122 ( Pt 9, 1765–80.
36. Coghill, RC, Sang, CN, Maisog, JM, Iadarola, MJ (1999) Pain intensity processing within the human brain: a bilateral, distributed mechanism. *J. Neurophysiol.* 82, 1934–43.
37. Ploner, M, Schmitz, F, Freund, HJ, Schnitzler, A (1999) Parallel activation of primary and secondary somatosensory cortices in human pain processing. *J. Neurophysiol.* 81, 3100–4.
38. Treede, RD, Kief, S, Hölzer, T, Bromm, B (1988) Late somatosensory evoked cerebral potentials in response to cutaneous heat stimuli. *Electroencephalogr. Clin. Neurophysiol.* 70, 429–41.
39. Fulbright, RK, Troche, CJ, Skudlarski, P, Gore, JC, Wexler, BE (2001) Functional MR imaging of regional brain activation associated with the affective experience of pain. *AJR.*

- Am. J. Roentgenol.* 177, 1205–10.
40. Rainville, P, Duncan, GH, Price, DD, Carrier, B, Bushnell, MC (1997) Pain affect encoded in human anterior cingulate but not somatosensory cortex. *Science* 277, 968–71.
  41. Mesulam, MM, Mufson, EJ (1982) Insula of the old world monkey. I. Architectonics in the insulo-orbito-temporal component of the paralimbic brain. *J. Comp. Neurol.* 212, 1–22.
  42. Berthier, M, Starkstein, S, Leiguarda, R (1988) Asymbolia for pain: a sensory-limbic disconnection syndrome. *Ann. Neurol.* 24, 41–9.
  43. Starr, CJ, Sawaki, L, Wittenberg, GF, Burdette, JH, Oshiro, Y, Quevedo, AS, Coghill, RC (2009) Roles of the insular cortex in the modulation of pain: insights from brain lesions. *J. Neurosci.* 29, 2684–94.
  44. Ostrowsky, K, Magnin, M, Rylvlin, P, Isnard, J, Guenot, M, Mauguière, F (2002) Representation of pain and somatic sensation in the human insula: a study of responses to direct electrical cortical stimulation. *Cereb. Cortex* 12, 376–85.
  45. Beydoun, A, Morrow, TJ, Shen, JF, Casey, KL (1993) Variability of laser-evoked potentials: attention, arousal and lateralized differences. *Electroencephalogr. Clin. Neurophysiol.* 88, 173–81.
  46. Johansen, JP, Fields, HL (2004) Glutamatergic activation of anterior cingulate cortex produces an aversive teaching signal. *Nat. Neurosci.* 7, 398–403.
  47. Porro, CA, Baraldi, P, Pagnoni, G, Serafini, M, Facchin, P, Maieron, M, Nichelli, P (2002) Does anticipation of pain affect cortical nociceptive systems? *J. Neurosci.* 22, 3206–3214.
  48. Lorenz, J, Cross, DJ, Minoshima, S, Morrow, TJ, Paulson, PE, Casey, KL (2002) A unique representation of heat allodynia in the human brain. *Neuron* 35, 383–93.
  49. Heinricher, MM, Tavares, I, Leith, JL, Lumb, BM (2009) Descending control of nociception: Specificity, recruitment and plasticity. *Brain Res. Rev.* 60, 214–225.
  50. Heinricher, MM, Fields, HL (Elsevier/Churchill Livingstone, 2013). in *Wall and Melzack's Textbook of Pain* (eds. Wall, P. D., McMahon, S. B. & Koltzenburg, M.) 129–142.
  51. Lima, D, Almeida, A (2002) The medullary dorsal reticular nucleus as a pronociceptive centre of the pain control system. *Prog. Neurobiol.* 66, 81–108.
  52. Tavares, I, Lima, D (2002) The caudal ventrolateral medulla as an important inhibitory modulator of pain transmission in the spinal cord. *J. Pain* 3, 337–46.
  53. Price, DD (2000) Psychological and neural mechanisms of the affective dimension of pain. *Science* 288, 1769–72.

54. Mayer, EA, Berman, S, Suyenobu, B, Labus, J, Mandelkern, MA, Naliboff, BD, Chang, L (2005) Differences in brain responses to visceral pain between patients with irritable bowel syndrome and ulcerative colitis. *Pain* 115, 398–409.
55. Fields, HL, Heinricher, MM (1985) Anatomy and physiology of a nociceptive modulatory system. *Philos. Trans. R. Soc. Lond. B. Biol. Sci.* 308, 361–74.
56. Mayer, DJ, Price, DD (1976) Central nervous system mechanisms of analgesia. *Pain* 2, 379–404.
57. Levy, R, Deer, TR, Henderson, J (2010) Intracranial neurostimulation for pain control: a review. *Pain Physician* 13, 157–65.
58. Rizvi, T a, Ennis, M, Behbehani, MM, Shipley, MT (1991) Connections between the central nucleus of the amygdala and the midbrain periaqueductal gray: topography and reciprocity. *J. Comp. Neurol.* 303, 121–31.
59. Floyd, NS, Price, JL, Ferry, AT, Keay, KA, Bandler, R (2000) Orbitomedial prefrontal cortical projections to distinct longitudinal columns of the periaqueductal gray in the rat. *J. Comp. Neurol.* 422, 556–78.
60. Bandler, R, Keay, KA (1996) Columnar organization in the midbrain periaqueductal gray and the integration of emotional expression. *Prog. Brain Res.* 107, 285–300.
61. Almeida, A, Cobos, A, Tavares, I, Lima, D (2002) Brain afferents to the medullary dorsal reticular nucleus: A retrograde and anterograde tracing study in the rat. *Eur. J. Neurosci.* 16, 81–95.
62. Beitz, AJ (1982) The organization of afferent projections to the midbrain periaqueductal gray of the rat. *Neuroscience* 7, 133–59.
63. Potrebic, SB, Fields, HL, Mason, P (1994) Serotonin immunoreactivity is contained in one physiological cell class in the rat rostral ventromedial medulla. *J. Neurosci.* 14, 1655–1665.
64. Tavares, I, Lima, D (1994) Descending projections from the caudal medulla oblongata to the superficial or deep dorsal horn of the rat spinal cord. *Exp. Brain Res.* 99, 455–463.
65. Almeida, A, Tavares, I, Lima, D (2000) Reciprocal connections between the medullary dorsal reticular nucleus and the spinal dorsal horn in the rat. *Eur. J. Pain* 4, 373–387.
66. Almeida, A, Cobos, A, Tavares, I, Lima, D (2002) Brain afferents to the medullary dorsal reticular nucleus: a retrograde and anterograde tracing study in the rat. *Eur. J. Neurosci.* 16, 81–95.

67. Almeida, A, Tjølsen, A, Lima, D, Coimbra, A, Hole, K (1996) The medullary dorsal reticular nucleus facilitates acute nociception in the rat. *Brain Res. Bull.* 39, 7–15.
68. Almeida, A, Størkson, R, Lima, D, Hole, K, Tjølsen, A (1999) The medullary dorsal reticular nucleus facilitates pain behaviour induced by formalin in the rat. *Eur. J. Neurosci.* 11, 110–22.
69. Amorim, D, Viisanen, H, Wei, H, Almeida, A, Pertovaara, A, Pinto-Ribeiro, F (2015) Galanin-mediated behavioural hyperalgesia from the dorsomedial nucleus of the hypothalamus involves two independent descending pronociceptive pathways. *PLoS One* 10, e0142919.
70. Zhang, L, Zhang, Y, Zhao, ZQ (2005) Anterior cingulate cortex contributes to the descending facilitatory modulation of pain via dorsal reticular nucleus. *Eur. J. Neurosci.* 22, 1141–1148.
71. Bouhassira, D, Villanueva, L, Bing, Z, le Bars, D (1992) Involvement of the subnucleus reticularis dorsalis in diffuse noxious inhibitory controls in the rat. *Brain Res.* 595, 353–357.
72. Ossipov, MH, Dussor, GO, Porreca, F (2010) Central modulation of pain. *J. Clin. Invest.* 120, 3779–87.
73. Morgan, MM (1999) Paradoxical inhibition of nociceptive neurons in the dorsal horn of the rat spinal cord during a nociceptive hindlimb reflex. *Neuroscience* 88, 489–98.
74. Le Bars, D, Villanueva, L (1988) Electrophysiological evidence for the activation of descending inhibitory controls by nociceptive afferent pathways. *Prog. Brain Res.* 77, 275–99.
75. Fishman, S, Ballantyne, J, Rathmell, JP, Bonica, JJ (Lippincott, Williams & Wilkins, 2010). *Bonica's Management of Pain.*
76. Merskey, H, Bogduk, N, Sloan, PA (1995) Classification of Chronic Pain, 2nd ed. *Can. J. Anaesth.* 42, 753.
77. Goldberg, DS, McGee, SJ (2011) Pain as a global public health priority. *BMC Public Health* 11, 770.
78. Viallon, A, Marjollet, O, Guyomarch, P, Robert, F, Berger, C, Guyomarch, S, Navez, ML, Bertrand, J-C (2007) Analgesic efficacy of orodispersible paracetamol in patients admitted to the emergency department with an osteoarticular injury. *Eur. J. Emerg. Med.* 14, 337–42.
79. Buchner, M, Neubauer, E, Zahlten-Hinguranage, A, Schiltewolf, M (2007) The influence of

- the grade of chronicity on the outcome of multidisciplinary therapy for chronic low back pain. *Spine (Phila. Pa. 1976)*. 32, 3060–6.
80. Amorim, D, David-Pereira, A, Pertovaara, A, Almeida, A, Pinto-Ribeiro, F (2014) Amitriptyline reverses hyperalgesia and improves associated mood-like disorders in a model of experimental monoarthritis. *Behav. Brain Res.* 265, 12–21.
  81. Pais-Vieira, M, Aguiar, P, Lima, D, Galhardo, V (2012) Inflammatory pain disrupts the orbitofrontal neuronal activity and risk-assessment performance in a rodent decision-making task. *Pain* 153, 1625–35.
  82. Finnerup, NB, Attal, N, Haroutounian, S, McNicol, E, Baron, R, Dworkin, RH, Gilron, I, Haanpää, M, Hansson, P, Jensen, TS, Kamerman, PR, Lund, K, Moore, A, Raja, SN, Rice, ASC, Rowbotham, M, Sena, E, Siddall, P, Smith, BH, Wallace, M (2015) Pharmacotherapy for neuropathic pain in adults: a systematic review and meta-analysis. *Lancet. Neurol.* 14, 162–73.
  83. Schaible, HG (Springer Berlin Heidelberg, 2007). in *Analgesia* (ed. Stein, C.) 3–28.
  84. Treede, R, Rief, W, Barke, A, Aziz, Q, Bennett, MI, Benoliel, R, Cohen, M, Evers, S, Finnerup, NB, First, MB, Giamberardino, MA, Kaasa, S, Kosek, E, Lavand'homme, P, Nicholas, M, Perrot, S, Scholz, J, Schug, S, Smith, BH, Svensson, P, Vlaeyen, JWS, Wang, S (2015) A classification of chronic pain for ICD-11. *Pain* 156, 1003–7.
  85. Martel-Pelletier, J, Pelletier, JP (Research Signpost, 2000). *Understanding Osteoarthritis from Bench to Bedside*.
  86. Cross, M, Smith, E, Hoy, D, Nolte, S, Ackerman, I, Fransen, M, Bridgett, L, Williams, S, Guillemin, F, Hill, CL, Laslett, LL, Jones, G, Cicuttini, F, Osborne, R, Vos, T, Buchbinder, R, Woolf, A, March, L (2014) The global burden of hip and knee osteoarthritis: estimates from the Global Burden of Disease 2010 study. *Ann. Rheum. Dis.* 73, 1323–1330.
  87. Zhang, Y, Jordan, JM (2010) Epidemiology of Osteoarthritis. *Clin. Geriatr. Med.* 26, 355–369.
  88. Neugebauer, V, Han, JS, Adwanikar, H, Fu, Y, Ji, G (2007) Techniques for assessing knee joint pain in arthritis. *Mol. Pain* 3, 8.
  89. Loeser, RF, Goldring, SR, Scanzello, CR, Goldring, MB (2012) Osteoarthritis: a disease of the joint as an organ. *Arthritis Rheum.* 64, 1697–707.
  90. Bijlsma, JWJ, Berenbaum, F, Lefeber, FPJG (2011) Osteoarthritis: an update with relevance for clinical practice. *Lancet* 377, 2115–26.

91. Berenbaum, F (2013) Osteoarthritis as an inflammatory disease (osteoarthritis is not osteoarthrosis!). *Osteoarthr. Cartil.* 21, 16–21.
92. Bondeson, J, Blom, AB, Wainwright, S, Hughes, C, Caterson, B, van den Berg, WB (2010) The role of synovial macrophages and macrophage-produced mediators in driving inflammatory and destructive responses in osteoarthritis. *Arthritis Rheum.* 62, 647–57.
93. Sherbourne, CD, Asch, SM, Shugarman, LR, Goebel, JR, Lanto, AB, Rubenstein, L V., Wen, L, Zubkoff, L, Lorenz, KA (2009) Early identification of co-occurring pain, depression and anxiety. *J. Gen. Intern. Med.* 24, 620–5.
94. Bair, MJ, Robinson, RL, Katon, W, Kroenke, K (2003) Depression and pain comorbidity. *Arch. Intern. Med.* 163, 2433.
95. Lampropoulou-Adamidou, K, Lelovas, P, Karadimas, E V., Liakou, C, Triantafillopoulos, IK, Dontas, I, Papaioannou, NA (2014) Useful animal models for the research of osteoarthritis. *Eur. J. Orthop. Surg. Traumatol.* 24, 263–71.
96. Mogil, JS (2009) Animal models of pain: progress and challenges. *Nat. Rev. Neurosci.* 10, 283–94.
97. Hunter, DJ, McDougall, JJ, Keefe, FJ (2008) The symptoms of osteoarthritis and the genesis of pain. *Rheum. Dis. Clin. North Am.* 34, 623–43.
98. La Porta, C, Bura, SA, Negrete, R, Maldonado, R (2014) Involvement of the endocannabinoid system in osteoarthritis pain. *Eur. J. Neurosci.* 39, 485–500.
99. Wang, T, Wen, C-Y, Yan, C-H, Lu, W-W, Chiu, K-Y (2013) Spatial and temporal changes of subchondral bone proceed to microscopic articular cartilage degeneration in guinea pigs with spontaneous osteoarthritis. *Osteoarthr. Cartil.* 21, 574–81.
100. Säämänen, AMK, Salminen, HJ, Dean, PB, De Crombrughe, B, Vuorio, EI, Metsäranta, MPH (2000) Osteoarthritis-like lesions in transgenic mice harboring a small deletion mutation in type II collagen gene. *Osteoarthr. Cartil.* 8, 248–257.
101. Longo, UG, Loppini, M, Fumo, C, Rizzello, G, Khan, WS, Maffulli, N, Denaro, V (2012) Osteoarthritis: new insights in animal models. *Open Orthop. J.* 6, 558–63.
102. Pomonis, JD, Boulet, JM, Gottshall, SL, Phillips, S, Sellers, R, Bunton, T, Walker, K (2005) Development and pharmacological characterization of a rat model of osteoarthritis pain. *Pain* 114, 339–46.
103. Fernihough, J, Gentry, C, Malcangio, M, Fox, A, Rediske, J, Pellas, T, Kidd, B, Bevan, S, Winter, J (2004) Pain related behaviour in two models of osteoarthritis in the rat knee. *Pain*

- 112, 83–93.
104. Adães, S, Mendonça, M, Santos, TN, Castro-Lopes, JM, Ferreira-Gomes, J, Neto, FL (2014) Intra-articular injection of collagenase in the knee of rats as an alternative model to study nociception associated with osteoarthritis. *Arthritis Res. Ther.* 16, R10.
  105. Marker, CL, Pomonis, JD (2012) The monosodium iodoacetate model of osteoarthritis pain in the rat. *Methods Mol. Biol.* 851, 239–248.
  106. Yu, YC, Koo, ST, Kim, CH, Lyu, Y, Grady, JJ, Chung, JM (2002) Two variables that can be used as pain indices in experimental animal models of arthritis. *J. Neurosci. Methods* 115, 107–13.
  107. Sluka, KA, Westlund, KN (1993) Behavioral and immunohistochemical changes in an experimental arthritis model in rats. *Pain* 55, 367–377.
  108. Leite-Almeida, H, Pinto-Ribeiro, F, Almeida, A (2015) Animal models for the study of comorbid pain and psychiatric disorders. *Mod. Trends Pharmacopsychiatry* 30, 1–21.
  109. Radhakrishnan, R, Moore, S a., Sluka, K a. (2003) Unilateral carrageenan injection into muscle or joint induces chronic bilateral hyperalgesia in rats. *Pain* 104, 567–577.
  110. Berge, O-G (Elsevier/Churchill Livingstone, 2013). in *Wall and Melzack's Textbook of Pain* (eds. Wall, P. D., McMahon, S. B. & Koltzenburg, M.) 170–181.
  111. Kellgren, JH, Samuel, EP (1950) The sensitivity and innervation of the articular capsule. *J. Bone Jt. Surgery. Br.* 32–B, 84–92.
  112. Schaible, H-G, Ebersberger, A, Von Banchet, GS (2002) Mechanisms of pain in arthritis. *Ann. N. Y. Acad. Sci.* 966, 343–354.
  113. Schaible, HG (Elsevier/Churchill Livingstone, 2013). in *Wall and Melzack's Textbook of Pain* (eds. Wall, P. D., McMahon, S. B. & Koltzenburg, M.) 609–619.
  114. Schaible, HG, Schmidt, RF (1985) Effects of an experimental arthritis on the sensory properties of fine articular afferent units. *J. Neurophysiol.* 54, 1109–1122.
  115. Schaible, HG, Schmidt, RF (1988) Time course of mechanosensitivity changes in articular afferents during a developing experimental arthritis. *J. Neurophysiol.* 60, 2180–2195.
  116. Coggeshall, RE, Hong, KA, Langford, LA, Schaible, HG, Schmidt, RF (1983) Discharge characteristics of fine medial articular afferents at rest and during passive movements of inflamed knee joints. *Brain Res.* 272, 185–8.
  117. Schaible, HG, Grubb, BD (1993) Afferent and spinal mechanisms of joint pain. *Pain* 55, 5–54.



118. Vanegas, H, Schaible, HG (2004) Descending control of persistent pain: Inhibitory or facilitatory? *Brain Res. Rev.* 46, 295–309.
119. Latremoliere, A, Woolf, CJ (2009) Central sensitization: a generator of pain hypersensitivity by central neural plasticity. *J. Pain* 10, 895–926.
120. Hoheisel, U, Koch, K, Mense, S (1994) Functional reorganization in the rat dorsal horn during an experimental myositis. *Pain* 59, 111–8.
121. Neugebauer, V, Schaible, HG (1990) Evidence for a central component in the sensitization of spinal neurons with joint input during development of acute arthritis in cat's knee. *J. Neurophysiol.* 64, 299–311.
122. Martindale, JC, Wilson, AW, Reeve, AJ, Chessell, IP, Headley, PM (2007) Chronic secondary hypersensitivity of dorsal horn neurones following inflammation of the knee joint. *Pain* 133, 79–86.
123. Sluka, KA, Westlund, KN (1993) An experimental arthritis model in rats: the effects of NMDA and non-NMDA antagonists on aspartate and glutamate release in the dorsal horn. *Neurosci. Lett.* 149, 99–102.
124. Schaible, HG, Jarrott, B, Hope, PJ, Duggan, AW (1990) Release of immunoreactive substance P in the spinal cord during development of acute arthritis in the knee joint of the cat: a study with antibody microprobes. *Brain Res.* 529, 214–23.
125. Hope, PJ, Jarrott, B, Schaible, HG, Clarke, RW, Duggan, AW (1990) Release and spread of immunoreactive neurokinin A in the cat spinal cord in a model of acute arthritis. *Brain Res.* 533, 292–9.
126. Schaible, HG, Freudenberger, U, Neugebauer, V, Stiller, RU (1994) Intraspinal release of immunoreactive calcitonin gene-related peptide during development of inflammation in the joint in vivo—a study with antibody microprobes in cat and rat. *Neuroscience* 62, 1293–305.
127. Woolf, CJ, Salter, MW (2000) Neuronal plasticity: increasing the gain in pain. *Science* 288, 1765–9.
128. Neugebauer, V, Lücke, T, Schaible, HG (1993) N-methyl-D-aspartate (NMDA) and non-NMDA receptor antagonists block the hyperexcitability of dorsal horn neurons during development of acute arthritis in rat's knee joint. *J. Neurophysiol.* 70, 1365–77.
129. Vanegas, H, Schaible, HG (2001) Prostaglandins and cyclooxygenases in the spinal cord. *Prog. Neurobiol.* 64, 327–63.

130. Hsieh, JC, Belfrage, M, Stone-Elander, S, Hansson, P, Ingvar, M (1995) Central representation of chronic ongoing neuropathic pain studied by positron emission tomography. *Pain* 63, 225–36.
131. Fukumoto, M, Ushida, T, Zinchuk, VS, Yamamoto, H, Yoshida, S (1999) Contralateral thalamic perfusion in patients with reflex sympathetic dystrophy syndrome. *Lancet* 354, 1790–1.
132. Tillisch, K, Mayer, EA, Labus, JS (2011) Quantitative meta-analysis identifies brain regions activated during rectal distension in irritable bowel syndrome. *Gastroenterology* 140, 91–100.
133. Dworkin, RH (2002) An overview of neuropathic pain: syndromes, symptoms, signs, and several mechanisms. *Clin. J. Pain* 18, 343–9.
134. Apkarian, AV, Baliki, MN, Geha, PY (2009) Towards a theory of chronic pain. *Prog. Neurobiol.* 87, 81–97.
135. Neugebauer, V, Galhardo, V, Maione, S, Mackey, SC (2009) Forebrain pain mechanisms. *Brain Res. Rev.* 60, 226–242.
136. Apkarian, VA, Hashmi, JA, Baliki, MN (2011) Pain and the brain: Specificity and plasticity of the brain in clinical chronic pain. *Pain* 152, S49–S64.
137. Baliki, MN, Chialvo, DR, Geha, PY, Levy, RM, Harden, RN, Parrish, TB, Apkarian, AV (2006) Chronic pain and the emotional brain: specific brain activity associated with spontaneous fluctuations of intensity of chronic back pain. *J. Neurosci.* 26, 12165–73.
138. Baliki, MN, Geha, PY, Fields, HL, Apkarian, AV (2010) Predicting value of pain and analgesia: nucleus accumbens response to noxious stimuli changes in the presence of chronic pain. *Neuron* 66, 149–60.
139. Braz, JM, Nassar, MA, Wood, JN, Basbaum, AI (2005) Parallel ‘pain’ pathways arise from subpopulations of primary afferent nociceptor. *Neuron* 47, 787–93.
140. Monconduit, L, Villanueva, L (2005) The lateral ventromedial thalamic nucleus spreads nociceptive signals from the whole body surface to layer I of the frontal cortex. *Eur. J. Neurosci.* 21, 3395–402.
141. Apkarian, AV, Sosa, Y, Sonty, S, Levy, RM, Harden, RN, Parrish, TB, Gitelman, DR (2004) Chronic back pain is associated with decreased prefrontal and thalamic gray matter density. *J. Neurosci.* 24, 10410–5.
142. Courtney, SM, Ungerleider, LG, Keil, K, Haxby, J V (1997) Transient and sustained activity

- in a distributed neural system for human working memory. *Nature* 386, 608–611.
143. Lorenz, J, Minoshima, S, Casey, KL (2003) Keeping pain out of mind: the role of the dorsolateral prefrontal cortex in pain modulation. *Brain* 126, 1079–91.
  144. Goel, V, Dolan, RJ (2003) Explaining modulation of reasoning by belief. *Cognition* 87, B11–22.
  145. Grachev, ID, Fredrickson, BE, Apkarian, A V (2000) Abnormal brain chemistry in chronic back pain: an in vivo proton magnetic resonance spectroscopy study. *Pain* 89, 7–18.
  146. Seifert, F, Bschorer, K, De Col, R, Filitz, J, Peltz, E, Koppert, W, Maihöfner, C (2009) Medial prefrontal cortex activity is predictive for hyperalgesia and pharmacological antihyperalgesia. *J. Neurosci.* 29, 6167–75.
  147. Bechara, A, Damasio, AR, Damasio, H, Anderson, SW (1994) Insensitivity to future consequences following damage to human prefrontal cortex. *Cognition* 50, 7–15.
  148. Apkarian, AV, Sosa, Y, Krauss, BR, Thomas, PS, Fredrickson, BE, Levy, RE, Harden, RN, Chialvo, DR (2004) Chronic pain patients are impaired on an emotional decision-making task. *Pain* 108, 129–136.
  149. Condés-Lara, M, Omaña Zapata, I, León-Olea, M, Sánchez-Alvarez, M (1989) Dorsal raphe and nociceptive stimulations evoke convergent responses on the thalamic centralis lateralis and medial prefrontal cortex neurons. *Brain Res.* 499, 145–52.
  150. Wise, SP (2008) Forward frontal fields: phylogeny and fundamental function. *Trends Neurosci.* 31, 599–608.
  151. Preuss, TM (1995) Do rats have prefrontal cortex? The rose-woolsey-akert program reconsidered. *J. Cogn. Neurosci.* 7, 1–24.
  152. Uylings, HBM, Groenewegen, HJ, Kolb, B (2003) Do rats have a prefrontal cortex? *Behav. Brain Res.* 146, 3–17.
  153. Leonard, CM (2016) Finding prefrontal cortex in the rat. *Brain Res.* 1645, 1–3.
  154. Pribram, KH, Wilson, WA, Connors, J (1962) Effects of lesions of the medial forebrain on alternation behavior of rhesus monkeys. *Exp. Neurol.* 6, 36–47.
  155. Calejesan, AA, Kim, SJ, Zhuo, M (2000) Descending facilitatory modulation of a behavioral nociceptive response by stimulation in the adult rat anterior cingulate cortex. *Eur. J. Pain* 4, 83–96.
  156. Yoon, T, Okada, J, Jung, MW, Kim, JJ (2008) Prefrontal cortex and hippocampus subserve different components of working memory in rats. *Learn. Mem.* 15, 97–105.

157. Birrell, JM, Brown, VJ (2000) Medial frontal cortex mediates perceptual attentional set shifting in the rat. *J. Neurosci.* 20, 4320–4.
158. Sawaguchi, T, Goldman-Rakic, PS (1994) The role of D1-dopamine receptor in working memory: local injections of dopamine antagonists into the prefrontal cortex of rhesus monkeys performing an oculomotor delayed-response task. *J. Neurophysiol.* 71, 515–28.
159. Kolb, B (1984) Functions of the frontal cortex of the rat: a comparative review. *Brain Res.* 320, 65–98.
160. Vertes, RP (2004) Differential projections of the infralimbic and prelimbic cortex in the rat. *Synapse* 51, 32–58.
161. Vertes, RP (2006) Interactions among the medial prefrontal cortex, hippocampus and midline thalamus in emotional and cognitive processing in the rat. *Neuroscience* 142, 1–20.
162. Zhang, R, Tomida, M, Katayama, Y, Kawakami, Y (2004) Response durations encode nociceptive stimulus intensity in the rat medial prefrontal cortex. *Neuroscience* 125, 777–785.
163. Cao, Z, Wu, X, Chen, S, Fan, J, Zhang, R, Owyang, C, Li, Y (2008) Anterior cingulate cortex modulates visceral pain as measured by visceromotor responses in viscerally hypersensitive rats. *Gastroenterology* 134, 535–43.
164. Li, X-Y, Ko, H-G, Chen, T, Descalzi, G, Koga, K, Wang, H, Kim, SS, Shang, Y, Kwak, C, Park, S-W, Shim, J, Lee, K, Collingridge, GL, Kaang, B-K, Zhuo, M (2010) Alleviating neuropathic pain hypersensitivity by inhibiting PKMzeta in the anterior cingulate cortex. *Science* 330, 1400–4.
165. Johansen, JP, Fields, HL, Manning, BH (2001) The affective component of pain in rodents: direct evidence for a contribution of the anterior cingulate cortex. *Proc. Natl. Acad. Sci. U. S. A.* 98, 8077–82.
166. Gao, Y-J, Ren, W-H, Zhang, Y-Q, Zhao, Z-Q (2004) Contributions of the anterior cingulate cortex and amygdala to pain- and fear-conditioned place avoidance in rats. *Pain* 110, 343–53.
167. Seminowicz, DA, Laferriere, AL, Millevamps, M, Yu, JSC,Coderre, TJ, Bushnell, MC (2009) MRI structural brain changes associated with sensory and emotional function in a rat model of long-term neuropathic pain. *Neuroimage* 47, 1007–14.
168. Pais-Vieira, M, Lima, D, Galhardo, V (2007) Orbitofrontal cortex lesions disrupt risk

- assessment in a novel serial decision-making task for rats. *Neuroscience* 145, 225–31.
169. Ji, G, Sun, H, Fu, Y, Li, Z, Pais-Vieira, M, Galhardo, V, Neugebauer, V (2010) Cognitive impairment in pain through amygdala-driven prefrontal cortical deactivation. *J. Neurosci.* 30, 5451–5464.
  170. Ohara, PT, Vit, J-P, Jasmin, L (2005) Cortical modulation of pain. *Cell. Mol. Life Sci.* 62, 44–52.
  171. Hardy, SG (1985) Analgesia elicited by prefrontal stimulation. *Brain Res.* 339, 281–4.
  172. Metz, AE, Yau, H-J, Centeno, MV, Apkarian, a V, Martina, M (2009) Morphological and functional reorganization of rat medial prefrontal cortex in neuropathic pain. *Proc. Natl. Acad. Sci. U. S. A.* 106, 2423–2428.
  173. Zhang, Z, Gadotti, VM, Chen, L, Souza, IA, Stemkowski, PL, Zamponi, GW (2015) Role of prelimbic GABAergic circuits in sensory and emotional aspects of neuropathic pain. *Cell Rep.* 12, 752–9.
  174. Ji, G, Neugebauer, V (2014) CB1 augments mGluR5 function in medial prefrontal cortical neurons to inhibit amygdala hyperactivity in an arthritis pain model. *Eur. J. Neurosci.* 39, 455–466.
  175. Ji, G, Neugebauer, V (2011) Pain-related deactivation of medial prefrontal cortical neurons involves mGluR1 and GABAA receptors. *J. Neurophysiol.* 106, 2642–2652.
  176. Kiritoshi, T, Ji, G, Neugebauer, V (2016) Rescue of impaired mGluR5-driven endocannabinoid signaling restores prefrontal cortical output to inhibit pain in arthritic rats. *J. Neurosci.* 36, 837–50.
  177. Wang, G-Q, Cen, C, Li, C, Cao, S, Wang, N, Zhou, Z, Liu, X-M, Xu, Y, Tian, N-X, Zhang, Y, Wang, J, Wang, L-P, Wang, Y (2015) Deactivation of excitatory neurons in the prelimbic cortex via Cdk5 promotes pain sensation and anxiety. *Nat. Commun.* 6, 7660.
  178. Jiang, ZC, Pan, Q, Zheng, C, Deng, XF, Wang, JY, Luo, F (2014) Inactivation of the prelimbic rather than infralimbic cortex impairs acquisition and expression of formalin-induced conditioned place avoidance. *Neurosci. Lett.* 569, 89–93.
  179. Millecamps, M, Centeno, M V., Berra, HH, Rudick, CN, Lavarello, S, Tkatch, T, Apkarian, VA (2007) d-Cycloserine reduces neuropathic pain behavior through limbic NMDA-mediated circuitry. *Pain* 132, 108–123.
  180. McNally, GP (1999) Pain facilitatory circuits in the mammalian central nervous system: their behavioral significance and role in morphine analgesic tolerance. *Neurosci. Biobehav.*

- Rev.* 23, 1059–78.
181. Bingel, U, Tracey, I (2008) Imaging CNS modulation of pain in humans. *Physiology (Bethesda)*. 23, 371–80.
  182. Sevcik, MA, Jonas, BM, Lindsay, TH, Halvorson, KG, Ghilardi, JR, Kuskowski, MA, Mukherjee, P, Maggio, JE, Mantyh, PW (2006) Endogenous opioids inhibit early-stage pancreatic pain in a mouse model of pancreatic cancer. *Gastroenterology* 131, 900–10.
  183. Zambreanu, L, Wise, RG, Brooks, JCW, Iannetti, GD, Tracey, I (2005) A role for the brainstem in central sensitisation in humans. Evidence from functional magnetic resonance imaging. *Pain* 114, 397–407.
  184. Mainero, C, Zhang, W-T, Kumar, A, Rosen, BR, Sorensen, AG (2007) Mapping the spinal and supraspinal pathways of dynamic mechanical allodynia in the human trigeminal system using cardiac-gated fMRI. *Neuroimage* 35, 1201–10.
  185. Porreca, F, Ossipov, MH, Gebhart, GF (2002) Chronic pain and medullary descending facilitation. *Trends Neurosci.* 25, 319–25.
  186. Gebhart, GF (2004) Descending modulation of pain. *Neurosci. Biobehav. Rev.* 27, 729–737.
  187. Ren, K, Dubner, R (1996) Enhanced descending modulation of nociception in rats with persistent hindpaw inflammation. *J. Neurophysiol.* 76, 3025 LP-3037.
  188. Schaible, HG, Neugebauer, V, Cervero, F, Schmidt, RF (1991) Changes in tonic descending inhibition of spinal neurons with articular input during the development of acute arthritis in the cat. *J. Neurophysiol.* 66, 1021 LP-1032.
  189. Wei, F, Dubner, R, Ren, K (1999) Nucleus reticularis gigantocellularis and nucleus raphe magnus in the brain stem exert opposite effects on behavioral hyperalgesia and spinal Fos protein expression after peripheral inflammation. *Pain* 80, 127–41.
  190. Basbaum, AI (Elsevier, 2008). *The senses: a comprehensive reference*.
  191. Tsuruoka, M, Willis, WD (1996) Bilateral lesions in the area of the nucleus locus coeruleus affect the development of hyperalgesia during carrageenan-induced inflammation. *Brain Res.* 726, 233–6.
  192. Urban, MO, Jiang, MC, Gebhart, GF (1996) Participation of central descending nociceptive facilitatory systems in secondary hyperalgesia produced by mustard oil. *Brain Res.* 737, 83–91.
  193. Kauppila, T, Kontinen, VK, Pertovaara, A (1998) Influence of spinalization on spinal

- withdrawal reflex responses varies depending on the submodality of the test stimulus and the experimental pathophysiological condition in the rat. *Brain Res.* 797, 234–242.
194. Herrero, JF, Cervero, F (1996) Supraspinal influences on the facilitation of rat nociceptive reflexes induced by carrageenan monoarthritis. *Neurosci. Lett.* 209, 21–24.
  195. Urban, MO, Coutinho, S V., Gebhart, GF (1999) Involvement of excitatory amino acid receptors and nitric oxide in the rostral ventromedial medulla in modulating secondary hyperalgesia produced by mustard oil. *Pain* 81, 45–55.
  196. Miki, K, Zhou, Q-Q, Guo, W, Guan, Y, Terayama, R, Dubner, R, Ren, K (2002) Changes in gene expression and neuronal phenotype in brain stem pain modulatory circuitry after inflammation. *J. Neurophysiol.* 87, 750–60.
  197. Guan, Y, Guo, W, Zou, S-P, Dubner, R, Ren, K (2003) Inflammation-induced upregulation of AMPA receptor subunit expression in brain stem pain modulatory circuitry. *Pain* 104, 401–13.
  198. Kincaid, W, Neubert, MJ, Xu, M, Kim, CJ, Heinricher, MM (2006) Role for medullary pain facilitating neurons in secondary thermal hyperalgesia. *J. Neurophysiol.* 95, 33–41.
  199. Pinto-Ribeiro, F, Ansah, OB, Almeida, A, Pertovaara, A (2008) Influence of arthritis on descending modulation of nociception from the paraventricular nucleus of the hypothalamus. *Brain Res.* 1197, 63–75.
  200. Suzuki, R, Rygh, LJ, Dickenson, AH (2004) Bad news from the brain: Descending 5-HT pathways that control spinal pain processing. *Trends Pharmacol. Sci.* 25, 613–617.
  201. Schadrack, J, Neto, FL, Ableitner, A, Castro-Lopes, JM, Willoch, F, Bartenstein, P, Zieglgänsberger, W, Tölle, TR (1999) Metabolic activity changes in the rat spinal cord during adjuvant monoarthritis. *Neuroscience* 94, 595–605.
  202. Lantéri-Minet, M, Weil-Fugazza, J, de Pommery, J, Menétrey, D (1994) Hindbrain structures involved in pain processing as revealed by the expression of c-Fos and other immediate early gene proteins. *Neuroscience* 58, 287–98.
  203. Dugast, C, Almeida, A, Lima, D (2003) The medullary dorsal reticular nucleus enhances the responsiveness of spinal nociceptive neurons to peripheral stimulation in the rat. *Eur. J. Neurosci.* 18, 580–588.
  204. Sotgiu, ML, Valente, M, Storchi, R, Caramenti, G, Mario Biella, GE (2008) Contribution by DRt descending facilitatory pathways to maintenance of spinal neuron sensitization in rats. *Brain Res.* 1188, 69–75.

205. Ambriz-Tututi, M, Palomero-Rivero, M, Ramirez-López, F, Millán-Aldaco, D, Drucker-Colín, AR (2013) Role of glutamate receptors in the dorsal reticular nucleus in formalin-induced secondary allodynia. *Eur. J. Neurosci.* 38, 3008–3017.
206. Martins, I, de Vries, MG, Teixeira-Pinto, A, Fadel, J, Wilson, SP, Westerink, BHC, Tavares, I (2013) Noradrenaline increases pain facilitation from the brain during inflammatory pain. *Neuropharmacology* 71, 299–307.
207. Martins, I, Costa-Araújo, S, Fadel, J, Wilson, SP, Lima, D, Tavares, I (2010) Reversal of neuropathic pain by HSV-1-mediated decrease of noradrenaline in a pain facilitatory area of the brain. *Pain* 151, 137–45.
208. Pinto, M, Sousa, M, Lima, D, Tavares, I (2008) Participation of  $\mu$ -opioid, GABA B , and NK1 receptors of major pain control medullary areas in pathways targeting the rat spinal cord: Implications for descending modulation of nociceptive transmission. *J. Comp. Neurol.* 510, 175–187.
209. Neto, FL, Carvalhosa, AR, Ferreira-Gomes, J, Reguenga, C, Castro-Lopes, JM (2008) Delta opioid receptor mRNA expression is changed in the thalamus and brainstem of monoarthritic rats. *J. Chem. Neuroanat.* 36, 122–7.
210. Martins, I, Carvalho, P, de Vries, MG, Teixeira-Pinto, A, Wilson, SP, Westerink, BHC, Tavares, I (2015) GABA acting on GABAB receptors located in a medullary pain facilitatory area enhances nociceptive behaviors evoked by intraplantar formalin injection. *Pain* 156, 1555–65.
211. Gereau, RW, Swanson, GT, Hampson, DR, Rose, EM, Antflick, JE (Humana Press, 2008). *The Glutamate Receptors.*
212. Ji, R-R, Kohno, T, Moore, KA, Woolf, CJ (2003) Central sensitization and LTP: do pain and memory share similar mechanisms? *Trends Neurosci.* 26, 696–705.
213. South, SM, Kohno, T, Kaspar, BK, Hegarty, D, Vissel, B, Drake, CT, Ohata, M, Jenab, S, Sailer, AW, Malkmus, S, Masuyama, T, Horner, P, Bogulavsky, J, Gage, FH, Yaksh, TL, Woolf, CJ, Heinemann, SF, Inturrisi, CE (2003) A conditional deletion of the NR1 subunit of the NMDA receptor in adult spinal cord dorsal horn reduces NMDA currents and injury-induced pain. *J. Neurosci.* 23, 5031–40.
214. Basbaum, AI, Bushnell, MC (Academic, 2008). *Science of Pain.*
215. Quartaroli, M, Fasdelli, N, Bettelini, L, Maraia, G, Corsi, M (2001) GV196771A, an NMDA receptor/glycine site antagonist, attenuates mechanical allodynia in neuropathic rats and



- reduces tolerance induced by morphine in mice. *Eur. J. Pharmacol.* 430, 219–27.
216. Efficacy and Safety of GLYX-13 in Subjects With Inadequate/Partial Response to Antidepressants. Available at: <https://clinicaltrials.gov/ct2/show/study/NCT01684163>. (Accessed: 14th February 2017).
  217. Nicoletti, F, Bockaert, J, Collingridge, GL, Conn, PJ, Ferraguti, F, Schoepp, DD, Wroblewski, JT, Pin, JP (2011) Metabotropic glutamate receptors: from the workbench to the bedside. *Neuropharmacology* 60, 1017–41.
  218. Cartmell, J, Schoepp, DD (2000) Regulation of neurotransmitter release by metabotropic glutamate receptors. *J. Neurochem.* 75, 889–907.
  219. Saugstad, JA, Ingram, SL (Humana Press, 2008). in *The Glutamate Receptors* (eds. Gereau, R. W. & Swanson, G. T.) 387–464.
  220. Ferraguti, F, Shigemoto, R (2006) Metabotropic glutamate receptors. *Cell Tissue Res.* 326, 483–504.
  221. Romano, C, Sesma, MA, McDonald, CT, O'Malley, K, Van den Pol, AN, Olney, JW (1995) Distribution of metabotropic glutamate receptor mGluR5 immunoreactivity in rat brain. *J. Comp. Neurol.* 355, 455–469.
  222. Ferraguti, F, Crepaldi, L, Nicoletti, F (2008) Metabotropic glutamate 1 receptor: current concepts and perspectives. *Pharmacol. Rev.* 60, 536–81.
  223. Goudet, C, Magnaghi, V, Landry, M, Nagy, F, Gereau, RW, Pin, J-P (2009) Metabotropic receptors for glutamate and GABA in pain. *Brain Res. Rev.* 60, 43–56.
  224. Gereau, RW, Conn, PJ (1995) Multiple presynaptic metabotropic glutamate receptors modulate excitatory and inhibitory synaptic transmission in hippocampal area CA1. *J. Neurosci.* 15, 6879–89.
  225. Vincent, K, Cornea, VM, Jong, Y-JI, Laferrière, A, Kumar, N, Mickeviciute, A, Fung, JST, Bandegi, P, Ribeiro-da-Silva, A, O'Malley, KL, Coderre, TJ (2016) Intracellular mGluR5 plays a critical role in neuropathic pain. *Nat. Commun.* 7, 10604.
  226. Aronica, E, van Vliet, E a, Mayboroda, O a, Troost, D, da Silva, FH, Gorter, J a (2000) Upregulation of metabotropic glutamate receptor subtype mGluR3 and mGluR5 in reactive astrocytes in a rat model of mesial temporal lobe epilepsy. *Eur. J. Neurosci.* 12, 2333–44.
  227. van den Pol, AN, Romano, C, Ghosh, P (1995) Metabotropic glutamate receptor mGluR5 subcellular distribution and developmental expression in hypothalamus. *J. Comp. Neurol.* 362, 134–50.

228. Panatier, A, Robitaille, R (2016) Astrocytic mGluR5 and the tripartite synapse. *Neuroscience* 323, 29–34.
229. Johnson, MP, Schoepp, DD (Humana Press, 2008). in *The Glutamate Receptors* (eds. Gereau, R. W. & Swanson, G. T.) 465–488.
230. Nakanishi, S, Nakajima, Y, Masu, M, Ueda, Y, Nakahara, K, Watanabe, D, Yamaguchi, S, Kawabata, S, Okada, M (1998) Glutamate receptors: brain function and signal transduction. *Brain Res. Rev.* 26, 230–5.
231. Neugebauer, V (Humana Press, 2008). in *The Glutamate Receptors* (eds. Gereau, R. W. & Swanson, G. T.) 489–508.
232. Shigemoto, R, Kinoshita, A, Wada, E, Nomura, S, Ohishi, H, Takada, M, Flor, PJ, Neki, A, Abe, T, Nakanishi, S, Mizuno, N (1997) Differential presynaptic localization of metabotropic glutamate receptor subtypes in the rat hippocampus. *J. Neurosci.* 17, 7503–22.
233. Corti, C, Aldegheri, L, Somogyi, P, Ferraguti, F (2002) Distribution and synaptic localisation of the metabotropic glutamate receptor 4 (mGluR4) in the rodent CNS. *Neuroscience* 110, 403–20.
234. Bradley, SR, Rees, HD, Yi, H, Levey, AI, Conn, PJ (1998) Distribution and developmental regulation of metabotropic glutamate receptor 7a in rat brain. *J. Neurochem.* 71, 636–45.
235. Iacovelli, L, Bruno, V, Salvatore, L, Melchiorri, D, Gradini, R, Caricasole, A, Barletta, E, De Blasi, A, Nicoletti, F (2002) Native group-III metabotropic glutamate receptors are coupled to the mitogen-activated protein kinase/phosphatidylinositol-3-kinase pathways. *J. Neurochem.* 82, 216–23.
236. Chiechio, S, Nicoletti, F (2012) Metabotropic glutamate receptors and the control of chronic pain. *Curr. Opin. Pharmacol.* 12, 28–34.
237. Bhave, G, Karim, F, Carlton, SM, Gereau, RW (2001) Peripheral group I metabotropic glutamate receptors modulate nociception in mice. *Nat. Neurosci.* 4, 417–23.
238. Dogrul, A, Ossipov, MH, Lai, J, Malan, TP, Porreca, F (2000) Peripheral and spinal antihyperalgesic activity of SIB-1757, a metabotropic glutamate receptor (mGluR(5)) antagonist, in experimental neuropathic pain in rats. *Neurosci. Lett.* 292, 115–8.
239. Masuoka, T, Nakamura, T, Kudo, M, Yoshida, J, Takaoka, Y, Kato, N, Ishibashi, T, Imaizumi, N, Nishio, M (2015) Biphasic modulation by mGlu5 receptors of TRPV1-mediated intracellular calcium elevation in sensory neurons contributes to heat sensitivity. *Br. J. Pharmacol.* 172, 1020–33.

240. Hu, H-J, Bhave, G, Gereau, RW (2002) Prostaglandin and protein kinase A-dependent modulation of vanilloid receptor function by metabotropic glutamate receptor 5: potential mechanism for thermal hyperalgesia. *J. Neurosci.* 22, 7444–52.
241. Karim, F, Wang, CC, Gereau, RW (2001) Metabotropic glutamate receptor subtypes 1 and 5 are activators of extracellular signal-regulated kinase signaling required for inflammatory pain in mice. *J. Neurosci.* 21, 3771–9.
242. Hu, H-J, Gereau, RW (2011) Metabotropic glutamate receptor 5 regulates excitability and Kv4.2-containing K<sup>+</sup> channels primarily in excitatory neurons of the spinal dorsal horn. *J. Neurophysiol.* 105, 3010–21.
243. Lax, NC, George, DC, Ignatz, C, Kolber, BJ (2014) The mGluR5 antagonist fenobam induces analgesic conditioned place preference in mice with spared nerve injury. *PLoS One* 9, e103524.
244. Bordi, F, Quartaroli, M (2000) Modulation of nociceptive transmission by NMDA/glycine site receptor in the ventroposterolateral nucleus of the thalamus. *Pain* 84, 213–24.
245. Salt, TE, Binns, KE (2000) Contributions of mGlu1 and mGlu5 receptors to interactions with N-methyl-D-aspartate receptor-mediated responses and nociceptive sensory responses of rat thalamic neurons. *Neuroscience* 100, 375–80.
246. Salt, TE, Jones, HE, Copeland, CS, Sillito, AM (2014) Function of mGlu1 receptors in the modulation of nociceptive processing in the thalamus. *Neuropharmacology* 79, 405–411.
247. Li, W, Neugebauer, V (2004) Differential roles of mGluR1 and mGluR5 in brief and prolonged nociceptive processing in central amygdala neurons. *J. Neurophysiol.* 91, 13–24.
248. Ren, W, Neugebauer, V (2010) Pain-related increase of excitatory transmission and decrease of inhibitory transmission in the central nucleus of the amygdala are mediated by mGluR1. *Mol. Pain* 6, 93.
249. Neugebauer, V, Li, W, Bird, GC, Bhave, G, Gereau, RW (2003) Synaptic plasticity in the amygdala in a model of arthritic pain: differential roles of metabotropic glutamate receptors 1 and 5. *J. Neurosci.* 23, 52–63.
250. Luongo, L, De Novellis, V, Gatta, L, Palazzo, E, Vita, D, Guida, F, Giordano, C, Siniscalco, D, Marabese, I, De Chiaro, M, Boccella, S, Rossi, F, Maione, S (2013) Role of metabotropic glutamate receptor 1 in the basolateral amygdala-driven prefrontal cortical deactivation in inflammatory pain in the rat. *Neuropharmacology* 66, 317–329.

251. Palazzo, E, Marabese, I, De Novellis, V, Oliva, P, Rossi, F, Berrino, L, Rossi, FS, Maione, S (2001) Metabotropic and NMDA glutamate receptors participate in the cannabinoid-induced antinociception. *Neuropharmacology* 40, 319–326.
252. Maione, S, Oliva, P, Marabese, I, Palazzo, E, Rossi, F, Berrino, L, Filippelli, A (2000) Periaqueductal gray matter metabotropic glutamate receptors modulate formalin-induced nociception. *Pain* 85, 183–9.
253. de Novellis, V, Mariani, L, Palazzo, E, Vita, D, Marabese, I, Scafuro, M, Rossi, F, Maione, S (2005) Periaqueductal grey CB1 cannabinoid and metabotropic glutamate subtype 5 receptors modulate changes in rostral ventromedial medulla neuronal activities induced by subcutaneous formalin in the rat. *Neuroscience* 134, 269–81.
254. Yang, D, Gereau, RW (2003) Peripheral group II metabotropic glutamate receptors mediate endogenous anti-allodynia in inflammation. *Pain* 106, 411–7.
255. Carlton, SM, Du, J, Zhou, S (2009) Group II metabotropic glutamate receptor activation on peripheral nociceptors modulates TRPV1 function. *Brain Res.* 1248, 86–95.
256. Yang, D, Gereau, RW (2004) Group II metabotropic glutamate receptors inhibit cAMP-dependent protein kinase-mediated enhancement of tetrodotoxin-resistant sodium currents in mouse dorsal root ganglion neurons. *Neurosci. Lett.* 357, 159–162.
257. Gerber, G, Zhong, J, Youn, D, Randic, M (2000) Group II and group III metabotropic glutamate receptor agonists depress synaptic transmission in the rat spinal cord dorsal horn. *Neuroscience* 100, 393–406.
258. Valerio, A, Paterlini, M, Boifava, M, Memo, M, Spano, P (1997) Metabotropic glutamate receptor mRNA expression in rat spinal cord. *Neuroreport* 8, 2695–2699.
259. Wang, H, Jiang, W, Yang, R, Li, Y (2011) Spinal metabotropic glutamate receptor 4 is involved in neuropathic pain. *Neuroreport* 22, 244–8.
260. Dolan, S, Gunn, MD, Biddlestone, L, Nolan, AM (2009) The selective metabotropic glutamate receptor 7 allosteric agonist AMN082 inhibits inflammatory pain-induced and incision-induced hypersensitivity in rat. *Behav. Pharmacol.* 20, 596–604.
261. Kiritoshi, T, Neugebauer, V (2015) Group II mGluRs modulate baseline and arthritis pain-related synaptic transmission in the rat medial prefrontal cortex. *Neuropharmacology* 95, 388–94.
262. Li, W, Neugebauer, V (2006) Differential changes of group II and group III mGluR function in central amygdala neurons in a model of arthritic pain. *J. Neurophysiol.* 96, 1803–15.

263. Palazzo, E, Marabese, I, Luongo, L, Boccella, S, Bellini, G, Giordano, ME, Rossi, F, Scafuro, M, Novellis, V de, Maione, S (2013) Effects of a metabotropic glutamate receptor subtype 7 negative allosteric modulator in the periaqueductal grey on pain responses and rostral ventromedial medulla cell activity in rat. *Mol. Pain* 9, 44.
264. Palazzo, E, Fu, Y, Ji, G, Maione, S, Neugebauer, V (2008) Group III mGluR7 and mGluR8 in the amygdala differentially modulate nocifensive and affective pain behaviors. *Neuropharmacology* 55, 537–45.
265. Marabese, I, Rossi, F, Palazzo, E, de Novellis, V, Starowicz, K, Cristino, L, Vita, D, Gatta, L, Guida, F, Di Marzo, V, Rossi, F, Maione, S (2007) Periaqueductal gray metabotropic glutamate receptor subtype 7 and 8 mediate opposite effects on amino acid release, rostral ventromedial medulla cell activities, and thermal nociception. *J. Neurophysiol.* 98, 43–53.
266. Palazzo, E, Marabese, I, Soukupova, M, Luongo, L, Boccella, S, Giordano, C, de Novellis, V, Rossi, F, Maione, S (2011) Metabotropic glutamate receptor subtype 8 in the amygdala modulates thermal threshold, neurotransmitter release, and rostral ventromedial medulla cell activity in inflammatory pain. *J. Neurosci.* 31, 4687–97.
267. Chiang, CY, Sessle, BJ, Dostrovsky, JO (2012) Role of astrocytes in pain. *Neurochem. Res.* 37, 2419–2431.
268. Ren, K, Dubner, R (2008) Neuron–glia crosstalk gets serious: role in pain hypersensitivity. *Curr. Opin. Anaesthesiol.* 21, 570–579.
269. Dheen, ST, Kaur, C, Ling, E-A (2007) Microglial activation and its implications in the brain diseases. *Curr. Med. Chem.* 14, 1189–97.
270. Kaur, C, Ling, EA (1991) Study of the transformation of amoeboid microglial cells into microglia labelled with the isolectin Griffonia simplicifolia in postnatal rats. *Acta Anat. (Basel)*. 142, 118–25.
271. Ling, EA, Ng, YK, Wu, CH, Kaur, C (2001) Microglia: its development and role as a neuropathology sensor. *Prog. Brain Res.* 132, 61–79.
272. Verkhratsky, A, Butt, A (John Wiley & Sons, Ltd, 2013). *Glial Physiology and Pathophysiology*.
273. Nakamura, Y (2002) Regulating factors for microglial activation. *Biol. Pharm. Bull.* 25, 945–53.
274. Perry, VH (2004) The influence of systemic inflammation on inflammation in the brain: implications for chronic neurodegenerative disease. *Brain. Behav. Immun.* 18, 407–13.

275. Banati, RB, Gehrmann, J, Schubert, P, Kreutzberg, GW (1993) Cytotoxicity of microglia. *Glia* 7, 111–8.
276. Colton, CA (2009) Heterogeneity of microglial activation in the innate immune response in the brain. *J. Neuroimmune Pharmacol.* 4, 399–418.
277. Block, ML, Zecca, L, Hong, J-S (2007) Microglia-mediated neurotoxicity: uncovering the molecular mechanisms. *Nat. Rev. Neurosci.* 8, 57–69.
278. Le, W, Rowe, D, Xie, W, Ortiz, I, He, Y, Appel, SH (2001) Microglial activation and dopaminergic cell injury: an in vitro model relevant to Parkinson's disease. *J. Neurosci.* 21, 8447–55.
279. Gehrmann, J, Matsumoto, Y, Kreutzberg, GW (1995) Microglia: intrinsic immuneffector cell of the brain. *Brain Res. Rev.* 20, 269–87.
280. Tang, Y, Le, W (2016) Differential roles of M1 and M2 microglia in neurodegenerative diseases. *Mol. Neurobiol.* 53, 1181–94.
281. Glass, CK, Saijo, K, Winner, B, Marchetto, MC, Gage, FH (2010) Mechanisms underlying inflammation in neurodegeneration. *Cell* 140, 918–34.
282. Block, ML, Hong, J-S (2005) Microglia and inflammation-mediated neurodegeneration: multiple triggers with a common mechanism. *Prog. Neurobiol.* 76, 77–98.
283. Fu, KY, Light, AR, Maixner, W (2000) Relationship between nociceptor activity, peripheral edema, spinal microglial activation and long-term hyperalgesia induced by formalin. *Neuroscience* 101, 1127–35.
284. Sweitzer, SM, Colburn, RW, Rutkowski, M, DeLeo, JA (1999) Acute peripheral inflammation induces moderate glial activation and spinal IL-1beta expression that correlates with pain behavior in the rat. *Brain Res.* 829, 209–21.
285. Clark, AK, Gentry, C, Bradbury, EJ, McMahon, SB, Malcangio, M (2007) Role of spinal microglia in rat models of peripheral nerve injury and inflammation. *Eur. J. Pain* 11, 223–30.
286. Hua, X-Y, Svensson, CI, Matsui, T, Fitzsimmons, B, Yaksh, TL, Webb, M (2005) Intrathecal minocycline attenuates peripheral inflammation-induced hyperalgesia by inhibiting p38 MAPK in spinal microglia. *Eur. J. Neurosci.* 22, 2431–40.
287. Echeverry, S, Shi, XQ, Zhang, J (2008) Characterization of cell proliferation in rat spinal cord following peripheral nerve injury and the relationship with neuropathic pain. *Pain* 135, 37–47.

288. Calvo, M, Bennett, DLH (2012) The mechanisms of microgliosis and pain following peripheral nerve injury. *Exp. Neurol.* 234, 271–82.
289. Beggs, S, Salter, MW (2007) Stereological and somatotopic analysis of the spinal microglial response to peripheral nerve injury. *Brain. Behav. Immun.* 21, 624–633.
290. Daulhac, L, Mallet, C, Courteix, C, Etienne, M, Duroux, E, Privat, A, Eschalier, A, Fialip, J (2006) Diabetes-induced mechanical hyperalgesia involves spinal mitogen-activated protein kinase activation in neurons and microglia via N-methyl-D-aspartate-dependent mechanisms. *Mol. Pharmacol.* 70, 1246–54.
291. Zhou, D, Chen, M-L, Zhang, Y-Q, Zhao, Z-Q (2010) Involvement of spinal microglial P2X7 receptor in generation of tolerance to morphine analgesia in rats. *J. Neurosci.* 30, 8042–7.
292. Sun, S, Cao, H, Han, M, Li, T-T, Pan, H-L, Zhao, Z-Q, Zhang, Y-Q (2007) New evidence for the involvement of spinal fractalkine receptor in pain facilitation and spinal glial activation in rat model of monoarthritis. *Pain* 129, 64–75.
293. Molander, C, Hongpaisan, J, Svensson, M, Aldskogius, H (1997) Glial cell reactions in the spinal cord after sensory nerve stimulation are associated with axonal injury. *Brain Res.* 747, 122–9.
294. Ji, R-R, Berta, T, Nedergaard, M (2013) Glia and pain: is chronic pain a gliopathy? *Pain* 154, S10-28.
295. Hathway, GJ, Vega-Avelaira, D, Moss, A, Ingram, R, Fitzgerald, M (2009) Brief, low frequency stimulation of rat peripheral C-fibres evokes prolonged microglial-induced central sensitization in adults but not in neonates. *Pain* 144, 110–8.
296. Hamilton, NB, Attwell, D (2010) Do astrocytes really exocytose neurotransmitters? *Nat. Rev. Neurosci.* 11, 227–38.
297. Calvo, M, Zhu, N, Tsantoulas, C, Ma, Z, Grist, J, Loeb, JA, Bennett, DLH (2010) Neuregulin-ErbB signaling promotes microglial proliferation and chemotaxis contributing to microgliosis and pain after peripheral nerve injury. *J. Neurosci.* 30, 5437–50.
298. Trang, T, Beggs, S, Wan, X, Salter, MW (2009) P2X4-receptor-mediated synthesis and release of brain-derived neurotrophic factor in microglia is dependent on calcium and p38-mitogen-activated protein kinase activation. *J. Neurosci.* 29, 3518–28.
299. Clark, AK, Staniland, AA, Marchand, F, Kaan, TKY, McMahan, SB, Malcangio, M (2010) P2X7-dependent release of interleukin-1beta and nociception in the spinal cord following

- lipopolysaccharide. *J. Neurosci.* 30, 573–82.
300. Clark, AK, Yip, PK, Malcangio, M (2009) The liberation of fractalkine in the dorsal horn requires microglial cathepsin S. *J. Neurosci.* 29, 6945–54.
301. Clark, AK, D'Aquisto, F, Gentry, C, Marchand, F, McMahon, SB, Malcangio, M (2006) Rapid co-release of interleukin 1beta and caspase 1 in spinal cord inflammation. *J. Neurochem.* 99, 868–80.
302. Johnston, IN, Milligan, ED, Wieseler-Frank, J, Frank, MG, Zapata, V, Campisi, J, Langer, S, Martin, D, Green, P, Fleshner, M, Leinwand, L, Maier, SF, Watkins, LR (2004) A role for proinflammatory cytokines and fractalkine in analgesia, tolerance, and subsequent pain facilitation induced by chronic intrathecal morphine. *J. Neurosci.* 24, 7353–65.
303. Guo, W, Wang, H, Watanabe, M, Shimizu, K, Zou, S, LaGraize, SC, Wei, F, Dubner, R, Ren, K (2007) Glial-cytokine-neuronal interactions underlying the mechanisms of persistent pain. *J. Neurosci.* 27, 6006–18.
304. Coull, J a M, Beggs, S, Boudreau, D, Boivin, D, Tsuda, M, Inoue, K, Gravel, C, Salter, MW, De Koninck, Y (2005) BDNF from microglia causes the shift in neuronal anion gradient underlying neuropathic pain. *Nature* 438, 1017–21.
305. Ren, K, Dubner, R (2010) Interactions between the immune and nervous systems in pain. *Nat. Med.* 16, 1267–76.
306. Suter, MR, Wen, Y-R, Decosterd, I, Ji, R-R (2007) Do glial cells control pain? *Neuron Glia Biol.* 3, 255–68.
307. Raghavendra, V, Tanga, F, DeLeo, JA (2003) Inhibition of microglial activation attenuates the development but not existing hypersensitivity in a rat model of neuropathy. *J. Pharmacol. Exp. Ther.* 306, 624–630.
308. Cui, Y, Liao, XX, Liu, W, Guo, RX, Wu, ZZ, Zhao, CM, Chen, PX, Feng, JQ (2008) A novel role of minocycline: Attenuating morphine antinociceptive tolerance by inhibition of p38 MAPK in the activated spinal microglia. *Brain. Behav. Immun.* 22, 114–123.
309. Miyoshi, K, Obata, K, Kondo, T, Okamura, H, Noguchi, K (2008) Interleukin-18-mediated microglia/astrocyte interaction in the spinal cord enhances neuropathic pain processing after nerve injury. *J. Neurosci.* 28, 12775–87.
310. Gao, Y-J, Xu, Z-Z, Liu, Y-C, Wen, Y-R, Decosterd, I, Ji, R-R (2010) The c-Jun N-terminal kinase 1 (JNK1) in spinal astrocytes is required for the maintenance of bilateral mechanical allodynia under a persistent inflammatory pain condition. *Pain* 148, 309–19.



311. Gao, Y-J, Zhang, L, Samad, OA, Suter, MR, Yasuhiko, K, Xu, Z-Z, Park, J-Y, Lind, A-L, Ma, Q, Ji, R-R (2009) JNK-induced MCP-1 production in spinal cord astrocytes contributes to central sensitization and neuropathic pain. *J. Neurosci.* 29, 4096–108.
312. Kawasaki, Y, Xu, Z-Z, Wang, X, Park, JY, Zhuang, Z-Y, Tan, P-H, Gao, Y-J, Roy, K, Corfas, G, Lo, EH, Ji, R-R (2008) Distinct roles of matrix metalloproteases in the early- and late-phase development of neuropathic pain. *Nat. Med.* 14, 331–336.
313. Kim, D, Figueroa, KW, Li, K, Boroujerdi, A, Yolo, T, Luo, DZ (2009) Profiling of dynamically changed gene expression in dorsal root ganglia post peripheral nerve injury and a critical role of injury-induced glial fibrillary acetic protein in maintenance of pain behaviors. *Pain* 143, 114–122.
314. Choi, BH, Lapham, LW (1978) Radial glia in the human fetal cerebrum: a combined Golgi, immunofluorescent and electron microscopic study. *Brain Res.* 148, 295–311.
315. Misson, JP, Edwards, MA, Yamamoto, M, Caviness, VS (1988) Identification of radial glial cells within the developing murine central nervous system: studies based upon a new immunohistochemical marker. *Brain Res. Dev. Brain Res.* 44, 95–108.
316. Zerlin, M, Levison, SW, Goldman, JE (1995) Early patterns of migration, morphogenesis, and intermediate filament expression of subventricular zone cells in the postnatal rat forebrain. *J. Neurosci.* 15, 7238–49.
317. Bushong, E a, Martone, ME, Jones, YZ, Ellisman, MH (2002) Protoplasmic astrocytes in CA1 stratum radiatum occupy separate anatomical domains. *J. Neurosci.* 22, 183–92.
318. Halassa, MM, Fellin, T, Haydon, PG (2007) The tripartite synapse: roles for gliotransmission in health and disease. *Trends Mol. Med.* 13, 54–63.
319. Hansen, RR, Malcangio, M (2013) Astrocytes-multitaskers in chronic pain. *Eur. J. Pharmacol.* 716, 120–8.
320. Khakh, BS, Sofroniew, M V (2015) Diversity of astrocyte functions and phenotypes in neural circuits. *Nat. Neurosci.* 18, 942–52.
321. Verkhratsky, A, Orkand, RK, Kettenmann, H (1998) Glial calcium: homeostasis and signaling function. *Physiol. Rev.* 78, 99–141.
322. Verkhratsky, A (2010) Physiology of neuronal-glia networking. *Neurochem. Int.* 57, 332–43.
323. Khakh, BS, McCarthy, KD (2015) Astrocyte calcium signaling: from observations to functions and the challenges therein. *Cold Spring Harb. Perspect. Biol.* 7, a020404.

324. Bazargani, N, Attwell, D (2016) Astrocyte calcium signaling: the third wave. *Nat. Neurosci.* 19, 182–9.
325. Shigetomi, E, Patel, S, Khakh, BS (2016) Probing the complexities of astrocyte calcium signaling. *Trends Cell Biol.* 26, 300–12.
326. Petravicz, J, Fiacco, TA, McCarthy, KD (2008) Loss of IP3 receptor-dependent Ca<sup>2+</sup> increases in hippocampal astrocytes does not affect baseline CA1 pyramidal neuron synaptic activity. *J. Neurosci.* 28, 4967–73.
327. Shigetomi, E, Tong, X, Kwan, KY, Corey, DP, Khakh, BS (2011) TRPA1 channels regulate astrocyte resting calcium and inhibitory synapse efficacy through GAT-3. *Nat. Neurosci.* 15, 70–80.
328. Srinivasan, R, Huang, BS, Venugopal, S, Johnston, AD, Chai, H, Zeng, H, Golshani, P, Khakh, BS (2015) Ca<sup>2+</sup> signaling in astrocytes from Ip3r2<sup>-/-</sup> mice in brain slices and during startle responses in vivo. *Nat. Neurosci.* 18, 708–717.
329. Shigetomi, E, Kracun, S, Sofroniew, M V, Khakh, BS (2010) A genetically targeted optical sensor to monitor calcium signals in astrocyte processes. *Nat. Neurosci.* 13, 759–66.
330. Kanemaru, K, Sekiya, H, Xu, M, Satoh, K, Kitajima, N, Yoshida, K, Okubo, Y, Sasaki, T, Moritoh, S, Hasuwa, H, Mimura, M, Horikawa, K, Matsui, K, Nagai, T, Iino, M, Tanaka, KF (2014) In vivo visualization of subtle, transient, and local activity of astrocytes using an ultrasensitive Ca(2+) indicator. *Cell Rep.* 8, 311–8.
331. Garrison, CJ, Dougherty, PM, Kajander, KC, Carlton, SM (1991) Staining of glial fibrillary acidic protein (GFAP) in lumbar spinal cord increases following a sciatic nerve constriction injury. *Brain Res.* 565, 1–7.
332. Garrison, CJ, Dougherty, PM, Carlton, SM (1994) GFAP expression in lumbar spinal cord of naive and neuropathic rats treated with MK-801. *Exp. Neurol.* 129, 237–43.
333. Xie, YF, Zhang, S, Chiang, CY, Hu, JW, Dostrovsky, JO, Sessle, BJ (2007) Involvement of glia in central sensitization in trigeminal subnucleus caudalis (medullary dorsal horn). *Brain. Behav. Immun.* 21, 634–41.
334. Meller, ST, Dykstra, C, Grzybycki, D, Murphy, S, Gebhart, GF (1994) The possible role of glia in nociceptive processing and hyperalgesia in the spinal cord of the rat. *Neuropharmacology* 33, 1471–8.
335. Khurgel, M, Koo, AC, Ivy, GO (1996) Selective ablation of astrocytes by intracerebral injections of alpha-aminoadipate. *Glia* 16, 351–8.

336. Rodríguez, MJ, Martínez-Sánchez, M, Bernal, F, Mahy, N (2004) Heterogeneity between hippocampal and septal astroglia as a contributing factor to differential in vivo AMPA excitotoxicity. *J. Neurosci. Res.* 77, 344–53.
337. Gao, Y-J, Ji, R-R (2010) Targeting astrocyte signaling for chronic pain. *Neurotherapeutics* 7, 482–93.
338. Menetski, J, Mistry, S, Lu, M, Mudgett, JS, Ransohoff, RM, DeMartino, JA, MacIntyre, DE, Abbadie, C (2007) Mice overexpressing chemokine ligand 2 (CCL2) in astrocytes display enhanced nociceptive responses. *Neuroscience* 149, 706–714.
339. Rothstein, JD, Dykes-Hoberg, M, Pardo, CA, Bristol, LA, Jin, L, Kuncl, RW, Kanai, Y, Hediger, MA, Wang, Y, Schielke, JP, Welty, DF (1996) Knockout of glutamate transporters reveals a major role for astroglial transport in excitotoxicity and clearance of glutamate. *Neuron* 16, 675–86.
340. Mao, J, Sung, B, Ji, R-R, Lim, G (2002) Chronic morphine induces downregulation of spinal glutamate transporters: implications in morphine tolerance and abnormal pain sensitivity. *J. Neurosci.* 22, 8312–23.
341. Xin, W-J, Weng, H-R, Dougherty, PM (2009) Plasticity in expression of the glutamate transporters GLT-1 and GLAST in spinal dorsal horn glial cells following partial sciatic nerve ligation. *Mol. Pain* 5, 15.
342. Sung, B, Lim, G, Mao, J (2003) Altered expression and uptake activity of spinal glutamate transporters after nerve injury contribute to the pathogenesis of neuropathic pain in rats. *J. Neurosci.* 23, 2899–910.
343. Weng, H-R, Chen, JH, Cata, JP (2006) Inhibition of glutamate uptake in the spinal cord induces hyperalgesia and increased responses of spinal dorsal horn neurons to peripheral afferent stimulation. *Neuroscience* 138, 1351–1360.
344. Bas, DB, Abdelmoaty, S, Sandor, K, Codeluppi, S, Fitzsimmons, B, Steinauer, J, Hua, XY, Yaksh, TL, Svensson, CI (2015) Spinal release of tumour necrosis factor activates c-Jun N-terminal kinase and mediates inflammation-induced hypersensitivity. *Eur. J. Pain* 19, 260–70.
345. Ren, K (2010) Emerging role of astroglia in pain hypersensitivity. *Jpn. Dent. Sci. Rev.* 46, 86–92.
346. Nie, H, Weng, H (2009) Glutamate transporters prevent excessive activation of NMDA receptors and extrasynaptic glutamate spillover in the spinal dorsal horn. *J. Neurophysiol.*

101, 2041–51.

347. Ren, B, Gu, X, Zheng, Y, Liu, C, Wang, D, Sun, Y, Ma, Z (2012) Intrathecal injection of metabotropic glutamate receptor subtype 3 and 5 agonist/antagonist attenuates bone cancer pain by inhibition of spinal astrocyte activation in a mouse model. *Anesthesiology* 116, 122–32.
348. Wei, F, Guo, W, Zou, S, Ren, K, Dubner, R (2008) Supraspinal glial-neuronal interactions contribute to descending pain facilitation. *J. Neurosci.* 28, 10482–10495.
349. Kim, SK, Hayashi, H, Ishikawa, T, Shibata, K, Shigetomi, E, Shinozaki, Y, Inada, H, Roh, SE, Kim, SJ, Lee, G, Bae, H, Moorhouse, AJ, Mikoshiba, K, Fukazawa, Y, Koizumi, S, Nabekura, J (2016) Cortical astrocytes rewire somatosensory cortical circuits for peripheral neuropathic pain. *J. Clin. Invest.* 126, 1983–97.
350. Chen, F-L, Dong, Y-L, Zhang, Z-J, Cao, D-L, Xu, J, Hui, J, Zhu, L, Gao, Y-J (2012) Activation of astrocytes in the anterior cingulate cortex contributes to the affective component of pain in an inflammatory pain model. *Brain Res. Bull.* 87, 60–6.





Ana David-Pereira, Diana Amorim, Antónia Palhares Lima, Rosete Nogueira, Hélder Pereira, Antti  
Pertovaara, Armando Almeida, Filipa Pinto-Ribeiro

**Injection of kaolin/carrageenan in the rat knee joint induces progressive  
experimental knee osteoarthritis.**

*(Manuscript under preparation)*





**Injection of kaolin/carrageenan in the rat knee joint induces progressive experimental knee osteoarthritis.**

Ana David-Pereira<sup>1,2</sup>, Diana Amorim<sup>1,2</sup>, Antónia Palhares Lima<sup>1,2</sup>, Rosete Nogueira<sup>1,2</sup>, Helder Pereira<sup>2,3</sup>, Antti Pertovaara<sup>4</sup>, Armando Almeida<sup>1,2</sup>, Filipa Pinto-Ribeiro<sup>1,2,\*</sup>

<sup>1</sup>Life and Health Sciences Research Institute (ICVS), School of Medicine, University of Minho, Braga, Portugal

<sup>2</sup>ICVS/3B's - PT Government Associate Laboratory, Braga/Guimarães, Portugal

<sup>3</sup>3B's Research Group-Biomaterials, Biodegradables and Biomimetics, Minho University, Headquarters of the European Institute of Excellence on Tissue Engineering and Regenerative Medicine, Guimarães, Portugal.

<sup>4</sup>Institute of Biomedicine/Physiology, University of Helsinki, Helsinki, Finland

*\*Corresponding author:*

[filiparibeiro@med.uminho.pt](mailto:filiparibeiro@med.uminho.pt)

## **Abstract**

Osteoarthritis (OA), the most common joint disorder worldwide, is characterized by progressive degeneration of articular and periarticular structures, leading to physical and emotional impairments that greatly impact the patients' quality of life. In young individuals, prevalence of OA is higher in men, but in the elderly it is higher in women. Unfortunately, no therapy has been able to halt the progression of the disease.

Due to the complexity of OA, most animal models are able only to mimic a specific stage or feature of the human disorder. In this work we demonstrate the intra-articular injection of kaolin/carrageenan leads to the progressive degeneration of the rat's knee joint that is accompanied by mechanical hyperalgesia and allodynia, gait impairments (reduced contact area of the affected limb), and radiographical and histopathological findings concomitant with advanced stages of OA in human patients. Additionally, animals also display emotional impairments, such as anxiety- and depressive-like behaviors, important and common comorbidities of human OA patients.

Overall, our model offers the possibility of inducing a progressive experimental model of OA that mimics several important features of the human disorder of interest to all those involved in OA research.

## **Introduction**

Osteoarthritis (OA) is the most common joint disorder, affecting 10-15% of the world population (Anderson and Loeser, 2009; Neogi and Zhang, 2013). It is the main cause of work disability in pre-retirement individuals (>50 years of age) and of disability in the elderly, with an incidence of 60% and 70% in men and women over 65 years of age, respectively (Plotnikoff et al., 2015). OA is considered the fastest growing (Tadano et al., 2016) and the most pressing public health problem (Hunter et al., 2008). Ageing, obesity, genetic predisposition, inflammatory diseases, trauma, overuse and sedentarism are main risk factors for the development of OA. In primary (idiopathic) OA, more common in middle-aged women, the aging process of joints is accelerated and aggravated by overuse, but its etiology is not well defined. Secondary OA, more common in men, results from joint abnormalities secondary to inflammatory, metabolic or endocrine diseases, misalignment or instability of the joints and traumatic injuries and deformities. OA is frequently asymmetric and the knees, hips, hands, neck, and lumbar spine joints are the most affected structures. Unfortunately, up-to-now no therapeutic interventions have been able to stop the progression of the disease.

OA is characterized by chronic progressive degeneration of weight bearing joints resulting from an imbalance between articular breakdown and repair mechanisms and hypertrophic changes in the bone (Bijlsma et al., 2011). Clinical diagnosis is primarily based on the patient's medical history, physical examination and radiography, and classified according to the Kellgren and Lawrence grading score (1963). The major cause for patients to seek medical care, however, is pain, and while its diagnosis is not difficult, it is often made at a time when OA is already well established. Initially pain is sporadic, resulting from recurrent episodes of articular inflammation that are a common feature of OA. Consequently, there is increased intra-articular pressure due to synovial inflammation and reduced blood flow. Besides the mechanical effect of increased pressure, the release of pro-inflammatory mediators, such as bradykinin, cytokines and substance P, causes pain by activating nociceptors in menisci, adipose tissue, synovium, and periosteum. Additional sensitization also occurs as a consequence of leakage of these mediators to periarticular structures (articular margins, the capsule insertion points and tendons). These events lead to the development of spontaneous pain, primary hyperalgesia and pain during otherwise innocuous movement (Bijlsma et al., 2011, Hunter et al., 2008).

Later in the process, pain aggravates due to remodeling of the bone, subchondral microfractures, periostitis, meniscal abnormalities, nerve compression and increased joint volume due to osteophyte formation. At this stage, pain might become intense enough to interfere with sleep and to enhance sensitivity to mechanical stimuli outside the area of injury (secondary hyperalgesia). Changes in central pain modulation pathways lead to the development of radiating pain and decrease pain thresholds in unaffected joints. Commonly, OA pain worsens with activity, especially after rest (gelling phenomenon), and limitation of motion range due to pain is present in all forms of OA (Bijlsma et al., 2011, Hunter et al., 2008).

A mismatch between the level of reported pain, disability and disease severity is frequent (Hunter et al., 2008), as only 12% of patients over 55 present symptomatic OA and concomitant radiographic features (Peat et al., 2001). Of the remaining, 50% of patients with radiographic knee OA do not complain of pain and the other 50% have pain but do not present a definite radiographic profile. The use of radiography is fundamental for the exclusion of other joint-associated pathologies (Cibere, 2006; Hunter et al., 2008), although it is non-essential for the diagnosis and management of OA in primary care (Bedson and Croft, 2008; Hunter et al., 2008). Radiography allows to identify joint space narrowing, subchondral bone sclerosis, subchondral cysts and osteophyte formation, as well as their severity and location (the two tibiofemoral joint compartments and the patellofemoral joint) (Kellgren and Lawrence, 1957; Peat et al., 2001; Kuyinu et al., 2016). However, changes to joint soft tissues cannot be visualized on plain film X-rays (Lane et al., 2011), which may account for the inefficiency of this method to diagnose OA at earlier stages. More recently, magnetic resonance imaging (MRI) yielded a better correspondence between reported pain severity and structural changes in the joint at earlier time points (Hunter et al., 2008), as it allows the visualization of bone marrow lesions, sub-articular bone attrition, synovitis and effusion (Tadano et al., 2016).

Although its clinical applicability is not very high in OA patients, histopathological scoring is commonly used in preclinical studies to establish the progression of OA and to classify the severity of lesions. According to the histopathology grading scale proposed by Pritzker et al. (2006), OA progressively affects cartilage from superficial to deeper structures. In healthy cartilage, the surface is smooth and the extracellular matrix and chondron columns are organized. Superficial fibrillation (microscopic cracks), focal or generalized cartilage matrix edema, cartilage and chondrocyte hypertrophy, proliferation/death of chondrocytes and disorganization of chondron columns are considered first stage OA changes (Grade 1), that progressively worsen to denudation and

fibrocartilaginous repair of bone surface, thickening of the articular bone plate with the formation of new ridges and grooves and to the formation of osteophytes in later stages of OA (Grades 5 and 6) (Pritzker et al., 2006; Pritzker and Aigner, 2010).

Although hand OA is the most common, knee and hip OA are the most debilitating for the patient (Loeser, 2010). Patients with lower limb OA display several postural alterations, including decreased muscle flexibility, walking speed, walking endurance, cadence, longer support time, reduced range of motion, joint instability, and shorter stride length (Messier et al., 1992; Barrois et al., 2016). Tanado et al. (2016) also showed during stance, ankle joints abduct less to avoid adduction at the knee level, an effect that increases with OA severity.

Besides the physical limitations, anxiety and depression, although extensively overlooked by primary care physicians (Turner, 2000; Margaretten et al., 2013; Paskins et al., 2014), are highly prevalent among OA patients, and aggravate the burden of OA significantly (Rosemann et al. 2008; Sharma et al., 2016). OA patients experiencing emotional comorbidities report more pain, display increased physical limitations, visit their primary care physicians more frequently, and take more medication; furthermore, pharmacological and surgical therapies have lower efficacy on treatment of these patients (Sharma et al., 2016). Interestingly, perceived pain, along with other factors, is positively correlated to the degree of depression and is a predictor of depression severity (Rosemann et al., 2007).

OA is therefore a multidimensional disease and the improvement of therapeutic strategies requires that clinical and preclinical research take them all into account. No single animal model is able to perfectly match the progression of human OA (Lampropoulou-Adamidou et al., 2014); instead, most models are used to study specific stages and features of the disease. The injection of a mixture of kaolin/carrageenan in the synovial cap of rodent knees has been used as a model of early inflammatory stages in arthritis (Amorim et al., 2014; König et al., 2014; Salinas-Sánchez et al., 2015; Cragg et al., 2016). In this work we demonstrate that prolonging this model in time leads to the development of several OA-like features in a progressive way in the rat including altered nociception, gait and emotional impairments and radiographic and histopathological findings.

## **Material and Methods**

### **Animals and ethical considerations**

The experiments were performed in Wistar han rats (n=32), weighing between 200–250g at the beginning of the experiments; Charles Rivers, Barcelona, Spain). Animals were housed under standard laboratory conditions in a thermostatically controlled room at  $22.0 \pm 0.5^{\circ}\text{C}$  with a normal 12h light/dark cycle (light cycle from 8.00a.m. to 8.00p.m.). The animals received commercial pelleted rat feed (CRM-P pellets, Special Diets Services, Witham, Essex, England) and water *ad libitum*. All experimental protocols followed the European Community Council Directive 86/609/EEC and 2010/63/EU concerning the use of animals for scientific purposes and were approved by the Institutional Ethical Commission.

### **Induction of the K/C model**

For the K/C model induction, animals were anaesthetized with a mixture of ketamine (0.75mg/Kg, i.p.; Imalgene, Merial, Oeiras, Portugal) and medetomidine (0.5mg/Kg, i.p.; Dorbene, Esteve, Carnaxide, Portugal). Then, 3% kaolin and 3% carrageenan (Sigma-Aldrich, Sintra, Portugal) were freshly dissolved in sterile saline solution (0.9%) and injected into the synovial cavity of the right knee joint (K/C) at a volume of 0.1mL using a 26 gauge needle, as described elsewhere (Amorim et al. 2014). Control animals (SHAM) were injected with 0.1mL saline in the synovial cavity of the right knee joint. After this procedure, ten flexions and extensions of the right leg were performed in SHAM and K/C animals. The anesthesia was reversed by administering atipamezole hydrochloride (1mg/Kg, i.p.; Antisedan, Pfizer, Oeiras, Portugal). Animals were monitored until fully awake (grooming and eating). The body weight of the animals was recorded weekly in order to monitor the general health status of the animals.

At the end of the experimental period, animals were euthanized with an overdose of pentobarbital (80mg/Kg, i.p.; CEVA, Portugal), transcardially perfused with a fresh 4% paraformaldehyde (PanReac AppliChem, Darmstadt, Germany) solution. Both knees were excised and post fixed in the same fixative for posterior analysis.

### **Assessment of mechanical allodynia - the flexion-extension test**

Animals were securely held by the experimenter and submitted to five consecutive flexion-extension movements of the injected knee. The number of audible vocalizations during the five movements was recorded and considered as an indicator of the development of mechanical allodynia.

### **Assessment of mechanical hyperalgesia - the pressure application measurement test**

The application of noxious pressure to the primary site of injury is a classical approach to measure mechanical hyperalgesia, both in humans and animals. The pressure application measurement (PAM) method was used to evaluate mechanical hyperalgesia four weeks after the intra-articular injection by the application of a force range between 0–1500g. Before the beginning of the test the experimenter practiced the correct application of the desired force by following a linear graph provided by the PAM software. To perform the test and with the animal securely held, the force transducer unit (fitted to the experimenter's thumb) was placed on one side of the animal's knee joint and the forefinger on the other. Then, an increasing force is applied across the joint at a rate of approximately  $300\text{g}\cdot\text{s}^{-1}$ , as defined in the software, until a behavioral response is observed (limb withdrawal, freezing of whisker movement, wriggling or vocalization) with a cut-off of 5s. The peak force applied immediately prior to the behavioral response was recorded, by the real-time measurement system of the PAM software, as the limb withdrawal threshold (LWT). Two measurements of the ipsilateral and contralateral limbs were performed at 1min intervals. The mean LWTs were calculated per animal.

### **Gait analysis**

To evaluate gait pattern, the footprint test was used. To obtain footprints, the hind and forepaws of the animals were coated with blue and pink non-toxic paints, respectively. A strip of white paper was placed on the floor of a runway for each run. The animals were allowed to walk along a 100cm length  $\times$  4.2cm width  $\times$  10cm height corridor towards the home cage grid. To evaluate the gait pattern of each animal, the stride length and contact area were determined by measuring these parameters in three consecutive steps. The mean stride length and contact area were calculated per animal.

### **Evaluation of anxiety-like and locomotor behaviors – the open field test**

The open field (OF) test was used to evaluate locomotor ability and anxiety-like behavior of animals following a protocol previously described (Amorim et al., 2014). The OF test was performed in a square arena (50cm wide) in a brightly illuminated room. The test started when the animal was placed at the center of the arena and its exploratory activity was videotaped for 5min. The arena was cleaned with 10% alcohol solution between each trial.

The total distance travelled by the animal inside the arena was used as an assessment of locomotor ability, by counting the number of squares crossed (5x5cm) by each animal during the behavioral session. The time spent in the center of the arena (corresponding to a square 30cm wide and equidistant from the borders) vs. the time spent in the periphery was used as a measure of anxiety-like behavior.

### **Assessment of depressive-like behavior – the forced-swimming test**

Learned helplessness was evaluated using the forced-swimming test (FST) and followed a protocol previously implemented in our lab. Animals were submitted to a pre-test session (5min) in which they were individually placed in cylinders filled with water (25°C; depth 30cm). Twenty-four hours later animals were again placed in the cylinders for a 5min period and the testing session was recorded with a video camera. The quantification of (i) latency to immobility, (ii) time spent immobile, and (iii) time spent swimming and climbing was performed using the Kinoscope software. Learned helplessness behavior was defined as decreased latency to immobility and increased immobility times.

### **Assessment of depressive-like behavior – the sucrose preference test**

Reduction in sucrose preference (SPT) was used as a measure of anhedonia, an important component of depression (Castagné et al., 2009). At the beginning of the experiment animals were presented with a bottle of water containing a 1% sucrose solution. Four weeks after the induction of experimental OA, during the night period, animals were again presented with two pre-weighted bottles, one containing water and the other a 1% sucrose solution. Sucrose preference was calculated according to the formula:



Sucrose preference (%) = [Sucrose solution consumption (g)/Total liquid consumption (g)]x100

### **Radiographical analysis of preserved knee joints**

Severity of knee OA was determined using the Kellgren and Lawrence score (1957), where grade 0 corresponds to no radiographic features of OA present; grade 1: doubtful joint space narrowing (JSN) and possible osteophytic lipping; grade 2: definite osteophytes and possible JSN on anteroposterior weight-bearing radiograph; grade 3: multiple osteophytes, definite JSN, sclerosis, possible bony deformity; and grade 4: large osteophytes, marked JSN, severe sclerosis and definite bony deformity.

### **Histopathological analysis**

The preserved knee joints were decalcified in EDTA solution for 1 week. Knee samples were then cut in the transverse plane and paraffin-embedded. Serial sections 4µm thick were obtained. Hematoxylin and eosin (H&E) staining was used to evaluate changes in general knee morphology. Masson's Trichrome staining was used to assess changes in collagen content, and Safranin-O Fast Green stain was used to analyze general knee morphology and proteoglycan loss in cartilage ground substance.

Knee degeneration was evaluated using the scores proposed by Pritzker et al. (2006) and Pearson et al. (2011) for human OA and Gerwin et al. (2010) for rats as shown in **Table 1**.

### **Statistical analysis**

The statistical analysis was performed using the GraphPad Prism 6 software (GraphPad Software Inc, La Jolla, CA, USA). All data sets were tested for normality. When results displayed a normal distribution, comparisons between groups were performed using unpaired t-tests. Two-way analysis of variance (ANOVA) followed by a t-test with a Bonferroni correction for multiple comparisons was used to analyze differences in body weight, gait and mechanical hyperalgesia between SHAM and K/C animals throughout experimental time. Statistical significance was accepted for  $p < 0.05$ . Data are expressed as mean ± standard error of the mean (SEM).

## Results

### Animal wellbeing

At the end of the experiment, K/C animals gained less weight than SHAM animals (main effect of experimental group:  $F_{1,130}=12.73$ ,  $p=0.0005$ ), an effect that did not vary with time (main effect of interaction:  $F_{4,130}=1.22$ ;  $p=0.31$ ). *Post-hoc* tests show K/C animals weighted significantly less than SHAM animals four weeks after K/C induction (**Fig. 1**).

### Mechanical hyperalgesia and allodynia

All K/C animals vocalized during the flexion-extension test throughout the experimental period indicating the development of mechanical allodynia (data not shown).

The evaluation of mechanical hyperalgesia in rats using the PAM test showed the LWT was significantly altered between K/C and SHAM animals (main effect of experimental group:  $F_{1,50}=5.67$ ;  $p=0.02$ ) and between the ipsi- and contralateral sides (main effect of side:  $F_{1,50}=12.09$ ,  $p=0.001$ ). *Post-hoc* tests showed the ipsilateral LWT of K/C animals was significantly lower than the K/C contralateral LWT and the ipsilateral LWT of SHAM animals (**Fig. 2**).

### Gait analysis

K/C induction had no effect on stride length on the contralateral side (main effect of experimental group:  $F_{5,61}=0.15$ ,  $p=0.70$ ) and throughout the experimental period (main effect of time:  $F_{1,40}=1.62$ ,  $p=0.21$ , **Fig. 3A**). Conversely, stride length on the ipsilateral side was significantly altered (main effect of experimental group:  $F_{1,40}=8.93$ ,  $p=0.005$ ). Stride length varied throughout the experimental period (main effect of time:  $F_{3,40}=5.18$ ,  $p=0.004$ ) with *post-hoc* test showing a significant decrease in stride length in K/C animals four weeks post-induction (**Fig. 3B**).

SHAM animals showed no difference in stride length between the ipsi- and contralateral side (main effect of side:  $F_{1,40}=0.89$ ,  $p=0.35$ ) and throughout the experimental period (main effect of time:  $F_{3,40}=1.80$ ,  $p=0.16$ ). In K/C animals, stride length was significantly different between the ipsi- and contralateral hind paws (main effect of side:  $F_{1,40}=12.02$ ,  $p=0.001$ ) and throughout the experimental period (main effect of time:  $F_{3,40}=5.52$ ,  $p=0.003$ ).

K/C induction significantly altered paw contact area (main effect of experimental group:  $F_{1,56}=17.39$ ,  $p=0.0001$ ). Paw contact area was also altered throughout the experimental period (main effect of time:  $F_{3,56}=3.62$ ,  $p=0.02$ ). *Post-hoc* tests showed a significant decrease in the ipsi/contralateral side ratio in K/C animals between one and two weeks post-induction when compared to controls (**Fig. 3C**).

### **Locomotor activity**

In the OF test, the analysis of the total distance travelled by animals of each experimental group showed no differences in the locomotor activity between SHAM and K/C animals four weeks after induction ( $t_{25}=0.44$ ,  $p=0.66$ ; **Fig. 4A**).

### **Anxiety-like behavior**

Data from the OF test supports the development of an anxious-like behavior phenotype in K/C animals four weeks after induction, as these animals spent significantly less time in the center of the arena ( $t_{25}=2.21$ ,  $p=0.04$ ; **Fig. 4C**) and avoided entering the center of the arena ( $t_{25}=2.31$ ,  $p=0.03$ ; **Fig. 4D**) when compared to SHAM.

### **Depressive-like behavior**

Our results show K/C animals displayed a depressive-like phenotype. Four weeks after the induction of the model, K/C animals displayed a lower latency to immobility ( $t_{25}=2.22$ ,  $p=0.04$ ; **Fig. 5A**) when compared to SHAM animals. Concomitantly, the time spent immobile was decreased in K/C animals ( $t_{25}=2.34$ ,  $p=0.03$ ; **Fig. 5B**). While the time spent swimming was decreased in K/C animals ( $t_{25}=2.61$ ,  $p=0.02$ ; **Fig. 5C**), no differences were found concerning the time spent climbing ( $t_{25}=2.04$ ,  $p=0.052$ ; **Fig. 5D**).

In the SPT, the induction of the experimental model significantly altered sucrose preference (main effect of experimental group:  $F_{1,28}=8.03$ ,  $p=0.008$ ). Sucrose consumption also varied with time (main effect of time:  $F_{1,28}=5.62$ ,  $p=0.02$ ). *Post-hoc* tests show K/C animals decreased their consumption of a sucrose solution when compared their sucrose consumption at the beginning of

the experiment and in comparison with SHAM animals, indicating the development of anhedonic-like behavior (**Fig. 5E**).

### **Radiographical analysis**

Radiographical examples from SHAM and K/C animals are presented in **Fig. 6**. The distal end of the femur is characterized by two condyles, the medial condyle and the lateral condyles that articulate with the proximal tibia and interposed menisci to form the stifle joint. SHAM animals display no radiographic alterations of joints (**Fig. 6A**). Similarly, no differences in joint structures were observed during the first two weeks post induction (**Fig. 6B**). Three weeks after K/C injection to the stifle, animals display moderate narrowing of joint space (an indirect measure of cartilage loss; **Fig. 6C**) that is aggravated at four weeks when K/C animals also display subchondral bone sclerosis, flattening of the femoral and tibial plates and osteophyte formation (**Fig. 6D**).

### **Histopathology analysis**

The histopathological analysis of SHAM joints showed articular structures remained intact, the cartilage was healthy without loss of chondrocytes or proteoglycans and no changes in the subchondral bone (**Fig. 7A,G,M**). By contrast, in the K/C groups we observed significant pathological alterations that were aggravated with time. Up to one week after induction of the model, K/C animals display infiltration of polinucleated cells in articular and periarticular tissues (**Fig. 7N,O**), edema areas (**Fig. 7B,H**), fibrillation of cartilage (**Fig. 7I**) and chondrocyte disorganization (**Fig. 7C**). On week three, K/C animals display disorganization of chondron columns (**Fig. 7D**), cartilage hypocellularity (**Fig. 7P**) and narrowing of joint space (**Fig. 7J**). From week four onwards, bone sclerosis (**Fig. 7F,K**), depletion of cartilage (**Fig. 7L**), thickening of subchondral bone and cartilage lamination (**Fig. 7E**), the presence of synovial cists (**Fig. 7Q**) and inflammation (**Fig. 7R**) are evident in K/C animals.

## Discussion

In the work herein we demonstrate that K/C intra-articular injection in rats mimics several features of human OA. Adult male rats displayed mechanical hyperalgesia and allodynia from post-induction day three onwards. The increase in nociceptive sensitivity was accompanied by changes in gait, reflected by a decrease in the paw contact area of the affected limb. Radiography analysis revealed an OA-like phenotype (narrowing of joint space, bone sclerosis and presence of osteophytes) four weeks post-induction. Histopathological analysis of knee sections showed a progressive degeneration of articular and periarticular structures concomitant with Grade 4 OA according to the Pritzker and Pearson's grading scales in the same time point. Importantly, four weeks after the induction of the experimental model, in addition to physical impairments, animals displayed an anxiety- and depressive-like phenotype. Taken as a whole, we propose the K/C model presents several advantages over other experimental models of OA, as the severity of the physical impairments is progressive and animals display comorbid emotional sequelae, all of which are common in the human disorder. This model bridges the gap between structural and symptomatic aspects of OA, a common disadvantage of other experimental models.

Pain is a cardinal sign of OA and is associated with peripheral sensitization (Suokas et al., 2012; Fingleton et al., 2015). In a clinical context, the application of pressure stimuli to the affected joint is one of the most common and reliable methods for assessing somatosensory response abnormalities, or primary mechanical hyperalgesia, in OA patients (Arendt-Nielsen et al., 2010; Wylde et al., 2012). The application of a similar protocol to our experimental groups, the PAM test, clearly demonstrated the K/C model decreases nociceptive mechanical thresholds in the affected joint soon after the induction of the model. At early stages it is probable the observed increase in mechanical hyperalgesia is due to an inflammatory reaction to the injection of carrageenan in the tibio-femoral joint rather than the consequence of trauma. In fact, the histopathological analysis of joint sections sampled at time points up to one-week post-induction show the superficial articular cartilage remains intact and radiographical analysis also shows no joint structural abnormalities. These results mirror what happens in the clinics, where the occurrence of pain and pain severity are often not accompanied by significant radiographical findings (Bedson and Croft, 2008). On the other hand, at later stages of human OA, the severity of reported pain correlates with the level of radiographical knee joint damage. Again our experimental model replicates this event, as K/C animals also display mechanical hyperalgesia four weeks post-induction, long after the initial

inflammatory phase is resolved. As in human subjects, at later stages of the disease, knee joint damage in our animals was evident both in radiographical and histopathological evaluations.

Courtney et al. (2010) suggest persistent nociceptive pain leads to central sensitization and subsequently to the development of a neuropathic component of chronic musculoskeletal pain and thus to mechanical allodynia in OA patients, a feature indirectly confirmed in our K/C animals by the vocalization in the flexion-extension test. In this context, once again our model exhibits important features of human OA. It should be noted, however, that this concept is based on extrapolations of data for skin receptors and not in deep tissues, such as joints (Courtney et al., 2010). As such, it is possible that what we consider allodynia, or the application of non-nociceptive stimuli, which in this case would be painful during otherwise innocuous movement, is in fact the evaluation of primary hyperalgesia as we are stressing motion range by stretching the injured joint.

Patients with OA typically display gait compensations due to 'fear of movement' in attempt to avoid pain (Jacobs et al., 2014). Additionally, at later stages of OA, structural changes in joints also contribute to changes in the internal mechanics of an articulating joint (Jacobs et al., 2014). Of the several parameters evaluated in this work, the induction of our model resulted in decreased paw print area in the ipsilateral side. Decreased paw print areas classically reflect unilateral dynamic weight-bearing imbalances where weight loading is shifted to the contralateral limb (Vrinten and Hamers, 2003; Jacobs et al., 2014). Our results are in line with previous works using models of carrageenan-induced monoarthritis (Angeby-Möller et al., 2008), the MIA and collagenase models of OA, among others (Marker and Pomonis 2012, Adães et al., 2014), and nerve injury (Bozkurt et al., 2008). Changes in joint loading are also common in trauma-induced human OA and are considered a significant risk factor for its progression (Buckwalter, 1995). Although our evaluation was restricted to the analysis of spatial parameters, it is evident the K/C model reproduces an important compensatory mechanism in weight-bearing joints as observed in OA patients. Further studies using automatic gait evaluation would allow to further investigate temporal-dependent changes in gait, such as timing and synchronicity of foot-strike and toe-off events, enabling a better correlation with gait impairments in OA patients.

As mentioned previously, although new techniques are being applied to the study of OA, radiography remains the most accessible tool for the evaluation and scoring of the OA-affected joint (Braun and Gold, 2012). Importantly, soft tissues are not captured by radiography, thus decreased joint space is used as an indirect measure of cartilage integrity in the clinics. In our work, four

weeks post induction, K/C animals displayed narrowing of the joint space, subchondral bone sclerosis, subchondral cyst formation and formation of osteophytes, perfectly matching all structural hallmarks of OA progression in patients. In fact, these features, according to the Kellgren and Lawrence scale, are concomitant with Grade 4 OA. Unlike the extensively used MIA model, in which events precipitate within a week post-induction, the K/C model displays a slower temporal summation of radiographical markers that are more closely related to the slow development of human OA.

The temporal analysis of histopathological data further confirmed the radiographic findings, showing a progressive and severe degeneration of articular structures. A strong initial inflammatory component is accompanied by patellar distension, synovial effusion and edema. Interestingly, although patellar distension is an early feature of OA, it was easily visualized in the x-rays of OA animals in early time points. As in the human disorder, eburnation and joint space narrowing precede the flattening of joint plates and the occurrence of osteolytic foci. Ultimately, total loss of cartilage and the formation of osteophytes is evident in later stages of the disease.

OA is frequently accompanied by emotional disorders, such as anxiety and depression. These comorbid affective disorders can interfere with daily activities, thus exerting a major negative effect on the quality of life of patients (Argoff, 2007; Asmundson and Katz, 2009; Campbell et al., 2003). In this work, K/C rats displayed comorbid emotional impairments, namely anxiety- and depressive-like behavior. The complexity of OA does not allow associating the development of emotional-like impairments to a specific OA feature. Chronic pain and emotional disorders are common comorbid findings in patients, however disability and decreased quality of life are also closely related to the development of psychiatric disorders. OA patients diagnosed with depression report more pain, higher disability scores, and lower therapy outcomes than non-depressed OA patients (Sharma et al., 2016).

In conclusion, the work here presented indicates the intra-articular K/C injection in rats leads to the development of several OA behavioral and structural symptoms in a slow and progressive fashion that closely mirror the human pathology. Instead of reflecting only a specific stage of OA, like many of the currently used OA preclinical models, several stages are represented in a relatively small time window, which allows to establish a progression timeline and to correlate it with particular markers of the disease. It also presents a good opportunity to study the mechanisms

underlying the development of comorbid behavioral impairments such as anxiety and depression, and to provide patients with better therapies that target the multiple symptoms of OA.



## REFERENCES

- Adães S, Mendonça M, Santos TN, Castro-Lopes JM, Ferreira-Gomes J, Neto FL. Intra-articular injection of collagenase in the knee of rats as an alternative model to study nociception associated with osteoarthritis. *Arthritis Res Ther*. 2014, 16, R10.
- Amorim D, David-Pereira A, Pertovaara A, Almeida A, Pinto-Ribeiro F. Amitriptyline reverses hyperalgesia and improves associated mood-like disorders in a model of experimental monoarthritis. *Behav Brain Res*. 2014, 265:12-21.
- Angeby-Möller K, Berge OG, Hamers FP. Using the CatWalk method to assess weight-bearing and pain behaviour in walking rats with ankle joint monoarthritis induced by carrageenan: effects of morphine and rofecoxib. *J Neurosci Methods*. 2008, 174(1):1-9.
- Arendt-Nielsen L, Nie H, Laursen MB, Laursen BS, Madeleine P, Simonsen OH, Graven-Nielsen T. Sensitization in patients with painful knee osteoarthritis. *Pain*. 2010, 149(3):573-581.
- Argoff CE. The coexistence of neuropathic pain, sleep, and psychiatric disorders: a novel treatment approach. *Clin J Pain*. 2007, 23(1):15-22.
- Asmundson GJ, Katz J. Understanding pain and posttraumatic stress disorder comorbidity: do pathological responses to trauma alter the perception of pain? *Pain*. 2008, 138(2):247-249.
- Barrois R, Gregory T, Oudre L, Moreau T, Truong C, Aram Pulini A, Vienne A, Labourdette C, Vayatis N, Buffat S, Yelnik A, Waele C, Laporte S, Vidal PP, Ricard D. An automated recording method in clinical consultation to rate the limp in lower limb osteoarthritis. *PLoS One*. 2016, 11(10):e0164975.
- Bedson J, Croft PR. The discordance between clinical and radiographic knee osteoarthritis: a systematic search and summary of the literature. *BMC Musculoskelet Disord*. 2008, 9:116.
- Bijlsma JWJ, Berenbaum F, Lefeber FPJG. Osteoarthritis: an update with relevance for clinical practice. *Lancet*. 2011, 377:2115-2126.
- Bozkurt A, Deumens R, Scheffel J, O'Dey DM, Weis J, Joosten EA, Führmann T, Brook GA, Pallua N. CatWalk gait analysis in assessment of functional recovery after sciatic nerve injury. *J Neurosci Methods*. 2008, 173(1):91-98.
- Braun, HJ, Gold, GE. Diagnosis of Osteoarthritis: Imaging. *Bone*. 2012, 51(2):278–288.

Buckwalter JA. Osteoarthritis and articular cartilage use, disuse, and abuse: experimental studies. *J Rheumatol Suppl.* 1995, 43:13-15.

Campbell I. The obesity epidemic: can we turn the tide? *Heart.* 2003, 89 Suppl 2:22-24.

Castagné V, Moser P, Porsolt RD. Behavioral assessment of antidepressant activity in rodents. In *Methods of Behavior Analysis in Neuroscience.* Ed. Buccafusco JJ. CRC Press/Taylor & Francis. 2009, Boca Raton (FL).

Cibere J. Do we need radiographs to diagnose osteoarthritis? *Best Pract Res Clin Rheumatol.* 2006, 20(1):27-38.

Courtney CA, Kavchak AE, Lowry CD, O'Hearn MA. Interpreting joint pain: quantitative sensory testing in musculoskeletal management. *J Orthop Sports Phys Ther.* 2010, 40(12):818-825.

Cragg B, Ji G, Neugebauer V. Differential contributions of vasopressin V1A and oxytocin receptors in the amygdala to pain-related behaviors in rats. *Mol Pain.* 2016, 11;12.

Fingleton C, Smart K, Moloney N, Fullen BM, Doody C. Pain sensitization in people with knee osteoarthritis: a systematic review and meta-analysis. *Osteoarthritis and Cartilage.* 2015, 23(7):1043-1056.

Gerwin N, Bendele AM, Glasson S, Carlson CS. The OARSI histopathology initiative - recommendations for histological assessments of osteoarthritis in the rat. *Osteoarthritis Cartilage.* 2010, 18 Suppl 3:S24-34.

Hunter DJ, McDougall JJ, Keefe FJ. The symptoms of osteoarthritis and the genesis of pain. *Rheum Dis Clin North Am.* 2008, 34(3):623-643.

Jacobs, BY, Kloefkorn HE, Allen KD. Gait analysis methods for rodent models of osteoarthritis. *Curr Pain Headache Rep.* 2014, 18(10):456.

Kellgren J, Lawrence J. Atlas of standard radiographs. The epidemiology of chronic rheumatism. Vol. 2. Blackwell Scientific Publications; Oxford: 1963.

Kellgren J, Lawrence J. Radiological assessment of osteo-arthritis. *Ann Rheum Dis.* 1957, 16(4):494-502.

König C, Zharsky M, Möller C, Schaible HG, Ebersberger A. Involvement of peripheral and spinal tumor necrosis factor- $\alpha$  in spinal cord hyperexcitability during knee joint inflammation in rats. *Arthritis Rheumatol*. 2014, 66(3):599-609.

Kuyinu EL, Narayanan G, Nair LS, Laurencin CT. Animal models of osteoarthritis: classification, update, and measurement of outcomes. *J Orthop Surg Res*. 2016, 2:11-19.

Lampropoulou-Adamidou K, Lelovas P, Karadimas EV, Liakou C, Triantafillopoulos IK, Dontas I, Papaioannou NA. Useful animal models for the research of osteoarthritis. *Eur J Orthop Surg Traumatol*. 2014, 24(3):263-271.

Lane NE, Brandt K, Hawker G, Peeva E, Schreyer E, Tsuji W, Hochberg MC. OARSI-FDA initiative: defining the disease state of osteoarthritis. *Osteoarthritis Cartilage*. 2011, 19(5):478-482.

Loeser RF. Age-related changes in the musculoskeletal system and the development of osteoarthritis. *Clin Geriatr Med*. 2010, 26(3):371-386.

Margaretten ME, Katz P, Schmajuk G, Yelin E. Missed opportunities for depression screening in patients with arthritis in the United States. *J Gen Intern Med*. 2013, 28(12):1637-1642.

Marker CL, Pomonis JD. The monosodium iodoacetate model of osteoarthritis pain in the rat. *Methods Mol Biol*. 2012, 851:239-248.

Messier SP, Loeser RF, Hoover JL, Semble EL, Wise CM. Osteoarthritis of the knee: effects on gait, strength, and flexibility. *Arch Phys Med Rehabil*. 1992, 73(1):29-36.

Neogi T, Zhang Y. Epidemiology of OA. *Rheum Dis Clin North Am*. 2013, 39(1):1-19.

Paskins Z, Sanders T, Hassell AB. Comparison of patient experiences of the osteoarthritis consultation with GP attitudes and beliefs to OA: a narrative review. *BMC Fam Pract*. 2014, 19:15-46.

Pearson RG, Kurien T, Shu KS, Scammell BE. Histopathology grading systems for characterisation of human knee osteoarthritis—reproducibility, variability, reliability, correlation, and validity. *Osteoarthritis Cartilage*. 2011, 19(3):324-31.

Peat G, Croft P, Hay E. Clinical assessment of the osteoarthritis patient. *Best Pract Res Clin Rheumatol*. 2001, 15(4):527-544.

Plotnikoff R, Karunamuni N, Lytvyak E, Penfold C, Schopflocher D, Imayama I, Johnson S, Raine K. Osteoarthritis prevalence and modifiable factors: a population study. *BMC Public Health*. 2015, 15:1195.

Pritzker KP, Aigner T. Terminology of osteoarthritis cartilage and bone histopathology - a proposal for a consensus. *Osteoarthritis Cartilage*. 2010, 18 Suppl 3:S7-9.

Pritzker KP, Gay S, Jimenez SA, Ostergaard K, Pelletier JP, Revell PA, Salter D, van den Berg WB. Osteoarthritis cartilage histopathology: grading and staging. *Osteoarthritis Cartilage*. 2006, 14(1):13-29.

Rosemann T, Gensichen J, Sauer N, Laux G, Szecsenyi J. The impact of concomitant depression on quality of life and health service utilization in patients with osteoarthritis. *Rheumatol Int*. 2007, 27(9):859-863.

Rosemann T, Laux G, Szecsenyi J, Wensing M, Grol R. Pain and osteoarthritis in primary care: factors associated with pain perception in a sample of 1,021 patients. *Pain Med*. 2008, 9(7):903-910.

Salinas-Sánchez DO, Zamilpa A, Pérez S, Herrera-Ruiz M, Tortoriello J, González-Cortazar M, Jiménez-Ferrer E. Effect of hautriwaic acid isolated from *Dodonaea viscosa* in a model of kaolin/carrageenan-induced monoarthritis. *Planta Med*. 2015, 81(14):1240-1247.

Shane Anderson A, Loeser RF. Why is osteoarthritis an age-related disease? *Best Pract Res Clin Rheumatol*. 2010, 24(1):15-26.

Sharma A, Kudesia P, Shi Q, Gandhi R. Anxiety and depression in patients with osteoarthritis: impact and management challenges. *Open Access Rheumatol*. 2016, 31(8):103-113.

Suokas AK, Walsh DA, McWilliams DF, Condon L, Moreton B, Wylde V, Arendt-Nielsen L, Zhang W. Quantitative sensory testing in painful osteoarthritis: a systematic review and meta-analysis. *Osteoarthritis Cartilage*. 2012, 20(10):1075-1085.

Tadano S, Takeda R, Sasaki K, Fujisawa T, Tohyama H. Gait characterization for osteoarthritis patients using wearable gait sensors (H-Gait systems). *J Biomech*. 2016, 49(5):684-690.

Turner J, Kelly B. Emotional dimensions of chronic disease. *West J Med*. 2000, 172(2):124-128.

Vrinten DH, Hamers FF. 'CatWalk' automated quantitative gait analysis as a novel method to assess mechanical allodynia in the rat; a comparison with von Frey testing. *Pain*. 2003, 102(1-2):203-209.

Wylde V, Palmer S, Learmonth ID, Dieppe P. Somatosensory abnormalities in knee OA *Rheumatology (Oxford)*. 2012, 51:535-543.

**Table 1** – Parameters used for the histopathological grading of the K/C model.

	Pritzker et al. (2006)	Pearson et al. 2011	Gerwin et al. (2010)
Grade 0	Intact, uninvolved cartilage.	Cartilage surface and morphology intact. Normal architecture of matrix. Intact cells with appropriate orientation.	No cartilage degeneration, Osteophytes in marginal zone <200µm. No changes in calcified cartilage and subchondral bone damage (1–2 layers of synovial lining cells).
Grade 1	Cells intact and cell death. Superficial cartilage intact, edema and/or fibrillation. Proliferation of cells (clusters) and cell hypertrophy.	Matrix intact, edema and/or superficial fibrillation (abrasion), focal superficial matrix condensation. Cell death, proliferation (clusters), hypertrophy, in the superficial zone.	Minimal degeneration; 5–10% of the total projected cartilage area affected by matrix or chondrocyte loss. Small osteophytes (200–299µm). Increased basophilia at tidemark, no fragmentation of tidemark, no or minimal/focal marrow changes. Increased thickening of subchondral bone subjacent to the area of greatest articular cartilage lesion severity. Increased number of lining cell layers (≥3–4 layers) or slight proliferation of subsynovial tissue.
Grade 2	Fibrillation through the superficial zone, surface abrasion with matrix loss within superficial zone. ±Discontinuity at superficial zone. ±Cationic stain matrix depletion (Safranin O or Toluidine Blue) upper 1/3 of cartilage (mid zone). ±Disorientation of chondron columns.	Surface discontinuity due to deep fibrillation of superficial zone, cationic stain matrix depletion of upper 1/3 of cartilage. Focal perichondral increased stain (mid zone). Disorientation of chondron columns. Cell death, proliferation (clusters) and hypertrophy.	Mild degeneration: 11–25% affected. Moderate osteophytes (300–399µm). Increased basophilia at tidemark, mild focal fragmentation of calcified cartilage of tidemark, mesenchymal change in marrow (fibroblastic cells) involving about 1/4 of subchondral region under lesion, increased thickening of subchondral bone subjacent to the area of greatest articular cartilage lesion severity. Increased number of lining cell layers (≥3–4 layers) and/or proliferation of subsynovial tissue.
Grade 3	Branched/complex fissures ±Cationic stain depletion (Safranin O or Toluidine Blue) into lower 2/3 of cartilage (deep zone) ±New collagen formation (polarized light microscopy, Picro Sirius Red stain).	Vertical fissures (clefts) into mid zone, branched fissures. Cationic stain depletion (Safranin O or Toluidine Blue) into lower 2/3 of cartilage (deep zone). New collagen formation (polarized light microscopy, Picro Sirius Red stain). Cell death, regeneration (clusters), hypertrophy in cartilage domains adjacent to fissures.	Moderate degeneration: 26–50% affected. Large osteophytes (400–499µm). Increased basophilia at tidemark, mild to marked fragmentation (multiple larger areas) of calcified cartilage/subchondral bone loss, mesenchymal change in marrow in up to 3/4 of total area, areas of marrow chondrogenesis may be evident but no major collapse of articular cartilage into epiphyseal bone (definite depression in surface). Increased number of lining cell layers (>4 layers) and/or proliferation of subsynovial tissue and infiltration of few inflammatory cells.

Grade 4	Superficial zone delamination and mid zone excavation. Cartilage matrix loss and cyst formation within cartilage matrix.	Erosion and loss of cartilage matrix. Delamination of superficial layer, mid layer cyst formation. Excavation of matrix superficial layer and mid zone.	Marked degeneration: 51–75% affected. Very large osteophytes ( $\geq 500\mu\text{m}$ ). Increased basophilia at tidemark, marked to severe fragmentation of calcified cartilage, marrow mesenchymal change involves up to 3/4 of area, articular cartilage has collapsed into the epiphysis to a depth of 250 $\mu\text{m}$ or less from tidemark (see definite depression in surface cartilage). Increased number of lining cell layers (>4 layers) and/or proliferation of subsynovial tissue, infiltration of large number of inflammatory cells.
Grade 5	Bone surface intact but reparative tissue surface present. Surface is sclerotic bone or reparative tissue including fibrocartilage.	Denudation, sclerotic bone or reparative tissue including fibrocartilage within denuded surface. Microfracture with repair limited to bone surface.	Severe degeneration: greater than 75% affected. Increased basophilia at tidemark, marked to severe fragmentation of calcified cartilage, marrow mesenchymal change involves up to 3/4 of area, articular cartilage has collapsed into the epiphysis to a depth of greater than 250 $\mu\text{m}$ from tidemark.
Grade 6	Joint margin and central osteophytes. Bone remodeling. Deformation of articular surface contour (more than osteophyte formation only) and includes microfracture and repair.	Deformation and bone remodeling (more than osteophyte formation only). It includes microfracture with fibrocartilaginous and osseous repair extending above the previous surface.	Non-applicable.

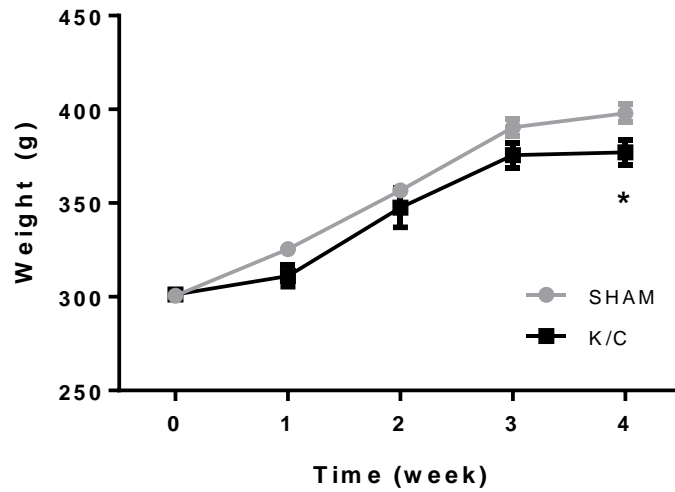


**Figure 1** – Weight gain in SHAM and K/C animals throughout the experimental period. Graphs show means + SEM. \* $p < 0.05$ .  $n_{\text{SHAM}} = 16$ ;  $n_{\text{ARTH}} = 16$ .

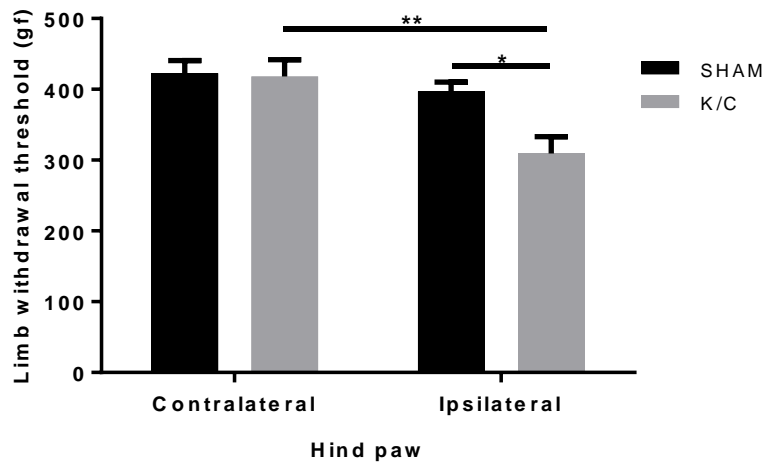


**Figure 2** – Mechanical hyperalgesia values measured with the PAM test 4 weeks after K/C intra-articular injection. Graphs show means + SEM. \* $p < 0.05$ ; \*\* $p < 0.01$ .  $n_{\text{SHAM}} = 16$ ;  $n_{\text{ARTH}} = 16$ .



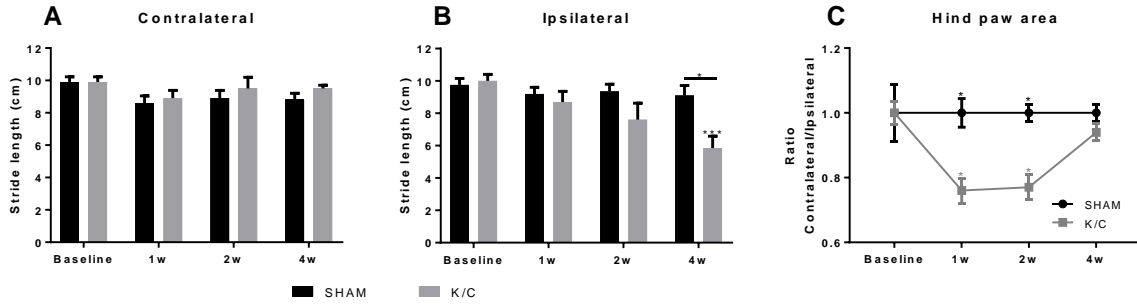


**Figure 3** – Gait evaluation before and after K/C intra-articular injection. **A** – Contralateral hind paw stride length in SHAM and K/C animals. **B** – Ipsilateral hind paw stride length in SHAM and K/C animals. **C** – Ratio of ipsi/contralateral contact area in SHAM and K/C animals. Graphs show means + SEM. \* $p < 0.05$ ; \*\*\* $p < 0.001$ .  $n_{\text{SHAM}}=6$ ;  $n_{\text{ARTH}}=6$ .

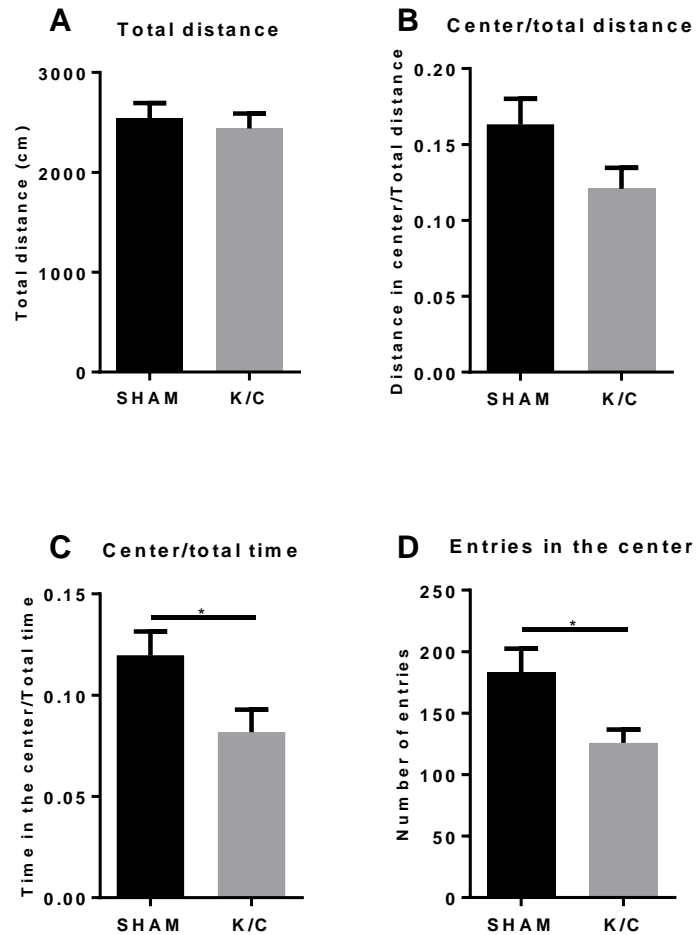


**Figure 4** – Locomotor and anxiety-like behaviors measured in the OF test 4 weeks after K/C intra-articular injection. **A** – Total distance travelled. **B** – Ratio of distance travelled in the center divided by the total distance travelled. **C** – Ratio of total time spent in the center by the total time of the

test. **D** – Number of total entries in the center of the arena. Graphs show means + SEM. \* $p < 0.05$ .  
 $n_{\text{SHAM}} = 16$ ;  $n_{\text{ARTH}} = 16$ .

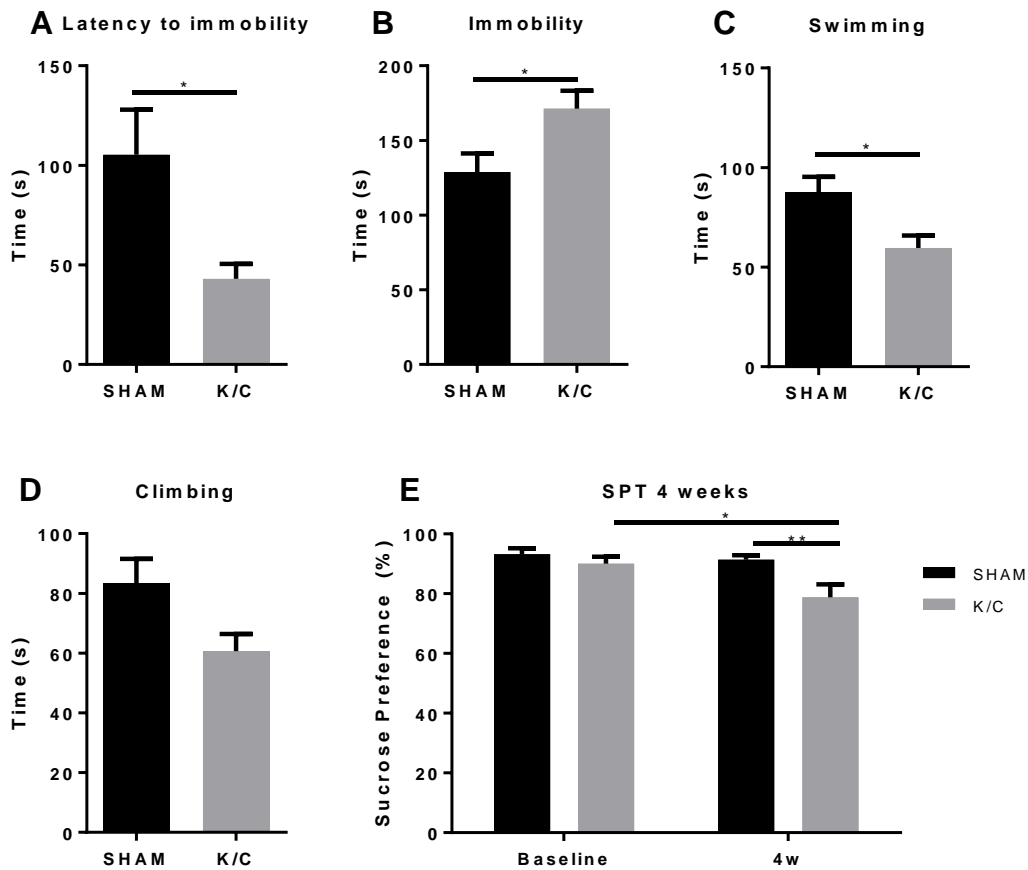


**Figure 5** – Depression-like behavior measured in the FST and SPT tests 4 weeks after K/C intra-articular injection. **A** – Latency to immobility in the FST test. **B** – Total time spent immobile in the FST test. **C** – Total time spent swimming in the FST test. **D** – Total time spent climbing in the FST test. **E** – Percentage of sucrose preference before and 6 weeks after K/C induction. Graphs show means + SEM. \* $p < 0.05$ ; \*\* $p < 0.01$ .  $n_{\text{SHAM}} = 16$ ;  $n_{\text{ARTH}} = 16$ .

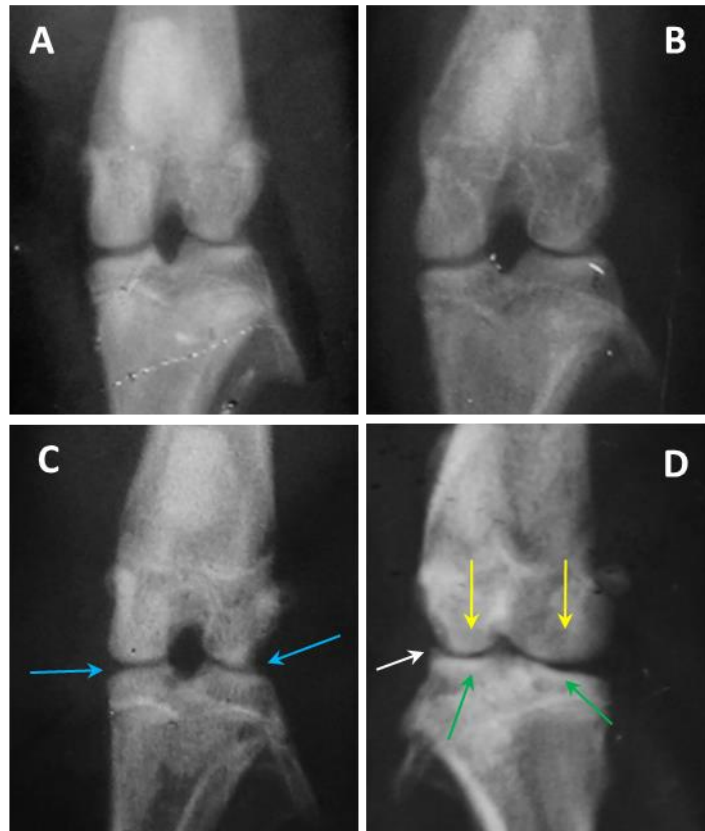


**Figure 6** – Progression of the radiographical findings in knee antero-posterior plane radiography of K/C animals. **A** – SHAM animals display normal articular structures. **B** – Up to week 2 post-induction, ARTH animals display no significant radiographical abnormalities. **C** – 3 weeks post-induction, ARTH animals show moderate (blue arrows) decrease of joint space. **D** – At 4 weeks, severe narrowing of joint space is evident (yellow arrows) as well as the development of osteophytes (white arrow) and sclerosis of subchondral bone (green arrows) corresponding to grade 4 of Kellgren and Lawrence's grading scale.

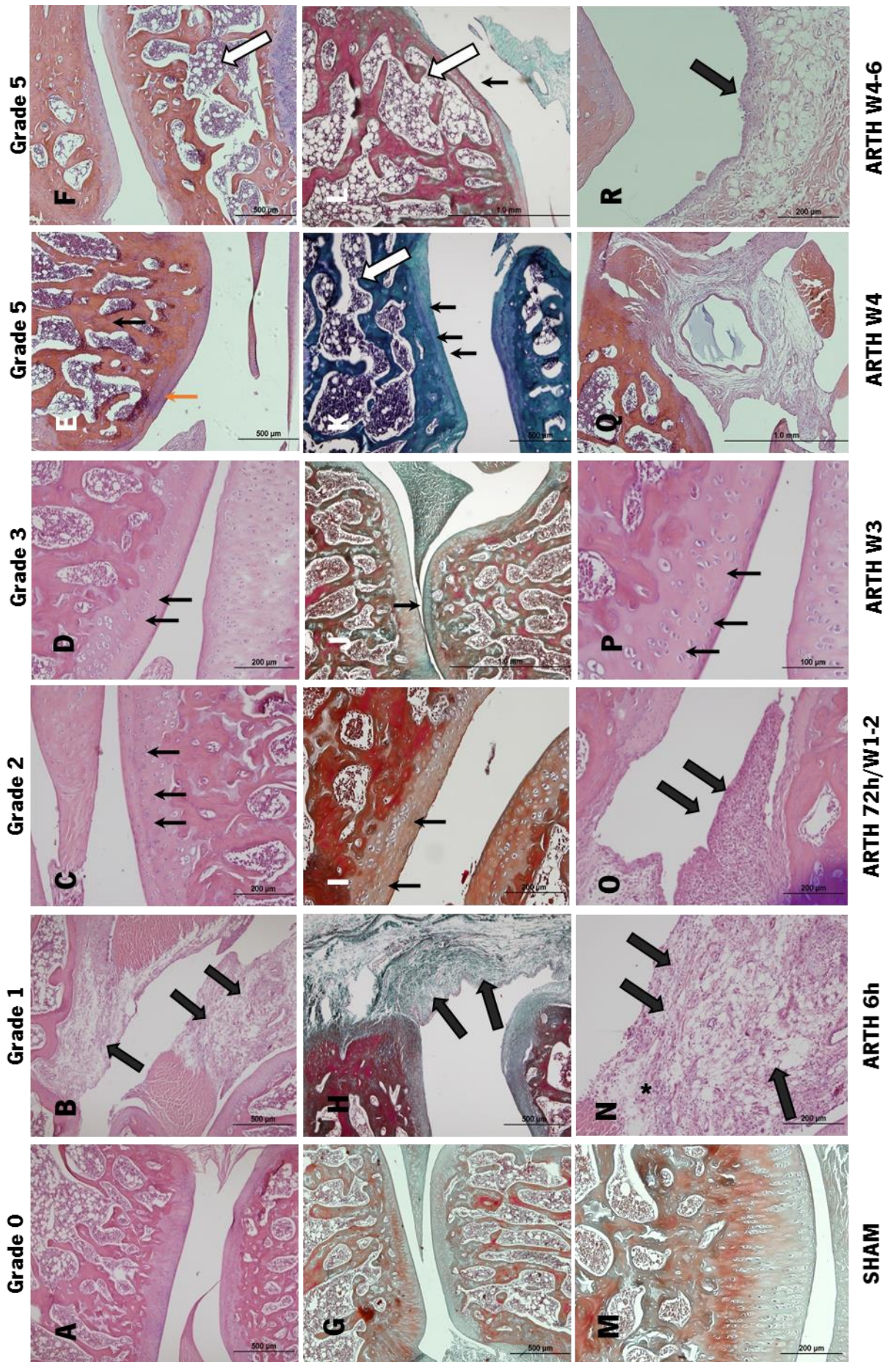


**Figure 7** – Histopathological evaluation of knee joint sections. SHAM animals display no changes in articular structures (**A,G,M**). K/C animals from 6 hours after induction display inflammatory reactions (**B,H,N**) and edema (**N**). From 72 hours up to 2 weeks, K/C animals display inflammatory reaction (**O**), chondrocyte disorganization (**C,I**) and cartilage fibrillation (**I**) while in week 3 the disorganization of chondron columns (**D,P**), narrowing of joint space (**J**) and hypocellularity of cartilage (**P**) is evident. At 4 weeks post induction K/C animals display thickening of subchondral bone trabeculae (**E** – black arrow), cartilage lamination (**E** – orange arrow), bone sclerosis (**K** – white arrows) and synovial cists (**Q**). Finally, from 4 weeks onwards, K/C animals display bone sclerosis (**F,L** – white arrows), cartilage depletion (**L** – black arrow) and inflammation (**R**). (**A-F; N-R**) Hematoxylin-eosin stain; (**G-M**) Masson's trichrome stain; (**M-R**) detail views of specific pathological aspects; \*edema; thick black arrow - inflammatory reaction; thin black arrow - focal disorganization of chondrocyte column; white arrows - bone sclerosis.



---

Ana David-Pereira, Sónia Puga, Sara Gonçalves, Diana Amorim, Cristina Silva, Antti Pertovaara,

Armando Almeida, Filipa Pinto-Ribeiro

**Metabotropic glutamate 5 receptor in the infralimbic cortex contributes to descending pain facilitation in healthy and arthritic animals**

*Neuroscience, 312:108-119*

2016





# METABOTROPIC GLUTAMATE 5 RECEPTOR IN THE INFRALIMBIC CORTEX CONTRIBUTES TO DESCENDING PAIN FACILITATION IN HEALTHY AND ARTHRITIC ANIMALS

A. DAVID-PEREIRA,<sup>a,b</sup> S. PUGA,<sup>a,b</sup> S. GONÇALVES,<sup>a,b</sup>  
D. AMORIM,<sup>a,b</sup> C. SILVA,<sup>a,b</sup> A. PERTOVAARA,<sup>c</sup>  
A. ALMEIDA,<sup>a,b</sup> AND F. PINTO-RIBEIRO<sup>a,b\*</sup>

<sup>a</sup> Life and Health Sciences Research Institute (ICVS), School of Health Sciences (ECS), Campus of Gualtar, University of Minho, 4750-057 Braga, Portugal

<sup>b</sup> ICVS/3B's – PT Government Associate Laboratory, Braga/Guimarães, Portugal

<sup>c</sup> Biomedicum Helsinki, Institute of Biomedicine/Physiology, University of Helsinki, Helsinki, Finland

**Abstract**—The involvement of the prefrontal cortex in pain processing has been recently addressed. We studied the role of the infralimbic cortex (IL) and group I metabotropic glutamate receptors (mGluRs) in descending modulation of nociception in control and monoarthritic (ARTH) conditions. Nociception was assessed using heat-induced paw withdrawal while drugs were microinjected in the IL of rats. Local anesthesia of the IL or the adjacent prelimbic cortex (PL) facilitated nociception, indicating that IL and PL are tonically promoting spinal antinociception. Phasic activation with glutamate (GLU) revealed opposing roles of the PL and IL; GLU in the PL had a fast antinociceptive action, while in the IL it had a slow onset pronociceptive action. IL administration of a local anesthetic or GLU produced identical results in ARTH and control animals. An mGluR5 agonist in the IL induced a pronociceptive effect in both groups, while mGluR5 antagonists had no effect in controls but induced antinociception in ARTH rats. Activation of the IL mGluR1 (through co-administration of mGluR1/5 agonist and mGluR5 antagonist) did not alter nociception in controls but induced antinociception in ARTH animals. IL administration of an mGluR1 antagonist failed to alter nociception in either experimental group. Finally, mGluR5 but not mGluR1 antagonists blocked the pronociceptive action

of GLU in both groups. The results indicate that IL contributes to descending modulation of nociception. mGluR5 in the IL enhance nociception in healthy control and monoarthritic animals, an effect that is tonic in ARTH. Moreover, activation of IL mGluR1s attenuates nociception following the development of monoarthritis. © 2015 IBRO. Published by Elsevier Ltd. All rights reserved.

**Key words:** infralimbic cortex, metabotropic glutamate receptor 5, experimental monoarthritis, pronociception.

## INTRODUCTION

In the last decade, there has been increasing evidence of the involvement of the prefrontal cortex (PFC) in the processing of the affective component of pain. It has been shown in both humans and animal models that, in chronic pain conditions, the PFC undergoes morphological and functional changes. These changes include decreased gray matter density in patients with chronic back pain (Apkarian et al., 2004). Increased medial PFC (mPFC) activation is correlated with the intensity and duration of spontaneous pain in patients with chronic pain (Baliki et al., 2006). Increases in the length, number of branches and spine density of basal dendrites of mPFC neurons as well as an increase in the NMDA/AMPA receptors ratio have been described in a rat model of neuropathic pain (Metz et al., 2009). Additionally, high-frequency electrical stimulation of the dorsal component of the mPFC, the anterior cingulate cortex (ACC), has been shown to be pronociceptive, decreasing heat-evoked paw withdrawal latencies (Zhang et al., 2005). Less is known, however, of the pain modulatory role of the anatomically and functionally distinct ventral mPFC (Heidbreder and Groenewegen, 2003; Vertes, 2006) that consists of the prelimbic (PL) and infralimbic (IL) cortices in the rodent brain. Zhang et al. (2004) have evaluated the electrophysiological responses of mPFC neurons (ACC, PL and IL) to mechanical noxious stimulation of the rat's tail, and were able to distinguish two subsets of responding neurons (nociceptive specific and wide-dynamic range-like neurons) that seem to encode nociceptive stimulus intensity.

In the present work, we studied the contribution of the IL to the modulation of nociception in the rat. We used local cerebral microinjections to generally activate and

\*Correspondence to: F. Pinto-Ribeiro, Life and Health Sciences Research Institute (ICVS), School of Health Sciences (ECS), Campus of Gualtar, University of Minho, 4750-057 Braga, Portugal. Tel: +351-253604852; fax: +351-253604820.

E-mail address: filiparibeiro@ecs.uminho.pt (F. Pinto-Ribeiro).

**Abbreviations:** ACC, anterior cingulate cortex; ARTH, K/C-induced monoarthritis; CHPG, (RS)-2-chloro-5-hydroxyglycine (mGluR5 agonist); DHPG, (S)-3,5-dihydroxyphenylglycine (mGluR1/5 agonist); GLU, glutamate; i.p., intraperitoneal; IL, infralimbic cortex; LIDO, lidocaine; LWT, limb withdrawal threshold; LY367385, (S)-(+)- $\alpha$ -amino-4-carboxy-2-methylbenzeneacetic acid (mGluR1 antagonist); mGluR, metabotropic glutamate receptor; MPEP, 6-methyl-2-(phenylethynyl)pyridine (mGluR5 antagonist); MTEP, 3-((2-methyl-1,3-thiazol-4-yl)ethynyl)pyridine hydrochloride (mGluR5 antagonist); mPFC, medial prefrontal cortex; PAM, pressure application measurement; PFC, prefrontal cortex; PL, prelimbic cortex; PWL, paw withdrawal latency; SHAM, control animals.

inhibit the IL, in order to evaluate its role upon the descending modulation of nociceptive behavior of rats. Furthermore, we used specific receptor agonists and antagonists for group I glutamate metabotropic receptors (mGluRs; includes receptors 1 and 5 – mGluR1 and mGluR5), in order to assess their involvement in IL-mediated descending modulation of nociception. The role of these receptors upon nociceptive modulation has been studied in several supraspinal brain areas (Palazzo et al., 2001; Neugebauer, 2002; Li and Neugebauer, 2004; Ren and Dubner, 2010), including the PL in the mPFC, where the blockade of mGluR1 can reverse the inhibition of neuronal spontaneous firing observed in sustained inflammatory pain (Ji and Neugebauer, 2011). Lastly, we investigated the impact of experimental monoarthritis upon IL-driven descending modulation of nociception.

## EXPERIMENTAL PROCEDURES

### Animals, anesthetics and ethical issues

The experiments were performed in adult Wistar Han male rats weighting 250–300 g (Charles River, France). The experimental protocol was approved by the Institutional Ethics Commission and followed the European Community Council Directive 2010/63/EU concerning the use of animals for scientific purposes. All efforts were made to minimize animal suffering and to use only the number of animals necessary to produce reliable scientific data.

During intracerebral cannula implantation, anesthesia was induced through the intraperitoneal (i.p.) administration of a mixture of ketamine (0.75 mg/kg, i.p.; Imalgene, Merial Lyon, France) and medetomidine (0.5 mg/kg, i.p.; Dorbene, Esteve Veterinaria, León, Spain). After the surgical procedures, anesthesia was reverted with atipamezole hydrochloride (1 mg/kg, i.p.; Antisedan, Orion Pharma, Orion Corporation, Espoo, Finland) and the animals were monitored until they were fully recovered. After the completion of the behavioral tasks, animals received a lethal dose of pentobarbitone and the brains were removed for histological confirmation of cannula placement (Fig. 1).

### Procedures for intracerebral injections

For intracerebral drug administration, cannulae were implanted as described by Pinto-Ribeiro et al. (2011). Briefly, rats were placed in a stereotaxic frame, a longitudinal incision was made in the scalp, which was retracted as well as the subcutaneous fascia, and a sterilized stainless-steel guide cannula (26 gauge; Plastics One, Roanoke, VA, USA) was implanted in the brain through a hole drilled in the skull. The tip of the guide cannula was positioned 1 mm above the right IL or PL (as a placement control) using the following stereotaxic coordinates: IL: 2.76 mm frontal to bregma; 0.6 mm lateral to midline; depth 4.2 mm; and PL: 2.76 mm frontal to the bregma; 0.6 mm lateral to midline; depth 3.5 mm (Paxinos and Watson, 2005). The guide cannula was fixed to the skull with screws and dental acrylic cement and the skin sutured around it. A dummy cannula (Plastics One) was

inserted into the guide cannula to prevent contamination and the animals were allowed to recover from the surgery for at least one week.

Test drugs were administered through a 33-gauge injection cannula (Plastics One) protruding 1 mm beyond the tip of the guide cannula. The microinjection was performed using a 5.0  $\mu$ L Hamilton syringe connected to the injection cannula by a polyethylene catheter (PE-10; Plastics One). The injection volume was 0.5  $\mu$ L and therefore, the spread of the injected drugs within the brain was expected to have a diameter of 1 mm (Myers, 1966). The efficacy of the injection was monitored by observing the movement of a small air bubble through the tubing. The injection lasted at least 20 s and the injection cannula was left in place for additional 30 s to minimize the return of drug solution back to the injection cannula.

### Induction of monoarthritis

The induction of a model of monoarthritis (ARTH) was performed 21 days before the beginning of the experiments, as described in detail elsewhere (Pinto-Ribeiro et al., 2013). Briefly, 3% kaolin and 3% carrageenan (Sigma–Aldrich, St. Louis, MO, USA) were dissolved in distilled water and injected into the synovial cavity of the right knee joint at a volume of 0.1 mL. This model produces mechanical hyperalgesia, which begins just in a few hours after surgery and extends up to 8 weeks (Radhakrishnan et al., 2003). In each animal, ARTH development was verified 1–2 h prior to each experiment. Only those rats that audibly vocalized every time after five flexion–extension movements of the knee joint were considered to have monoarthritis, and they were included in the ARTH group (Pinto-Ribeiro et al., 2011, 2013; Amorim et al., 2014). Control animals (SHAM) were injected with 0.1 mL saline in the synovial cavity of the right knee joint. SHAM animals did not vocalize to any of the five consecutive flexion–extension movements of the knee joint.

Additionally, we used the pressure application measurement (PAM) to verify the development of primary mechanical hyperalgesia in ARTH animals (Barton et al., 2007). To perform the test, the animal is held securely while the force transducer unit (fitted to the experimenter's thumb) is placed on one side of the knee joint and the forefinger on the other. Increasing force (0–1500 g) is gradually applied across the joint until a behavioral response is observed (paw-withdrawal, vocalization, wriggling or vocalization), with a cut-off of 5 s. The peak force (in grams of force (gf)) applied immediately prior to the behavioral response is registered as the limb withdrawal threshold (LWT). LWT was measured twice in both the ipsilateral and contralateral limbs at 1-min intervals. The mean LWTs were calculated per animal. At the end of the session animals were returned to their home cage.

### Behavioral assessment of nociception – Hargreaves model

Prior to performing the behavioral tests, rats were habituated to the experimental conditions (i) by allowing them to spend 1–2 h daily in the testing room during the week preceding any testing, and (ii) by performing daily

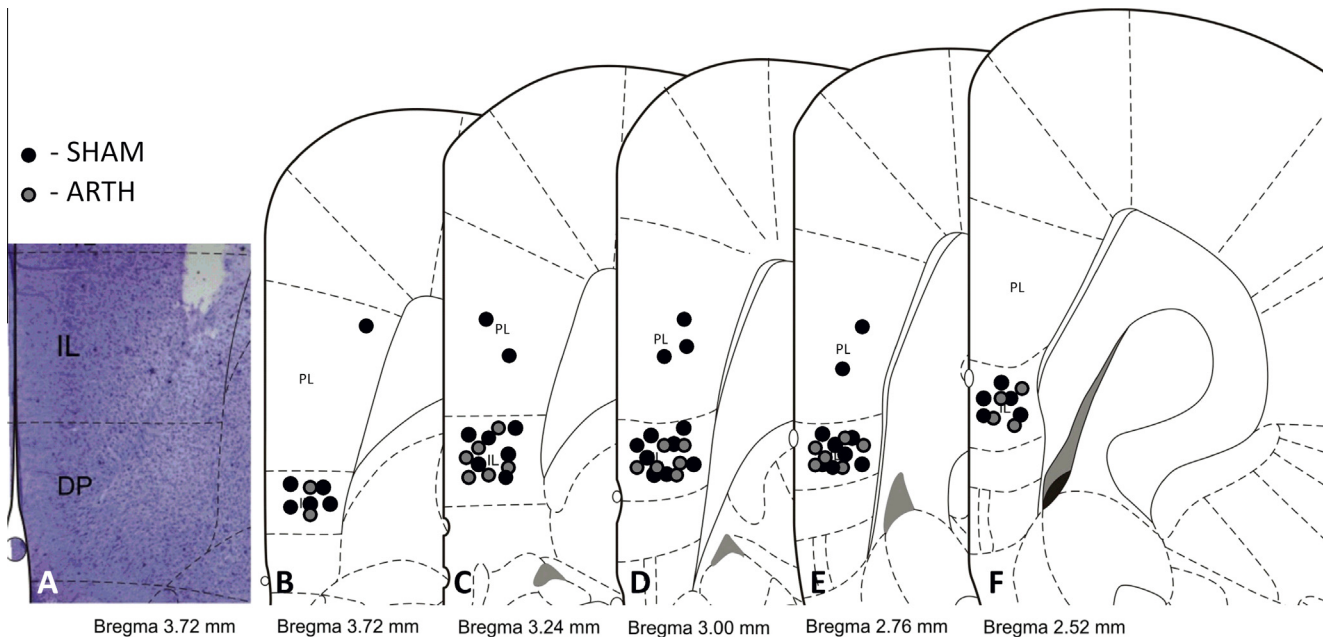


**Fig. 1.** Anatomical confirmation of drug injection sites in the prelimbic (PL) and infralimbic (IL) cortices. (A) Photomicrograph of an example of the drug injection site in the IL of the rat brain (AP: +3.72 mm from bregma) superimposed with the appropriate legend of Paxinos and Watson (2005) stereotaxic atlas. (B–F) Schematic representation of other injection sites in the PL and IL (B: +3.72 mm, C: +3.24 mm, D: +3.00 mm, E: +2.76 mm; F: +2.52 mm). DP – dorsal peduncular cortex; IL – infralimbic cortex; PL – prelimbic cortex.

handling sessions. For assessing nociception in unanesthetized animals, the latency of hindpaw withdrawal following radiant heat stimulation (Hargreaves test; Plantar Test Device Model 37370, Ugo Basile, Comerio, Italy) was determined. In each behavioral session, the withdrawal latency was assessed prior to drug administration and at various intervals following the intracerebral injections (Fig. 2). At each time point, the measurements were repeated twice at an interval of 1 min (except for glutamate (GLU) due to its fast effect) and the mean of these values was used in further calculations. The cut-off time for radiant-heat exposure was set at 15 s in order to avoid any damage to the skin.

## Drugs

GLU (Merck, Darmstadt, Germany), (RS)-2-chloro-5-hydroxyglycine (CHPG; mGluR5 agonist), (S)-3,5-dihydroxyphenylglycine (DHPG; mGluR1/5 agonist; Tocris, Bristol, United Kingdom), and 3-((2-Methyl-1,3-thiazol-4-yl) ethynyl)pyridine hydrochloride (MTEP; mGluR5 antagonist, Tocris, Bristol, United Kingdom) solutions for intracerebral drug injection were prepared with sterilized saline solution 0.9% (Unither, Amiens, France; pH 7.2). 6-Methyl-2-(phenylethynyl)pyridine (MPEP; mGluR5 antagonist; Tocris, Bristol, United Kingdom) was dissolved in 10% dimethyl sulfoxide (DMSO). (S)-(+)- $\alpha$ -Amino-4-carboxy-2-methylbenzeneacetic acid (LY367385; mGluR1 antagonist) was dissolved in 2% sodium hydroxide solution (NaOH). Lidocaine (2%; LIDO) was acquired as a solution (B. Braun Medical, Barcarena, Portugal).

Previous studies showed that the 50 nmol dose of GLU (Pinto-Ribeiro et al., 2011), DHPG, CHPG (Anshah et al., 2009) and MPEP (Movsesyan et al., 2001) and the 40 nmol dose of LY367385 (de Novellis et al., 2005)

are effective in activating/blocking mGluRs after intracerebral microinjection in the rat. Since there are studies suggesting that MPEP has significant non-specific actions, including inhibition of NMDA receptors (Lea and Faden, 2006) and positive allosteric modulation of mGluR4 (Mathiesen et al., 2003), MTEP was also used and their effects compared. The MTEP dose (50 nmol) used was the same as for MPEP to allow the comparison of the two antagonists' efficacy. An observation window of 50 min was determined by evaluating alterations in nociceptive behavior at fixed time points (Fig. 2) until the drug effect was no longer observed. Control injections with the respective vehicle (VEH) solutions were performed as control values, in order to avoid any bias that might result from injecting the solution itself.

## Rotarod test

To exclude motor effects of drug injection in the IL, motor performance was evaluated on a Rotarod equipment (3376-4R; TSE Systems, USA) using an accelerating protocol. In this protocol, SHAM and ARTH animals were placed on a rod that accelerated smoothly from 4 to 40 rotations per minute (rpm) over a period of 5 min. The first 3 days of protocol served as training. In each day, rats underwent the accelerating protocol for a total of 4 trials per day, with a rest of at least 20 min between each trial. On the following days, the effect of each drug upon motor performance was tested on the same accelerating protocol and the latency to fall was recorded (Monville et al., 2006). Due to the small window of drug action observed in the Hargreaves model, during drug testing animals underwent only two trials of the accelerating protocol, 10 and 30 min after drug administration (Fig. 2).

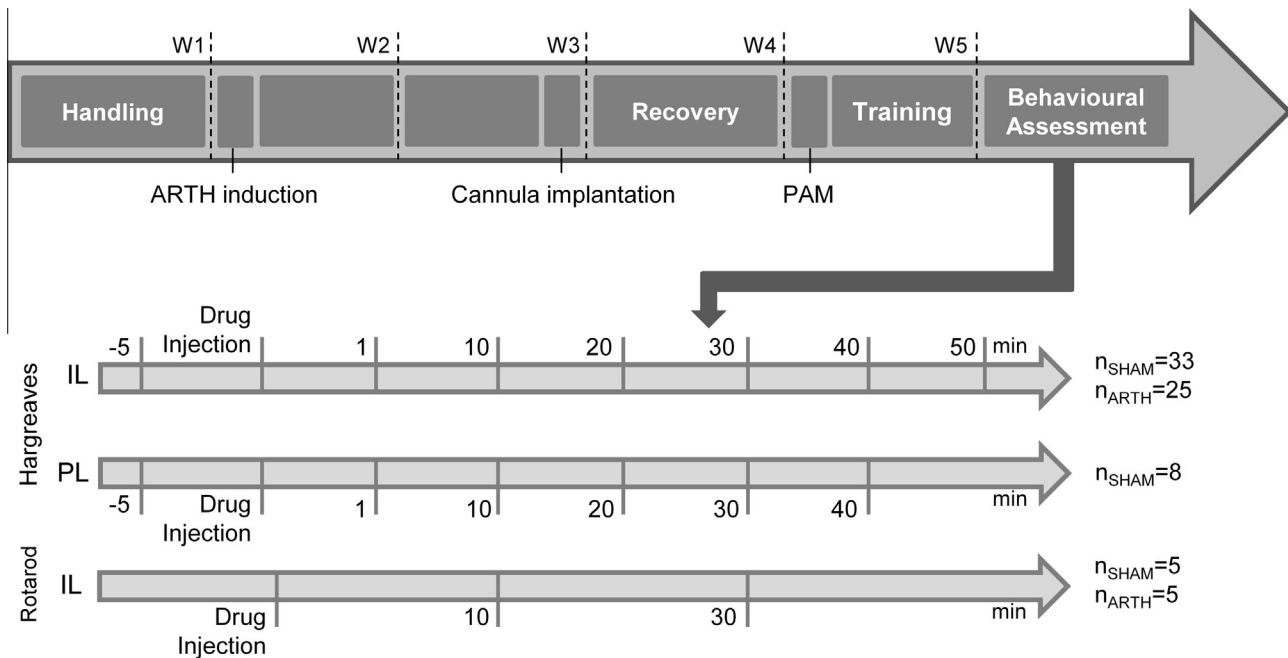


**Fig. 2.** Schematic representation of the experimental design timeline. Rats were habituated to the laboratory and the experimenter for 5 days. After habituation, animals belonging to the arthritic (ARTH) group received an intra-synovial injection of 3% kaolin/carrageenan while control (SHAM) animals received an intra-synovial injection of saline solution. Two weeks after monoarthritis induction, animals were implanted with a guide cannula in the infralimbic (IL) or in the prelimbic (PL) cortices. After recovery (one week), rats performed the pressure application measurement (PAM) and were trained in the paw-withdrawal apparatus. Pharmacological tests were performed at the same time points for all the drugs. min – minutes; W1–5 – weeks 1 to 5.

### Course of the behavioral study

Three weeks after ARTH induction and at least one week after guide cannula implantation, animals were trained in the Hargreaves test. Four weeks after ARTH induction, the tonic and phasic action of the IL and PL and the effect of the activation/inactivation of mGluR1 and/or mGluR5 in the IL upon nociceptive behavior were determined in unanesthetized animals through the assessment of changes in paw withdrawal latency (PWL) after drug injection. Withdrawal latencies were assessed 1, 10, 20, 30, 40 and 50 min following intracerebral injections (Fig. 2). The interval between behavioral assessments of different drugs was of at least three days. The order for testing each different drug was randomized among animals. Animals were injected with a maximum of five different drugs, in random order.

### Statistics

Using the GraphPad Prism 5 software (GraphPad Software Inc., La Jolla, CA, USA), a two-way analysis of variance (ANOVA) followed by *t*-test with a Bonferroni correction for multiple comparisons was used to compare behavioral results among experimental groups.  $P < .05$  was considered to represent a significant difference. Data are presented as mean  $\pm$  standard error of the mean (SEM).

## RESULTS

### Healthy animals

*GLU-induced activation of PL and IL has opposite phasic effects on nociceptive behavior in healthy rats.* In 100

order to study a possible phasic role of the PL and the IL upon nociceptive behavior in healthy rats, we microinjected GLU into these areas and evaluated changes in the heat-evoked PWL of SHAM animals. Overall, GLU administration in the PL had an antinociceptive effect in SHAM animals, as revealed by an increase in the PWL (main effect of GLU:  $F_{1,120} = 4.99$ ;  $P = 0.0273$ ), and this effect varied with time (interaction drug effect  $\times$  time:  $F_{5,120} = 2.36$ ,  $P = 0.0415$ ). *Post hoc* tests showed that GLU treatment of the PL induced a short-lasting antinociceptive effect that was maximal 1 min after GLU injection and that disappeared within 10 min (Fig. 3A). In contrast, GLU administration in the IL resulted in a pronociceptive effect as revealed by the decrease of the PWL in SHAM animals (main effect of GLU:  $F_{1,40} = 15.73$ ;  $P = 0.0003$ ), and this pronociceptive effect varied with time (interaction drug  $\times$  time:  $F_{5,40} = 3.88$ ,  $P = 0.0059$ ). While the antinociceptive effect induced by GLU in the PL was of rapid onset and short duration, *post hoc* tests indicated that GLU in the IL induced a pronociceptive effect that was significant from 10 to 30 min after GLU injection (Fig. 3C).

*Local anesthesia of both PL and IL reveals tonic antinociceptive effects in healthy rats.* To evaluate a possible tonic role of the PL and the IL in the descending control of nociceptive behavior in healthy rats, we microinjected LIDO, a local anesthetic, and evaluated changes in heat-evoked PWL of SHAM animals. Overall, the inhibition of PL and IL with LIDO significantly decreased PWL of SHAM animals (main effect of LIDO in PL:  $F_{1,103} = 11.63$ ,  $P = 0.0009$ ; main effect of LIDO in IL:  $F_{1,44} = 7.80$ ;  $P = 0.0077$ ), showing

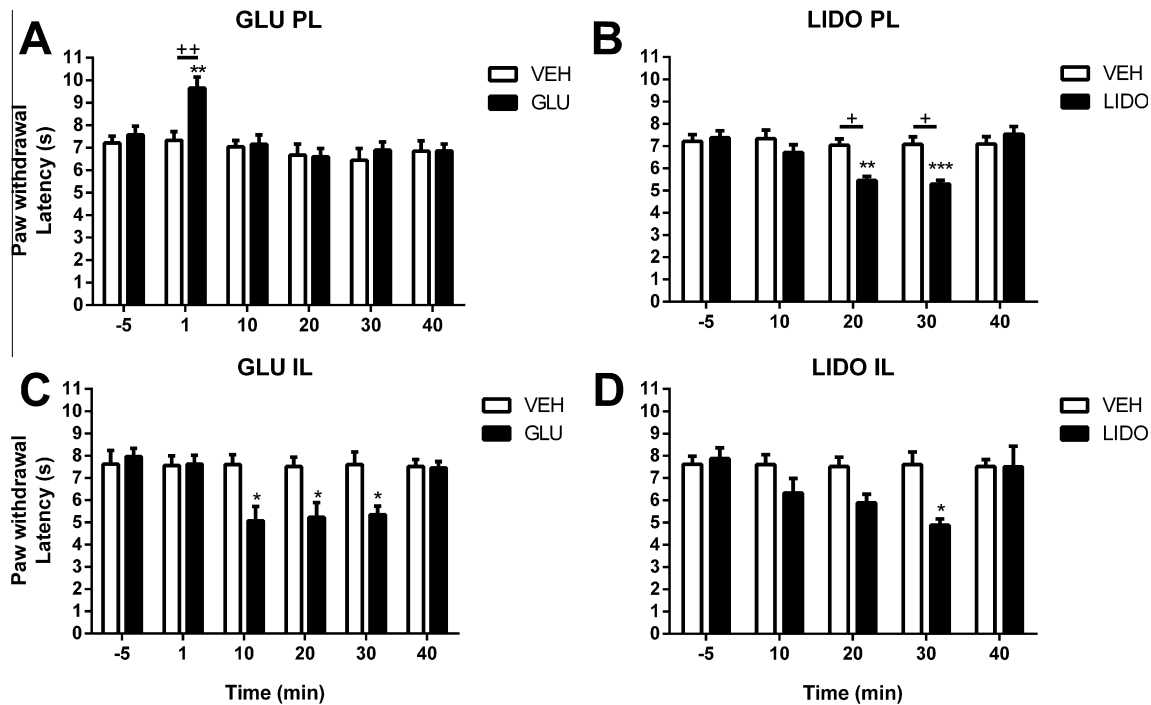


**Fig. 3.** Radiant heat-evoked paw withdrawal latencies (PWL) of healthy control animals after intracerebral drug administrations in the prelimbic (PL; A, B) or infralimbic (IL; C, D) cortex (GLU, glutamate, 50 nmol; LIDO, lidocaine, 2%; VEH, vehicle). (A) GLU in the PL increased the PWL 1 min after its administration; (B) LIDO in the PL decreased the PWL 10 and 20 min after its administration; (C) GLU in the IL decreased the PWL 10–30 min after its administration; (D) LIDO in the IL decreased the PWL 30 min after its administration. Graphs show the mean  $\pm$  SEM (VEH:  $n_{PL} = 10$ ;  $n_{IL} = 6$ ; GLU:  $n_{PL} = 10$ ;  $n_{IL} = 6$ ; LIDO:  $n_{PL} = 10$ ;  $n_{IL} = 7$ ). Drug injections were performed at time point 0.  $^+P < 0.05$ ;  $^{**/+}P < 0.01$ ;  $^{***}P < 0.001$  (*t*-test with a Bonferroni correction for multiple comparisons;  $^{+/+}$  represent the comparison of injection results with pre-injection (–5 min) value;  $^{+/+}$  represent the comparison of time point values of SHAM vs. ARTH).

that both these areas tonically inhibit nociception in healthy rats. *Post-hoc* tests showed that these LIDO-induced alterations in PWL lasted for 10–30 min (Fig. 3B, D).

The following experiments focused on the prolonged pronociceptive action of GLU in the IL.

### Effect of IL pharmacological manipulation upon nociceptive behavior

*The IL modulates heat-evoked nociceptive behavior of SHAM and ARTH animals.* To assess if the long-lasting pronociceptive effect of GLU microinjection in the IL was due to activation of metabotropic rather than ionotropic receptors, we selectively activated mGluR1 and mGluR5 in the IL and assessed its impact upon nociceptive behavior of SHAM and ARTH animals. Additionally, we also determined the time window during which drugs microinjected into the IL affected nociceptive behavior by testing noxious heat-evoked PWL in SHAM and ARTH rats at various time points after cortical drug administrations (Figs. 4–6). IL injection of the VEH failed to alter PWL (main effect of time after VEH treatment:  $F_{5,66} = 0.142$ ; Fig. 4A), independent of the experimental group (interaction experimental group  $\times$  time after vehicle treatment:  $F_{5,66} = 0.05$ ). GLU or LIDO in the IL significantly decreased PWL of SHAM and ARTH animals (main effect of time after GLU treatment:  $F_{5,59} = 14.80$ ,  $P < 0.0001$ ; main effect of time after LIDO

treatment:  $F_{5,61} = 8.70$ ,  $P < 0.0001$ ) for 10–30 min after drug injection (Figs. 4B, C). The pronociceptive effects of GLU or LIDO in the IL did not vary between the SHAM and ARTH groups (interaction experimental group  $\times$  time after GLU microinjection:  $F_{5,59} = 0.48$ ; interaction experimental group  $\times$  time after LIDO microinjection:  $F_{5,61} = 0.70$ ).

DHPG (an mGluR1/5 agonist) in IL significantly decreased PWL (main effect of time after DHPG treatment:  $F_{5,66} = 5.02$ ,  $P = 0.006$ ; Fig. 4D), an effect that varied with the experimental group (interaction experimental group  $\times$  time after cortical drug treatment:  $F_{5,66} = 3.76$ ,  $P = 0.0047$ ). *Post hoc* tests indicated that the pronociceptive effect of DHPG in IL was significantly stronger in SHAM than ARTH animals 30 min after drug treatment (Fig. 4C).

*Prolonged pronociceptive behavior elicited by GLU in the IL is not mediated by mGluR1 activation.* To assess if the mGluR1 was responsible for the long-lasting pronociceptive effect of GLU microinjection in the IL, we selectively activated and/or inhibited mGluR1 in the IL and assessed its impact on nociceptive behavior in SHAM and ARTH animals.

The IL co-administration of DHPG with MPEP (with the purpose of activating mGluR1) had a significant effect on PWL (main effect of time after DHPG + MPEP treatment:  $F_{5,74} = 4.07$ ,  $P = 0.0026$ ), that varied with the experimental group (interaction experimental group  $\times$  time after drug treatment:  $F_{5,75} = 7.96$ ,  $P < 0.0001$ ). *Post hoc* tests indicated that the combination of DHPG

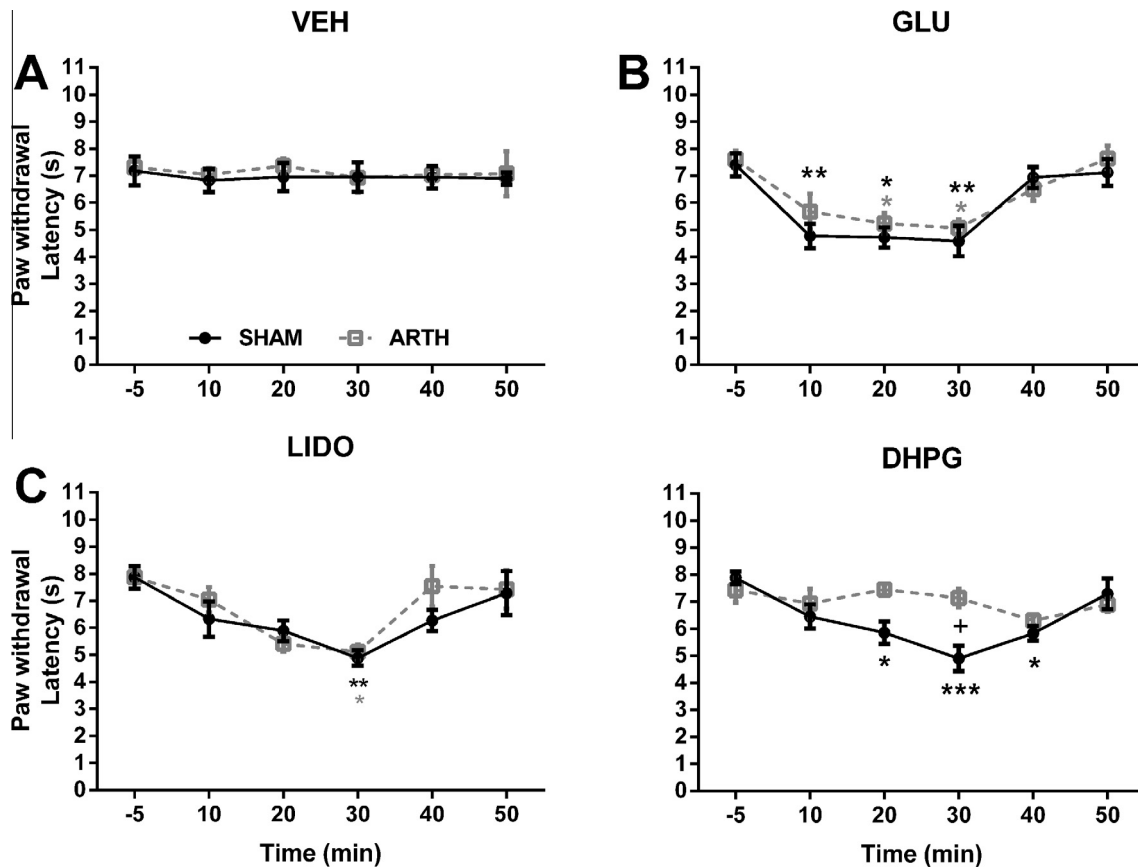


**Fig. 4.** Radiant heat-evoked paw withdrawal latencies (PWL) after intracerebral administration in the infralimbic cortex (IL). Effects of IL administration of vehicle (VEH; A), glutamate (GLU, 50 nmol; B), LIDO (2%; C) and DHPG (an mGluR1/5 agonist, 50 nmol; D) in control (SHAM, black full lines) and monoarthritic (ARTH, gray dashed lines) animals. Drug injections were performed at time point 0. Data are presented as mean  $\pm$  SEM. VEH:  $n_{\text{SHAM}} = 6$ ,  $n_{\text{ARTH}} = 8$ ; GLU:  $n_{\text{SHAM}} = 6$ ,  $n_{\text{ARTH}} = 6$ ; LIDO:  $n_{\text{SHAM}} = 7$ ,  $n_{\text{ARTH}} = 6$ ; DHPG:  $n_{\text{SHAM}} = 7$ ,  $n_{\text{ARTH}} = 6$ .  $^{\dagger}$   $P < 0.05$ ;  $^{**}$   $P < 0.01$ ;  $^{***}$   $P < 0.001$  (*t*-test with a Bonferroni correction for multiple comparisons;  $^{*†}$  represent the comparison of injection results with pre-injection (–5 min) value;  $^{+}$  represents the comparison of time point values of SHAM vs. ARTH).

and MPEP prolonged the PWL only in the ARTH group and this antinociceptive effect was significantly stronger in the SHAM than the ARTH group from 10 to 30 min after the drug treatment (Fig. 5B). LY367385 alone (an mGluR1 antagonist) did not alter PWL (main effect of time after LY367385 treatment:  $F_{5,60} = 0.4909$ ,  $P = 0.7818$ ; Fig. 5C), independent of the experimental group (interaction experimental group  $\times$  time after drug treatment:  $F_{5,60} = 0.16$ ). Co-administration of DHPG, MPEP and LY367385 in the IL failed to alter PWL (main effect of time after DHPG + MPEP + LY367358 treatment:  $F_{5,60} = 0.26$ ,  $P = 0.9321$ ), independent of the experimental group (interaction experimental group  $\times$  time after drug treatment:  $F_{5,60} = 0.70$ ; Fig. 5D).

IL co-administration of LY367385 and GLU significantly decreased PWL of SHAM and ARTH animals (main effect of time after LY367358 + GLU treatment:  $F_{5,128} = 25.60$ ,  $P < 0.0001$ ) for 20–30 min after drug injection (Fig. 5E). The pronociceptive effects of the combination of LY367385 and GLU in the IL did not vary between SHAM and ARTH groups (interaction experimental group  $\times$  time after microinjection:  $F_{5,128} = 0.94$ ).

No changes were observed in PWL after vehicle microinjection to the IL (main effect of time after VEH

treatment:  $F_{5,66} = 0.14$ ), independent of the experimental group (interaction experimental group  $\times$  time after drug treatment:  $F_{5,66} = 0.05$ ; Fig. 5A).

*mGluR5 mediates the prolonged pronociceptive behavior elicited by GLU in the IL.* To assess if the long-lasting pronociceptive effect of GLU microinjection was mediated through mGluR5 in the IL, we selectively activated and/or inhibited mGluR5 in the IL and assessed its impact on nociceptive behavior in SHAM and ARTH animals.

CHPG (an mGluR5 agonist) in the IL significantly decreased PWL of SHAM and ARTH animals (main effect of time after CHPG treatment:  $F_{5,120} = 16.38$ ,  $P < 0.0001$ ) for 10–40 min after drug injection (Fig. 6B). The pronociceptive effects of CHPG in the IL did not vary between the SHAM and ARTH groups (interaction experimental group  $\times$  time after microinjection:  $F_{5,120} = 0.30$ ). IL administration of MPEP or MTEP alone (mGluR5 antagonists) had a significant effect on PWL (main effect of time after MPEP treatment:  $F_{5,82} = 4.56$ ;  $P < 0.0001$ ; main effect of time after MTEP treatment:  $F_{5,77} = 5.02$ ;  $P = 0.0005$ ). The effect of MPEP or MTEP alone in IL varied with the experimental group (interaction experimental group  $\times$  time after MPEP administration:  $F_{5,82} = 4.56$ ,  $P < 0.0001$ ; interaction experimental

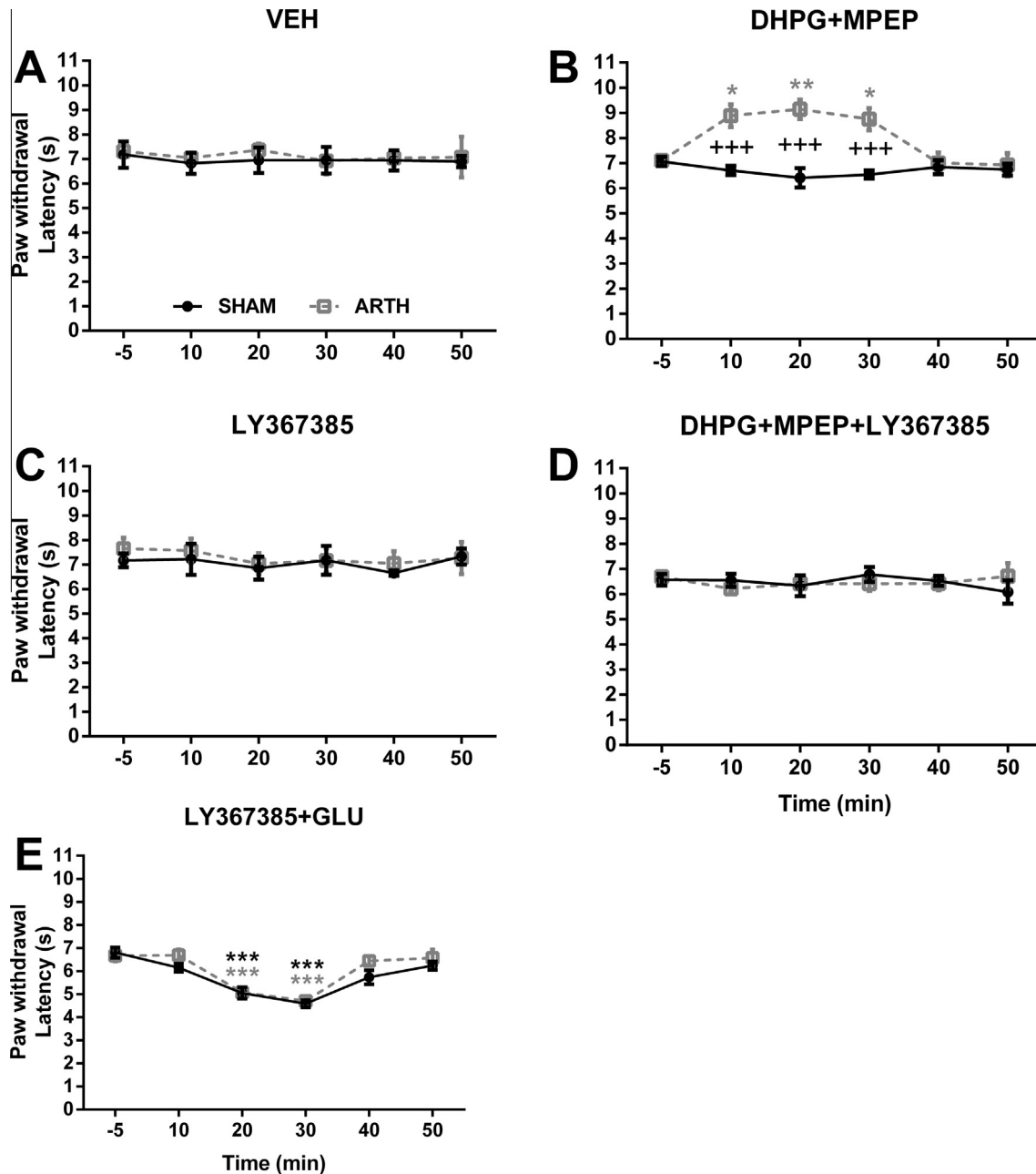


**Fig. 5.** Radiant heat-evoked paw withdrawal latencies (PWL) after intracerebral mGluR1 agonists/antagonists administration in the infralimbic cortex (IL). Effects of IL administration of vehicle (VEH; A), a combination of DHPG and MPEP (an mGluR1/5 agonist and an mGluR5 antagonist, respectively; 50 nmol each; B), LY367385 (an mGluR1 antagonist, 40 nmol; C), a combination of DHPG, MPEP and LY367385 (50 nmol DHPG and MPEP, 40 nmol LY367385; D) and a combination of LY367385 and GLU (40 nmol LY367385, 50 nmol GLU; E) in control (SHAM, black full lines) and monoarthritic (ARTH, gray dashed lines) animals. Drug injections were performed at time point 0. Data are presented as mean + SEM. VEH:  $n_{\text{SHAM}} = 6$ ,  $n_{\text{ARTH}} = 8$ ; DHPG + MPEP:  $n_{\text{SHAM}} = 9$ ,  $n_{\text{ARTH}} = 6$ ; LY367385:  $n_{\text{SHAM}} = 6$ ,  $n_{\text{ARTH}} = 6$ ; DHPG + MPEP + LY367385:  $n_{\text{SHAM}} = 6$ ,  $n_{\text{ARTH}} = 6$ ; LY367385 + GLU:  $n_{\text{SHAM}} = 11$ ,  $n_{\text{ARTH}} = 11$ .  $P < 0.05$ ;  $^{*}P < 0.01$ ;  $^{***}P < 0.001$  (t-test with a Bonferroni correction for multiple comparisons;  $^{*}/^{**}/^{***}$  represent the comparison of injection results with pre-injection (–5 min) value;  $^{++}/^{+++}$  represent the comparison of time point values of SHAM vs. ARTH).

group  $\times$  time after MPEP administration:  $F_{5,77} = 4.56$ ,  $P = 0.0010$ ). *Post hoc* tests indicated that PWL was prolonged after MPEP or MPEP in the ARTH but not in the SHAM group and that the PWL was significantly longer in the ARTH than the SHAM group 30–40 min after MPEP or MPEP administration (Figs. 6C, D).

Co-administration of MPEP/MTEP and GLU in the IL failed to alter PWL (main effect of time after MPEP + GLU treatment:  $F_{5,95} = 0.21$ ;  $P = 0.9568$ ; main effect of time after MTEP + GLU treatment:  $F_{5,66} = 0.25$ ;  $P = 0.9396$ ), independent of the experimental group (interaction experimental group  $\times$  time after

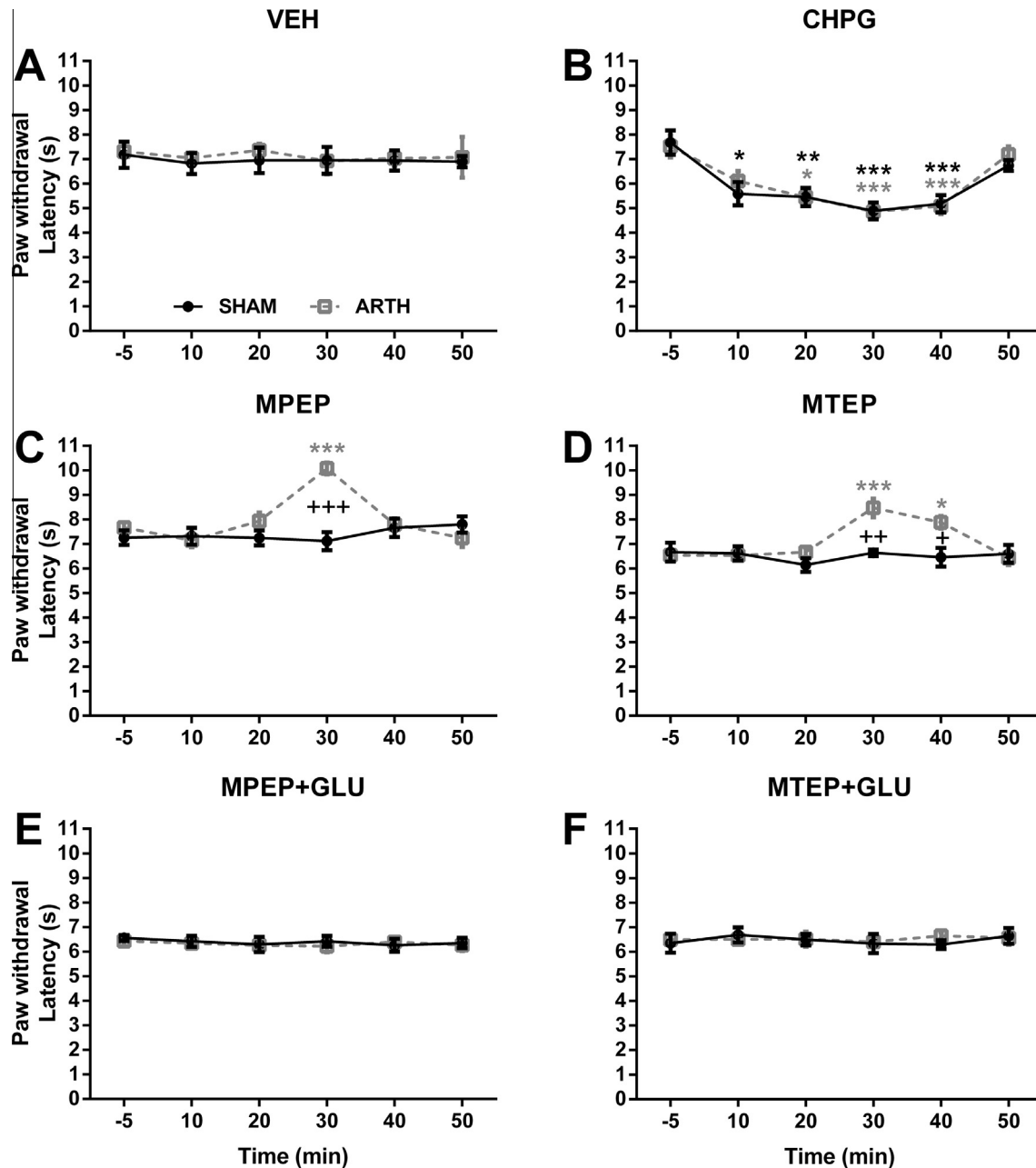


**Fig. 6.** Radiant heat-evoked paw withdrawal latencies (PWL) after intracerebral mGluR5 agonists/antagonists administration in the infralimbic cortex (IL). Effects of IL administration of vehicle (VEH; A), CHPG (an mGluR5 agonist, 50 nmol; B), MPEP (an mGluR5 antagonist, 50 nmol; C), MTEP (an mGluR5 receptor antagonist, 50 nmol; D), MPEP + GLU (50 nmol each; E) and MTEP + GLU (50 nmol each; F) in control (SHAM, black full lines) and monoarthritic (ARTH, gray dashed lines) animals. Drug injections were performed at time point 0. Data are presented as mean + SEM. VEH:  $n_{\text{SHAM}} = 6$ ,  $n_{\text{ARTH}} = 8$ ; CHPG:  $n_{\text{SHAM}} = 11$ ,  $n_{\text{ARTH}} = 11$ ; MPEP:  $n_{\text{SHAM}} = 7$ ,  $n_{\text{ARTH}} = 9$ ; MTEP:  $n_{\text{SHAM}} = 6$ ,  $n_{\text{ARTH}} = 9$ ; MPEP + GLU:  $n_{\text{SHAM}} = 11$ ,  $n_{\text{ARTH}} = 7$ ; MTEP + GLU:  $n_{\text{SHAM}} = 6$ ,  $n_{\text{ARTH}} = 7$ .  $^{*}P < 0.05$ ;  $^{***}P < 0.001$  ( $t$ -test with a Bonferroni correction for multiple comparisons;  $^{*}/^{**}/^{***}$  represent the comparison of injection results with pre-injection (–5 min) value;  $^{+}/^{++}/^{+++}$  represent the comparison of time point values of SHAM vs. ARTH).

MPEP + GLU treatment:  $F_{5,95} = 0.11$ ; interaction experimental group  $\times$  time after MTEP + GLU treatment:  $F_{5,66} = 0.26$ ; Figs. 6E, F).

No changes were observed in PWL after vehicle microinjection to the IL (main effect of time after VEH treatment:  $F_{5,66} = 0.14$ ), independent of the experimental group (interaction experimental group  $\times$  time after drug treatment:  $F_{5,66} = 0.05$ ; Fig. 6A).

ARTH animals present mechanical hyperalgesia in the affected knee joint. Four weeks after ARTH induction, mechanically evoked LWT of the knee joint of ARTH animals was significantly decreased when compared to SHAM (main effect of experimental group:  $F_{1,26} = 6.50$ ;  $P = 0.0171$ ), an effect dependent of the tested limb (interaction: experimental group  $\times$  limb:  $F_{1,26} = 12.53$ ;  $P = 0.0015$ ). *Post hoc* tests indicate that LWT in the



ipsilateral joint of ARTH animals is significantly decreased when compared to the contralateral knee joint of the ARTH group and to the ipsilateral knee joint of SHAM group (Fig. 7A).

*Motor performance was not altered after drug microinjection in the IL.* Locomotor performance was assessed in the Rotarod test to evaluate potential motor effects elicited by drug administration. The results obtained show that although ARTH animals have a significantly decreased latency to fall when compared to the SHAM group (main effect of experimental group:  $F_{1,64} = 6.39$ ,  $P = 0.0140$ ), none of the microinjected drugs had an effect on motor performance of SHAM and ARTH rats at the time points tested in the nociceptive assessment (main effect of drug treatment:  $F_{7,64} = 0.10$ ,  $P = 0.9980$ ). This effect was independent of the experimental group (interaction experimental group  $\times$  drug treatment:  $F_{7,64} = 0.12$ ; Fig. 7B).

## DISCUSSION

In the present work, we demonstrate for the first time that administration of GLU to the IL induces prolonged behavioral hyperalgesia. This effect is mediated by the mGluR5, since IL administration of a selective mGluR5 agonist mimicked the behavioral pronociceptive effect evoked by GLU in both SHAM and ARTH animals. Moreover, previous administration of an antagonist of mGluR5, but not mGluR1, in the IL was effective in blocking the pronociceptive effect of GLU in both experimental groups. The increase in withdrawal latency (antinociception) observed after blocking IL mGluR5 in ARTH animals only, suggests an increased tonic activation of these receptors in chronic inflammation of the joint.

The effect induced by activation of mGluR1 in the IL was studied indirectly by IL co-administration of an mGluR1/5 agonist and an mGluR5 antagonist. The antinociceptive effect induced by this combination of drugs in ARTH but not in SHAM animals suggests that following the development of monoarthritis, the net effect of the descending pathways recruited by mGluR1 is antinociceptive. It might be argued that the antinociception induced by IL co-administration of the mGluR1/5 agonist and mGluR5 antagonist in the ARTH group was due to blocking of the mGluR5-driven pronociceptive drive rather than activation of the mGluR1; however, previous administration of an mGluR1 antagonist blocked this antinociceptive effect, indicating an activation of mGluR1 instead of the inactivation of mGluR5. Additionally, the findings that IL administration of an mGluR5 agonist alone had a pronociceptive action whereas the mGluR1/5 agonist alone failed to alter nociception, support the proposal that mGluR1 in the IL of ARTH animals has indeed an antinociceptive effect.

### Technical considerations

In this work, we have chosen to evaluate heat-evoked PWL, a test in which the baseline values of SHAM and

ARTH animals are similar (Fig. 4A), instead of mechanical LWT, where ARTH animals have significantly decreased values when compared to SHAM (Fig. 7A). Our choice was based on the technical differences between the PAM and the Hargreaves tests. The PAM test requires not only that the animals are heavily handled by the researcher during each experimental session, but also that the knee joint is noxiously stimulated twice at each time point before and after drug administration. Thus, one test would imply the affected joint to undergo 12 noxious stimulations in a short period of time (60 min) which by itself might bias the evaluation, as the mechanical hyperalgesia in K/C model is use-dependent. By contrast, in the Hargreaves test animals are placed in a compartment for the duration of the experimental session (no handling is involved) and the thermal stimulus is applied from underneath the plantar surface of the hindpaw, thus sparing the joint, but still activating ascending and descending pain modulatory pathways. Therefore, we are not showing a reversion of mechanical hyperalgesia when treating ARTH animals, but that the IL promotes descending facilitation both in health and in disease, and that this effect is mediated by mGluR, mainly mGluR5.

### The opposing roles of the PL and IL in descending modulation of nociception are associated to the activation of different types of GLU receptors

The dorsal portion of the mPFC, that includes the ACC, is among the most studied cortical areas in pain processing (Apkarian et al., 2005; Tracey and Mantyh, 2007), but only a few studies have been centered in the PL and IL cortices in the rodent brain. So far, these areas have been mostly implicated in the attentional and cognitive processing of pain (Apkarian et al., 2005), but there is some evidence that they actively modulate nociception. In fact, reports show that sustained pain conditions lead to a decrease of basal neuronal activity in the mPFC (Ji and Neugebauer, 2011; Luongo et al., 2013). The behavioral data of the present study shows that the PL and the IL modulate nociception and that the blockade of these regions with LIDO decreased PWL, suggesting a tonic antinociceptive role in pain control.

Since the PL and the IL are adjacent to one another, it could be argued that there is widespread diffusion of drugs, resulting in a simultaneous activation/inactivation of these areas due to drug spillage outside of the targeted area of administration. However, GLU administration to the PL and IL had opposite effects on heat-evoked PWL, increasing and decreasing withdrawal latencies, respectively. Interestingly, GLU in the PL increased withdrawal latencies within 30–60 s, a short onset of action typical of the activation of ionotropic GLU receptors. Indeed, Millecamps et al. (2007) reported that activation of NMDA receptors in PL induced analgesia. By contrast, GLU in the IL decreased PWL, but only 10–30 min after drug administration, a response typically associated with the activation of mGluRs. This hypothesis is supported firstly, by the decrease in PWL observed after the IL microinjection of

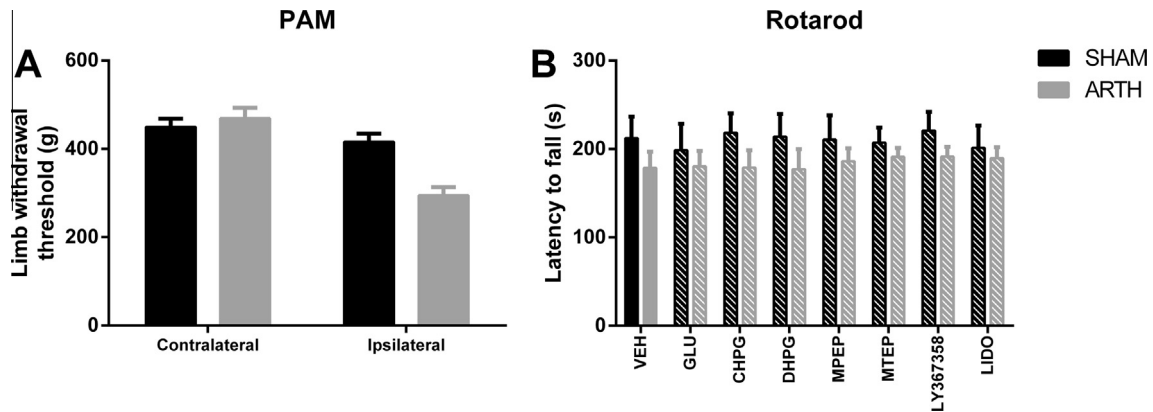


**Fig. 7.** (A) Evaluation of limb withdrawal threshold (LWT) in the pressure application measurement (PAM) 4 weeks after arthritis induction. The LWT of ARTH ( $n = 7$ ) animals was significantly decreased when compared to results of control SHAM ( $n = 8$ ) animals (mechanical hyperalgesia). (B) Drug effects on locomotion. Evaluation of performance in the rotarod test after drug injection in the infralimbic cortex (IL) of SHAM and ARTH rats showed that none of the drugs had an effect on the latency to fall 10–30 min after administration in the IL. Data are presented as mean + SEM. \*\* $P < 0.01$ ; \*\*\* $P < 0.001$ .

CHPG, an mGluR5 selective agonist, which mimicked the effect of GLU in the IL; and secondly, by the lack of changes in nociceptive behavior when GLU microinjection was preceded by administration of MPEP or MTEP, two different mGluR5 antagonists.

Interestingly, GLU and CHPG microinjection decreased PWL similar to what observed after LIDO microinjection. A potential explanation for this finding is that the effect of mGluR5 activation triggers an inhibitory mechanism, leading to suppression of neuronal discharge in the IL. In line with this hypothesis, a recent study by Pollard et al. (2014) has shown that mGluR5 activation leads to inhibition of neuronal activity in the ventral mPFC by promoting feed-forward inhibition. However, there are also contrasting reports that show mGluR5 activation in the ventral mPFC increases neuronal excitability by reducing the release of presynaptic GABA (Kiritoshi et al., 2013; Ji and Neugebauer, 2014). As a modulator of neuronal excitability (Schoepp, 2001), mGluR5 activation/inactivation can affect several mechanisms, thus, further studies are still needed to fully understand the pathways underlying descending modulation of nociception modulated by mGluR5 in the IL.

#### mGluRs mediate GLU-driven descending facilitation from the IL

In the present work, IL administration of the selective mGluR5 agonist CHPG as well as of exogenous GLU induced delayed and long-lasting pronociceptive effects that were identical in both SHAM and ARTH animals. Although the mechanism driving this effect is not fully understood, a study by Ji and Neugebauer (2014) showed the administration of an mGluR5-positive allosteric modulator (which increases receptor availability without activating it) increases background and evoked activity of IL pyramidal cells in healthy animals. However, in animals with sustained inflammatory pain, this facilitatory effect was only observed following co-application of a CB1 receptor agonist with the mGluR5 allosteric modulator (Ji and Neugebauer, 2014). This finding indicates that

sustained inflammatory pain promotes remodeling of signaling pathways involving the IL and mGluRs. In line with this evidence, we observed that MPEP or MTEP, both mGluR5 antagonists, in the IL produced antinociception only in ARTH animals, further suggesting that mGluR5 in the IL plays a role in tonic facilitation of nociception in chronic inflammatory disorders. Other studies using animal models of inflammatory pain have reported antinociception (Hudson et al., 2002; Zhu et al., 2004) and inhibition of spontaneous burst activity in the mPFC (Houmayoun and Moghaddam, 2006) after systemic administration of an mGluR5 antagonist. Together, the effects observed after blocking mGluR5 suggest this receptor plays an important role in the modulation of nociceptive transmission in chronic inflammatory pain states. Although we cannot directly compare the effect of systemically administered drugs to the effect of local microinjections in a specific brain area, the present and earlier results (Ji and Neugebauer, 2014) are in line with the proposal that the mGluR5-mediated mechanisms in the IL contribute to the descending control of nociception and its modulation in inflammatory conditions.

Activation of mGluR1 with a combination of DHPG and MPEP in the IL of SHAM animals had no effect upon nociceptive behavior, while it increased heat-evoked PWL (antinociception) in the ARTH group. These results suggest that in experimental monoarthritis a descending antinociceptive pathway can be activated if mGluR1 in the IL are recruited. Yet, inactivation of mGluR1 in the IL with antagonist LY367385 had no effect on PWL of SHAM or ARTH animals, indicating that mGluR1 are not tonically activated in the IL. Interestingly, an earlier electrophysiological study showed PL mGluR1 are important players in the decrease of the spontaneous activity of PL neurons caused by pain-induced hyperactivity of the amygdala in sustained inflammatory conditions (Ji and Neugebauer, 2014). Overall, although we were able to evoke an antinociceptive effect after the activation of mGluR1 in the IL, the impact of this pathway toward nociception remains unclear, since the blockade of mGluR1 had no

effect upon nociceptive behavior and the pronociceptive effect of mGluR5 prevailed in controls and animals with experimental monoarthritis.

## CONCLUSIONS

Drugs acting at mGluRs have more subtle effects on glutamatergic transmission than agonists and antagonists of ionotropic GLU receptors, as well as fewer side effects on normal functions (Conn and Pin, 1997; Schoepp, 2001; Neugebauer, 2002). Hence, the modulation of mGluRs allows a fine-tuning of cellular responses to glutamatergic inputs. The results of this study provide strong evidence the IL is involved in the descending modulation of nociception and mGluRs, particularly mGluR5, might contribute to inflammatory hyperalgesia.

*Acknowledgments*—This study was supported by grants from the Portuguese Science Foundation (FCT) Project PTDC/SAU-NEU/108557/2008, FEDER-COMPETE, by the Academy of Finland and the Sigrid Juselius Foundation, Helsinki, Finland and co-financed by the Portuguese North Regional Operational Program (ON.2 – O Novo Norte) under the National Strategic Reference Framework (QREN), through the European Regional Development Fund (FEDER). ADP was supported by FCT grant SFRH/BD/90374/2012 and DA was supported by FCT grant SFRH/BD/71219/2010.

## REFERENCES

- Amorim D, David-Pereira A, Pertovaara A, Almeida A, Pinto-Ribeiro F (2014) Amitriptyline reverses hyperalgesia and improves associated mood-like disorders in a model of experimental monoarthritis. *Behav Brain Res* 265:12–21.
- Ansah OS, Gonçalves L, Almeida A, Pertovaara A (2009) Enhanced pronociception by amygdaloid group I metabotropic glutamate receptors in nerve-injured animals. *Exp Neurol* 216:66–74.
- Apkarian AV, Bushnell MC, Treede RD, Zubieta JK (2005) Human brain mechanisms of pain perception and regulation in health and disease. *Eur J Pain* 9:463–484.
- Apkarian AV, Sosa Y, Sonty S, Levy RM, Harden RN, Parrish TB, Gitelman DR (2004) Chronic back pain is associated with decreased prefrontal and thalamic gray matter density. *J Neurosci* 24:10410–10415.
- Baliki MN, Chialvo DR, Geha PY, Levy RM, Harden RN, Parrish TB, Apkarian AV (2006) Chronic pain and emotional brain: specific brain activity associated with spontaneous fluctuations of intensity of chronic back pain. *J Neurosci* 26:12165–12173.
- Barton NJ, Strickland IT, Bond SM, Brash HM, Bate ST, Wilson AW, Chessell IP, Reeve AJ, McQueen DS (2007) Pressure application measurement (PAM): a novel behavioural technique for measuring hypersensitivity in a rat model of joint pain. *J Neurosci Methods* 163:67–75.
- Conn PJ, Pin JP (1997) Pharmacology and functions of metabotropic glutamate receptors. *Annu Rev Pharmacol Toxicol* 37:205–237.
- de Novellis V, Mariani L, Palazzo E, Vita D, Marabese I, Scafuro M, Rossi F, Maione S (2005) Periaqueductal grey CB1 cannabinoid and metabotropic glutamate subtype 5 receptors modulate changes in rostral ventromedial medulla neuronal activities induced by subcutaneous formalin in the rat. *Neuroscience* 134:269–281.
- Heidbreder CA, Groenewegen HJ (2003) The medial prefrontal cortex in the rat: evidence for a dorso-ventral distinction based upon functional and anatomical characteristics. *Neurosci Biobehav Rev* 27:555–579.
- Houmayoun H, Moghaddam B (2006) Bursting of prefrontal cortex neurons in awake rats is regulated by metabotropic glutamate 5 (mGlu5) receptors: rate-dependent influence and interaction with NMDA receptors. *Cereb Cortex* 16:93–105.
- Hudson LJ, Bevan S, McNair K, Gentry C, Fox A, Kuhn R, Winter J (2002) Metabotropic glutamate receptor 5 upregulation in A-fibers after spinal nerve injury: 2-methyl-6-(phenylethynyl)-pyridine (MPEP) reverses the induced thermal hyperalgesia. *J Neurosci* 22:2660–2668.
- Ji G, Neugebauer V (2011) Pain-related deactivation of medial prefrontal cortical neurons involves mGluR1 and GABA<sub>A</sub> receptors. *J Neurophysiol* 106:2642–2652.
- Ji G, Neugebauer V (2014) CB1 augments mGluR5 function in medial prefrontal cortical neurons to inhibit amygdala hyperactivity in an arthritis pain model. *Eur J Neurosci* 39:455–466.
- Kiritoshi T, Sun H, Ren W, Stauffer SR, Lindsley CW, Conn PJ, Neugebauer V (2013) Modulation of pyramidal cell output in the medial prefrontal cortex by mGluR5 interacting with CB1. *Neuropharmacology* 66:170–178.
- Li W, Neugebauer V (2004) Differential roles of mGluR1 and mGluR5 in brief and prolonged nociceptive processing in central amygdala neurons. *J Neurophysiol* 91:13–24.
- Lea PMT, Faden AI (2006) Metabotropic glutamate receptor subtype 5 antagonists MPEP and MTEP. *CNS Drug Rev* 12:149–166.
- Luongo L, de Novellis V, Gatta L, Palazzo E, Vita D, Guida F, Giordano C, Siniscalco D, Marabese I, De Chiaro M, Boccella S, Rossi F, Maione S (2013) Role of metabotropic glutamate receptor 1 in the basolateral amygdala-driven prefrontal cortical deactivation in inflammatory pain in the rat. *Neuropharmacology* 66:317–329.
- Mathiesen JM, Svendsen N, Brauner-Osborne H, Thomsen C, Ramirez MT (2003) Positive allosteric modulation of the human metabotropic glutamate receptor 4 (hmGluR4) by SIB-1893 and MPEP. *Br J Pharmacol* 138:1026–1030.
- Metz AE, Yau HJ, Centeno MV, Apkarian AV, Martina M (2009) Morphological and functional reorganization of rat medial prefrontal cortex in neuropathic pain. *Proc Natl Acad Sci USA* 106:2423–2428.
- Millecamps M, Centeno MV, Berra HH, Rudick CN, Lavarello S, Tkatch T, Apkarian AV (2007) D-Cycloserine reduces neuropathic pain behavior through limbic NMDA-mediated circuitry. *Pain* 132:108–123.
- Monville C, Torres EM, Dunnett SB (2006) Comparison of incremental and accelerating protocols of the rotarod test for the assessment of motor deficits in the 6-OHDA model. *J Neurosci Methods* 158:219–223.
- Movsesyan VA, O'Leary DM, Fan L, Bao W, Mullins PGM, Knoblach SM, Faden AI (2001) mGluR5 antagonists 2-methyl-6-(phenylethynyl)-pyridine and (E)-2-methyl-6-(2-phenylethynyl)-pyridine reduce traumatic neuronal injury in vitro and in vivo by antagonizing N-methyl-D-aspartate receptors. *J Pharmacol Exp Ther* 296:41–47.
- Myers RD (1966) Injection of solutions into cerebral tissue: relation between volume and diffusion. *Physiol Behav* 1:171–174.
- Neugebauer V (2002) Metabotropic glutamate receptors – important modulators of nociception and pain behaviour. *Pain* 98:1–8.
- Palazzo E, Marabese I, de Novellis V, Oliva P, Rossi F, Berrino L, Rossi F, Maione S (2001) Metabotropic and NMDA glutamate receptors participate in the cannabinoid-induced antinociception. *Neuropharmacology* 40:319–326.
- Paxinos G, Watson C (2005) The rat brain in stereotaxic coordinates. Sydney: Academic Press.
- Pinto-Ribeiro F, Amorim D, David-Pereira A, Monteiro AM, Costa P, Pertovaara A, Almeida A (2013) Pronociception from the dorsomedial nucleus of the hypothalamus is mediated by the rostral ventromedial medulla in healthy controls but is absent in arthritic animals. *Brain Res Bull* 99:100–108.
- Pinto-Ribeiro F, Ansah OB, Almeida A, Pertovaara A (2011) Response properties of nociceptive neurons in the caudal ventrolateral medulla (CVLM) in monoarthritic and healthy control rats: Modulation of responses by the paraventricular nucleus of the hypothalamus (PVN). *Brain Res Bull* 86:82–90.

- Pollard M, Bartolome JM, Conn PJ, Steckler T, Shaban H (2014) Modulation of neuronal microcircuit activities within the medial prefrontal cortex by mGluR5 positive allosteric modulator. *J Psychopharmacol* 28:935–946.
- Radhakrishnan R, Moore SA, Sluka KA (2003) Unilateral carrageenan injection into muscle or joint chronic bilateral hyperalgesia in rats. *Pain* 104:567–577.
- Ren K, Dubner R (2010) Glutamate and GABA receptors in pain transmission. In: Beaulieu P, Lussier D, Porreca F, Dickenson AH, editors. *Pharmacology of pain*. Seattle: IASP Press, International Association for the Study of Pain. p. 207–239.
- Schoepp DD (2001) Unveiling the functions of presynaptic metabotropic glutamate receptors in the central nervous system. *J Pharmacol Exp Ther* 299:12–20.
- Tracey I, Mantyh PW (2007) The cerebral signature for pain perception and its modulation. *Neuron* 55:377–391.
- Vertes RP (2006) Interactions among the medial prefrontal cortex, hippocampus and midline thalamus in emotional and cognitive processing in the rat. *Neuroscience* 142:1–20.
- Zhang L, Zhang Y, Zhao ZQ (2005) Anterior cingulate cortex contributes to the descending facilitatory modulation of pain via dorsal reticular nucleus. *Eur J Neurosci* 22(5):1141–1148.
- Zhang R, Tomida M, Katayama Y, Kawakami Y (2004) Response durations encode nociceptive stimulus intensity in the rat medial prefrontal cortex. *Neuroscience* 126:777–785.
- Zhu CZ, Wilson SG, Mikusa JP, Wismer CT, Gauvin DM, Lynch 3rd JJ, Wade CL, Decker MW, Honore P (2004) Assessing the role of metabotropic glutamate receptor 5 in multiple nociceptive modalities. *Eur J Pharmacol* 506:107–118.

*(Accepted 30 October 2015)*  
*(Available online 6 November 2015)*

Ana David-Pereira, Sara Gonçalves, Antti Pertovaara, Armando Almeida, Filipa Pinto-Ribeiro

**Astrocytic mGluR5 in the infralimbic cortex are engaged in descending nociceptive modulation in experimental monoarthritis**

*(Manuscript under preparation)*



**Astrocytic mGluR5 in the infralimbic cortex are engaged in descending nociceptive modulation in experimental monoarthritis**

Ana David-Pereira<sup>1,2,\*</sup>, Sara Gonçalves<sup>1,2,\*</sup>, Antti Pertovaara<sup>3</sup>, Armando Almeida<sup>1,2</sup>, Filipa Pinto-Ribeiro<sup>1,2</sup>

<sup>1</sup>Life and Health Sciences Research Institute (ICVS), School of Medicine, Campus of Gualtar, University of Minho, 4750-057 Braga, Portugal

<sup>2</sup>ICVS/3B's - PT Government Associate Laboratory, Braga/Guimarães, Portugal

<sup>3</sup>Department of Physiology, Faculty of Medicine, POB 63, University of Helsinki, 00014 Helsinki, Finland

*\* Corresponding author.*

E-mail address: [filiparibeiro@ecsaude.uminho.pt](mailto:filiparibeiro@ecsaude.uminho.pt) (F. Pinto-Ribeiro)

## **Abstract**

Metabotropic glutamate receptor 5 (mGluR5) partly mediates medial prefrontal cortex (mPFC) output and regulates its activity in pain. mGluR5 are present not only in neurons but also in astrocytes, whose relevance in chronic pain is becoming increasingly evident. Here the role of infralimbic cortex (IL) mGluR5 in the descending modulation of pain in healthy and monoarthritic rats was assessed, with special emphasis on the contribution of astrocytic mGluR5 towards this effect.

Firstly, nociceptive behavior was assessed before and after intracerebral injection of drugs in the IL of healthy and monoarthritic rats. mGluR5 activation in healthy animals facilitated mechanical and thermal nociceptive behavior, but mGluR5 antagonist had no effect. In ARTH animals, mGluR5 agonist produced thermal hyperalgesia and did not worsen the pre-existent primary mechanical hyperalgesia while mGluR5 antagonist induced thermal and mechanical antinociception.

Secondly, the gliotoxin L- $\alpha$  amino adipate (L $\alpha$ AA) was administered to both experimental groups in order to ablate astrocytic function in the IL. L $\alpha$ AA had no effect on the basal nociceptive behavior of animals. Identically, astrocytic ablation did not alter the behavioral effect of mGluR5 agonist. However, the antinociceptive effect of mGluR5 antagonist in ARTH animals' mechanical and thermal nociceptive behavior was lost after astrocyte ablation.

The results indicate mGluR5 in the IL facilitate nociception in healthy and monoarthritic animals. Moreover, tonic alterations in mGluR5 activity after experimental monoarthritis are partly dependent on astrocytic mGluR5.

## **Keywords**

Infralimbic cortex; Metabotropic glutamate receptor 5; Experimental monoarthritis; Astrocytes; L- $\alpha$  amino adipate.



## Introduction

With the increasing need to understand the mechanisms leading to the development and establishment of chronic pain, the role of non-neuronal cell types, such as astrocytes, and their interactions between themselves and with neurons is beginning to be addressed. Being the most abundant cells in the central nervous system (CNS), astrocytes hold multiple roles as house-keeping cells, regulating blood flow; maintaining fluid, ion, pH and transmitter homeostasis; and intervening in CNS metabolism<sup>1</sup>. Astrocytes are in a privileged position to contribute to the central mechanisms of pain modulation, as they form physically coupled networks with surrounding astrocytes through which intercellular transmission of  $\text{Ca}^{2+}$  signaling and exchange of cytosolic contents occurs<sup>2</sup>. Astrocytes are also an integral part of the “tripartite synapse”, playing a key role in the regulation of synaptic transmission and neuronal excitability<sup>3</sup>.

In response to peripheral and CNS damage, spinal neurons release glutamate, activating local astrocytes and increasing the intercellular transmission of  $\text{Ca}^{2+}$  currents<sup>4</sup>. Activation of astrocytes leads to the release of several gliotransmitters, including several known pronociceptive mediators such as ATP, D-serine, cytokines, chemokines and glutamate, which in turn regulate neuronal activity<sup>5</sup>. Astrocyte activation in animal models of chronic pain occurs at late and prolonged stages of the disease, reflecting long duration pain responses<sup>6</sup>. Chronic astrocyte activation affects the function of glutamate regulatory transporters<sup>7</sup>, leading to an imbalance in glutamate uptake and an overall increase in excitatory synaptic transmission<sup>8-10</sup>, one of the hallmarks of chronic pain<sup>11</sup>. Intrathecal administration of pharmacological glial inhibitors, such as fluoroacetate or L- $\alpha$ -amino adipate (L- $\alpha$ -AA), blocks or attenuates hyperalgesia and/or allodynia in models of inflammatory<sup>12,13</sup> and neuropathic pain<sup>14,15</sup>, further highlighting the importance of glial cells in development and maintenance of chronic pain.

Metabotropic glutamate receptors type 5 (mGluR5) are one of the best studied glial receptors that play a regulatory role in synaptic transmission. Astrocytic mGluR5 detects and regulates glutamatergic transmission, leading to increased  $\text{Ca}^{2+}$  transmission in the astrocyte. This  $\text{Ca}^{2+}$  wave can affect local synaptic transmission or propagate through astrocytic junctions proportionally to the number of mGluR5 activated<sup>16</sup>. Interestingly, spinal mGluR5 and glial fibrillary acidic protein (GFAP, a marker of astrocytes) expression are upregulated in a model of bone cancer pain and intrathecal administration of an mGluR5 antagonist attenuates spontaneous pain, mechanical allodynia and thermal hyperalgesia, as well as reducing the pain-related spinal GFAP expression<sup>17</sup>.

Although spinal astrocytic activation in animals models of chronic pain is already under scrutiny, less is known about supraspinal mechanisms. Wei and colleagues found prolonged activation of astrocytes in the rostral ventromedial medulla (RVM) after chronic constriction injury (CCI) of the infraorbital nerve in rats<sup>18</sup>, indicating that glial-neuronal interactions contribute to the descending modulation of pain at the supraspinal level. Additionally, a recent study found increased expression of astrocytic mGluR5 in the somatosensory cortex I of rats with chronic neuropathic pain, which, when blocked, suppressed mechanical allodynia<sup>19</sup>. In previous works, we showed that prolonged monoarthritis leads to a tonic activation of mGluR5 in the infralimbic cortex (IL) of rats<sup>20</sup>. Here we tested if monoarthritis-induced tonic activation of mGluR5 in the IL is dependent on a neuronal or an astrocytic pathway. For this purpose, the effect of IL astrocyte ablation upon IL mGluR5-mediated nociceptive behavior was evaluated in healthy and monoarthritic rats.

## **Methods**

### **Animals, ethical issues and anesthetics**

The experiments were performed in adult Wistar Han male rats weighting 250-300g at the beginning of the experiment (Charles River, France). The experimental protocol was approved by the Institutional Ethical Commission and followed the European Community Council Directive 2010/63/EU concerning the use of animals for scientific purposes. All efforts were made to minimize animal suffering and to use only the number of animals necessary to produce reliable scientific data.

For all surgical procedures, anesthesia was induced through the intraperitoneal (i.p.) administration of a mixture of ketamine (0.75 mg/kg, i.p.; Imalgene, Merial Lyon, France) and medetomidine (0.5 mg/kg, i.p.; Dorbene, Esteve Veterinaria, León, Spain). Anesthesia was reverted with atipamezole hydrochloride (1mg/kg, i.p.; Antisedan, Orion Pharma, Orion Corporation, Espoo, Finland) and the animals were monitored until fully recovered. After the completion of the behavioral tasks, animals received a lethal dose of pentobarbital and the brains were removed for histological confirmation of cannula placement and injection efficacy.

### **Induction of monoarthritis**

Induction of monoarthritis (ARTH) was performed 28 days before the beginning of the experiments, as described in detail elsewhere<sup>21</sup>. Briefly, 0.1mL of a solution of 3% kaolin and 3% carrageenan (Sigma-Aldrich, St. Louis, MO, USA) dissolved in sterile saline solution was injected intrasynovially in the right knee joint of ARTH rats. The same volume of sterile saline solution was injected in the right knee joints of SHAM animals. Mechanical hyperalgesia development is observable a few hours after surgery and can be observed up to 8 weeks<sup>22,23</sup>. ARTH development was verified 1–2h prior to each behavioral session in each animal. To be considered monoarthritic, rats had to vocalized audibly during each one of five consecutive flexion–extension movements of the knee joint<sup>22</sup>. SHAM animals did not vocalize during any of the flexion–extension movements of the knee joint.

### **Intracerebral cannula implantation**

For intracerebral drug administration, cannulas were implanted as described elsewhere<sup>24</sup>. Briefly, anesthetized rats were placed in a standard stereotaxic frame, where the skull was exposed and a craniotomy performed. A sterilized stainless-steel guide cannula (26 gauge; Plastics One, Roanoke, VA, USA) was implanted in the brain with the tip positioned 1mm above the right IL, [2.76mm frontal to bregma; 0.6mm lateral to midline; depth 4.2mm<sup>25</sup> (**Fig. 1A,C-G**)], fixed to the skull with screws and dental acrylic cement and the skin sutured around it. To prevent contamination, a dummy cannula (Plastics One) was inserted into the guide cannula.

### **Drugs**

As described in previous studies, (RS)-2-Chloro-5-hydroxyglycine (CHPG, 100nmol/ $\mu$ L; mGluR5 agonist; Tocris, Bristol, United Kingdom) and 3-((2-Methyl-1,3-thiazol-4-yl)ethynyl)pyridine hydrochloride (MTEP, 50nmol/ $\mu$ L; mGluR5 antagonist, Tocris, Bristol, United Kingdom) solutions for intracerebral drug injection were prepared with sterilized saline solution 0.9% (B. Braun Oy, Espoo, Finland; pH 7,2)<sup>20</sup>. L- $\alpha$ -amino adipate (L $\alpha$ AA, 25 $\mu$ g/ $\mu$ L; Sigma Aldrich) was prepared in phosphate buffer saline (PBS)<sup>14,26</sup>.

A 33-gauge injection cannula (Plastics One) protruding 1mm beyond the tip of the guide cannula and connected to a 5.0 $\mu$ L Hamilton syringe by a polyethylene catheter (PE-10; Plastics One) was

used to inject drugs. The injection volume of L $\alpha$ AA was 2 $\mu$ L, delivered using an automated injector (0.5 $\mu$ L/min). The expected drug injection spread was of 2.4mm in diameter<sup>27</sup>. The injection volume of drugs for behavioral tests was 0.5 $\mu$ L, with an expected drug injection spread within the brain of 1mm in diameter<sup>27</sup>. The efficacy of injection was monitored by noting the movement of a small air bubble through the tubing. The minimum duration for drug microinjection was of at least 20s and the injection cannula was left in place for an additional 30s to minimize drug solution return through the injection cannula.

Alterations in nociceptive behavior were evaluated at fixed time points (**Fig. 2**) until the drug effect was no longer observed. The behavioral results presented are for the peak effect of drugs, which was determined to be 30min after drug injection. Control injections were performed with the vehicle solution.

## **Behavioral assessment of nociception**

### ***Hargreaves model***

Secondary heat hyperalgesia in unanesthetized animals was determined by measuring hind paw withdrawal latency (PWL) following radiant heat stimulation (Hargreaves test; Plantar Test Device Model 37370, Ugo Basile, Varese, Italy). In each behavioral session, PWL was assessed before and at fixed intervals following intracerebral drug administration (**Fig. 2**). At each time point, the measurements were repeated twice at an interval of 1min. The mean of these values was used in further calculations. To avoid any damage to the skin, the cut-off time for radiant-heat exposure was set at 15s.

### ***Pressure application measurement***

Primary mechanical nociception was evaluated using the pressure application measurement (PAM), which allows to accurately measure primary mechanical hyperalgesia by the application of a force range of 0-1500g on the knee joint<sup>28</sup>. To perform the test, the animal is held securely while the force transducer unit (fitted to the experimenter's thumb) is placed on one side of the knee joint and the forefinger on the other. Increasing force is gradually applied across the joint until a behavioral response is observed (paw-withdrawal, vocalization, wriggling or vocalization), with a cut-off of 5s. The peak force (in grams of force (gf)) applied immediately prior to the behavioral response is registered as the limb withdrawal threshold (LWT). To avoid excessive testing and

damage of the knee joint, in each behavioral session, LWT was measured before and at the time point of maximum drug effect determined during the Hargreaves test. At each time point, measurements were performed twice in both the ipsilateral and contralateral limbs at 1min intervals. The mean LWTs were calculated per animal. At the end of the session animals were returned to their home cage.

### **Course of the behavioral study**

Rats were habituated to the experimental conditions by performing daily handling sessions with the experimenter and by allowing them to spend 1h daily in the testing room and apparatus during the week preceding any testing. Animals were sub-divided in 2 experimental groups: (i) animals tested in the Hargreaves test ( $n_{\text{SHAM}}=12$ ;  $n_{\text{ARTH}}=12$ ) and (ii) animals tested with the PAM apparatus ( $n_{\text{SHAM}}=8$ ;  $n_{\text{ARTH}}=8$ ). 3 weeks after ARTH induction, intracerebral cannulas were implanted in SHAM and ARTH animals. 1 week after guide cannula implantation, animals were habituated to the Hargreaves/PAM apparatus. 4 weeks after ARTH induction, astrocytic ablation was performed by administering L $\alpha$ AA or PBS through the guide cannula of all rats. The following day, changes in nociceptive behavior of animals after drug administration in the IL were determined by assessing PWL before and at the peak of drug action previously determined (30min) following the first drug administration for the Hargreaves and PAM tests. Nociceptive behavior was assessed after ablating astrocytes until a maximum of 7 days post-L $\alpha$ AA injection, after which animals received a lethal dose of pentobarbitone, were intracardially perfused with 4% paraformaldehyde solution and the brains excised for posterior confirmation of cannula placement and L $\alpha$ AA efficacy (**Fig. 1**). Drug testing was randomized among animals. All animals were treated with all drug combinations.

### **Histology**

Coronal sections 50  $\mu$ m thick were obtained from frozen brains in a cryostat (Leica CM1900). Sections were washed thrice in TBS and incubated in TBS-T with 10% goat serum (ThermoFisher, USA) during 30min to block unspecific reactivity, after which they were incubated overnight with primary anti-glial fibrillary acidic protein (GFAP) antibody (mouse, 1:800; Sigma-Aldrich, St. Louis, MO, USA) in TBS-T with 4% goat serum. The following day sections were incubated with secondary anti-mouse antibody (1:1000; Sigma-Aldrich, St. Louis, MO, USA) in TBS-T for 2h at room

temperature, followed by DAPI (4',6-Diamidino-2'-phenylindole dihydrochloride, 1:1000; Sigma-Aldrich) for 10min. Slides were coverslip using Permafluor mounting media (Thermo Scientific Shandon; **Fig. 1**).

## Statistics

Statistical analysis was performed using two-way analysis of variance (ANOVA) with repeated measures, followed by *t*-test with a Bonferroni correction for multiple comparison. Analysis was performed with SPSS software and graphs were built with GraphPad Prism 6 software (GraphPad Software Inc., La Jolla, CA, USA).  $p < 0.05$  was considered to represent a significant difference. Data are presented as mean  $\pm$  standard error of the mean (SEM).

## Results

### Effect of astrocyte ablation on heat-evoked paw withdrawal latency in SHAM and ARTH animals

To assess if IL mGluR5-mediated pronociception depends on astrocytic mGluR5, we studied the effects of mGluR5 activation/inactivation upon heat-evoked PWL before and after ablating astrocytes in the IL.  $\alpha$ AA administration does not alter baseline PWL (main effect of ablation:  $F_{1,174}=0.023$ ;  $p=0.881$ ) independently of the experimental group (interaction of ablation vs. experimental group:  $F_{1,174}=0.004$ ;  $p=0.951$ ). Vehicle administration in the IL does not alter PWL (main effect of drug:  $F_{1,61}=2.636$ ;  $p=0.110$ ), independently of the experimental group tested (interaction of drug vs. experimental group:  $F_{1,61}=0.340$ ;  $p=0.562$ ), astrocyte ablation (interaction of drug vs. ablation:  $F_{1,61}=1.227$ ;  $p=0.272$ ) or the combination of both factors (interaction of drug vs. experimental group vs. ablation:  $F_{1,61}=0.220$ ;  $p=0.641$ ; **Fig. 2A**).

CHPG microinjection significantly decreases PWL (main effect of drug:  $F_{1,60}=184,742$ ;  $p < 0.0001$ ), independently of experimental group (interaction of drug vs. experimental group:  $F_{1,60}=0.187$ ;  $p=0.667$ ), ablation (interaction drug vs. ablation:  $F_{1,60}=0.095$ ;  $p=0.759$ ) or combination of both factors (interaction of drug vs. experimental group vs. ablation:  $F_{1,60}=1,729$ ;  $p=0.193$ ). *Post hoc* tests show that 30min after CHPG administration PWL is significantly decreased in SHAM and ARTH animals and that astrocyte ablation does not alter mGluR5 pronociception (**Fig. 2B**).

Overall, MTEP administration does not significantly alter PWL (main effect of drug:  $F_{1,45}=0.412$ ;  $p=0.412$ ). The effect of the experimental group alone is not significantly different (interaction of drug vs. experimental group:  $F_{1,45}=3.135$ ;  $p=0.083$ ); however, astrocyte ablation significantly alters the effect of MTEP (interaction of drug vs. ablation:  $F_{1,45}=7.393$ ;  $p=0.009$ ) in a way that is dependent of the experimental group (interaction of drug vs. experimental group vs. ablation:  $F_{1,45}=9.084$ ;  $p=0.004$ ). *Post hoc* tests show that MTEP does not alter PWL in SHAM animals and is antinociceptive in ARTH animals. Moreover, astrocyte ablation results in the loss of MTEP antinociceptive effect in the ARTH group (**Fig. 2C**).

### **Effect of astrocyte ablation on mechanical-evoked limb withdrawal threshold in SHAM and ARTH animals**

To assess if mGluR5 activation in the IL also elicits mechanical pronociception, and if the effect is dependent on astrocytic mGluR5, we studied the effects of mGluR5 activation/inactivation in LWT as measured by the PAM test before and after ablating astrocytes in the IL.

The LWT of ARTH animals is significantly lower when compared to SHAM (main effect of group:  $F_{1,59}=163.247$ ;  $p<0.001$ ), a behavioral correlate of monoarthritis. The administration of L $\alpha$ AA does not alter baseline values of neither experimental group (main effect of ablation:  $F_{1,59}=0.115$ ;  $p=0.736$ ).

Overall, CHPG significantly alters LWT (main effect of drug:  $F_{1,30}=53.498$ ;  $p<0.001$ ). This effects depends on the experimental group tested (interaction drug vs. experimental group:  $F_{1,30}=20.980$ ;  $p<0.001$ ) but not on astrocyte ablation (interaction drug vs. ablation:  $F_{1,30}=0.0003$ ;  $p=0.986$ ; interaction drug vs. experimental group vs. ablation:  $F_{1,30}=0.881$ ;  $p=0.355$ ). *Post hoc* tests indicate that CHPG administration decreases the LWT of SHAM, but not of ARTH, animals, a result that is not altered by astrocyte ablation (**Fig. 3A**).

MTEP administration significantly alters LWT (main effect of drug:  $F_{1,25}=4.298$ ;  $p=0.049$ ), independently of the experimental group and astrocyte ablation (interaction of drug vs. experimental group:  $F_{1,25}=2.189$ ;  $p=0.152$ ; interaction of drug vs. ablation:  $F_{1,25}=1.722$ ;  $p=0.201$ ; interaction of drug vs. experimental group vs. ablation:  $F_{1,25}=2.858$ ;  $p=0.103$ ). *Post hoc* tests indicate that MTEP has no effect upon LWT of SHAM animals; however, it increases LWT of ARTH animals to levels similar to those of animals without monoarthritis. Additionally, similarly to the

results in PWL measurements, astrocyte ablation impairs the effect of MTEP in ARTH animals (**Fig. 3B**)

## **Discussion**

In the present work, we demonstrate mGluR5 activation in the IL facilitates nociceptive responses in two modalities of peripheral noxious stimulation, thermal and mechanical, in healthy rats. mGluR5-mediated thermal pronociception is also present in animals with monoarthritis, although primary hyperalgesic behavior is not exacerbated by mGluR5 agonist. IL-mediated pronociception does not depend on astrocytic mGluR5, as pharmacological astrocyte ablation does not impair IL mGluR5-induced hyperalgesia. Previous results indicate tonic activation of IL mGluR5 occurs after 4 weeks of monoarthritis<sup>20</sup>, a result we replicate in the present study. Additionally, we confirm that blocking IL mGluR5 in ARTH, but not SHAM, animals elicits behavioral antinociception not only in thermal, but also in mechanically evoked nociceptive behavior. Importantly, we demonstrate for the first time that astrocyte ablation results in loss of behavioral antinociception after IL mGluR5 inhibition. This result suggests prolonged monoarthritis leads to tonic activation of astrocytic mGluR5, and IL astrocytes contribute to nociceptive changes in monoarthritis.

In previous publications, we showed glutamate microinjected into the IL acts preferentially upon mGluRs instead of ionotropic receptors to facilitate nociceptive behavior in both SHAM and ARTH animals<sup>20</sup>. We also proposed monoarthritis leads to a tonic activation of mGluR5, which when blocked promotes analgesia. In the aforementioned work we studied only alterations in noxious heat-evoked behavior applied to non-inflamed skin, showing the IL descending contribution to pain modulation is altered by monoarthritis induction. In the present work, we have extended these results by evaluating IL mGluR5 impact upon mechanical noxious behavior in an area with heightened noxious inputs (primary hyperalgesia). IL mGluR5 contribution to pronociception is similar in the two different modalities of peripheral stimulation in healthy animals; however, mGluR5 activation does not worsen monoarthritis-induced mechanical hyperalgesia. In contrast to our results, Kiritoshi and colleagues described that enhancing IL mGluR5 signaling 5-6h after K/C monoarthritis induction reverses mechanical hyperalgesia in rats<sup>29</sup>. The different testing time points could account for the opposing results obtained. In fact, persistent inflammatory pain is characterized by time-dependent plastic changes at several levels of the ascending and descending nociceptive pathways. Behaviorally, induction of monoarthritis with the K/C model induces both



primary and secondary hyperalgesia in acute stage of inflammation, while only primary hyperalgesia remains in chronic stages<sup>22,30,31</sup>. These phenotypic alterations are related to molecular, morphological and functional changes in neuronal circuitries such as those occurring, for example, in the RVM (reviewed by Vanegas and Schaible, 2004<sup>32</sup>), but also to time-dependent changes in the activation state of glial cells<sup>4,9</sup>.

To study the role of astrocytes upon IL descending nociceptive modulatory effect we compare mGluR5 agonist/antagonist actions before and after astrocyte ablation. CHPG administration induces pronociception in both SHAM and ARTH animals, independently of whether astrocyte function is intact or not. These findings suggest that CHPG-induced pronociception is dependent on neuronal mGluR5. It is important to consider that L $\alpha$ AA at the concentration used in our study selectively ablates astrocytes, without affecting neurons, oligodendrocytes or microglia<sup>33,34</sup>. Therefore, it is possible that CHPG is also acting on microglial mGluR5. *In vitro* studies show microglia express mGluR5, and their activation reduces microglia-related neuroinflammation and toxicity<sup>35</sup>, but to the best of our knowledge there are no studies on microglial mGluR5 role in pain modulation. The pattern of microglial reactivity after chronic pain onset argue against the involvement of these cells in CHPG effect, as, overall, microglial proliferation is very marked in the first stages of chronic pain, but usually is not found for more than 3 days after inflammation onset<sup>9,36</sup>. Without further studies, however, it is impossible to rule out microglia involvement in mGluR5-mediated pronociception.

On the other hand, ablation of IL astrocytes abolishes antinociception after mGluR5 inhibition in ARTH animals, suggesting chronic monoarthritis tonically activates mGluR5 specifically in astrocytes. Interestingly, astrogliosis is observed only a few days after inflammation onset, remaining for long periods, therefore being proposed to maintain long-term pathological states<sup>4,37,38</sup>. Increased astrogliosis is reported in the spinal cord, brainstem and forebrain of rats with chronic inflammatory pain<sup>39</sup>; particularly, increased GFAP expression occurs in the ACC 3 and 14 days after CFA, but not before<sup>33</sup>. One caveat for our hypothesis that astrocytic mGluR5 contributes to IL-mediated antinociception is that despite being described as an important regulator of synaptic transmission, mGluR5 expression in astrocytes peaks during developmental stages and is drastically reduced in adulthood<sup>16</sup>. Nonetheless, a recent study describes that following peripheral neuropathic pain induction, GFAP expression increases in the rat somatosensory cortex; more importantly, it is accompanied by a reemergence of astrocytic mGluR5 spines, which when blocked

reverses mechanical allodynia<sup>19</sup>. The mechanism described in this study constitutes an interesting proposal to explain the involvement of astrocytic mGluR5 in the behavioral changes observed in our monoarthritic rats. Future studies will test this hypothesis.

Finally, one interesting observation is that astrocyte ablation by itself does not alter nociceptive baselines in SHAM or ARTH animals. It is well established that inhibition of glial cells, either astrocytes or microglia, does not alter normal pain processing<sup>40</sup>. However, when administered in the spinal cord, pharmacological astrocyte inhibitors abolish nociceptive behaviors in animals with inflammatory<sup>12,13</sup> and neuropathic pain<sup>14,15</sup> and the same occurs when astrocytes are inhibited in the nociceptive modulatory RVM<sup>41</sup>. Considering this evidence, it seems that, in our study, IL astrocytes do not directly contribute to mechanical hyperalgesia in monoarthritis. On the other hand, the IL is proposed, in the majority of studies on its role in nociception, to modulate the cognitive and affective dimensions of pain. In fact, the IL is implicated in inflammatory pain-driven impairments in decision-making tasks<sup>42</sup> and in the modulation of anxiety behaviors<sup>43</sup>, which are comorbidities associated with chronic pain<sup>22</sup>. It is possible that the IL is modulating cognitive/affective dimensions of pain as well as contributing to sensory-discriminative nociceptive modulation through mGluR5 signaling. In line with this proposal, ablating astrocytes in the ACC, an area important for aversive-like negative affect of pain<sup>44</sup>, does not affect CFA-related mechanical allodynia, but reverses pain avoidance behavior<sup>33</sup>.

In conclusion, mGluR5 activation in the IL facilitates nociception in healthy and monoarthritic animals, highlighting the role of the IL in pain modulation. Additionally, tonic alterations in mGluR5 activity after experimental monoarthritis are partly dependent on astrocytic mGluR5. Therefore, the present work adds to the growing evidence that glial cells, and more specifically astrocytes, give an important contribution towards chronic pain conditions.

### **Author contributions**

ADP and FPR developed the concept and designed experiments. AP and SG performed and analyzed all of the experiments. ADP, SG and FPR wrote the paper. AP and AA revised the manuscript. All authors discussed and revised the manuscript.

## **Acknowledgements**

This study was supported by grants from the Portuguese Science Foundation (FCT) Project nu PTDC/SAU-NEU/108557/2008, by FEDER funds, through the Competitiveness Factors Operational Programme (COMPETE); by National funds, through the FCT, under the scope of the project POCI-01-0145-FEDER-007038. ADP was supported by FCT grant SFRH/BD/90374/2012.

## References

1. Bélanger, M. & Magistretti, P. J. The role of astroglia in neuroprotection. *Dialogues Clin. Neurosci.* 11, 281–95 (2009).
2. Hansen, R. R. & Malcangio, M. Astrocytes-multitaskers in chronic pain. *Eur. J. Pharmacol.* 716, 120–8 (2013).
3. Haydon, P. G. Glia: listening and talking to the synapse. *Nat. Rev. Neurosci.* 2, 185–93 (2001).
4. Ji, R.-R., Berta, T. & Nedergaard, M. Glia and pain: is chronic pain a gliopathy? *Pain* 154 Suppl, S10-28 (2013).
5. Hamilton, N. B. & Attwell, D. Do astrocytes really exocytose neurotransmitters? *Nat. Rev. Neurosci.* 11, 227–38 (2010).
6. Fellin, T. *et al.* Bidirectional astrocyte-neuron communication: the many roles of glutamate and ATP. *Novartis Found. Symp.* 276, 208-17-21, 233–7, 275–81 (2006).
7. Tawfik, V. L. *et al.* Induction of astrocyte differentiation by propentofylline increases glutamate transporter expression in vitro: heterogeneity of the quiescent phenotype. *Glia* 54, 193–203 (2006).
8. Sung, B., Lim, G. & Mao, J. Altered expression and uptake activity of spinal glutamate transporters after nerve injury contribute to the pathogenesis of neuropathic pain in rats. *J. Neurosci.* 23, 2899–910 (2003).
9. Ren, K. Emerging role of astroglia in pain hypersensitivity. *Jpn. Dent. Sci. Rev.* 46, 86–92 (2010).
10. Nie, H. & Weng, H. Glutamate transporters prevent excessive activation of NMDA receptors and extrasynaptic glutamate spillover in the spinal dorsal horn. *J. Neurophysiol.* 101, 2041–51 (2009).
11. Woolf, C. J. & Salter, M. W. Neuronal plasticity: increasing the gain in pain. *Science* 288, 1765–9 (2000).
12. Xie, Y. F. *et al.* Involvement of glia in central sensitization in trigeminal subnucleus caudalis (medullary dorsal horn). *Brain. Behav. Immun.* 21, 634–41 (2007).

13. Meller, S. T., Dykstra, C., Grzybycki, D., Murphy, S. & Gebhart, G. F. The possible role of glia in nociceptive processing and hyperalgesia in the spinal cord of the rat. *Neuropharmacology* 33, 1471–8 (1994).
14. Khurgel, M., Koo, A. C. & Ivy, G. O. Selective ablation of astrocytes by intracerebral injections of alpha-aminoadipate. *Glia* 16, 351–8 (1996).
15. Rodríguez, M. J., Martínez-Sánchez, M., Bernal, F. & Mahy, N. Heterogeneity between hippocampal and septal astroglia as a contributing factor to differential in vivo AMPA excitotoxicity. *J. Neurosci. Res.* 77, 344–53 (2004).
16. Panatier, A. & Robitaille, R. Astrocytic mGluR5 and the tripartite synapse. *Neuroscience* 323, 29–34 (2016).
17. Ren, B. *et al.* Intrathecal injection of metabotropic glutamate receptor subtype 3 and 5 agonist/antagonist attenuates bone cancer pain by inhibition of spinal astrocyte activation in a mouse model. *Anesthesiology* 116, 122–32 (2012).
18. Wei, F., Guo, W., Zou, S., Ren, K. & Dubner, R. Supraspinal glial-neuronal interactions contribute to descending pain facilitation. *J Neurosci* 28, 10482–10495 (2008).
19. Kim, S. K. *et al.* Cortical astrocytes rewire somatosensory cortical circuits for peripheral neuropathic pain. *J. Clin. Invest.* 126, 1983–97 (2016).
20. David-Pereira, A. *et al.* Metabotropic glutamate 5 receptor in the infralimbic cortex contributes to descending pain facilitation in healthy and arthritic animals. *Neuroscience* 312, 108–119 (2016).
21. Pinto-Ribeiro, F. *et al.* Pronociception from the dorsomedial nucleus of the hypothalamus is mediated by the rostral ventromedial medulla in healthy controls but is absent in arthritic animals. *Brain Res. Bull.* 99, 100–108 (2013).
22. Amorim, D., David-Pereira, A., Pertovaara, A., Almeida, A. & Pinto-Ribeiro, F. Amitriptyline reverses hyperalgesia and improves associated mood-like disorders in a model of experimental monoarthritis. *Behav. Brain Res.* 265, 12–21 (2014).
23. Radhakrishnan, R., Moore, S. a. & Sluka, K. a. Unilateral carrageenan injection into muscle or joint induces chronic bilateral hyperalgesia in rats. *Pain* 104, 567–577 (2003).

24. Pinto-Ribeiro, F., Ansah, O. B., Almeida, A. & Pertovaara, A. Response properties of nociceptive neurons in the caudal ventrolateral medulla (CVLM) in monoarthritic and healthy control rats: modulation of responses by the paraventricular nucleus of the hypothalamus (PVN). *Brain Res. Bull.* 86, 82–90 (2011).
25. Paxinos, G. & Watson, C. *George Paxinos Charles Watson.* (1986).
26. Domin, H., Szewczyk, B., Woźniak, M., Wawrzak-Wleciał, A. & Śmiałowska, M. Antidepressant-like effect of the mGluR5 antagonist MTEP in an astroglial degeneration model of depression. *Behav. Brain Res.* 273, 23–33 (2014).
27. Myers, R. D. Injection of solutions into cerebral tissue: Relation between volume and diffusion. *Physiol. Behav.* 1, 171–IN9 (1966).
28. Barton, N. J. *et al.* Pressure application measurement (PAM): a novel behavioural technique for measuring hypersensitivity in a rat model of joint pain. *J. Neurosci. Methods* 163, 67–75 (2007).
29. Kiritoshi, T., Ji, G. & Neugebauer, V. Rescue of impaired mGluR5-driven endocannabinoid signaling restores prefrontal cortical output to inhibit pain in arthritic rats. *J. Neurosci.* 36, 837–50 (2016).
30. Sluka, K. A. & Westlund, K. N. Behavioral and immunohistochemical changes in an experimental arthritis model in rats. *Pain* 55, 367–377 (1993).
31. Ren, K. & Dubner, R. Inflammatory models of pain and hyperalgesia. *ILARJ.* 40, 111–118 (1999).
32. Vanegas, H. & Schaible, H. G. Descending control of persistent pain: Inhibitory or facilitatory? *Brain Res. Rev.* 46, 295–309 (2004).
33. Chen, F.-L. *et al.* Activation of astrocytes in the anterior cingulate cortex contributes to the affective component of pain in an inflammatory pain model. *Brain Res. Bull.* 87, 60–6 (2012).
34. Tsai, M. J., Chang, Y. F., Schwarcz, R. & Brookes, N. Characterization of L-alpha-amino adipic acid transport in cultured rat astrocytes. *Brain Res.* 741, 166–73 (1996).
35. Byrnes, K. R. *et al.* Metabotropic glutamate receptor 5 activation inhibits microglial

- associated inflammation and neurotoxicity. *Glia* 57, 550–60 (2009).
36. Suter, M. R., Wen, Y.-R., Decosterd, I. & Ji, R.-R. Do glial cells control pain? *Neuron Glia Biol.* 3, 255–68 (2007).
  37. Cui, Y. *et al.* A novel role of minocycline: Attenuating morphine antinociceptive tolerance by inhibition of p38 MAPK in the activated spinal microglia. *Brain. Behav. Immun.* 22, 114–123 (2008).
  38. Raghavendra, V., Tanga, F. & DeLeo, J. A. Inhibition of microglial activation attenuates the development but not existing hypersensitivity in a rat model of neuropathy. *J. Pharmacol. Exp. Ther.* 306, 624–630 (2003).
  39. Raghavendra, V., Tanga, F. Y. & DeLeo, J. A. Complete Freund's adjuvant-induced peripheral inflammation evokes glial activation and proinflammatory cytokine expression in the CNS. *Eur. J. Neurosci.* 20, 467–73 (2004).
  40. Chiang, C. Y., Sessle, B. J. & Dostrovsky, J. O. Role of astrocytes in pain. *Neurochem. Res.* 37, 2419–2431 (2012).
  41. Liu, X. *et al.* Inhibition of glial activation in rostral ventromedial medulla attenuates mechanical allodynia in a rat model of cancer-induced bone pain. *J. Huazhong Univ. Sci. Technol. - Med. Sci.* 32, 291–298 (2012).
  42. Ji, G. *et al.* Cognitive impairment in pain through amygdala-driven prefrontal cortical deactivation. *J. Neurosci.* 30, 5451–5464 (2010).
  43. Bi, L. L. *et al.* Enhanced excitability in the infralimbic cortex produces anxiety-like behaviors. *Neuropharmacology* 72, 148–156 (2013).
  44. Johansen, J. P. & Fields, H. L. Glutamatergic activation of anterior cingulate cortex produces an aversive teaching signal. *Nat. Neurosci.* **7**, 398–403 (2004).

## Figures

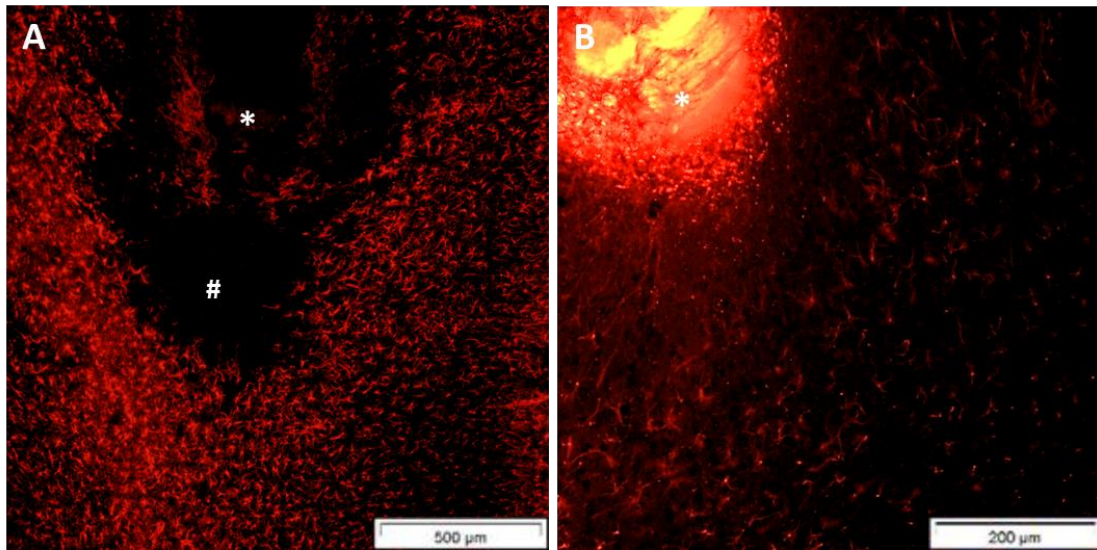


**Figure 1** – Anatomical confirmation of L- $\alpha$ -aminoadipate (L $\alpha$ AA) efficacy. Representative micrographs of GFAP stained brain sections obtained 7 days post injection of L $\alpha$ AA (**A**) or PBS (**B**). \* - glial scar from cannula placement; # - non-fluorescent halo representative of L $\alpha$ AA-induced astrocyte ablation.



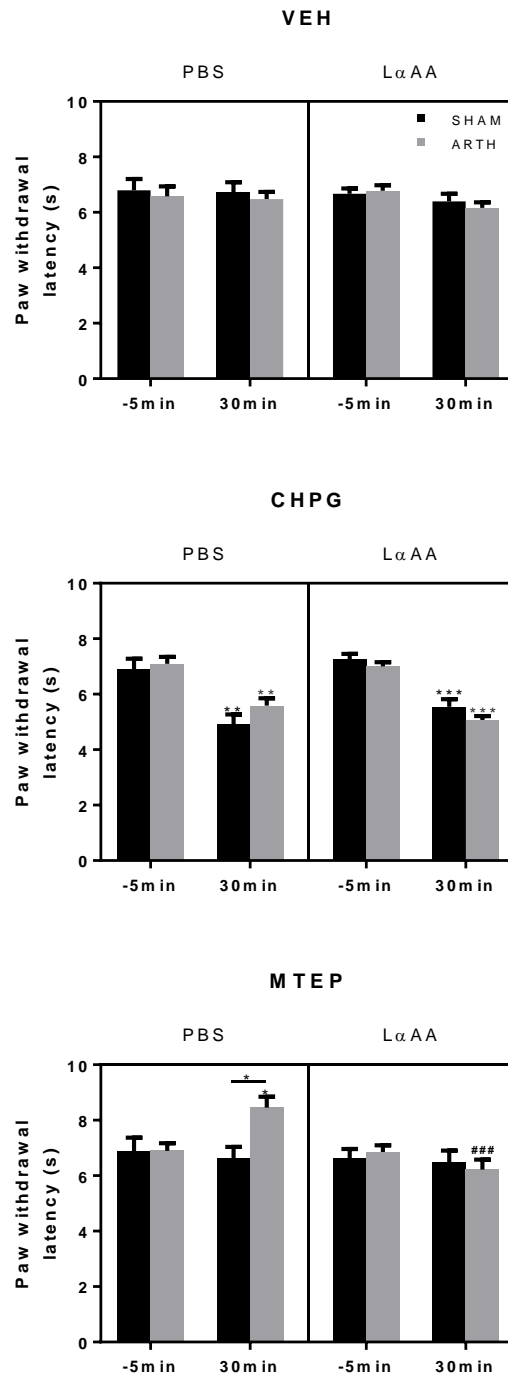


**Figure 2** – Effect of vehicle (VEH; **A**), mGlu5 activation with CHPG (**B**) and mGluR5 inhibition with MTEP (**C**) in the infralimbic cortex (IL) upon the heat-evoked paw withdrawal latencies (PWL) in control (SHAM) and arthritic (ARTH) rats before and after astrocyte ablation with L- $\alpha$ -aminoadipate (L $\alpha$ AA). Graphs show means + SEM. \*\*p<0.01; \*\*\*p<0.001. VEH/PBS: n<sub>SHAM</sub>=12; n<sub>ARTH</sub>=15; VEH/ L $\alpha$ AA: n<sub>SHAM</sub>=20; n<sub>ARTH</sub>=18; CHPG/PBS: n<sub>SHAM</sub>=9; n<sub>ARTH</sub>=15; CHPG/ L $\alpha$ AA: n<sub>SHAM</sub>=18; n<sub>ARTH</sub>=22; MTEP/PBS: n<sub>SHAM</sub>=11; n<sub>ARTH</sub>=14; MTEP/ L $\alpha$ AA: n<sub>SHAM</sub>=12; n<sub>ARTH</sub>=12.

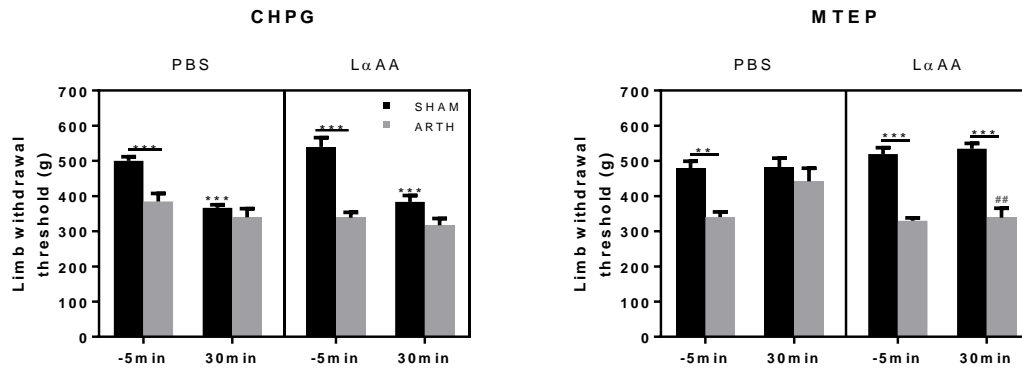


**Figure 3** – Effect of mGlu5 activation with CHPG (**A**) and mGluR5 inhibition with MTEP (**B**) in the infralimbic cortex (IL) upon the mechanical-evoked limb withdrawal threshold (LWT) in control (SHAM) and arthritic (ARTH) rats before and after astrocyte ablation with L- $\alpha$ -aminoadipate (L $\alpha$ AA). Graphs show means + SEM. \*\* $p < 0.01$ ; \*\*\* $p < 0.001$ . CHPG/PBS:  $n_{\text{SHAM}}=8$ ;  $n_{\text{ARTH}}=8$ ; CHPG/ L $\alpha$ AA:  $n_{\text{SHAM}}=8$ ;  $n_{\text{ARTH}}=10$ ; MTEP/PBS:  $n_{\text{SHAM}}=4$ ;  $n_{\text{ARTH}}=8$ ; MTEP/ L $\alpha$ AA:  $n_{\text{SHAM}}=8$ ;  $n_{\text{ARTH}}=9$ .

Chapter 2.4

---

Ana David-Pereira, Boriss Sagalajev, Hong Wei, Armando Almeida, Antti Pertovaara, Filipa Pinto-

Ribeiro

**The medullary dorsal reticular nucleus as a relay for descending pronociception induced by the mGluR5 in the rat infralimbic cortex**

*Neuroscience, in press*

2017



Please cite this article in press as: David-Pereira A et al. The medullary dorsal reticular nucleus as a relay for descending pronociception induced by the mglur5 in the rat infralimbic cortex. *neuroscience* (2017), <http://dx.doi.org/10.1016/j.neuroscience.2017.02.046>

*Neuroscience xxx (2017) xxx–xxx*

## THE MEDULLARY DORSAL RETICULAR NUCLEUS AS A RELAY FOR DESCENDING PRONOCICEPTION INDUCED BY THE mGluR5 IN THE RAT INFRALIMBIC CORTEX

ANA DAVID-PEREIRA,<sup>a,b</sup> BORISS SAGALAJEV,<sup>c</sup>  
HONG WEI,<sup>c</sup> ARMANDO ALMEIDA,<sup>a,b</sup>  
ANTTI PERTOVAARA<sup>c,\*†</sup> AND FILIPA PINTO-RIBEIRO<sup>a,b,\*†</sup>

<sup>a</sup> *Life and Health Sciences Research Institute (ICVS), School of Medicine (EM), Campus of Gualtar, University of Minho, 4710-057 Braga, Portugal*

<sup>b</sup> *ICVS/3B's – PT Government Associate Laboratory, Braga/Guimarães, Portugal*

<sup>c</sup> *Department of Physiology, Faculty of Medicine, POB 63, University of Helsinki, 00014 Helsinki, Finland*

**Abstract—Metabotropic glutamate receptor 5 (mGluR5) activation in the infralimbic cortex (IL) induces pronociceptive behavior in healthy and monoarthritic rats. Here we studied whether the medullary dorsal reticular nucleus (DRt) and the spinal TRPV1 are mediating the IL/mGluR5-induced spinal pronociception and whether the facilitation of pain behavior is correlated with changes in spinal dorsal horn neuron activity. For drug administrations, all animals had a cannula in the IL as well as a cannula in the DRt or an intrathecal catheter. Heat-evoked paw withdrawal was used to assess pain behavior in awake animals. Spontaneous and heat-evoked discharge rates of single DRt neurons or spinal dorsal horn wide-dynamic range (WDR) and nociceptive-specific (NS) neurons were evaluated in lightly anesthetized animals. Activation of the IL/mGluR5 facilitated nociceptive behavior in both healthy and monoarthritic animals, and this effect was blocked by lidocaine or GABA receptor agonists in the DRt. IL/mGluR5 activation increased spontaneous and heat-evoked DRt discharge rates in healthy but not monoarthritic rats. In the spinal dorsal horn, IL/mGluR5 activation increased spontaneous activity of WDR neurons in healthy animals only, whereas heat-evoked responses**

of WDR and NS neurons were increased in both experimental groups. Intrathecally administered TRPV1 antagonist prevented the IL/mGluR5-induced pronociception in both healthy and monoarthritic rats. The results suggest that the DRt is involved in relaying the IL/mGluR5-induced spinal pronociception in healthy control but not monoarthritic animals. Spinally, the IL/mGluR5-induced behavioral heat hyperalgesia is mediated by TRPV1 and associated with facilitated heat-evoked responses of WDR and NS neurons. © 2017 IBRO. Published by Elsevier Ltd. All rights reserved.

**Key words:** infralimbic cortex, metabotropic glutamate receptor 5, experimental monoarthritis, pronociception, dorsal reticular nucleus, spinal TRPV1.

### INTRODUCTION

Increased nociceptive sensitivity in chronic pain results from sensitization of peripheral and central pathways (Schaible et al., 2002). Central sensitization translates as hyperalgesia and allodynia resulting in hypersensitivity of nociceptive neurons to suprathreshold and previously subthreshold stimuli, respectively. Consequently, a pain facilitatory state arises due to changes in brain activity that can be detected through electrophysiological and imaging techniques (Apkarian, 2004; Metz et al., 2009; Woolf, 2011). These secondary neuroplastic changes, fundamental for the establishment and maintenance of chronic pain, occur throughout the pain matrix and range from frontal areas, such as the medial prefrontal cortex (mPFC), to caudal modulatory regions, such as the rostral ventromedial medulla (RVM) and the dorsal reticular nucleus (DRt) (Pertovaara et al., 1996; Ossipov et al., 2000; Lima and Almeida, 2002; Heinricher et al., 2009; Baron et al., 2013).

The DRt is a pain modulatory brain region better known for its facilitatory action (Almeida et al., 1996, 1999; Lima and Almeida, 2002; Martins et al., 2013). Electrolytic lesion or chemical block of the DRt increases tail-flick latency in healthy animals (Almeida et al., 1996) and decreases pain behavior in the formalin test (Almeida et al., 1999). DRt neurons receive afferent projections from spinal neurons (Almeida et al., 1993, 2000) activated by noxious stimulation (Almeida and Lima, 1997; Dugast et al., 2003). Its receptive fields encompass the entire body surface and are activated exclusively or preferentially by noxious stimuli

\*Corresponding authors. Address: Life and Health Sciences Research Institute (ICVS), School of Medicine (EM), Campus of Gualtar, University of Minho, 4710-057 Braga, Portugal (F. Pinto-Ribeiro). E-mail addresses: [antti.pertovaara@helsinki.fi](mailto:antti.pertovaara@helsinki.fi) (A. Pertovaara), [filipa.ribeiro@ecea.uminho.pt](mailto:filipa.ribeiro@ecea.uminho.pt) (F. Pinto-Ribeiro).

<sup>†</sup> These authors share the last authorship.  
**Abbreviations:** AMG, AMG 9810 (TRPV1 antagonist); ANOVA, analysis of variance; ARTH, kaolin/carrageenan induced monoarthritis; CHPG, (RS)-2-Chloro-5-hydroxyglycine (mGluR5 agonist); CNS, central nervous system; DRt, dorsal reticular nucleus; GABA,  $\gamma$ -aminobutyric acid; i.p., intraperitoneal; i.t., intrathecal; IL, infralimbic cortex; LIDO, lidocaine; mGluR5, metabotropic glutamate receptor 5; MPEP, 6-Methyl-2-(phenylethynyl)pyridine; mPFC, medial prefrontal cortex; MUSC, muscimol; NS, nociceptive-specific; ONDAN, ondansetron hydrochloride (5-HT<sub>3</sub>R antagonist); PAG, periaqueductal gray area; PFC, prefrontal cortex; PSTH, peristimulus time histogram; PWL, (heat-evoked hind) paw withdrawal latency; RVM, rostral ventromedial medulla; SAL, saline; SEM, standard error of the mean; TRPV1, transient receptor potential cation channel subfamily V member 1; WDR, wide-dynamic range.

(Villanueva et al., 1988, 1996). The DRt projects to several brain areas implicated in pain processing and modulation (Leite-Almeida et al., 2006) and also targets spinal dorsal horn neurons located in laminae I and IV–VI (Almeida et al., 1993, 2000; Tavares and Lima, 1994; Villanueva et al., 1995). This descending pathway seems to be directly involved in nociceptive facilitation in healthy (Almeida et al., 1999; Zhang et al., 2005; Amorim et al., 2015) and neuropathic animals (Sotgiu et al., 2008).

The DRt receives axonal projections from many brain regions implicated in pain processing and modulation (Almeida et al., 2002), including the infralimbic cortex (IL), a region shown to induce heat hyperalgesia in rodents after local activation of metabotropic glutamate receptor 5 (mGluR5) (David-Pereira et al., 2016). Conversely, mGluR5 block in the IL leads to heat analgesia, an effect observed only in rats with prolonged inflammatory pain, suggesting that experimental monoarthritis may lead to neuroplastic changes in the IL (David-Pereira et al., 2016). However, not much is known about the functional role of descending pathways between the IL and various spinally-projecting pain modulatory regions/relays, such as the DRt. In this work, electrophysiological and behavioral techniques were used to study whether the DRt is involved in relaying the descending pronociceptive effect induced by activation of the mGluR5 in IL in monoarthritic as well as healthy control animals.

We also attempted to assess which receptor mediates the IL/mGluR5-induced descending pronociceptive effect at the spinal cord level. In particular, we tested the potential involvement of the pronociceptive transient receptor potential cation channel subfamily V member 1 (TRPV1), best known for its important role in transduction of noxious signals in the peripheral terminals of primary afferent nociceptors (Caterina et al., 2000). In the spinal dorsal horn, TRPV1 is expressed on central terminals of nociceptive nerve fibers where it amplifies transmission on excitatory interneurons, and postsynaptically where it facilitates responses of presumed pain-relay neurons (Valtschanoff et al., 2001; Zhou et al., 2009). Earlier, it has been shown that pharmacological blocking of the spinal TRPV1 attenuates pain-related behavior in various arthritis models (Cui et al., 2006), but the role of spinal TRPV1 in descending facilitation of nociception is not yet known. Here we administered intrathecally a selective TRPV1 antagonist to assess whether spinal TRPV1 is involved in mediating the IL/mGluR5-induced descending pronociceptive effect in monoarthritic and/or healthy control animals.

## EXPERIMENTAL PROCEDURES

### Animals, anesthetics and ethical issues

The experiments were performed in adult Wistar Han male rats with 200–300 g (Envigo, Blackthorn, UK). The experimental protocol was approved by the Experimental Animal Ethics Committee of the Provincial Government of Southern Finland (Hämeenlinna, Finland; permission # ESAVI/7863/04.10.07/2013) and followed the European Community Council Directive 2010/63/EU concerning the use of animals for scientific

purposes. All efforts were made to minimize animal suffering and to use only the number of animals necessary to produce reliable scientific data.

For all surgical and electrophysiological procedures, anesthesia was induced through the intraperitoneal (i.p.) administration of sodium pentobarbitone (60 mg/kg; Mebunat, OrionPharma, Espoo, Finland). Anesthesia level was assessed by observation of pupil size, general muscle tone and by assessing withdrawal responses to noxious pinching; anesthesia was maintained by administering additional doses of sodium pentobarbitone (15–20 mg/kg) as required. During the electrophysiological experiments, anesthesia was kept at a level at which no spontaneous movement of extremities was observed.

When performing the surgical procedures for insertion of chronic guide cannulas and/or an intrathecal catheter, anesthesia was induced and maintained as described above. After completion of the surgical procedure, animals were monitored until they were fully recovered. To prevent post-operative pain, animals were treated subcutaneously with 0.01 mg/kg of buprenorphine (Temgesic, Reckitt Benckiser, Berkshire, UK) twice a day for 3 days, and were allowed to recover for at least a week before the beginning of the behavioral experiments.

After the completion of the experiments, animals received a lethal dose of sodium pentobarbitone and the brains were removed for histological confirmation of cannula and/or electrode placement.

### Induction of monoarthritis

Induction of monoarthritis (ARTH) was performed 28 days before the beginning of the experiments, as described in detail elsewhere (Pinto-Ribeiro et al., 2013). Briefly, 3% kaolin and 3% carrageenan (Sigma–Aldrich, St. Louis, MO, USA) were dissolved in distilled water and injected intrasynovially in the right knee joint at a volume of 0.1 mL. Mechanical hyperalgesia begins development a few hours after surgery and can be observed up to 8 weeks (Radhakrishnan et al., 2003; Amorim et al., 2014). ARTH development was verified 1–2 h prior to each behavioral/electrophysiological session in each animal. Only rats that audibly vocalized during each one of the five flexion–extension movements of the knee joint were considered to be monoarthritic and included in the ARTH group (Amorim et al., 2014). Saline solution (0.1 mL) was injected intrasynovially in the right knee joint of control animals (SHAM). SHAM animals did not vocalize during any of the five consecutive flexion–extension movements of the knee joint.

### Procedures for intracerebral microinjections

For intracerebral drug administration, cannulas were implanted as described elsewhere (Pinto-Ribeiro et al., 2011). Rats were placed in a standard stereotaxic frame, the skull was exposed, one or two holes drilled and sterilized stainless-steel guide cannulas (26 gauge; Plastics One, Roanoke, VA, USA) were implanted in the brain. The coordinates in this and other sections refer to the

atlas of Paxinos and Watson (1986). The tip of the guide cannula was positioned 1 mm above the right IL [2.76 mm frontal to bregma; 0.6 mm lateral to midline; depth 4.2 mm (Fig. 1A, C–G)] and the right DRt [–14.04 mm frontal to bregma; 1.4 mm lateral to midline; depth 8.6 mm (Fig. 1B, H–L)], fixed to the skull with screws and dental acrylic cement, and the skin sutured around it. A dummy cannula (Plastics One) was inserted into the guide cannula to prevent contamination.

Test drugs were administered through a 33-gauge injection cannula (Plastics One) protruding 1 mm beyond the tip of the guide cannula and connected to a 5.0- $\mu$ L Hamilton syringe by a polyethylene catheter (PE-10; Plastics One). The injection volume was 0.5  $\mu$ L, with an expected drug injection spread within the brain of 1 mm in diameter (Myers, 1966). The efficacy of injection was monitored by noting the movement of a small air bubble through the tubing. The minimum duration for drug microinjection was of at least 20 s and the injection cannula was left in place for an additional 30 s to minimize drug solution return through the injection cannula.

#### 186 Procedures for intrathecal injections

187 For spinal cord drug delivery at the lumbar level,  
188 intrathecal (i.t.) catheters (Intramedic PE-10, Becton  
189 Dickinson and Company, Sparks, MD, USA) were  
190 implanted as originally described by Størkson and  
191 colleagues (1996). The following day, the correct physio-  
192 logical placement of the catheter was confirmed by  
193 administering lidocaine (LIDO; 10  $\mu$ L, 4%; OrionPharma,  
194 Espoo, Finland) with a 50- $\mu$ L Hamilton syringe (Hamilton  
195 Company, Bonaduz, Switzerland). Only those rats that  
196 presented no motor impairment before LIDO injection  
197 but had bilateral paralysis of their hind limbs after i.t.  
198 administration of LIDO were used in further studies. After  
199 the test, animals were monitored until they regained  
200 motor control of their hind limbs. When administering  
201 the studied drugs i.t., the volume of drug injections was  
202 10  $\mu$ L.

#### 203 Drugs

204 (RS)-2-chloro-5-hydroxyglycine (CHPG; mGluR5 agonist;  
205 Tocris, Bristol, UK), 6-Methyl-2-(phenylethynyl)pyridine  
206 (MPEP; mGluR5 antagonist; Tocris, Bristol, UK), 5-  
207 aminomethyl-3-hydroxyisoxazole (Muscimol – MUSC;  
208 GABA<sub>A</sub> receptor agonist; Tocris, Bristol, UK) and  $\gamma$ -  
209 aminobutyric acid (GABA, Tocris; Bristol, UK) solutions  
210 for intracerebral drug injection were prepared with  
211 sterilized saline solution 0.9% (B. Braun Oy, Espoo,  
212 Finland; pH 7.2). (2E)-N-(2,3-Dihydro-1,4-benzodioxin-6-  
213 yl)-3-[4-(1,1-dimethylethyl)phenyl]-2-propenamide (AMG  
214 9810; TRPV1 antagonist; Tocris, Bristol, UK) was  
215 dissolved in a solution of 5% ethanol + 5% Tween-80.  
216 LIDO (4%) was acquired as a solution (Orion).

217 Previous studies showed that an intracerebral dose of  
218 50 nmol of CHPG (Ansah et al., 2009; David-Pereira  
219 et al., 2016) and 50 nmol of MPEP (David-Pereira et al.,  
220 2016) are effective in activating/inhibiting mGluR5 in the  
221 rat and that intracerebral doses of 30 ng of MUSC and  
222 50 nmol of GABA were effective in activating GABA

receptors (Frye et al., 1983; Lacerda et al., 2003). An  
intrathecal dose of at least 15  $\mu$ g of AMG 9810 (AMG)  
was shown to reverse mechanical and thermal hyperalge-  
sia in a rat model of inflammatory pain (Yu et al., 2008).  
Alterations in nociceptive behavior were evaluated at  
fixed time points (Fig. 2) until the drug effect was no  
longer observed. The behavioral and electrophysiological  
results presented are for the peak effect of drugs, which  
was determined to be 30 min after drug injection. Control  
injections were performed with the respective vehicle  
(VEH) solutions.

#### 234 BEHAVIORAL ASSESSMENT OF NOCICEPTION

##### 235 Hargreaves model

236 Rats were habituated to the experimental conditions by  
237 performing daily handling sessions with the  
238 experimenter and by allowing them to spend 1 h daily in  
239 the testing room and apparatus during the week  
240 preceding any testing. Nociception in unanesthetized  
241 animals was determined by measuring hind paw  
242 withdrawal latency (PWL) following radiant heat  
243 stimulation (Hargreaves test; Plantar Test Device Model  
244 37370, Ugo Basile, Varese, Italy). In each behavioral  
245 session, PWL was assessed before and at fixed  
246 intervals following intracerebral and/or i.t. drug  
247 administration (Fig. 2). At each time point, the  
248 measurements were repeated twice at an interval of  
249 1 min. The mean of these values was used in further  
250 calculations. To avoid any damage to the skin, the cut-  
251 off time for radiant-heat exposure was set at 15 s.

##### 252 Skin temperature

253 The temperature of the hind paws was measured before  
254 each PWL measurement by placing a contact thermode  
255 on the plantar skin of each hind paw (Physitemp, Model  
256 BAT-12, Physitemp Instruments Inc., Clifton, NJ, USA).  
257 This measurement was performed to exclude a drug-  
258 induced change in the skin temperature as a  
259 confounding factor when assessing radiant heat-induced  
260 response latencies (Luukko et al., 1994).

#### 261 ELECTROPHYSIOLOGICAL RECORDINGS

##### 262 DRt recordings

263 Single-unit recordings of DRt neurons were performed  
264 under sodium pentobarbitone anesthesia. Animals were  
265 breathing spontaneously and the body temperature was  
266 maintained within physiological range using a warming  
267 blanket.

268 Animals were placed in a standard stereotaxic  
269 apparatus, the skull was exposed and holes were drilled  
270 to allow the placement of a guide cannula in the IL  
271 (2.76 mm frontal to bregma; 0.6 mm lateral to midline;  
272 depth 4.2 mm; Fig. 1A, C–G) and a recording electrode  
273 in the DRt (14.04 mm frontal to bregma; 1.4 mm lateral  
274 to midline; depth 8.6 mm; Fig. 1B, H–L). Single neuron  
275 activity was recorded with lacquer-coated tungsten  
276 electrodes (impedance 3–10 M $\Omega$  at 1KHz; FCH Inc.,  
277 Bowdoin, ME, USA).

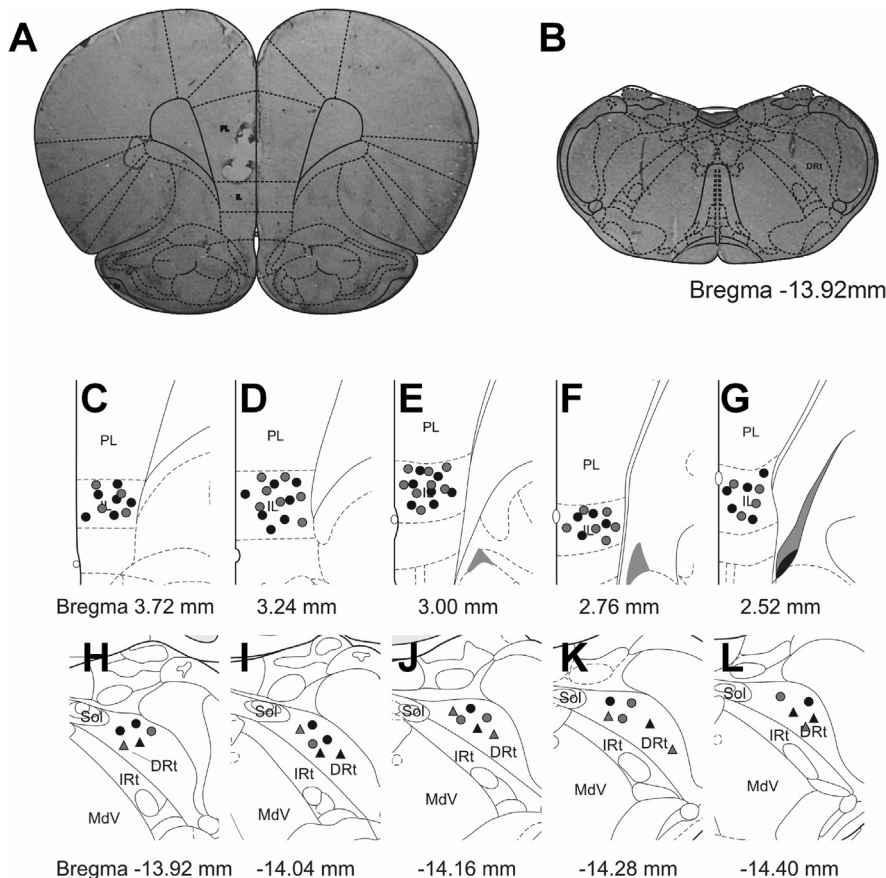


**Fig. 1.** Anatomical confirmation of drug injection and neuronal recordings. (A) Photomicrograph of an example of the cannula placement in the infralimbic cortex (IL) of the rat brain (AP: +3.72 mm from bregma) superimposed with the appropriate legend from Paxinos and Watson (2007) stereotaxic atlas. (B) Photomicrograph of an example of the recording site in the medullary dorsal reticular (DRt) of the rat brain (AP: -13.92 mm from bregma) superimposed with the appropriate legend from Paxinos and Watson (2007) stereotaxic atlas. (C-G) Schematic representation of other injection sites in the IL (C: +3.72 mm, D: +3.24 mm, E: +3.00 mm, F: +2.76 mm; G: +2.52 mm) in SHAM (black) and ARTH animals (gray). (H-L) Schematic representation of other injection (circles) or recording (triangles) sites in the DRt (H: -13.92 mm, I: -14.04 mm, J: -14.16 mm, K: -14.28 mm, L: -14.40 mm) in SHAM (black) and ARTH animals (gray). DRt – medullary dorsal reticular nucleus; IL – infralimbic cortex; IRT – intermediate reticular nucleus; MdV – medullary ventral reticular nucleus; PL – prelimbic cortex; Sol – nucleus of the solitary tract.

Spike 2 software (Cambridge Electronic Design, Cambridge, UK). Multiple spikes were isolated based on spike shape parameters from the neuronal signals using the spike shape template functions in Spike2. To ensure the same neurons were evaluated before and after drug injection, the template generated in the first recording was used for spike sorting in all consecutive recordings.

### Latency of DRt neuronal response to electric stimulation in the IL

To have an estimate of the time that it takes from activation of the IL to the activation of the DRt, the latency of DRt neuron response to electric stimulation of the IL was determined in two healthy control animals. For this purpose, recording and characterization of DRt neurons was performed as described in the above section. Additionally, a concentric bipolar stimulation electrode (SS80SNE-100, MicroProbes, Gaithersburg, MD, USA) was positioned in the right IL (2.76 mm frontal to bregma; 0.6 mm lateral to midline; depth 5.0 mm). After finding a neuron in the DRt that gave an excitatory response to noxious heat stimulation, single electrical stimuli (square pulses of 0.3-ms duration) were delivered in the IL using a constant-current stimulator (PSIU6 and Grass S88, Grass Instruments, Quincy, MA, USA). For assessment of latency and latency variation, a series of 10 stimuli at the intensity of 10.0 mA (real stimulus) or 0.0 mA (fake stimulus) were delivered consecutively at 2-s intervals. Peristimulus time histograms (PSTHs) were constructed from successive stimulation trials with 2-ms bins separately in the real and fake stimulus condition. PSTHs were normalized to give firing probability (spikes/bin). Based on earlier studies on corticofugal neurons, response of the DRt neurons was classified as a short latency response if the first impulse evoked by a real stimulus occurred in  $\geq 20\%$  of cases within 20 ms (Doig et al., 2014). In the present study, however, time window 0 ms – 9.5 ms could not be analyzed due to stimulus artifact produced by the currently used high stimulus intensity. Therefore, the response occurring between 9.5 ms and 20 ms was considered a short latency response in this study. Another criterion for possibly monosynaptic short latency response was that within 20 ms there was a histogram peak that had > 3 standard

278 To search for DRt neurons, the response to a noxious  
279 heat stimulus applied to the plantar skin of the right hind  
280 paw was used (54 °C for 10 s; LTS-3 Stimulator,  
281 Thermal Devices Inc., Golden Valley, MN, USA). A  
282 piezoceramic movement detector (Siemens Elema Ab,  
283 Solna, Sweden) was taped to the skin of a flexor muscle  
284 in the hind limb to allow correlating the changes in the  
285 activity of DRt cells with withdrawal responses.

286 The evaluation of the response of DRt cells to  
287 peripheral noxious stimulation consisted of the following  
288 assessments: (i) spontaneous activity (first 20 s of  
289 recording without any stimulation); (ii) response to  
290 noxious heating of the hind paw (10 s); and (iii) latency  
291 of the heat-induced limb-reflex (time from the start of  
292 the heat stimulus to the first movement of the hind limb).

293 The signals from the recordings were amplified and  
294 filtered by using standard techniques. Data sampling  
295 and spike sorting were performed with a computer  
296 connected to a CED Micro 1401 interface and using



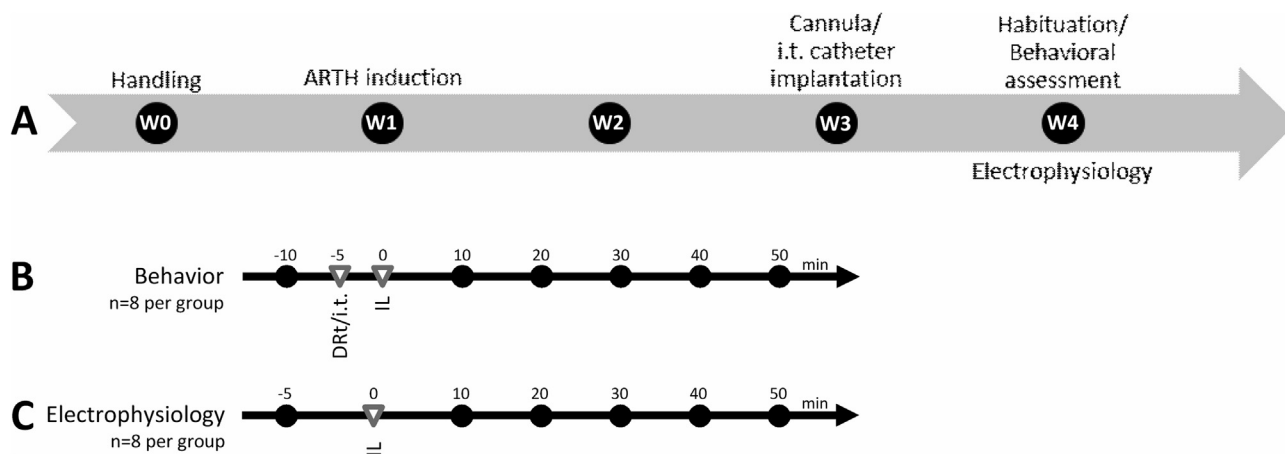


**Fig. 2.** Schematic representation of the experimental design timeline. (A) Rats were habituated to the laboratory and the experimenter for 5 days. After habituation, animals belonging to the monoarthritic (ARTH) group received an intra-synovial injection of 3% kaolin/carrageenan while control (SHAM) animals received an intra-synovial injection of saline solution. Two weeks after experimental monoarthritis induction, animals were implanted with a guide cannula in the infralimbic cortex (IL). After recovery (one week), rats were trained in the paw-withdrawal apparatus. (B) Behavioral testing was performed at the same time points for all the drug combinations. DRT/i.t. drug administration was performed 5 min before IL microinjection. (C) Electrophysiological recordings were performed at the same time points for all the drugs. DRT – dorsal reticular nucleus; IL – infralimbic cortex; i.t. – intrathecal; min – minutes; W0–4 – weeks 0 to 4.

356 deviations higher firing probability in the real than the cor-  
357 responding fake stimulus condition (Doigt et al., 2014).

### 358 Spinal dorsal horn neuron recordings

359 Single-unit recordings of spinal dorsal horn neurons were  
360 performed under sodium pentobarbitone anesthesia.  
361 Animals were breathing spontaneously and the body  
362 temperature was maintained within physiological range  
363 using a warming blanket.

364 With the animal deeply anesthetized, a laminectomy  
365 was performed at the level of the T12–L2 vertebrae to  
366 expose the L4–L6 segments of the spinal cord. The dura  
367 was cut and a pool of skin formed and filled with warm  
368 mineral oil (Mineral Oil, Sigma–Aldrich Finland, Helsinki,  
369 Finland) to prevent dehydration. The animal was placed  
370 in a standard stereotaxic frame and two spinal clamps,  
371 one rostral and one distal to the laminectomy, were  
372 used to stabilize the preparation. Single neuron activity  
373 was recorded as previously described using lacquer-  
374 coated tungsten electrodes (Viisanen et al., 2012).

375 To search for spinal dorsal horn neurons, a  
376 mechanical innocuous stimulus was applied with a  
377 brush on the plantar skin of the ipsilateral hind paw  
378 (brushing), followed by noxious heat stimulation of the  
379 plantar skin of the right hind paw (54 °C for 10 s; LTS-3  
380 Stimulator, Thermal Devices Inc., Golden Valley, MN,  
381 USA). If the neurons responded to both innocuous  
382 brush and noxious heat stimulation, the cell was  
383 classified as wide-dynamic range (WDR) neuron; if the  
384 neuron responded to the noxious thermal stimulation but  
385 failed to respond to the innocuous brushing, it was  
386 classified as a nociceptive-specific (NS) neuron (Willis  
387 and Coggeshall, 2004). Neurons that responded exclu-  
388 sively to innocuous stimuli were not further considered  
389 in this study. Only neurons that were considered to be

390 in the spinal dorsal horn according to the recording depth  
391 from the cord surface (< 1000 μm) were further analyzed.

392 The evaluation of the response of spinal dorsal horn  
393 cells to peripheral noxious stimulation consisted of the  
394 following assessments: (i) spontaneous activity (first  
395 20 s of recording without any stimulation) and (ii)  
396 response to noxious heating of the hind paw (10 s).

397 The signals from the recordings were amplified and  
398 processed as described in the previous section, using a  
399 computer connected to a CED Micro 1401 interface and  
400 using Spike 2 software (Cambridge Electronic Design,  
401 Cambridge, UK).

### 402 Course of the behavioral study

403 Animals used in the behavioral studies were sub-divided  
404 in two experimental groups: (i) animals with intracerebral  
405 cannulas in the IL and in the DRt ( $n_{\text{SHAM}} = 14$ ;  
406  $n_{\text{ARTH}} = 15$ ), and (ii) animals with an intracerebral  
407 cannula in the IL and an i.t. catheter ( $n_{\text{SHAM}} = 8$ ;  
408  $n_{\text{ARTH}} = 7$ ). Three weeks after ARTH induction and at  
409 least one week after guide cannula/i.t. catheter  
410 implantation, animals were habituated to the Hargreaves  
411 test apparatus as described previously. Four weeks  
412 after ARTH induction, changes in nociceptive behavior  
413 of unanesthetized animals after drug administration in  
414 the IL and DRt/spinal cord (5 min between each  
415 administration) were determined (Fig. 2A) by assessing  
416 PWL before and 10, 20, 30, 40 and 50 min following the  
417 first drug administration. Additionally, at these time  
418 points the temperature of the hind paw plantar skin was  
419 also assessed (Fig. 2B). Drug testing was randomized  
420 among animals. The interval between behavioral  
421 assessments in each rat was of at least three days. All  
422 animals were treated with all drug combinations.

## 423 COURSE OF THE ELECTROPHYSIOLOGICAL 424 STUDY

### 425 DRt neuron recordings

426 Electrophysiological recordings of DRt cells were  
427 performed 4 weeks after ARTH induction ( $n_{\text{SHAM}} = 7$ ;  
428  $n_{\text{ARTH}} = 7$ ). Pharmacological manipulations started after  
429 the spontaneous and noxious heat-evoked activity of  
430 responding cells had been recorded. In a single session,  
431 one to five neurons could be recorded simultaneously.  
432 The same cells were recorded throughout the whole  
433 session unless the neuron stopped responding for more  
434 than one hour, in which case another recording site was  
435 searched (Fig. 2C). In each session, a microinjection of  
436 SAL, CHPG or MPEP were administered at an interval  
437 of 1.5 h between injections. In general, one or two  
438 recording sessions were performed in each animal. At  
439 the end of the electrophysiological session, an  
440 electrolytic lesion was made in the last recording site to  
441 allow posterior confirmation of the recording site(s).

### 442 Latency of the DRt response to electric IL stimulation

443 The latency to response of DRt neurons to electric IL  
444 stimulation was measured in a separate experiment  
445 using two healthy control rats. Only one DRt neuron  
446 giving an excitatory response to noxious heat was  
447 tested in each animal. After completing the recording  
448 session, the animal was euthanized and the recording/  
449 stimulation sites were determined as described above.

### 450 Spinal dorsal horn neuron recordings

451 Electrophysiological recordings of spinal dorsal horn  
452 neurons were performed four weeks after ARTH  
453 induction ( $n_{\text{SHAM}} = 7$ ;  $n_{\text{ARTH}} = 8$ ). Pharmacological  
454 manipulations started after the neuron was classified as  
455 a WDR or NS cell and its spontaneous and noxious  
456 heat-evoked activity had been recorded in a baseline  
457 condition (i.e., before drug injection; Fig. 2C). In a single  
458 session, one to three neurons could be recorded  
459 simultaneously. The same cells were recorded  
460 throughout the whole session unless the neuron  
461 stopped responding for more than one hour, in which  
462 case another recording site was searched. In each  
463 session, the interval between IL microinjections of SAL  
464 and CHPG was 1.5 h. In general, one or two recording  
465 sessions were performed in each animal. Recording  
466 sites within the spinal dorsal horn were estimated based  
467 on the depth from the cord surface.

### 468 Statistics

469 Statistical analyses were performed using a two-way  
470 analysis of variance (ANOVA) followed by *t*-test with a  
471 Bonferroni correction for multiple comparison, except for  
472 comparisons between two groups, which were made  
473 using Student *t*-test. Analyses were performed with  
474 GraphPad Prism 6 software (GraphPad Software Inc.,  
475 La Jolla, CA, USA), and  $p < 0.05$  was considered to  
476 represent a significant difference. Data are presented as  
477 mean  $\pm$  standard error of the mean (SEM). Both 138

behavioral and electrophysiological data are presented 478  
as the difference ( $\Delta$ ) between values measured 30 min 479  
after drug administration and values measured before 480  
injection. 481

$$\Delta = 30 \text{ min} - (\text{baseline}) \quad 482$$

## 483 RESULTS

### 484 Blocking the DRt prevents heat hyperalgesia after IL/ 485 mGluR5 activation in both SHAM and ARTH animals

486 The effect of CHPG, an mGluR5 agonist, in the IL, was 487  
assessed in both SHAM and ARTH animals, while the 488  
DRt and the descending pathway relaying through it 489  
were blocked through the local microinjection of LIDO, 490  
MUSC or GABA. Baseline PWLs before drug injections 491  
were not significantly different between ARTH and 492  
SHAM groups ( $t_{173} = 1.111$ ,  $p = 0.268$ ; Fig. 3D). 493  
Overall, LIDO microinjection altered PWL (effect of drug 494  
microinjection:  $F_{3,89} = 42.34$ ,  $p < 0.0001$ ), independent 495  
of the experimental group (interaction of drug 496  
administration vs experimental group:  $F_{3,89} = 0.171$ , 497  
 $p = 0.915$ ). *Post hoc* tests indicate that administration 498  
of CHPG alone in the IL decreased PWL, LIDO alone in 499  
the DRt increased PWL, whereas the combination of 500  
CHPG in the IL and LIDO in the DRt did not alter PWL 501  
of SHAM or ARTH animals (Fig. 3A). Selectively 502  
blocking DRt neuronal activity with MUSC and GABA 503  
administration held results similar to the general 504  
inhibition with LIDO: drug microinjection altered PWL 505  
(effect of MUSC microinjection:  $F_{3,104} = 39.89$ , 506  
 $p < 0.0001$ ; effect of GABA microinjection: 507  
 $F_{3,101} = 40.09$ ,  $p < 0.0001$ ), independent of the 508  
experimental group tested (effect of MUSC 509  
microinjection:  $F_{3,104} = 0.311$ ,  $p = 0.817$ ; effect of 510  
GABA microinjection:  $F_{3,101} = 0.165$ ,  $p = 0.920$ ). *Post* 511  
*hoc* tests indicate that the combination of CHPG in the 512  
IL and MUSC (Fig. 3B) or GABA (Fig. 3C) in the DRt did 513  
not alter the PWL of SHAM or ARTH animals. 514

515 The temperature of the plantar skin was not affected 516  
by drug administrations (effect of drug microinjection: 517  
 $F_{7,99} = 1.213$ ,  $p = 0.303$ ), independent of the 518  
experimental group (interaction of drug administration vs 519  
experimental group:  $F_{7,99} = 0.334$ ,  $p = 0.937$ ; Fig. 3E). 520

### 521 mGluR5 activation in the IL increases spontaneous 522 and evoked activity of DRt neurons in SHAM, but not 523 in ARTH animals

524 In general, DRt neurons were spontaneously active and 525  
their receptive fields covered large areas of the body 526  
including the right sided hind limb and the tail. 527  
Receptive field stimulation with a noxious thermal 528  
stimulus but not innocuous brushing of the skin 529  
produced an excitatory response in DRt neurons 530  
(Fig. 4A).

531 The activity of nociceptive DRt cells was recorded 532  
before and after the administration of CHPG in the IL. In 533  
ARTH animals, the baseline spontaneous activity of DRt 534  
neurons before drug administrations was significantly 535  
higher than in SHAM animals ( $t_{77} = 2.156$ ,  $p = 0.034$ ;

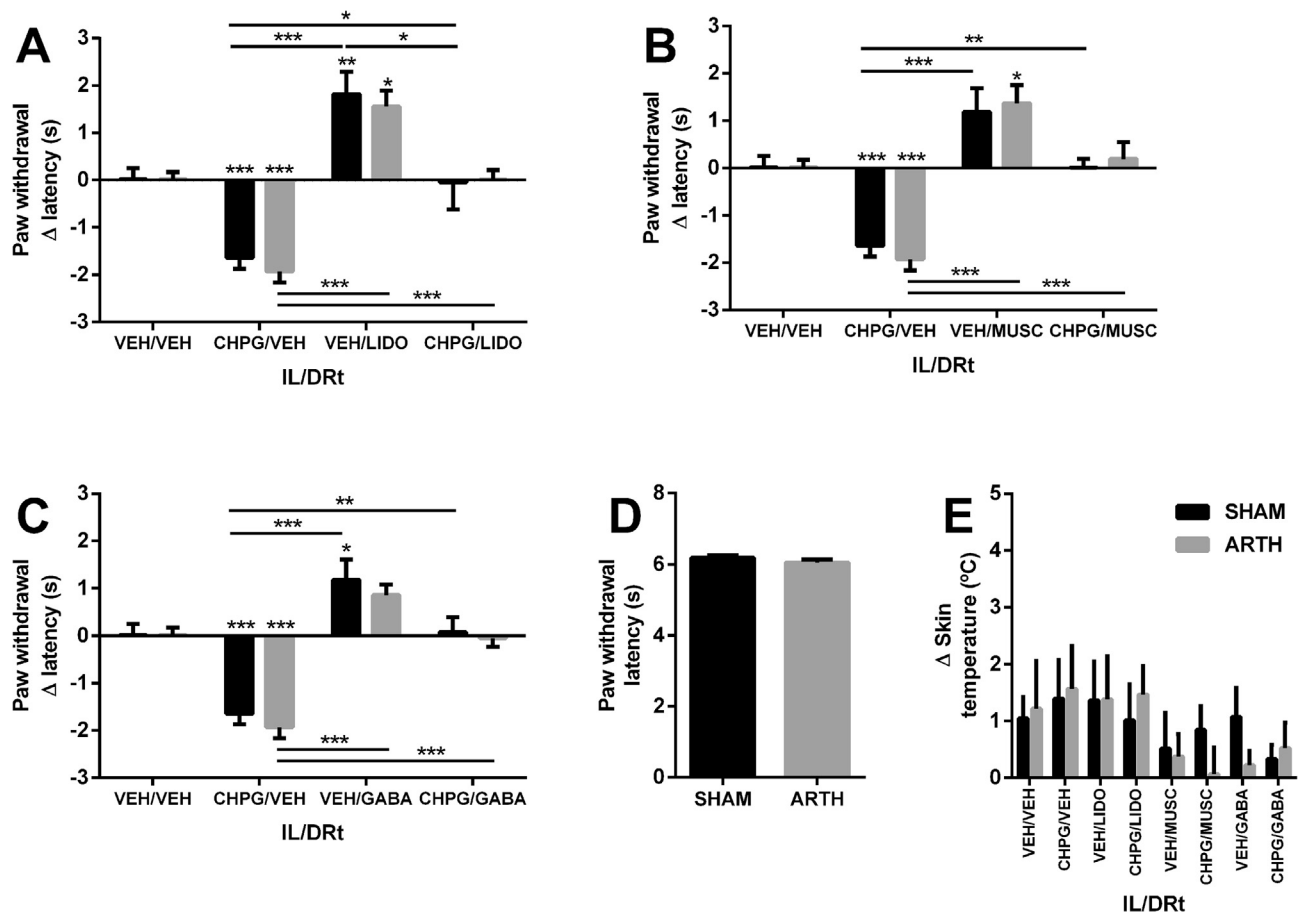


**Fig. 3.** (A–C) Paw withdrawal latency (PWL) variation 30 min after drug microinjection into the infralimbic cortex (IL) and dorsal reticular nucleus (DRt) of SHAM and ARTH animals. Effects of vehicle (VEH) in the IL and in the DRt; CHPG (mGluR5 agonist) in the IL and VEH in the DRt; VEH in the IL and lidocaine (LIDO)/muscimol (MUSC)/GABA in the DRt; and CHPG in the IL and LIDO/MUSC/GABA in the DRt. (D) PWL before drug microinjection in the IL and DRt in control (SHAM) and arthritic (ARTH) groups. (E) Skin temperature (°C) variation 30 min after drug injection into the IL and DRt of SHAM and ARTH animals.  $\Delta$  – (PWL30 min)–(PWL–5 min). Graphs A, B, C and E show  $\Delta$  mean + SEM; graph D shows mean + SEM. \* $p$  < 0.05; \*\* $p$  < 0.01; \*\*\* $p$  < 0.001. (VEH/VEH:  $n_{\text{SHAM}} = 20$ ;  $n_{\text{ARTH}} = 19$ ; CHPG/VEH:  $n_{\text{SHAM}} = 18$ ;  $n_{\text{ARTH}} = 15$ ; VEH/LIDO:  $n_{\text{SHAM}} = 6$ ;  $n_{\text{ARTH}} = 6$ ; CHPG/LIDO:  $n_{\text{SHAM}} = 6$ ;  $n_{\text{ARTH}} = 7$ ; VEH/MUSC:  $n_{\text{SHAM}} = 10$ ;  $n_{\text{ARTH}} = 10$ ; CHPG/MUSC:  $n_{\text{SHAM}} = 10$ ;  $n_{\text{ARTH}} = 10$ ; VEH/GABA:  $n_{\text{SHAM}} = 9$ ;  $n_{\text{ARTH}} = 9$ ; CHPG/GABA:  $n_{\text{SHAM}} = 7$ ;  $n_{\text{ARTH}} = 12$ ).

536 Fig. 4B), whereas there were no differences in the heat-  
 537 evoked baseline responses between SHAM and ARTH  
 538 animals ( $t_{89} = 0.1085$ ,  $p = 0.914$ ; Fig. 4C).  
 539 Administration of CHPG in the IL significantly changed  
 540 the spontaneous activity of DRt neurons (effect of drug  
 541 administration:  $F_{1,69} = 11.08$ ,  $p = 0.001$ ); this effect  
 542 varied with the experimental group (interaction between  
 543 drug administration and experimental group:  
 544  $F_{1,69} = 4.258$ ,  $p = 0.043$ ). *Post hoc* tests show CHPG  
 545 increased the spontaneous activity of DRt neurons in  
 546 SHAM but not ARTH animals, while VEH administration  
 547 did not alter spontaneous activity of DRt neurons in any  
 548 of the experimental groups (Fig. 4D).

549 CHPG administration significantly altered heat-  
 550 evoked DRt responses (effect of drug administration:  
 551  $F_{1,71} = 10.48$ ,  $p = 0.002$ ) and this effect varied with the  
 552 experimental group (interaction between drug  
 553 administration and experimental group:  $F_{1,71} = 6.293$ ,  
 554  $p = 0.014$ ). Similarly to what was observed for the  
 555 spontaneous activity, *post hoc* tests showed that the  
 556 heat-evoked DRt neuronal discharge increased in

557 SHAM but not ARTH animals after IL administration of  
 558 CHPG (Fig. 4E).

559 Administration of MPEP in the IL had no effect upon  
 560 the spontaneous and evoked activity of DRt neurons  
 561 (effect of drug administration upon spontaneous activity:  
 562  $F_{1,49} = 1.541$ ,  $p = 0.22$ ; effect of drug administration  
 563 upon evoked activity:  $F_{1,47} = 0.352$ ;  $p = 0.56$ ),  
 564 independent of the experimental group (interaction  
 565 between drug administration and experimental group for  
 566 spontaneous activity:  $F_{1,49} = 0.992$ ,  $p = 0.32$ ;  
 567 interaction between drug administration and  
 568 experimental group for evoked activity:  $F_{1,47} = 0.599$ ,  
 569  $p = 0.44$ ; Fig. 4F, G).

570 The time spent between the beginning of the noxious  
 571 heat stimulus and observing a change in neuronal activity  
 572 was not significantly altered by CHPG administration  
 573 (effect of drug administration:  $F_{2,36} = 2.604$ ,  $p = 0.088$ ),  
 574 and was independent of the experimental group  
 575 (interaction between drug administration and  
 576 experimental group:  $F_{2,36} = 0.011$ ,  $p = 0.989$ ).  
 577 However, DRt neurons in ARTH animals had a

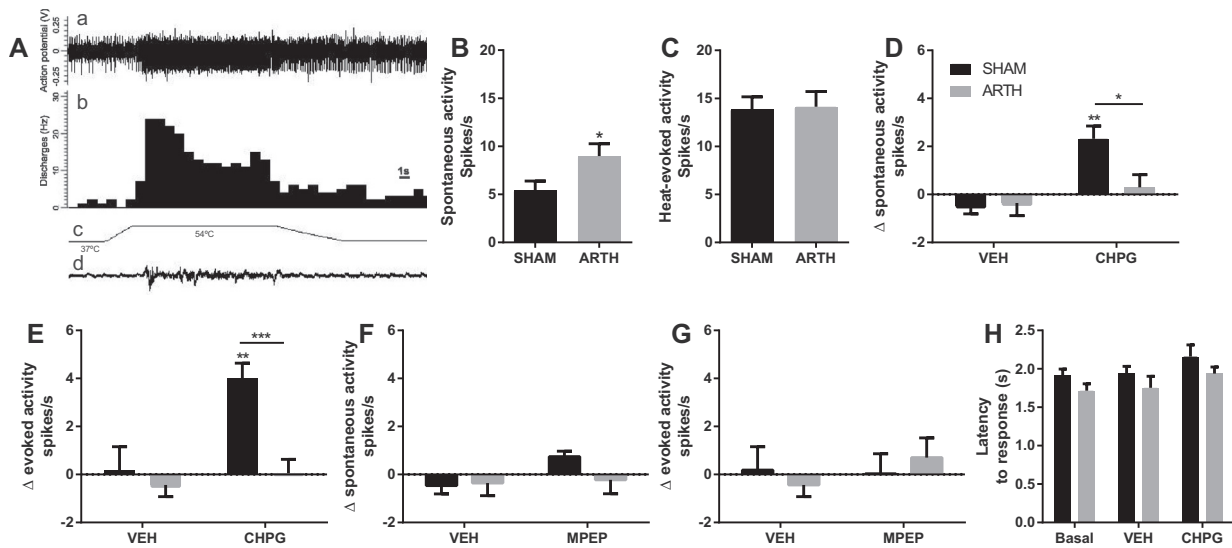


**Fig. 4.** Effect of mGluR5 activation/inactivation in the infralimbic cortex (IL) upon the spontaneous and heat-evoked activity of dorsal reticular nucleus (DRt) cells. (A) Example of an original recording of a DRt neuron in response to noxious heating of the right hind paw. a – raw data of neuronal responses; b – peristimulus time histogram showing the discharge of a DRt neuron; c – heat stimulus that starts from the baseline temperature of 37 °C and peaks at 54 °C; d – movement detection of a flexor muscle in the hind limb during hind paw heat stimulation. (B) Spontaneous activity of DRt neurons in healthy (SHAM) and arthritic (ARTH) animals. (C) Evoked activity of DRt neurons in healthy and arthritic animals. (D) Effect of IL CHPG administration upon the spontaneous activity of DRt neurons in SHAM and ARTH animals. (E) Effect of IL CHPG administration upon the noxious heat-evoked activity of DRt neurons in SHAM and ARTH animals. (F) Effect of IL MPEP administration upon the spontaneous activity of DRt neurons in SHAM and ARTH animals. (G) Effect of IL MPEP administration upon the noxious heat-evoked activity of DRt neurons in SHAM and ARTH animals. (H) Latency from the beginning of stimulation to cell/muscle response to stimulation. VEH – vehicle; CHPG – mGluR5 agonist; MPEP – mGluR5 antagonist;  $\Delta$  – (activity 30 min) – (activity-5 min). Graphs B, C and F show mean + SEM; graphs D-G show  $\Delta$  mean + SEM. \* $p$  < 0.05; \*\* $p$  < 0.01; \*\*\* $p$  < 0.001. (VEH:  $n_{SHAM}$  = 15,  $n_{ARTH}$  = 20; CHPG:  $n_{SHAM}$  = 19,  $n_{ARTH}$  = 22; MPEP:  $n_{SHAM}$  = 8,  $n_{ARTH}$  = 10).

578 significantly shorter latency to the onset of the heat-  
579 evoked response than DRt neurons in SHAM animals  
580 (effect of experimental group:  $F_{1,36}$  = 4.966,  $p$  = 0.032;  
581 Fig. 4H).

582 **Response latency of DRt neurons to electrical**  
583 **activation of the IL**

584 Recordings of two nociceptive DRt neurons in two healthy  
585 control animals indicated that the median latencies of the  
586 first impulse followed by electric stimulation of IL were  
587 14 ms (interquartile range: 12–65 ms) and 15 ms  
588 (14–34 ms), whereas the corresponding median  
589 latencies followed by fake stimulation of IL were 663 ms  
590 (160–1387 ms) and 650 ms (165–864 ms). Within 20 ms  
591 from the real IL stimulus, the firing probability was > 3  
592 SDs higher than within the same time window after the  
593 fake IL stimulus (Fig. 5).

594 **MGLUR5 ACTIVATION IN THE IL INCREASES**  
595 **DISCHARGE RATES OF SPINAL DORSAL**  
596 **HORN NEURONS IN BOTH SHAM AND ARTH**  
597 **ANIMALS**

598 **Wide-dynamic range (WDR) neurons**

599 Recordings of the studied WDR neurons were performed  
600 in the deep spinal dorsal horn as indicated by the  
601 recording depth that varied from 500 to 1000  $\mu$ m from  
602 the cord surface. The receptive fields of the studied  
603 neurons covered the plantar skin of the hind paw and

604 some surrounding areas (e.g. partial/complete toes or  
605 heel; Fig. 6A).

606 The baseline spontaneous activity of spinal WDR  
607 neurons before drug administration was higher in the  
608 ARTH than SHAM group ( $t_{39}$  = 2.505,  $p$  = 0.017;  
609 Fig. 6B). Drug administration in the IL had no significant  
610 overall effect on the spontaneous activity of WDR  
611 neurons (effect of drug administration:  $F_{1,47}$  = 1.280,  
612  $p$  = 0.264). However, the drug effect varied with the  
613 experimental group (interaction between drug  
614 administration and experimental group:  $F_{1,47}$  = 4.271,  
615  $p$  = 0.044). *Post hoc* tests showed the spontaneous  
616 activity of WDR neurons in SHAM animals was  
617 increased after CHPG administration, while in ARTH  
618 animals no drug-induced changes of spontaneous  
619 activity were observed (Fig. 6C).

620 Drug administration in the IL altered the heat-evoked  
621 response of spinal WDR neurons (effect of drug  
622 administration:  $F_{1,43}$  = 16.61,  $p$  = 0.0002), independent  
623 of the experimental group (interaction between drug  
624 administration and experimental group:  $F_{1,43}$  = 0.1525,  
625  $p$  = 0.698). *Post hoc* tests show that the heat-evoked  
626 responses of spinal WDR neurons both in SHAM and  
627 ARTH groups were significantly increased after IL  
628 administration of CHPG and that in the SHAM group the  
629 increase of the heat-evoked response was significantly  
630 higher than in the ARTH group (Fig. 6D).

631 **Nociceptive specific (NS) neurons**

632 Recordings of the studied NS neurons were performed in  
633 the superficial spinal dorsal horn as indicated by the

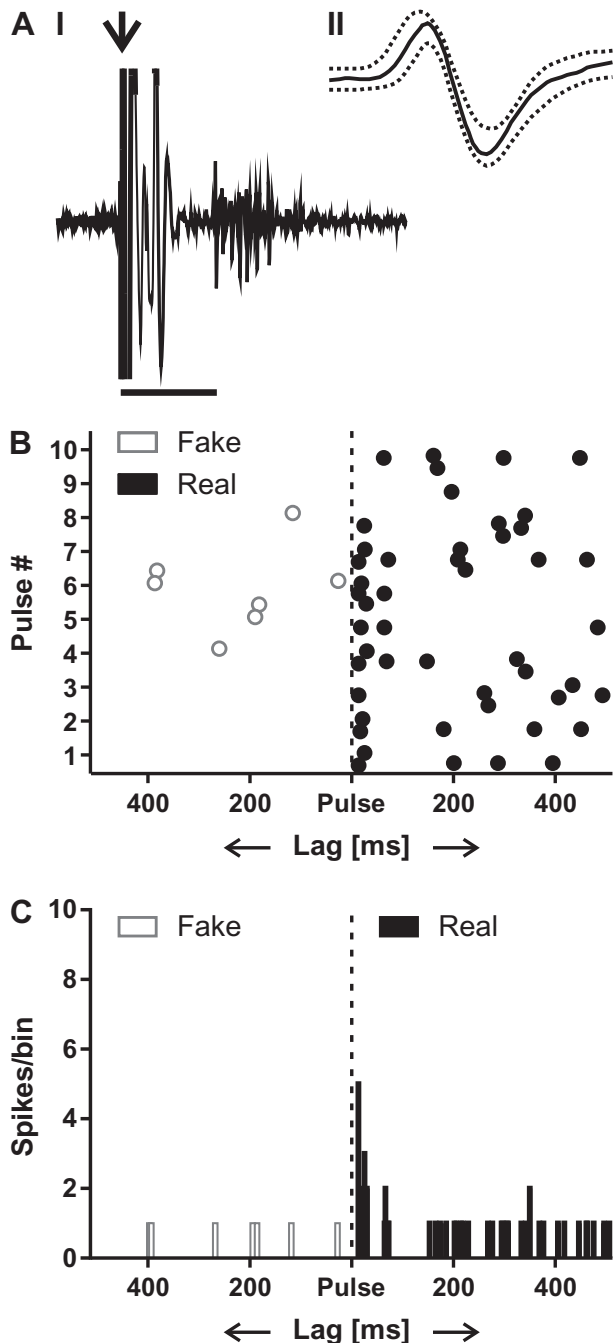


**Fig. 5.** Recording responses of a nociceptive dorsal reticular nucleus (DRt) neuron to electric stimulation of the infralimbic cortex (IL). (A, I) Ten consecutive superimposed responses to single pulse IL stimuli (0.3 ms, 10 mA, 0.5 Hz). The arrow indicates the electric stimulus that is followed by a stimulus-evoked noise signal lasting 9.5 ms. The horizontal calibration bars represents 17 ms. (A, II) The shape of the single action potential recorded in the DRt, and its template (dotted lines). (B) Raster plot of DRt neuron spiking following 10 consecutive real (10 mA) or fake (0 mA) IL stimulations. Responses following real IL stimulations are shown to the right from the midline, and responses to the fake IL stimulations are shown to the left from the midline. (C) Poststimulus time histograms of 10 repeated real (to the right from the midline) vs fake (to the left from the midline) IL stimulations. Bin width: 2 ms.

covered the plantar skin of the hind paw and some surrounding areas (e.g. partial/complete toes or heel; Fig. 6E).

Baseline spontaneous activity of spinal NS neurons was higher in the ARTH than the SHAM group ( $t_{31} = 3.881, p = 0.0005$ ; Fig. 6F). Drug administration in the IL had no significant effect on the spontaneous activity of spinal NS neurons (effect of drug administration:  $F_{1,20} = 0.602, p = 0.467$ ), independent of the experimental group (interaction between drug administration and experimental group:  $F_{1,20} = 0.009, p = 0.928$ ; Fig. 6G).

In contrast to spontaneous activity, heat-evoked responses of spinal NS neurons were significantly altered after CHPG microinjection in the IL (effect of drug administration:  $F_{1,23} = 9.496, p = 0.005$ ). This effect did not vary with the experimental group (interaction between drug administration and experimental group:  $F_{1,23} = 0.531, p = 0.474$ ; Fig. 6H).

#### Behavioral hyperalgesia after IL/mGluR5 activation is mediated by spinal TRPV1

Baseline PWLs were not significantly different between SHAM and ARTH animals before i.t. administration of AMG, a TRPV1 antagonist ( $t_{52} = 1.320, p = 0.193$ ; Fig. 7A).

When studying the role of spinal TRPV1 in IL-mediated pronociception, there was an overall change in PWL after drug administration (effect of drug microinjection:  $F_{3,46} = 16.33, p < 0.0001$ ), independent of the experimental group (interaction between drug administration and experimental group:  $F_{3,46} = 0.039, p = 0.990$ ). *Post hoc* analysis showed CHPG in the IL significantly decreased PWL both in SHAM and ARTH animals. I.t. AMG alone had no significant influence on PWL in either the SHAM or ARTH group, while AMG blocked pronociception induced by IL administration of CHPG (Fig. 7B). Paw skin temperature was not altered by drug administrations (effect of drug microinjection:  $F_{3,36} = 0.154, p = 0.926$ ) in any of the experimental groups (interaction between drug administration and experimental group:  $F_{3,36} = 0.425, p = 0.737$ ; Fig. 7C).

## DISCUSSION

In this work, we confirmed that mGluR5 activation in the IL by intracortical microinjection of CHPG enhances behavioral hyperalgesia and spinal neuronal activity in healthy (SHAM) and monoarthritic (ARTH) rats. Moreover, we showed for the first time that the medullary DRt is a relay nucleus for the IL/mGluR5-induced descending pronociceptive effect in healthy animals, but not in monoarthritic rats. The IL/mGluR5-induced behavioral hyperalgesia to heat was accompanied by facilitation of heat-evoked responses of spinal dorsal horn WDR and NS neurons in both experimental groups. Interestingly, pharmacological inhibition of spinal TRPV1 prevented the IL/mGluR5-induced hyperalgesia in both SHAM and ARTH groups suggesting that spinal TRPV1 is mediating the descending pronociceptive effect.

634 recording depth that varied from 50 to 250  $\mu\text{m}$  from the  
635 cord surface. The receptive fields of the studied neurons 141

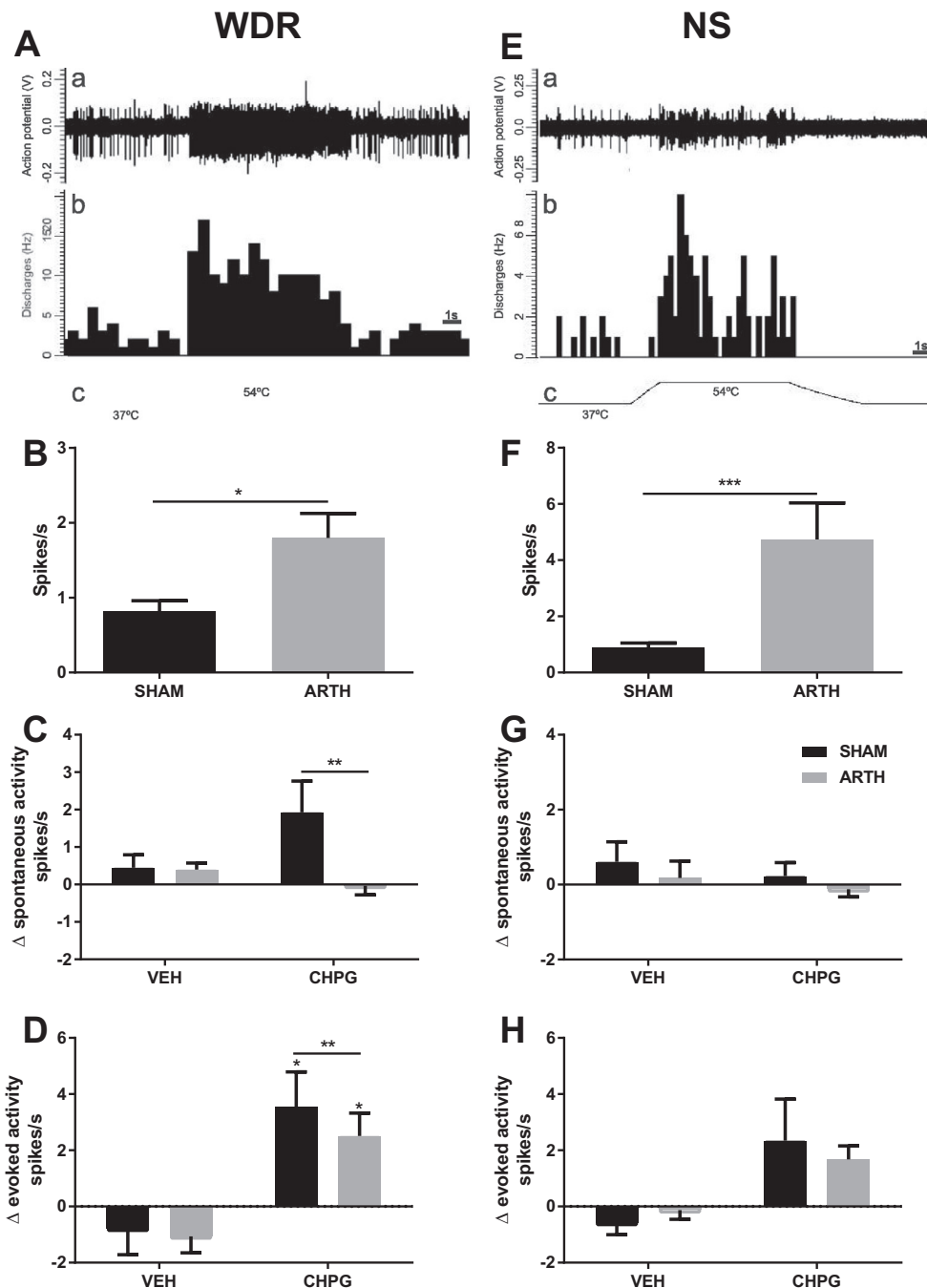


**Fig. 6.** Effect of mGluR5 activation in the infralimbic cortex (IL) upon the spontaneous and heat-evoked activity of L4-L6 spinal dorsal horn nociceptive neurons. (A) Example of an original recording of a wide-dynamic range (WDR) neuron in response to noxious heating of the right hind paw. a – raw data of neuronal responses; b – peristimulus time histogram showing the discharge of a spinal dorsal horn neuron; c – heat stimulus that starts from the baseline temperature of 37 °C and peaks at 54 °C. (B) Spontaneous activity of WDR neurons in control (SHAM) and arthritic (ARTH) animals. (C) Effect of IL drug administration upon the spontaneous activity of spinal WDR neurons in SHAM and ARTH animals. (D) Effect of IL drug administration upon the noxious heat-evoked activity of spinal WDR neurons in SHAM and ARTH animals. (E) Example of an original recording of a nociceptive specific (NS) neuron in response to noxious heating of the right hind paw. a – raw data of neuronal responses; b – peristimulus time histogram showing the discharge of a spinal dorsal horn neuron; c – heat stimulus that starts from the baseline temperature of 37 °C and peaks at 54 °C. (F) Spontaneous activity of NS neurons in SHAM and ARTH animals. (G) Effect of IL drug administration upon the spontaneous activity of spinal NS neurons in SHAM and ARTH animals. (H) Effect of IL drug administration upon the noxious heat-evoked activity of spinal NS neurons in SHAM and ARTH animals. VEH – vehicle; CHPG – mGluR5 agonist; Δ – (activity 30 min)–(activity-5 min). Graphs B and F show mean + SEM; graphs C, D, G and H show Δ mean + SEM. \**p* < 0.05; \*\**p* < 0.01; \*\*\**p* < 0.001. (WDR: VEH: *n*<sub>SHAM</sub> = 8, *n*<sub>ARTH</sub> = 12; CHPG: *n*<sub>SHAM</sub> = 12, *n*<sub>ARTH</sub> = 21. NS: VEH: *n*<sub>SHAM</sub> = 6, *n*<sub>ARTH</sub> = 8; CHPG: *n*<sub>SHAM</sub> = 6, *n*<sub>ARTH</sub> = 9).

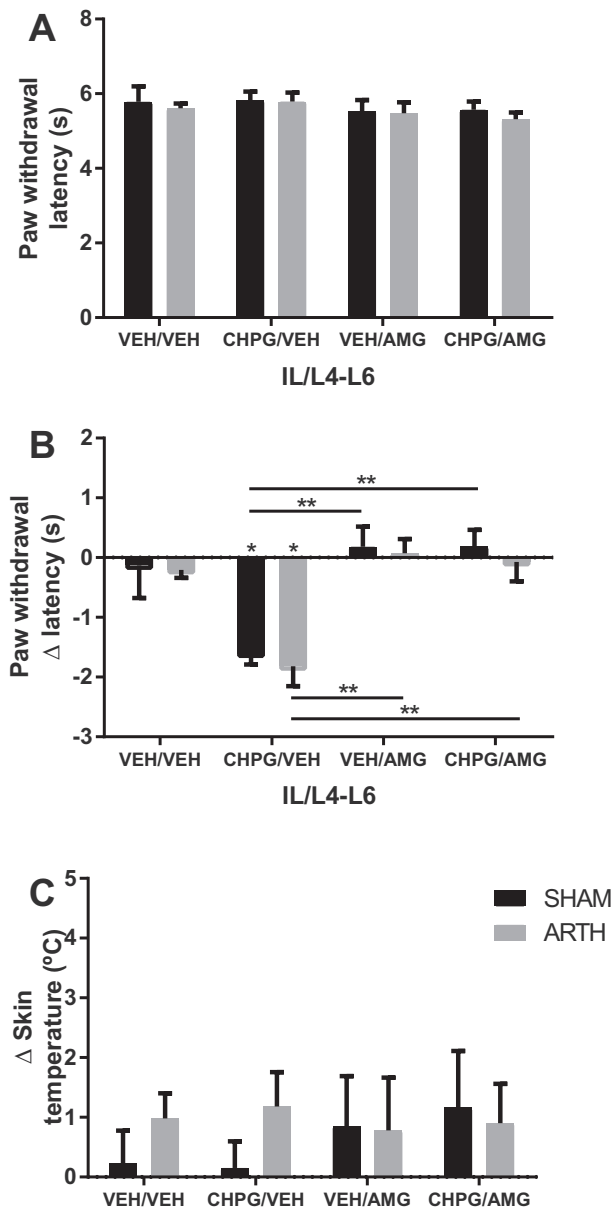


**Fig. 7.** (A) Paw withdrawal latency (PWL) before drug microinjection into the infralimbic cortex (IL) and the spinal cord (L4-L6) of control (SHAM) and arthritic (ARTH) animals. (B) PWL variation 30 min after drug microinjection in the IL and L4-L6 in SHAM and ARTH animals. Effects of vehicle (VEH) in the IL and in the L4-L6; CHPG (mGluR5 agonist) in the IL and SAL in the L4-L6; SAL in the IL and AMG-9810 (AMG; TRPV1 antagonist) in the L4-L6; and CHPG in the IL and AMG in the L4-L6. (C) Skin temperature (°C) variation 30 min after drug injection into the IL and L4-L6 of SHAM and ARTH animals. Δ – (PWL30 min)-(PWL-5 min). Graph A shows mean + SEM; graphs B and C show Δ mean + SEM; \**p* < 0.05; \*\**p* < 0.01; \*\*\**p* < 0.001. (VEH/VEH:  $n_{SHAM} = 5$ ,  $n_{ARTH} = 7$ ; CHPG/VEH:  $n_{SHAM} = 7$ ,  $n_{ARTH} = 6$ ; VEH/AMG:  $n_{SHAM} = 8$ ,  $n_{ARTH} = 7$ ; CHPG/AMG:  $n_{SHAM} = 7$ ,  $n_{ARTH} = 7$ ).

694 As previously reported (David-Pereira et al., 2016),  
695 CHPG injection in the IL facilitated nociceptive spinal-  
696 organized behavior in both SHAM and ARTH animals.  
697 Interestingly, a recent study showed the opposite effect  
698 when an mGluR5-positive allosteric modulator was  
699 administered in the IL of rats with K/C induced-  
700 monoarthritis, restoring mechanical hind limb withdrawal

701 threshold of monoarthritic rats to pre-arthritis values  
702 (Kiritoshi et al., 2016). The disparity between the two  
703 studies could result from the site, type or, particularly,  
704 time of stimulation; Kiritoshi and colleagues tested IL  
705 mGluR5 function on nociception by stimulating the knee  
706 joint of rats with mechanical pressure – primary hypersen-  
707 sitivity – 6 h after K/C injection. Contrastingly, we stimu-  
708 lated the distal hind paw with noxious heat 4 weeks  
709 after ARTH induction. Although at earlier time points the  
710 K/C model of monoarthritis is associated with both pri-  
711 mary and secondary hyperalgesia (Urban et al. 1999),  
712 at later stages monoarthritic rats only exhibit primary  
713 mechanical hyperalgesia (Sluka and Westlund, 1993;  
714 Ren and Dubner, 1999; Amorim et al., 2014). Interest-  
715 ingly, these alterations in behavior are mirrored by  
716 changes of neurotransmitter levels in the spinal cord.  
717 For example, glutamate expression correlates with sec-  
718 ondary hyperalgesia, and substance P and calcitonin  
719 gene-related peptide expressions correlate with primary  
720 hyperalgesia, reflecting a transition from acute to chronic  
721 inflammatory pain (Sluka and Westlund, 1993). Time-  
722 dependent behavioral alterations also benefit from  
723 descending inputs from supraspinal regions such as the  
724 RVM, which both inhibits and facilitates nociception. The  
725 balance between these opposing descending inputs var-  
726 ies according to the time elapsed since inflammatory pain  
727 onset (Vanegas and Schaible, 2004). Therefore, IL  
728 mGluR5 activation might yield opposing descending mod-  
729 ulatory effects at different stages of inflammatory pain;  
730 further observations, however, would require a longitu-  
731 dinal study of molecular, functional and behavioral impact  
732 of inflammatory pain in the IL.

733 To the best of our knowledge, direct projections from  
734 the IL to the spinal cord have not been described. We  
735 hypothesized that a downstream pain facilitatory area,  
736 such as the DRt, mediated at least partially the  
737 observed behavioral hyperalgesia. The assessment of  
738 DRt neuron response to electric IL stimulation suggests  
739 that although responses with a latency shorter than  
740 9.5 ms could not be appropriately assessed in the  
741 present conditions, according to recently described  
742 criteria for corticofugal projections some of the studied  
743 projections from the IL to the DRt might be oligo- or  
744 even monosynaptic (Doig et al., 2014). Furthermore, tran-  
745 sient block of the DRt with LIDO or inhibition of synaptic  
746 signaling with GABA agonists was able to prevent the  
747 IL/mGluR5-induced behavioral hyperalgesia in both  
748 SHAM and ARTH animals. The interpretation of this find-  
749 ing however is complicated by the antinociceptive action  
750 induced by LIDO, MUSC or GABA alone in the DRt of  
751 both SHAM and ARTH animals. In contrast, single-cell  
752 electrophysiological recordings in the DRt indicate that  
753 IL administration of CHPG increased spontaneous and  
754 heat-evoked activity of DRt neurons in SHAM but not in  
755 ARTH animals. Since activation of mGluR5 in the IL  
756 induces pronociceptive behavior in both experimental  
757 groups, we hypothesize the existence of another supraspi-  
758 nal area besides the DRt that relays the pronociceptive  
759 effect originating in the IL of ARTH animals. Moreover, it  
760 is possible that the DRt promotes nociception in parallel  
761 with this second relay also in healthy controls.

Our earlier behavioral results indicate that IL MPEP administration induced antinociception in ARTH animals and had no effect in SHAM animals (David-Pereira et al., 2016). This behavioral finding contrasts with the present electrophysiological result showing that IL MPEP failed to influence the discharge of DRt neurons in ARTH as well as SHAM animals. The discrepancy in the effect of IL MPEP on spinally organized behavior versus the discharge of DRt neurons in the ARTH group supports the hypothesis that unlike in SHAM animals, the DRt of ARTH animals may not be the only or the critical relay for the descending pronociceptive effect induced by the IL mGluR5, but another parallel pathway exerts a key role in the descending pronociceptive effect in the ARTH group.

Anatomical evidence on descending projections from the DRt to spinal cord laminae I and IV–V (Lima and Coimbra, 1988; Tavares and Lima, 1994; Almeida et al., 1995; Villanueva et al., 1995) and electrophysiological evidence showing that stimulating the DRt with glutamate increases WDR responses to noxious sciatic nerve stimulation (Dugast et al., 2003), indicate that the modulation of nociception by the DRt relies, at least in part, in the modulation of spinal WDR cell activity. Therefore, it is not surprising that our data indicate that IL/mGluR5 activation increases spontaneous activity of spinal WDR cells in SHAM but not ARTH animals. Additionally, the CHPG-induced facilitation of heat-evoked responses was significantly weaker in WDR neurons of the ARTH than SHAM group. However, as observed earlier with RVM ON-cell discharge in animals with peripheral nerve injury (Carlson et al., 2007), there is also the possibility that the noxious stimulation-induced responses of spinal WDR cells of ARTH animals were influenced by the ceiling effect. In line with this proposal, spontaneous activity of WDR neurons was significantly higher in the ARTH than SHAM group.

An interesting observation is that CHPG administration in the IL of SHAM animals increased both spontaneous and heat-evoked activity in WDR neurons, whereas only heat-evoked activity was increased in NS neurons. WDR neurons are considered important for perception of prolonged pain (Coghill et al., 1993; Fallis, 2006); functionally, there is evidence that WDR cells can be important for sensory/discriminative aspects of pain as, for instance, intensity-encoding deep-laminae WDR neurons heavily project through the spinothalamic tract (STT) to brain regions more commonly associated with the sensory-discriminative aspects of pain, such as the SI (Millan, 2002). On the other hand, NS neurons are considered to be involved in the phasic aspects of pain, such as the signaling of a new noxious stimulus and the activation of autonomic responses to a new challenge (Coghill et al., 1993; Fallis, 2006). In parallel with WDR cells, NS neurons from superficial dorsal horn laminae project through the STT to supraspinal regions associated with the emotional/cognitive dimensions of pain, such as the PFC (Millan, 2002). Although this distribution is not an absolute distinction between WDR and NS neuronal function, it is likely to have implications for pain development and its treatment.

Earlier studies have demonstrated IL neurons that encode nociception (Zhang et al., 2004). Moreover, the mPFC, including the IL, has been implicated in multiple other roles ranging from anxiety modulation (Bi et al., 2013) to decision-making (Ji et al., 2010). Together these earlier and the present findings raise a hypothesis that the activation of mGluR5 in the IL is among mechanisms contributing to the interaction of the emotional/cognitive state and pain through descending control of spinal pain-relay neurons.

It should be noted that when interpreting the IL/mGluR5-induced changes in the ongoing discharge rates of spinal dorsal horn as well as DRt neurons in terms of behavior, a limitation for the interpretations is that the analysis of pain behavior was based on heat-evoked behavioral responses and not on ongoing pain behavior assessed e.g. by drug-induced conditioned place-avoidance. Additionally, while the anesthesia level was kept as stable as possible, it cannot be excluded that anesthesia or a change in its level may have had an influence on neuronal responses. Importantly, however, since the anesthesia procedure was identical in all experimental conditions, the possible effects of anesthesia or a change in its level cannot explain the differences between the effects induced by IL administration of VEH vs mGluR5 agonist, differences between SHAM vs ARTH rats, or differences among different neuronal populations (DRt vs spinal dorsal horn WDR and NS neurons).

TRPV1 is tonically active and its ablation has been shown to prevent the development of nociceptive behaviors such as that evoked by thermal or chemical stimulation (Caterina et al., 1997, 2000). In the present study, when TRPV1 antagonist AMG 9810 was administered alone, it had no effect upon the PWL of SHAM or ARTH animals. The dose of AMG 9810 was chosen based on earlier results showing that when it was used intrathecally, it reversed mechanical and thermal hyperalgesia in a rat model of inflammatory pain (Yu et al., 2008). The currently used dose of AMG 9810 was not sufficient to alter baseline latencies in SHAM controls, or in the ARTH group four weeks after the induction of K/C monoarthritis when the arthritis was no longer accompanied by secondary hyperalgesia. Interestingly, expression of TRPV1 in different dorsal root ganglia cell types is variable depending on the time after chronic inflammatory pain induction (Yu et al., 2008), and, for instance, in the CFA model, TRPV1 expression peaks 14 days after induction, while at 28 days it returns to control levels (Luo et al., 2004). Concomitantly, hot plate latency responses decrease in those animals, with the lowest values registered 14 days after induction (Luo et al., 2004). Based on these earlier findings it is possible that the late time point of testing in the present ARTH group may attest for the lack of effect by a TRPV1 antagonist alone on heat nociception along with the lack of heat hyperalgesia.

While the spinally administered TRPV1 antagonist failed to influence the baseline PWL, it did prevent the IL mGluR5-mediated pronociception in both SHAM and ARTH groups. This finding indicates that spinal TRPV1 is mediating the IL mGluR5-induced pronociception at



884 the spinal cord level in ARTH as well as SHAM condition.  
885 Although until recently spinal TRPV1 was thought to be  
886 expressed only on central terminals of primary afferent  
887 nerve fibers, some studies showed the expression of  
888 TRPV1 on GABAergic interneurons in the superficial  
889 laminae of the spinal dorsal horn (Valtschanoff et al.,  
890 2001; Ferrini et al., 2010; Kim et al., 2012). Activation of  
891 spinal TRPV1 has been linked to increased excitability  
892 of spinal dorsal horn neurons, leading to mechanical allo-  
893 dyndia in neuropathic pain models (Cui et al., 2006). Tak-  
894 ing this evidence into account, one interesting possibility  
895 is that the IL mGluR5-induced pronociception involves  
896 activation of TRPV1 on spinal interneurons. However,  
897 intrathecal drug administration affects indiscriminately  
898 the target receptor, and therefore further studies are  
899 needed to distinguish between the functional roles of  
900 TRPV1 expressed on central endings of peripheral nerve  
901 terminals and spinal interneurons.

902 In healthy and monoarthritic animals, mGluR5  
903 activation in the IL facilitated spinally organized pain  
904 behavior as revealed by a decrease in the heat-evoked  
905 paw withdrawal latency. In healthy controls, this  
906 descending pronociceptive effect was accompanied by  
907 an increase in the heat-evoked discharge rate of  
908 medullary DRt neurons and spinal dorsal horn WDR and  
909 NS neurons. In experimental monoarthritis, the IL/  
910 mGluR5-induced descending facilitation of the heat-  
911 evoked responses was absent in medullary DRt neurons  
912 but still present in spinal dorsal horn WDR and NS  
913 neurons. Together these findings suggest the DRt is a  
914 relay in the descending pronociceptive pathway  
915 activated by IL/mGluR5 in healthy controls, but an  
916 additional descending pronociceptive pathway, which  
917 does not relay in the DRt, is likely to be recruited in  
918 experimental monoarthritis (in parallel, it may be  
919 involved also in healthy controls). Interestingly, one or  
920 both of these descending pronociceptive pathways  
921 target, at least partly, spinal TRPV1 as indicated by the  
922 loss of the IL/mGluR5-induced pronociceptive effect  
923 following pharmacological block of spinal TRPV1 in both  
924 healthy and arthritic animals.

## 925 AUTHOR CONTRIBUTIONS

926 ADP, AP and FPR developed the concept and designed  
927 experiments. ADP performed and analyzed all of the  
928 experiments. BS was involved in part of the  
929 electrophysiological experiments. HW assisted in the  
930 surgical procedures. ADP, AP and FPR wrote the  
931 paper. AA revised the manuscript. All authors discussed  
932 and revised the manuscript.

933 *Acknowledgements*—This study was supported by grants from  
934 the Portuguese Science Foundation (FCT) Project no PTDC/  
935 SAU-NEU/108557/2008, by FEDER funds, through the Compet-  
936 itiveness Factors Operational Programme (COMPETE); by  
937 National funds, through the FCT, under the scope of the project  
938 POCI-01-0145-FEDER-007038; by the Academy of Finland;  
939 and the Sigrid Jusélius Foundation, Helsinki, Finland. ADP was  
940 supported by FCT grant SFRH/BD/90374/2012.

## REFERENCES

- Almeida A, Cobos A, Tavares I, Lima D (2002) Brain afferents to the  
942 medullary dorsal reticular nucleus: A retrograde and anterograde  
943 tracing study in the rat. *Eur J Neurosci* 16:81–95. 944
- Almeida A, Lima D (1997) Activation by cutaneous or visceral noxious  
945 stimulation of spinal neurons projecting to the medullary dorsal  
946 reticular nucleus in the rat: a c-fos study. *Eur J Neurosci*  
947 9:686–695. 948
- Almeida A, Størkson R, Lima D, Hole K, Tjølsen A (1999) The  
949 medullary dorsal reticular nucleus facilitates pain behaviour  
950 induced by formalin in the rat. *Eur J Neurosci* 11:110–122. 951
- Almeida A, Tavares I, Lima D (1995) Projection sites of deep dorsal  
952 horn in the dorsal reticular nucleus. *Neuro Rep* 6:1245–1248. 953
- Almeida A, Tavares I, Lima D (2000) Reciprocal connections between  
954 the medullary dorsal reticular nucleus and the spinal dorsal horn  
955 in the rat. *Eur J Pain* 4:373–387. 956
- Almeida A, Tavares I, Lima D, Coimbra A (1993) Descending  
957 projections from the medullary dorsal reticular nucleus make  
958 synaptic contacts with spinal cord lamina I cells projecting to that  
959 nucleus: An electron microscopic tracer study in the rat.  
960 *Neuroscience* 55:1093–1106. 961
- Almeida A, Tjølsen A, Lima D, Coimbra A, Hole K (1996) The  
962 medullary dorsal reticular nucleus facilitates acute nociception in  
963 the rat. *Brain Res Bull* 39:7–15. 964
- Amorim D, David-Pereira A, Pertovaara A, Almeida A, Pinto-Ribeiro F  
965 (2014) Amitriptyline reverses hyperalgesia and improves  
966 associated mood-like disorders in a model of experimental  
967 monoarthritis. *Behav Brain Res* 265:12–21. 968
- Amorim D, Viisanen H, Wei H, Almeida A, Pertovaara A, Pinto-  
969 Ribeiro F (2015) Galanin-mediated behavioural hyperalgesia from  
970 the dorsomedial nucleus of the hypothalamus involves two  
971 independent descending pronociceptive pathways. *PLoS One*  
972 10:e0142919. 973
- Ansah OB, Gonçalves L, Almeida A, Pertovaara A (2009) Enhanced  
974 pronociception by amygdaloid group I metabotropic glutamate  
975 receptors in nerve-injured animals. *Exp Neurol* 216:66–74. 976
- Apkarian AV (2004) Chronic back pain is associated with decreased  
977 prefrontal and thalamic gray matter density. *J Neurosci*  
978 24:10410–10415. 979
- Baron R, Hans G, Dickenson AH (2013) Peripheral input and its  
980 importance for central sensitization. *Ann Neurol* 74:630–636. 981
- Bi LL, Wang J, Luo ZY, Chen SP, Geng F, Chen YH, Li SJ, Yuan CH,  
982 Lin S, Gao TM (2013) Enhanced excitability in the infralimbic  
983 cortex produces anxiety-like behaviors. *Neuropharmacology*  
984 72:148–156. 985
- Carlson JD, Maire JJ, Martenson ME, Heinricher MM (2007)  
986 Sensitization of pain-modulating neurons in the rostral  
987 ventromedial medulla after peripheral nerve injury. *J Neurosci*  
988 27:13222–13231. 989
- Caterina MJ, Leffler A, Malmberg AB, Martin WJ, Trafton J, Petersen-  
990 Zeitz KR, Koltzenburg M, Basbaum AI, Julius D (2000) Impaired  
991 nociception and pain sensation in mice lacking the capsaicin  
992 receptor. *Science* 288:306–313. 993
- Caterina MJ, Schumacher MA, Tominaga M, Rosen TA, Levine JD,  
994 Julius D (1997) The capsaicin receptor: a heat-activated ion  
995 channel in the pain pathway. *Nature* 389:816–824. 996
- Coghill RC, Mayer DJ, Price DD (1993) Wide dynamic range but not  
997 nociceptive-specific neurons encode multidimensional features of  
998 prolonged repetitive heat pain. *J Neurophysiol* 69:703–716. 999
- Cui M et al (2006) TRPV1 receptors in the CNS play a key role in  
1000 broad-spectrum analgesia of TRPV1 antagonists. *J Neurosci*  
1001 26:9385–9393. 1002
- David-Pereira A, Puga S, Gonçalves S, Amorim D, Silva C,  
1003 Pertovaara A, Almeida A, Pinto-Ribeiro F (2016) Metabotropic  
1004 glutamate 5 receptor in the infralimbic cortex contributes to  
1005 descending pain facilitation in healthy and arthritic animals.  
1006 *Neuroscience* 312:108–119. 1007

- 1008 Doig NM, Magill PJ, Apicella P, Bolam JP, Sharott A (2014) Cortical  
1009 and thalamic excitation mediate the multiphasic responses of  
1010 striatal cholinergic interneurons to motivationally salient stimuli. *J*  
1011 *Neurosci* 34:3101–3117.
- 1012 Dugast C, Almeida A, Lima D (2003) The medullary dorsal reticular  
1013 nucleus enhances the responsiveness of spinal nociceptive  
1014 neurons to peripheral stimulation in the rat. *Eur J Neurosci*  
1015 18:580–588.
- 1016 Fallis A (2006). In: Shimoji K, Willis WD, editors. *Evoked spinal cord*  
1017 *potentials*. Tokyo: Springer Japan. Available at: [http://link.](http://link.springer.com/10.1007/4-431-30901-2)  
1018 [springer.com/10.1007/4-431-30901-2](http://link.springer.com/10.1007/4-431-30901-2).
- 1019 Ferrini F, Salio C, Lossi L, Gambino G, Merighi A (2010) Modulation  
1020 of inhibitory neurotransmission by the vanilloid receptor type 1  
1021 (TRPV1) in organotypically cultured mouse substantia gelatinosa  
1022 neurons. *Pain* 150:128–140.
- 1023 Frye GD, McCown TJ, Breese GR (1983) Characterization of  
1024 susceptibility to audiogenic seizures in ethanol-dependent rats  
1025 after microinjection of gamma-aminobutyric acid (GABA) agonists  
1026 into the inferior colliculus, substantia nigra or medial septum. *J*  
1027 *Pharmacol Exp Ther* 227:663–670.
- 1028 Heinricher MM, Tavares I, Leith JL, Lumb BM (2009) Descending  
1029 control of nociception: Specificity, recruitment and plasticity. *Brain*  
1030 *Res Rev* 60:214–225.
- 1031 Ji G, Sun H, Fu Y, Li Z, Pais-Vieira M, Galhardo V, Neugebauer V  
1032 (2010) Cognitive impairment in pain through amygdala-driven  
1033 prefrontal cortical deactivation. *J Neurosci* 30:5451–5464.
- 1034 Kim YH, Back SK, Davies AJ, Jeong H, Jo HJ, Chung G, Na HS, Bae  
1035 YC, Kim SJ, Kim JS, Jung SJ, Oh SB (2012) TRPV1 in  
1036 GABAergic interneurons mediates neuropathic mechanical  
1037 allodynia and disinhibition of the nociceptive circuitry in the  
1038 spinal cord. *Neuron* 74:640–647.
- 1039 Kiritoshi T, Ji G, Neugebauer V (2016) Rescue of impaired mGluR5-  
1040 driven endocannabinoid signaling restores prefrontal cortical  
1041 output to inhibit pain in arthritic rats. *J Neurosci* 36:837–850.
- 1042 Lacerda JEC, Campos RR, Araujo GC, Andreatta-Van Leyen S,  
1043 Lopes OU, Guertzenstein PG (2003) Cardiovascular responses to  
1044 microinjections of GABA or anesthetics into the rostral  
1045 ventrolateral medulla of conscious and anesthetized rats. *Braz J*  
1046 *Med Biol Res* 36:1269–1277.
- 1047 Leite-Almeida H, Valle-Fernandes A, Almeida A (2006) Brain  
1048 projections from the medullary dorsal reticular nucleus: An  
1049 anterograde and retrograde tracing study in the rat.  
1050 *Neuroscience* 140:577–595.
- 1051 Lima D, Almeida A (2002) The medullary dorsal reticular nucleus as a  
1052 pronociceptive centre of the pain control system. *Prog Neurobiol*  
1053 66:81–108.
- 1054 Lima D, Coimbra A (1988) The spinothalamic system of the rat:  
1055 Structural types of retrogradely labelled neurons in the marginal  
1056 zone (lamina I). *Neuroscience* 27:215–230.
- 1057 Luo H, Cheng J, Han J-S, Wan Y (2004) Change of vanilloid receptor  
1058 1 expression in dorsal root ganglion and spinal dorsal horn during  
1059 inflammatory nociception induced by complete Freund's adjuvant  
1060 in rats. *Neuroreport* 15:655–658.
- 1061 Luukko M, Kontinen Y, Kempainen P, Pertovaara A, Petrovaara A  
1062 (1994) Influence of various experimental parameters on the  
1063 incidence of thermal and mechanical hyperalgesia induced by a  
1064 constriction mononeuropathy of the sciatic nerve. *Exp Neurol*  
1065 128:143–154.
- 1066 Martins I, de Vries MG, Teixeira-Pinto A, Fadel J, Wilson SP,  
1067 Westerink BHC, Tavares I (2013) Noradrenaline increases pain  
1068 facilitation from the brain during inflammatory pain.  
1069 *Neuropharmacology* 71:299–307.
- 1070 Metz AE, Yau H-J, Centeno MV, Apkarian AV, Martina M (2009)  
1071 Morphological and functional reorganization of rat medial  
1072 prefrontal cortex in neuropathic pain. *Proc Natl Acad Sci U S A*  
1073 106:2423–2428.
- 1074 Millan MJ (2002) Descending control of pain. *Prog Neurobiol*  
1075 66:355–474.
- 1076 Myers RD (1966) Injection of solutions into cerebral tissue: Relation  
1077 between volume and diffusion. *Physiol Behav* 1:171–174 IN9.
- 1078 Ossipov MH, Lai J, Malan TP, Porreca F (2000) Spinal and  
1079 supraspinal mechanisms of neuropathic pain. *Ann N Y Acad Sci*  
1080 909:12–24.
- 1081 Paxinos G, Watson C (1986) *George Paxinos Charles Watson*.  
1082 Pertovaara A, Wei H, Hämäläinen MM (1996) Lidocaine in the  
1083 rostroventromedial medulla and the periaqueductal gray  
1084 attenuates allodynia in neuropathic rats. *Neurosci Lett*  
1085 218:127–130.
- 1086 Pinto-Ribeiro F, Amorim D, David-Pereira A, Monteiro AM, Costa P,  
1087 Pertovaara A, Almeida A (2013) Pronociception from the  
1088 dorsomedial nucleus of the hypothalamus is mediated by the  
1089 rostral ventromedial medulla in healthy controls but is absent in  
1090 arthritic animals. *Brain Res Bull* 99:100–108.
- 1091 Pinto-Ribeiro F, Ansah OB, Almeida A, Pertovaara A (2011)  
1092 Response properties of nociceptive neurons in the caudal  
1093 ventrolateral medulla (CVLM) in monoarthritic and healthy  
1094 control rats: modulation of responses by the paraventricular  
1095 nucleus of the hypothalamus (PVN). *Brain Res Bull* 86:82–90.
- 1096 Radhakrishnan R, Moore SA, Sluka KA (2003) Unilateral  
1097 carrageenan injection into muscle or joint induces chronic  
1098 bilateral hyperalgesia in rats. *Pain* 104:567–577.
- 1099 Ren K, Dubner R (1999) Inflammatory models of pain and  
1100 hyperalgesia. *ILAR J* 40:111–118.
- 1101 Schaible H-G, Ebersberger A, Von Banchet GS (2002) Mechanisms  
1102 of pain in arthritis. *Ann N Y Acad Sci* 966:343–354.
- 1103 Sluka KA, Westlund KN (1993) Behavioral and immunohistochemical  
1104 changes in an experimental arthritis model in rats. *Pain*  
1105 55:367–377.
- 1106 Sotgiu ML, Valente M, Storch R, Caramenti G, Mario Biella GE  
1107 (2008) Contribution by DRt descending facilitatory pathways to  
1108 maintenance of spinal neuron sensitization in rats. *Brain Res*  
1109 1188:69–75.
- 1110 Starkson RV, Kjørsvik A, Tjølsen A, Hole K (1996) Lumbar  
1111 catheterization of the spinal subarachnoid space in the rat. *J*  
1112 *Neurosci Methods* 65:167–172.
- 1113 Tavares I, Lima D (1994) Descending projections from the caudal  
1114 medulla oblongata to the superficial or deep dorsal horn of the rat  
1115 spinal cord. *Exp Brain Res* 99:455–463.
- 1116 Valtchanoff JG, Rustioni A, Guo A, Hwang SJ (2001) Vanilloid  
1117 receptor VR1 is both presynaptic and postsynaptic in the  
1118 superficial laminae of the rat dorsal horn. *J Comp Neurol*  
1119 436:225–235.
- 1120 Vanegas H, Schaible HG (2004) Descending control of persistent  
1121 pain: Inhibitory or facilitatory? *Brain Res Rev* 46:295–309.
- 1122 Viisanen H, Ansah OB, Pertovaara A (2012) The role of the dopamine  
1123 D2 receptor in descending control of pain induced by motor cortex  
1124 stimulation in the neuropathic rat. *Brain Res Bull* 89:133–143.
- 1125 Villanueva L, Bernard JF, Le Bars D (1995) Distribution of spinal cord  
1126 projections from the medullary subnucleus reticularis dorsalis and  
1127 the adjacent cuneate nucleus: A phaseolus vulgaris-leucoagglutinin study in the rat. *J Comp Neurol* 352:11–32.
- 1128 Villanueva L, Bouhassira D, Bing Z, Le Bars D (1988) Convergence of  
1129 heterotopic nociceptive information onto subnucleus reticularis  
1130 dorsalis neurons in the rat medulla. *J Neurophysiol* 60:980–1009.
- 1131 Villanueva L, Bouhassira D, Le Bars D (1996) The medullary  
1132 subnucleus reticularis dorsalis (SRD) as a key link in both the  
1133 transmission and modulation of pain signals. *Pain* 67:231–240.
- 1134 Willis WD, Coggeshall RE (2004) *Sensory mechanisms of the spinal*  
1135 *cord: Volume 1 primary afferent neurons and the spinal dorsal*  
1136 *horn*. USA: Springer.
- 1137 Woolf CJ (2011) Central sensitization: Implications for the diagnosis  
1138 and treatment of pain. *Pain* 152:S2–S15.
- 1139 Yu L, Yang F, Luo H, Liu F-Y, Han J-S, Xing G-G, Wan Y (2008) The  
1140 role of TRPV1 in different subtypes of dorsal root ganglion  
1141 neurons in rat chronic inflammatory nociception induced by  
1142 complete Freund's adjuvant. *Mol Pain* 4:61.
- 1143

A. David-Pereira et al. / Neuroscience xxx (2017) xxx–xxx

15

- 1144 Zhang L, Zhang Y, Zhao ZQ (2005) Anterior cingulate cortex  
1145 contributes to the descending facilitatory modulation of pain via  
1146 dorsal reticular nucleus. *Eur J Neurosci* 22:1141–1148.
- 1147 Zhang R, Tomida M, Katayama Y, Kawakami Y (2004) Response  
1148 durations encode nociceptive stimulus intensity in the rat medial  
1149 prefrontal cortex. *Neuroscience* 125:777–785.
- Zhou HY, Chen SR, Chen H, Pan HL (2009) The glutamatergic  
nature of TRPV1-expressing neurons in the spinal dorsal horn. *J  
Neurochem* 108:305–318.

1153  
1154  
1155  
*(Received 4 July 2016, Accepted 21 February 2017)*  
*(Available online xxxx)*

UNCORRECTED PROOF



Ana David-Pereira, Sara Gonçalves, Armando Almeida, Filipa Pinto-Ribeiro

**The rostral ventromedial medulla relays descending pronociception induced by  
infralimbic cortex mGluR5 in monoarthritic, but not healthy, rats**

*(Manuscript under preparation)*



## **The rostral ventromedial medulla relays descending pronociception induced by infralimbic cortex mGluR5 in monoarthritic, but not healthy, rats**

Ana David-Pereira<sup>1,2</sup>, Sara Gonçalves<sup>1,2</sup>, Armando Almeida<sup>1,2</sup>, Filipa Pinto-Ribeiro<sup>1,2</sup>

<sup>1</sup>*Life and Health Sciences Research Institute (ICVS), School of Medicine (EM), Campus of Gualtar, University of Minho, 4710-057 Braga, Portugal*

<sup>2</sup>*ICVS/3B's - PT Government Associate Laboratory, Braga/Guimarães, Portugal*

We previously demonstrated metabotropic glutamate receptor 5 (mGluR5) activation in the infralimbic cortex (IL) induces pronociceptive behavior in healthy (SHAM) and monoarthritic (ARTH) rats (David-Pereira et al., 2016). In healthy animals, the dorsal reticular nucleus (DRt) relays the pronociceptive IL effect to the spinal cord, but in monoarthritic animals this pathway is disrupted (David-Pereira et al., 2017).

The periaqueductal gray matter-rostral ventromedial medulla (PAG-RVM) circuit is one of the best characterized pain modulatory pathways, of which the RVM is considered the output region (Heinricher et al., 2009). Nociceptive transmission can be exacerbated (pronociception) or inhibited (antinociception) by the activity of two types of RVM cells, ON- and OFF-cells, respectively. Electrophysiologically, ON-cells increase and OFF-cell decrease their activity in response to a noxious stimulus. A third cell type that does not respond to peripheral stimulation, known as NEUTRAL-cells, can also be found in the RVM.

The goal of the present work is to determine whether the RVM relays the pronociceptive effect of IL mGluR5 activation in ARTH animals. The effect of IL administration of CHPG (mGluR5 agonist) upon RVM neuronal activity of SHAM (intrasynovial injection of saline solution) and ARTH animals (intrasynovial injection of 3% kaolin/carrageenan solution) was evaluated. In lightly anesthetized animals, recordings of (i) spontaneous activity (first 20s of recording without any stimulation), (ii) the response to innocuous brushing of the back (5s) and (iii) the response to noxious heating of the tail (10s) of the RVM's three cell types were performed. RVM cells were characterized as ON, OFF or NEUTRAL-cells if their activity increased or decreased more than 10% or did not alter from baseline values, respectively. Additionally, ON and OFF cells were further divided into wide-dynamic range (WDR), if they responded to innocuous and noxious stimulation, or nociceptive specific (NS), if they responded only to noxious stimulation.

Overall, vehicle administration had no effect upon the spontaneous or heat evoked activity of RVM cells in any experimental group (**Table 1**). The spontaneous and heat-evoked discharge rates of NEUTRAL and ON-cells (WDR and NS) in SHAM and ARTH rats were not altered by CHPG administration. The same was observed for the spontaneous and heat-evoked activity of NS OFF-cells and the spontaneous activity of WDR OFF-cells in both experimental groups (**Table 1; Fig. 1**). However, WDR OFF-cells of SHAM and ARTH animals responded differently to noxious heat after CHPG administration (main effect of experimental group:  $F_{1,34}=9.53$ ,  $p=0.004$ ). *Post-hoc* tests showed that CHPG administration caused noxious heat-evoked response to be significantly smaller in WDR OFF-cells of ARTH, but not in SHAM animals (**Fig. 1I**).

The results herein suggest that in experimental monoarthritis, pronociception after IL mGluR5 activation is relayed through the RVM. Interestingly, the behavioral effect seems to result from a loss of antinociceptive OFF-cell response, particularly in cells that respond to polymodal inputs, rather than an increase in pronociceptive ON-cell activity. Additionally, CHPG-induced alterations in RVM neuronal activity are ARTH specific. Together with previous observations (David-Pereira et al., 2017), the present results suggest that prolonged monoarthritis causes the relay for IL pronociception to shift from a DRt-mediated pathway to a RVM-mediated one. Further studies are needed to ascertain the validity of our results; namely, the effect of mGluR5 antagonists, which are antinociceptive when administered only in the IL of ARTH animals (David-Pereira et al., 2016), upon RVM activity.

## References

David-Pereira A, Puga S, Gonçalves S, Amorim D, Silva C, Pertovaara A, Almeida A, Pinto-Ribeiro F (2016) Metabotropic glutamate 5 receptor in the infralimbic cortex contributes to descending pain facilitation in healthy and arthritic animals. *Neuroscience* 312:108–119.

David-Pereira A, Sagalajev B, Wei H, Almeida A, Pertovaara A, Pinto-Ribeiro F (2017) The medullary dorsal reticular nucleus as a relay for descending pronociception induced by the mGluR5 in the rat infralimbic cortex. *Neuroscience*, in press.

Heinricher MM, Tavares I, Leith JL, Lumb BM (2009) Descending control of nociception: Specificity, recruitment and plasticity. *Brain Res Rev* 60:214–225.



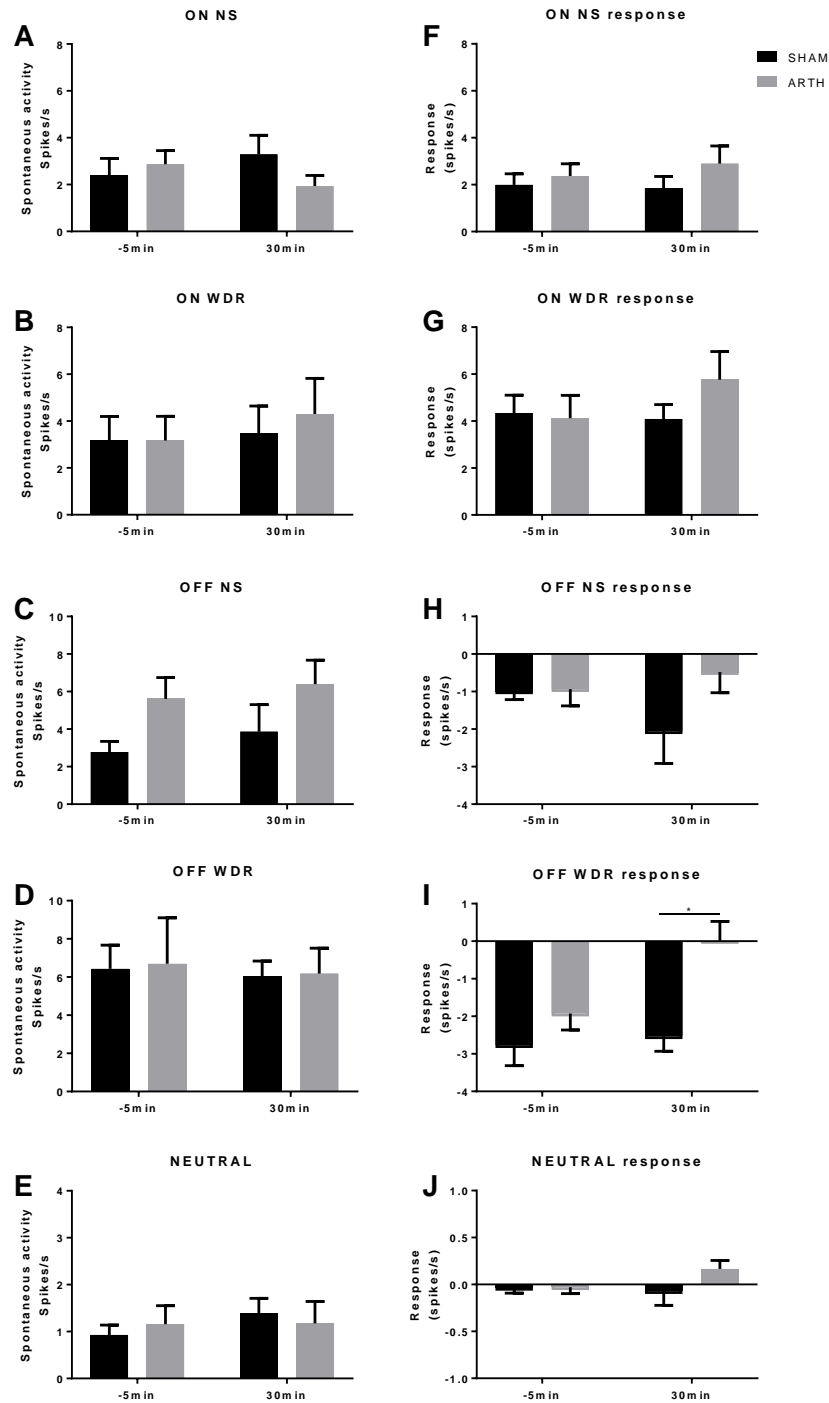


**Figure 1** - Effect of mGluR5 activation in the infralimbic cortex (IL) upon the spontaneous and heat-evoked activity of rostral ventromedial medulla (RVM) cells. **(A-E)** Spontaneous activity of RVM NS ON **(A)**, WDR ON **(B)**, NS OFF **(C)**, WDR OFF **(D)** and NEUTRAL **(E)** cells in healthy (SHAM) and monoarthritic (ARTH) animals. **(F-J)** Noxious heat-evoked activity of RVM NS ON **(F)**, WDR ON **(G)**, NS OFF **(H)**, WDR OFF **(I)** and NEUTRAL **(J)** cells in SHAM and ARTH animals. Graphs show means + SEM.  $p < 0.05$ .

**Table 1** – Summary of the two-way analyses of variance (ANOVA) results of the electrophysiological recordings of RVM neurons. Results show the main effect for the between factors (SHAMxARTH), within factors (-5minx30min) and interaction analysis.

Drug	Cell type	Type and time of evaluation	Two-way ANOVA (SHAMxARTH;-5minx30min)																						
			SHAM		ARTH		Main effect of group			Main effect of drug			Interaction												
			Mean±SD	N	Mean±SD	N	df	F	p	df	F	p	df	F	p										
SAL	ON NS	Spontaneous activity	-5min	2.28±1.89	12	1.43±1.42	13	1, 46	2.94	0.09	1, 46	0.26	0.62	1, 46	0.10	0.75									
			30min	1.93±1.29	12	1.36±1.17	13																		
		Response	-5min	4.25±3.40	12	3.16±2.79	13										1, 46	0.85	0.36	1, 46	0.007	0.94	1, 46	0.08	0.78
			30min	3.92±3.43	12	3.34±3.24	13																		
	ON WDR	Spontaneous activity	-5min	3.54±8.24	21	2.70±3.65	15	1, 68	0.38	0.54	1, 68	0.009	0.93	1, 68	0.004	0.95									
			30min	3.50±7.25	21	2.46±3.56	15																		
		Response	-5min	3.89±3.17	21	3.94±3.33	15										1, 68	0.15	0.70	1, 68	0.07	0.79	1, 68	0.11	0.75
			30min	3.42±3.38	21	3.98±3.34	15																		
	OFF NS	Spontaneous activity	-5min	5.38±1.26	2	4.93±0.63	2	1, 4	0.02	0.88	1, 4	0.10	0.77	1, 4	0.51	0.52									
			30min	4.85±0.39	2	5.13±0.02	2																		
		Response	-5min	-1.07±0.22	2	-1.26±1.09	2										1, 4	0.09	0.78	1, 4	0.03	0.87	1, 4	0.01	0.93
			30min	-1.03±0.76	2	-1.13±0.14	2																		
OFF WDR	Spontaneous activity	-5min	4.59±2.49	13	4.29±2.09	5	1, 32	0.11	0.74	1, 32	0.02	0.89	1, 32	0.001	0.97										
		30min	4.76±2.82	13	4.39±3.22	5																			
	Response	-5min	-1.97±1.16	13	-1.55±0.95	5										1, 32	1.46	0.24	1, 32	0.30	0.59	1, 32	0.15	0.70	
		30min	-1.88±1.70	13	-1.07±1.12	5																			
NEUTRAL	Spontaneous activity	-5min	0.81±0.75	8	1.49±2.06	9	1, 30	1.33	0.26	1, 30	0.0003	0.99	1, 30	0.02	0.89										
		30min	0.88±0.67	8	1.40±1.88	9																			
	Response	-5min	-3.03±0.21	8	0.04±0.22	9										1, 30	0.13	0.72	1, 30	0.82	0.37	1, 30	0.64	0.43	
		30min	0.25±0.31	8	0.06±0.82	9																			
CHPG	ON NS	Spontaneous activity	-5min	2.40±2.78	15	2.87±1.53	7	1, 40	0.28	0.60	1, 40	0.0007	0.98	1, 40	1.18	0.28									
			30min	3.29±3.14	15	1.94±1.19	7																		
		Response	-5min	1.99±1.69	15	2.37±1.37	7										1, 40	1.62	0.21	1, 40	0.11	0.75	1, 40	0.36	0.55
			30min	1.83±1.85	15	2.90±1.98	7																		
	ON WDR	Spontaneous activity	-5min	3.18±5.93	34	3.17±3.86	14	1, 92	0.09	0.76	1, 92	0.29	0.59	1, 92	0.10	0.76									
			30min	3.48±6.74	34	4.30±5.69	14																		
		Response	-5min	4.34±4.31	34	4.12±3.38	14										1, 92	0.69	0.41	1, 92	0.64	0.43	1, 92	1.81	0.28
			30min	4.98±3.46	34	5.76±4.16	14																		
	OFF NS	Spontaneous activity	-5min	2.78±1.13	4	5.62±1.60	2	1, 8	4.45	0.068	1, 8	0.53	0.49	1, 8	0.01	0.91									
			30min	3.86±2.88	4	6.40±1.80	2																		
		Response	-5min	-0.99±0.44	4	-0.93±0.63	2										1, 8	1.37	0.28	1, 8	0.19	0.67	1, 8	1.17	0.31
			30min	-2.06±1.71	4	-0.48±0.77	2																		
OFF WDR	Spontaneous activity	-5min	6.43±4.65	14	6.69±5.39	5	1, 34	0.02	0.90	1, 34	0.09	0.77	1, 34	0.002	0.96										
		30min	6.06±2.93	14	6.18±2.99	5																			
	Response	-5min	-2.77±1.81	14	-1.93±0.98	5										1, 34	9.53	0.004*	1, 34	3.93	0.056	1, 34	2.39	0.13	
		30min	-2.53±1.33	14	0.005±1.17	5																			
NEUTRAL	Spontaneous activity	-5min	0.93±0.72	12	1.16±1.18	9	1, 38	0.0005	0.98	1, 38	0.48	0.49	1, 38	0.41	0.52										
		30min	1.39±1.11	12	1.17±1.41	9																			
	Response	-5min	-0.04±0.21	12	-0.03±0.17	9										1, 38	1.24	0.27	1, 38	0.53	0.47	1, 38	1.10	0.30	
		30min	-0.07±0.57	12	0.17±0.22	9																			





### 3. Discussion

In the present thesis, the use of functional interventions associated to behavioral and electrophysiological approaches allowed to uncover some mechanisms underlying chronic inflammatory pain related changes. In **Chapter 2.1** we show the K/C model elicits behavioral hyperalgesia associated to profound morphological changes in the knee joint. In **Chapter 2.2** we describe the opposing antinociceptive and pronociceptive roles of the PL and the IL, respectively, in descending modulation, and demonstrate that glutamate administration in the IL acts preferentially through mGluR5 to facilitate nociception. Additionally, we show mGluR5 becomes tonically active 4 weeks after chronic inflammatory pain onset, an effect dependent on intact astrocyte function (**Chapter 2.3**). Chronic pain changes in nociceptive modulation by the IL also extend to its relay areas. In healthy animals, IL mGluR5 pronociception is associated to increased responses of DRt nociceptive neurons to noxious heating of the hind paw (**Chapter 2.4**), while in K/C animals the facilitatory effect is associated to the depression of RVM OFF-cells response to peripheral noxious heat (**Chapter 2.5; Fig. 1**). In **Chapter 2.4** we also show that mGluR5 activation in the IL promotes behavioral hyperalgesia by increasing the responses of spinal WDR and NS cells to noxious stimuli. Finally, we show blocking TRPV1 in the spinal cord inhibits IL mGluR5-mediated pronociception (**Chapter 2.4**). In summary, during the development of the present dissertation we uncovered new evidence indicating that sustained chronic inflammatory pain prompts plastic alterations in the brain and spinal cord, and that the IL plays a role in the descending modulation of nociception.

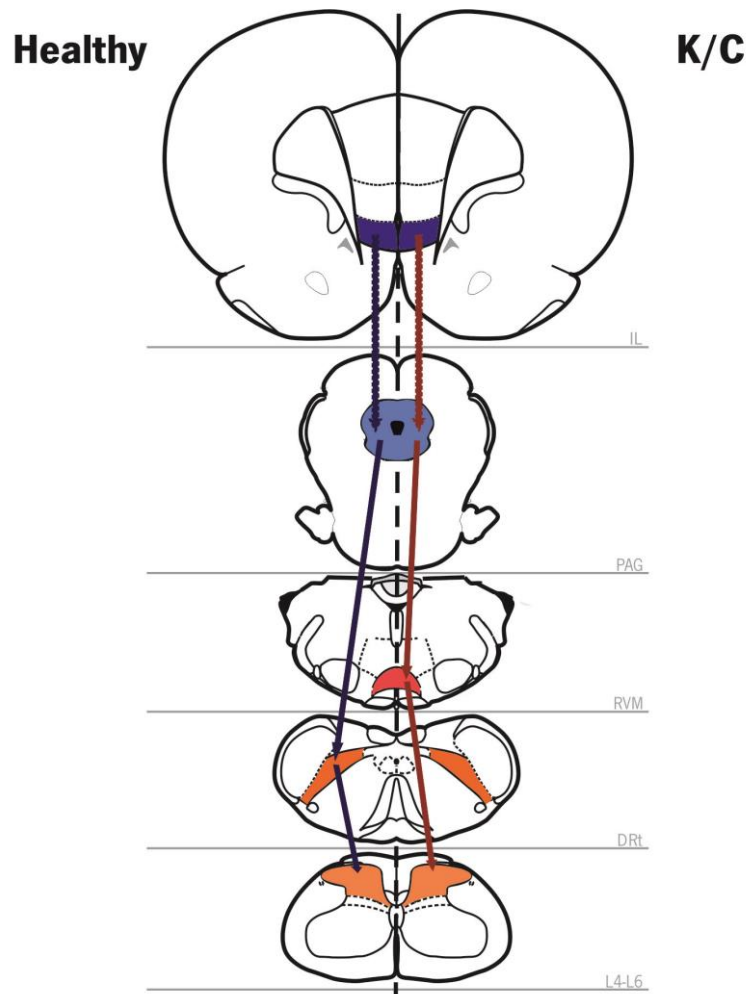


**Figure 1** - Schematic representation of possible pathways relaying IL pronociceptive drive in healthy and K/C rats. *Blue dotted lines* – hypothesized projection to the PAG; *blue full lines* – possible descending pathways in healthy animals; *red dotted lines* – possible descending pathways in K/C animals; *red full lines* – possible descending pathways in K/C animals; DRt – dorsal reticular nucleus; IL – infralimbic cortex; K/C – kaolin/carrageenan of inflammatory pain; PAG – periaqueductal gray matter; RVM – rostral ventromedial medulla; L4-L6 – spinal cord 4-6 lumbar segments) (Adapted from Paxinos and Watson, 2007).

### 3.1 Technical considerations

#### 3.1.1 Behavioral assessment of nociception

In animal models, nociceptive assessments consist mostly on the measurement of noxious evoked responses, which have proved useful in assessing alterations driven by pathological states or pharmacological treatments<sup>1</sup>. However, the most common complaint from chronic pain patients,

ongoing pain<sup>2</sup>, is frequently overlooked in preclinical studies. Quantification of ongoing pain in animal models is complicated by lack of self-report, as well as by the absence of displays of spontaneous pain behaviors or even by the researcher's inability to recognize them as such. For example, rodents only emit audible vocalizations in response to severe acute stimuli and in models of mild to moderate pain there are no postural alterations that can be easily discriminated and quantified<sup>3</sup>. In addition, in models of OA and monoarthritis, such as the one described in **Chapter 2.1**, the spontaneous behavior does not correspond to the level of degradation observed *post-mortem* in the knee joint<sup>4,5</sup>. Some simple behaviors, such as locomotion, weight bearing and gait, can be used to indirectly measure inflammatory pain. However, on their own they provide insufficient data and the use of evoked pain behaviors is still necessary for a better characterization of the models<sup>6</sup>. The main consequence of ignoring spontaneous pain symptoms is the low translational value of preclinically effective pharmacological therapies into clinical settings<sup>3</sup>. The improvement and development of pain assessments, progressing from evoked nociception to a more multidimensional evaluation of pain are therefore necessary to achieve higher translational values.

#### *3.1.1.1 Thermal hyperalgesia*

One of the preferred methods to test heat hyperalgesia is the Hargreaves model<sup>7</sup>. This test measures radiant heat-evoked paw withdrawal latencies, with the advantage of testing animals in a less stressful situation than the tail-flick test, for example, as they are unrestrained by the experimenter. Nevertheless, several factors can influence radiant heat-evoked results, such as the initial temperature of the testing surface and of the skin, the animals' state of alertness, the presence of inflammation or potential pharmacological effects<sup>8-10</sup>. To overcome these limitations several precautions were taken in our experimental protocols. Firstly, the testing surface was heated before the beginning of the experiments. Animals were also allowed to become familiar with the apparatus by performing training sessions previous to the testing days and by allowing them to explore at least 10 minutes at the beginning of each experimental session. In addition, the temperature of the plantar skin was measured at each tested time point, allowing to exclude potential side effects arising from the various pharmacological interventions on the autonomic nervous system, or due to the prolonged inflammation elicited by the experimental model used.

### *3.1.1.2 Mechanical hyperalgesia*

Increased sensitivity to noxious mechanical stimulation of joints is commonly described in OA patients<sup>11,12</sup>. The devices used to measure mechanical hyperalgesia include the Randall-Selitto, which applies increasing pressure to the paw<sup>13</sup>, and the pressure application measurement (PAM), where a mobile force transducer attached to the experimenters thumb is used to apply pressure to the area of interest<sup>14</sup>. Both tests present advantages and disadvantages when compared with each other: in the Randal-Selitto test, pressure is applied through an automated weight system, while in the PAM test the experimenter controls the rate of pressure increase, which requires a highly trained experimenter and even then presents more variability in the results. On the other hand, the Randall-Selitto only allows to test mechanical thresholds in the paws, while the PAM transducer can be applied to any joint. Both tests require animal restraining, and hence habituation to the procedure. Additionally, the experimenter needs to be able to detect one of several behaviors (paw-withdrawal, wriggling, vocalization or freezing of whisker movement) as a sign of pain from the animals<sup>14</sup>. Since our model presents knee pathology, the PAM test was a more appropriate choice for our experimental protocols. Due to the aggressiveness of the test and to avoid over-sensitization of injured knee joints, the effect of drug administration on mechanical hyperalgesia (**Chapter 2.3**) was evaluated only before drug microinjection and at the peak of drug effect, previously determined in the Hargreaves test (**Chapter 2.2**).

### *3.1.1.3 Indirect measures: gait analysis*

In models of OA, in addition to measurements of primary (and when present, secondary) hyperalgesia, evaluation of postural deficits can provide an indirect measure of OA-related nociception<sup>5,15</sup>. Load bearing is the parameter more commonly affected by OA and, interestingly, its values are directly correlated with mechanical allodynia scores<sup>5,16</sup>. Gait alterations can be assessed by the weight-bearing test<sup>17</sup> or the CatWalk test<sup>5,16</sup>. The weight bearing test measures load bearing on each hind limb in a static position. The CatWalk evaluates the same type of parameter, with the advantage of doing so during walking<sup>17</sup>. Hence, parameters not only related to single paws (intensity of paw print, relative paw placement, duration of limb placement), but also related to interlimb coordination can be assessed<sup>5,16,18</sup>.



Since we do not have access to an automated CatWalk apparatus, we used a manual system to perform gait analysis. Inherently, this method is associated to a higher error since all the scoring is done manually. It also involves covering the fore and hind paws of rats with paint, which adds a stressful factor to the test. Additionally, it does not allow a direct measurement of the values of load bearing; instead, they must be inferred from the area of paw print. Nonetheless, it proved to be sensible enough to observe gait alterations in K/C rats (**Chapter 2.1**).

### *3.1.2 Behavioral assessment of anxiety and depressive-like behaviors*

Several paradigms can be used to assess mood-like disorders. In **Chapter 2.1** we used the open field test (OF) to evaluate anxiety-like deficits in K/C animals, and the forced swimming test (FST) and sucrose preference test (SPT) to evaluate depressive-like phenotype.

The OF is used primarily to analyze motor function by examining the exploratory drive of the animal. However, it is also possible to determine an anxious state in rodents as, when exposed to a strange environment, mammals tend to freeze, reducing the chances of being spotted by a predator, and walk close to the walls, a behavior known as thigmotaxis. Decreased exploration and time spent in the center of the field are indicators of anxiety-like behavior<sup>19,20</sup>. This test needs to be performed in a highly controlled environment to ensure the accuracy of the results, as several factors can affect the outcome, including housing conditions, light intensity, circadian cycle variations, prior handling or stress exposure, and familiarity with the arena<sup>21</sup>. For example, prior exposure to stressful situations, such as other types of experimental testing, can significantly increase the anxiety levels of rodents. On the other hand, re-exposure to the paradigm can reduce anxiety-like behavior to levels comparable to that of treatment with anxiolytic drugs such as benzodiazepines<sup>21</sup>. In addition, the presence of the experimenter in the room can also influence the results. To overcome these difficulties, several precautions were taken during the experimental testing. Each animal was exposed to the OF only once and only to one test per day. Additionally, the test was performed in enclosed, dimly lit spaces where rats could not see the experimenters.

Alternatively, anxiety-like behaviors can be measured through other tests, such as the elevated plus maze, the light-dark box or the social interaction tests. The elevated plus maze and the light-dark box evaluate similar parameters, testing the conflict generated between the rodents' exploratory drive and their avoidance of the open arms or lit compartment<sup>21</sup>. In the social interaction test, the

time that two rats spend interacting is measured. When compared to the other tests described, the social interaction test presents one main advantage, as it does not rely on the exposure of the animals to an aversive situation<sup>22</sup>.

The FST was developed by Porsolt and colleagues and is used to evaluate depressive-like behavior and antidepressant activity<sup>23</sup>. When placed in an inescapable cylinder with water, rodents initially try to escape but tend to stop after a while. This immobility reflects a failure in persisting in escape-directed behavior, known as behavioral despair, or the development of passive behavior that disengages the animal from active forms of coping with stressful stimuli. The pretest session induces learned helplessness, which induces deficits in affect, cognition, sleep and motor performance, resembling many depressive symptoms<sup>24,25</sup>. Depression is a multifaceted condition, of which the primary symptoms (difficulty in concentration, low self-esteem, guilt, suicidal ideation, thoughts of death) are difficult to model in animals<sup>26</sup>. Depressed mood in human patients is proposed to be analogous to learned helplessness in rodents<sup>26</sup>, which can be measured not only through the FST, but also through the tail suspension test<sup>26</sup>. However, since the measured variable in this tests, immobility, is evoked by the test itself and is not measurable outside of the experimental setting, the FST and tail suspension procedures are more appropriate to evaluate antidepressant effects than depressive-like behavior *per se*. Furthermore, since the FST relies on differences in motor activity, it is also important to ensure that the results obtained are not caused by a locomotion deficit. In **Chapter 2.2**, we used the rotarod test in healthy and K/C animals to evaluate if drug microinjection in the IL has secondary locomotor effects, which retrospectively also allowed to confirm K/C animals do not show locomotor deficits.

Measures of decreased pleasure, or anhedonia, are also proposed to be analogous in patients and rodents. The most used test to measure anhedonia in rodents is the sucrose preference test<sup>26</sup>. However, in the specific case of chronic pain models, the overlap between pain and pleasure mechanisms and pathways can difficult the task of separating the symptoms of pain and depressive-like behaviors as measured by anhedonia<sup>27</sup>. Therefore, the combination of several approaches is necessary to increase the validity of the results. By combining measures of learned helplessness and anhedonia, we validate the results of each test.

### *3.1.3 Functional interventions*

#### *3.1.3.1 Pharmacological and electrical modulation*

The modulation of CNS activity and its translation into a specific behavior plays a fundamental part in neuroscience research. In the pain field, one of the most famous interventions was carried out by Reynolds (1969), who described that electrical stimulation delivered into the PAG induced deep analgesia that allowed to perform surgery in awake rats<sup>28</sup>. Since then, other approaches were used and developed that allow the permanent lesion or transient modulation of a specific area.

Electrical or pharmacological lesions can be used to determine the nociceptive role of a specific brain region. However, by causing permanent, indiscriminate damage in the neural populations, these approaches can have side effects that do not correspond to the actual function of the area of interest<sup>29,30</sup>. Alternatively, transient pharmacological blockade with local anesthetics such as lidocaine, which blocks Na<sup>+</sup> channels and prevents neuron depolarization<sup>31</sup>, or increasing the inhibitory tone in a region with GABA administration provides a more physiological result with a lower chance of secondary effects.

Gain of function strategies such as electrical stimulation or local injection of glutamate can also be used to determine the nociceptive potential of a region<sup>32</sup>. Pharmacological interventions are preferable to electrical ones, as they mimic physiological processes more closely than electrical stimulation. However, some care should be taken regarding the used concentrations, since glutamate, for example, is a highly excitotoxic neurotransmitter<sup>33,34</sup>. In addition to using glutamate to generally activate an area of interest, neural circuits can be studied by using specific receptor agonists and antagonists. In the work described in this dissertation, particularly in **Chapter 2.2**, the use of several group I mGluRs agonists and antagonists allowed us to dissect the receptors specific contribution to glutamate-driven IL pronociception. One of the main drawbacks of driving system function with a receptor agonist is the potential activation of a pathway that is otherwise inactive. In this sense, the use of receptor antagonists provides better information regarding the physiological function of the studied receptor/pathway. In addition, pharmacological interventions do not allow to distinguish among the cell types they act on, as we demonstrated in **Chapter 2.3**. Alternatively, the use of optogenetics allows the specific manipulation of the preferred cell type and receptor. This technique is however associated to higher costs and expertise, as it requires the expression of a light-sensitive channel, achieved by local injection of a virus targeted to the desired

cell type or through the breeding of a genetic mouse models that express the light-sensitive channels<sup>35</sup>.

### *3.1.3.2 L- $\alpha$ -amino adipate (L $\alpha$ AA)*

To study the astrocyte contribution for mGluR5-mediated hyperalgesia, we evaluated how inhibition of astrocyte function in the IL affected nociceptive behavior in SHAM and K/C animals (**Chapter 2.3**). L $\alpha$ AA is a natural product of lysine metabolism in the CNS that, as a structural homolog of glutamate, inhibits glutamate transport in astrocytes. Briefly, glutamate in the synaptic cleft is internalized by astrocytes and transformed by glutamine synthase into an inert form, glutamine. The inactive glutamine is transported back into the presynaptic neuronal terminal and reconverted into glutamate by the enzyme glutaminase, in a process known as the glutamine cycle. L $\alpha$ AA blocks glutamine synthase in astrocytes, leading to the accumulation of cytotoxic levels of glutamate inside the astrocyte<sup>36</sup>. L $\alpha$ AA-induced astrocyte pathology is progressively characterized by nuclear swelling, followed by astrocyte body swelling and membrane blebbing, and finally by cell vacuolation and breakage into spherical bodies<sup>36,37</sup>. Moreover, since astrocytes are physically connected with each other, the damage can extend to the surrounding cells<sup>36,38</sup>.

The selectivity of L $\alpha$ AA toxicity is subject to some controversy. For example, while Olney and colleagues reported the occurrence of neuronal necrosis after L $\alpha$ AA injection in the brain<sup>39</sup>, most studies indicate that L $\alpha$ AA selectively targets astrocytes, without affecting neurons or microglia for at least 7 days after administration<sup>36,37,40</sup>. The neurotoxicity observed by Olney and colleagues was instead proposed to result from the high concentration of L $\alpha$ AA used. In **Chapter 2.3**, we chose a concentration based on these observations to avoid altering neuronal or microglial activities. Nonetheless, even though L $\alpha$ AA can be considered a selective gliotoxin, it is important to consider the impact that astrocyte ablation entails for extracellular space homeostasis, excitatory neurotransmitter uptake and metabolic support functions. In line with these observations, Lima and colleagues observed that the expression of neuronal markers in the mPFC of adult rats is not altered by L $\alpha$ AA, but they found dendritic atrophy of pyramidal neurons in the area affected by L $\alpha$ AA, which aggravated with time<sup>41</sup>. Therefore, some degree of neuronal dysfunction should be expected after astrocyte ablation. To try and minimize this effect, we performed all the behavioral tests in the first 7 days after ablation, a time point after which the animals were sacrificed. Their

impact upon the observed behavioral results however, remains unknown and should be further investigated.

Other methods could be used to complement our results; for example, a reversible gliotoxin, such as fluoroacetate or fluorocitrate, could be used to avoid the secondary effects occurring at the neuronal level. However, neither of the substances is selective for astrocytes, and could affect microglia or oligodendrocytes activity as well<sup>42</sup>. The use of a genetically modified model, such as the inducible dominant negative SNARE mouse model (dnSNARE; blocks vesicle exocytosis from astrocytes, and concomitantly gliotransmitter release<sup>43</sup>) or the IP<sub>3</sub>R2 knockout model (blocks the release of intracellular Ca<sup>2+</sup> from the endoplasmic reticulum stores<sup>44</sup>) could provide a useful tool to study astrocyte function in nociception. However, these models are not completely well characterized, and in recent years some studies have been published that question the validity of their results<sup>45-47</sup>.

### *3.1.4 Anesthesia and electrophysiological recordings*

#### *3.1.4.1 Ketamine and medetomidine*

The recourse to anesthetics was necessary at one or more occasions during the course of our experimental procedures. Surgical implantation of intracerebral cannulas and intrathecal catheters, as well as the induction of the K/C model mostly relied on the use of a mixture of ketamine and medetomidine, with atipamezole, that reverses medetomidine effects, to induce rapid anesthesia recovery. Ketamine is a NMDA receptor antagonist that blocks the excitatory effects of glutamatergic transmission, preventing central sensitization<sup>48</sup>. It also stimulates cardiovascular activity by acting upon the sympathetic nervous system<sup>49</sup>. Anesthetic concentrations of ketamine peak at 5 minutes post administration and can last for about 25 minutes, making ketamine a short-duration anesthetic. Medetomidine, an  $\alpha$ 2-adrenoceptor agonist, causes sedation and analgesia, along with cardiovascular depression. In combination, the effect of the two drugs is potentiated to provide a more stable anesthesia. Additionally, the net balance of the cardiovascular effects when both drugs are administered is null<sup>50</sup>. In comparison with other injectable drugs, such as barbiturates, ketamine and medetomidine provide a more stable anesthesia, with a faster recovery due to the use of atipamezole, and therefore with fewer complications. However, these drugs have additional applications that might interfere with the subsequent results. For instance, in addition to

blocking NMDA receptor function, ketamine also potentiates glutamate transmission through AMPA receptors and has inhibitory effects on muscarinic acetylcholine receptors<sup>51</sup>. In fact, ketamine has been recently in the spotlight for its fast antidepressant effect: a single sub-anesthetic dose of ketamine can reverse symptoms in patients with treatment-resistant depression, and the effect lasts from a few days to a few weeks<sup>52</sup>. The antidepressant mechanism of ketamine involves the rapid enhancement of synaptic function in cortical regions<sup>53</sup>, resulting in increased activity of pyramidal neurons<sup>54</sup>. Due to our experimental timeline, where cannula implantation in K/C animals was performed 3 weeks after induction and 1 week before the beginning of experimental testing, and considering that the antidepressant results of ketamine can last for a few weeks, it is possible that ketamine administration influenced our results. Generally, however, we excluded this hypothesis because all of **Chapter 2.4**'s surgical procedures were performed with sodium pentobarbital, and the results obtained match those in the remaining Chapters.

#### *3.1.4.2 Sodium pentobarbital*

Electrophysiological recordings were performed in animals under pentobarbital anesthesia (**Chapters 2.4 and 2.5**). This protocol is one of the most widely used when recording nociceptive modulatory brainstem areas such as the RVM<sup>55,56</sup>; however, it presents several drawbacks. First, since pentobarbital is injected intraperitoneally, a stable anesthesia depth can be difficult to maintain. To minimize its impact on the results, the anesthesia level was frequently monitored by observing muscle tone and pupil dilation. Second, one of the major goals of anesthesia is the suppression of sensory pathways, and in particular pain, which represents a major drawback in pain studies. Different drugs can disrupt ascending and descending pain pathways at different levels. Overall, anesthetics have little or no effect upon peripheral nerve sensitivity, but have a high impact on spinal cord neurons<sup>57</sup>. As pentobarbital binds to GABA<sub>A</sub> receptors and acts by potentiating inhibitory GABAergic tone<sup>58</sup>, activity in different supraspinal CNS regions is more or less affected by the anesthetic depending on the GABA<sub>A</sub> composition<sup>59</sup>. As a consequence, differences between awake and anesthetized animals can be quite significant. For example, one study reported that RVM OFF-cells are not found during single unit electrophysiological recordings in awake rats; under barbiturate anesthesia, however, they become detectable<sup>60,61</sup>. Therefore, care should be taken when extrapolating conclusions from recordings in anesthetized animals and, whenever possible, they should be confirmed with or replaced by recordings in awake animals.

### *3.1.4.3 Type of electrophysiological recordings*

Some consideration must also be given to the advantages and disadvantages of the type of electrophysiological recording used. In the work here presented we used single unit electrophysiological recordings, which allow to differentiate functionally heterogeneous neuronal populations such as the RVM's ON-, OFF- and NEUTRAL-cells<sup>62</sup> and dorsal horn nociceptive WDR and NS cells<sup>63</sup>. This approach also allows to compare between the baseline and evoked activities of different experimental groups and pharmacological treatments. However, the conclusions based on this data must be considered with some reservation, especially when evaluating the activity of large heterogeneous brain regions, since the number of neurons analyzed in each recording is small and might not be representative of the entire area of interest<sup>64</sup>. To overcome this limitation, recordings using multielectrode arrays could be used; this technique allows the simultaneous recording of a brain region through evenly distributed electrodes and therefore provides data on the ensemble neural activity<sup>64</sup>. The usefulness of multielectrode recordings was shown for example by the discovery of large multiwhisker receptive fields in cortical neurons that respond dynamically in time after stimulation<sup>65</sup>. In addition, since multielectrode arrays can be chronically implanted in animals<sup>66</sup>, this method is not affected by neuronal alterations induced by anesthesia.

## **3.2 Suitability of the K/C model to study OA**

The K/C model is usually described as a monoarthritis model that mimics the recurrent inflammatory episodes that occur in human patients<sup>67,68</sup>. It produces inflammation, mechanical and thermal hyperalgesia, and neuroplastic changes in the CNS that peak at 5-6h after induction and can last for 1 week<sup>67-69</sup>. Despite being previously described that mechanical hyperalgesia can last for at least 8 weeks<sup>70</sup>, most studies that use the K/C model do not present data over 1 week after induction. However, we previously reported that 4 weeks after induction of the K/C model there were alterations in RVM and spinal dorsal horn activity concomitant with nociceptive facilitation<sup>55,71</sup>, and that rats developed anxiety and depressive-like behaviors at that time point<sup>72</sup>. Therefore, in **Chapter 2.1**, we studied the progressive effects of intra-synovial injection of a mixture containing kaolin and carrageenan in rats to evaluate the potential of the model in mimicking OA pathology. K/C injection caused animals to display mechanical hyperalgesia and allodynia, accompanied by a reduction of the contact area of the hind paw. The histopathological and radiological analysis of the affected joint showed severe alterations corresponding to a Grade 4 level in the Kellgren and

Lawrence scale of OA<sup>73,74</sup>. In later stages of the pathology, animals developed comorbid anxiety and depressive-like behaviors.

The most common complaint in OA patients is pain<sup>11</sup>. Its treatment, however, is not always effective and relies mostly on the topical or oral application of non-steroid anti-inflammatory drugs (NSAID) in less severe cases, progressing to local administration of steroids to suppress inflammatory reactions and, at very advanced stages, joint replacement<sup>11</sup>. The development of a preclinical model that reproduces closely the main features of human OA would be of great importance to the development of new therapies with higher translational value. Since the gold standard method used for the detection and classification of clinical OA is radiography<sup>75</sup>, we analyzed the radiographic profile of the affected knee joints throughout the progression of the K/C model and correlated them with histopathological findings. Although all groups present mechanical hypersensitivity, radiographic changes were first detected only 2 weeks after K/C injection, and correlated to mild histological changes including chondrocyte disorganization and inflammation. At the 4 week time point, radiography showed the development of subchondral bone sclerosis and formation of osteophytes, as well as narrowing of the joint space. Histological changes also increased in severity and, in line with radiographic findings, included bone sclerosis. Interestingly, radiographic reports in human patients are also limited to later stages of the disease when articular degeneration is present<sup>76</sup> and only about half of the patients with joint pain complaints display radiographic changes<sup>77</sup>. These results add significance to our proposal of the K/C model as a suitable model to study OA.

Patients with OA usually present altered gait patterns, adopting instinctive protective behaviors to avoid inflicting further damage in the damaged joint. In fact, OA is the most important cause of impaired mobility, constituting about 50% of all the musculoskeletal diseases in the work<sup>78</sup>. After K/C administration, our animals display subtle changes in the gait parameters assessed. The most prominent change is the smaller contact area of the affected hind paw, which can represent an indirect measure of load bearing changes, commonly reported in other preclinical OA models<sup>4,15,67</sup>.

Long-term exposure to the K/C model is also associated with the development of anxiety and depressive-like behaviors. Pain-related mood disorders such as anxiety, depression and sleep disorders are an important source of disability in chronic pain patients, which is often overlooked by clinicians and preclinical researchers alike<sup>79</sup>. Although over one third of OA patients suffer from one or more disorders<sup>79</sup>, the underlying mechanisms of pain and mood interactions are mostly



unknown. Therefore, the K/C model presents a good opportunity to study not only the more well-known symptoms of OA, but also to better understand the common mechanisms of comorbid pain and mood regulation.

Overall, the progression of joint degeneration and behavioral dysfunction described in **Chapter 2.1** closely mirror the progression of human OA, indicating the K/C model is a suitable model to study OA. As listed in the Introduction of this thesis, many models are described as suitable for the study of OA, including the well described MIA model. The main advantage of the K/C intra-articular administration in comparison with other chemically inducible models is the progressive development of physical impairments and articular degeneration, which allow to study OA at a particular time point of the disease, independently of whether the goal is to study disease progression mechanisms and markers, or therapeutic efficacy of interventions. In addition, this model is easy, inexpensive to implement and, at least until 1 week after induction<sup>67-69</sup>, the results reported in several studies show little variability between investigators and laboratories. These three characteristics further support the validity of the K/C model to study OA. In future studies, the progression of behavioral and morphological symptoms should be correlated to immune response markers of the disease, to further ascertain the validity of the K/C model to study OA. In addition, since gender and age are main risk factors to the development of OA<sup>78,80</sup>, the effect of K/C intra-articular administration in females, both healthy and ovariectomized to mimic a menopausal state, should be characterized.

### **3.3 Pain modulation by the mPFC**

#### *3.3.1 Dissociation of PL and IL functions*

The PL and the IL are commonly treated as a single region known as the ventral mPFC. It is usual to find publications that do not distinguish between the two subregions and that implicate them equally in behavioral flexibility<sup>81</sup>, spatial working memory<sup>82,83</sup>, anxiety behavior<sup>84</sup>, fear-extinction<sup>85</sup>, decision-making<sup>86</sup> and pain<sup>87</sup>. However, both the anatomical projections and the functional roles of the PL and IL diverge significantly when analyzed separately<sup>88-93</sup>. For example, Millicamps and colleagues described local infusion of NMDA produces antinociception in the PL, but has no effect when microinjected into the IL<sup>94</sup>. Similarly, our results in **Chapter 2.2** show a contrasting nociceptive behavioral effect elicited by glutamate microinjection in the PL and in the IL, adding to

the current evidence pointing to dissociated subregional contributions toward pain modulation from the mPFC. In addition, this functional dissociation also seems to extend to receptor involvement: while glutamate in the PL has a fast antinociceptive effect, indicative of ionotropic glutamate receptor-mediated effects, in the IL the pronociceptive effect is dependent on slow acting mGluRs, a result that is in line with Millecamps' observations<sup>94</sup>.

Although we did not further explore the dichotomy of PL and IL functions, the opposite functions of the PL and IL are also evident when considering their roles in the regulation of behaviors other than pain. For example, the regulation of conditioned fear memories stored in the AMY is dependent on mPFC activity<sup>95</sup>, as early studies show that lesions in the ventral mPFC impair the ability of rats to recall fear extinction<sup>96</sup>. When the particular involvement of each ventral mPFC subregion was explored, the IL alone was found to be responsible for consolidation of extinction of fear memories<sup>89</sup>. Moreover, Vidal-Gonzalez and colleagues described that independent stimulation of the PL and the IL had opposing effects: microstimulation of the IL reduced expression of fear responses to a conditionate stimulus and promoted extinction behavior, while PL microstimulation enhanced fear responses and prevented the formation of extinction behavior<sup>92</sup>. Although both the PL and the IL share bidirectional projections with the AMY, they project to different amygdalar subregions: glutamatergic PL projections target the basolateral AMY (BLA), while GABAergic IL projections target the central AMY (CeA)<sup>92</sup>.

What is more interesting is that these particular AMY-mPFC circuits are also extensively characterized in the context of inflammatory pain and share many similarities with fear-conditioning mechanisms<sup>97</sup>. Pain implies the formation of fear memories and fear conditioning towards an aversive, painful stimulus. A noxious stimulus causes a withdrawal reflex and the formation of a memory of the pain caused, that leads to its avoidance in future situations. In chronic pain, pain related fear can be more disabling than pain itself<sup>98,99</sup>. Therefore, it is not surprising that increased neurotransmission in fear related structures such as the AMY is found in chronic pain settings<sup>100,101</sup>, as well as in closely related areas such as the mPFC. Indeed, studies show that the AMY-mPFC circuitry contributes to the development and establishment of pain-related affective and cognitive disorders<sup>102-104</sup>, as well as enhancing monoarthritis-induced hyperalgesia<sup>105</sup>, though the specificity of each region is still incompletely determined.

### *3.3.2 Modulation of nociception by the IL*

The slow action of glutamate in the IL compared to the usually fast effect observed in the PL and reported by other studies<sup>55,71</sup>, led to the proposal that mGluRs are preferentially activated by glutamate to modulate nociception. By using a combination of agonists and antagonist for these receptors, we were able to prove that mGluR5 are activated by glutamate application in the IL (**Chapter 2.2**). Interestingly, mGluR5 activation was able to decrease the thresholds for thermal and mechanical stimulation in healthy animals; in K/C animals, IL mGluR5 activation lowered noxious-heat evoked nociceptive behavior in the distal paw, but not mechanically evoked behavior in the affected knee joint. This effect is most likely mediated by neuronal mGluR5, as astrocyte ablation did not modify the observed results. The induction of the inflammatory pain model also led to altered IL signaling, as antagonism of mGluR5 only affected K/C, but not healthy, animals, through a mechanism dependent on intact astrocytic function (**Chapter 2.3**).

The contribution of the IL to pain modulation and to its chronification is still considerably understudied. Morphological and functional alterations<sup>106</sup> as well as increased expression of neuronal activation markers were reported in the IL of rats with neuropathic pain<sup>107,108</sup>. In inflammatory pain, several studies indicate there is increased inhibitory transmission in the IL<sup>102-104,109</sup>, and by counteracting this inhibitory tone, inflammation-mediated hypersensitivity is abolished<sup>105,109</sup>. Interestingly, increased inhibition in the IL, along with inflammation-induced hyperalgesia, can be reversed by co-activation of mGluR5 and CB1 receptors<sup>104,105</sup>. These studies seem to contradict the results presented in this dissertation, where mGluR5 activation in the IL facilitated nociception in healthy and K/C rats, and mGluR5 inactivation had antinociceptive properties in K/C animals. We propose that different signaling pathways are favored by the disparate approaches used by us and by other authors. mGluR5 receptors are known to interact with and regulate a multitude of receptors to promote facilitation or inhibition of synaptic transmission in the PFC. For example, group I mGluR agonist DHPG can increase both inhibitory and excitatory transmission onto PFC pyramidal cells<sup>110,111</sup>. mGluR5 activation contributes to increased mPFC inhibitory tone by modulating cholinergic signaling<sup>112</sup>, but it also increases synaptic transmission in the mPFC through several other mechanisms, such as rate-dependent excitatory influence on spontaneous burst activity and intrinsic excitability<sup>113-115</sup>, potentiation of NMDA receptor mediated effects on firing rate and burst activity<sup>113</sup>, or long-term depression of GABAergic activity through retrograde endocannabinoid signaling<sup>104,105</sup>. Therefore, future studies should address the

underlying mechanism modulated by mGluR5 in our studies, as well as the effect that 4 weeks of inflammatory pain have upon the overall activity of mPFC subregions.

We also observed mGluR5 in the IL had no tonic effect upon nociceptive thresholds under physiological conditions. On the other hand, in chronic inflammatory pain conditions, IL mGluR5 antagonism was antinociceptive (**Chapter 2.2**). This could indicate that while driving mGluR5 signaling with an agonist can alter nociceptive behavior, in physiological conditions these receptors are not directly involved in the modulation of noxious evoked behaviors. In chronic pain conditions, which are frequently connected to the development of comorbid mood and cognitive impairments, i.e. alterations in the affective and cognitive dimensions of pain<sup>72,116,117</sup>, IL mGluR5 signaling is altered. Remarkably, chronic pain alterations are dependent on astrocytic function, as the tonic effect of mGluR5 antagonist on K/C animals is abolished by astrocyte ablation with L $\alpha$ AA (**Chapter 2.3**). Due to the homeostatic role of astrocytes<sup>38</sup>, the results hint at considerable remodeling occurring at the synaptic level due to prolonged experimental peripheral inflammation, altering not only neuron-neuron communication, but also neuron-glia interactions. In this context, our results point to a tonic activation of mGluR5 specifically in astrocytes due to the exposure to prolonged inflammatory pain. This tonic activation state could be due to increased astrocyte reactivity, increased expression of mGluR5 by astrocytes, or a combination of both. As described in the Introduction of this dissertation, in recent years there has been an increased focus on the contribution of glial cells towards the development and maintenance of pathological states. Increased astrocyte reactivity has been found in the forebrain, brainstem and spinal cord of rats for prolonged periods (28 days) after CFA administration<sup>118</sup>. Moreover, in the ACC, augmented astrocyte reactivity is associated to alterations in the affective dimension of pain, as astrocyte ablation inhibits escape/avoidance behavior in rats with prolonged inflammatory pain<sup>119</sup>. Although we do not have a full picture of the mechanisms underlying astrocytic function in pain perception, several lines of evidence have emerged that indicate astrocytes can influence synaptic and brain activity through many different processes. A recent study showed astrocytes in the spinal cord drive an alternative form of LTP that could explain secondary hypersensitivity. This form of gliogenic LTP is dependent on the binding of diffusible extracellular messenger such as D-serine and TNF $\alpha$ , meaning that it can spread in the cerebrospinal fluid and affect remote sites<sup>120</sup>.

On a different note, the parallel astrocyte-astrocyte communication propagated through Ca<sup>2+</sup> waves is also involved in pain, as expression of gap junction protein Cx43 (the main type of protein in

astrocyte-astrocyte gap junctions<sup>36</sup>), is increased after CFA-induced inflammation<sup>121</sup>; concurrently, gap junction inhibition produces analgesia in several pain models<sup>122</sup>. Interestingly, the generation of Ca<sup>2+</sup> waves can be induced by astrocytic mGluR5. These receptors are proposed to detect glutamatergic transmission in astrocytes and regulate synaptic transmission accordingly<sup>123</sup>. The number of astrocytic mGluR5 receptors activated is proportional to the magnitude of the Ca<sup>2+</sup> wave observed, indicating that larger synaptic events elicit higher responses in astrocytes that can propagate further from the origin of the signal<sup>123</sup>. Although mGluR5 expression in adulthood is quite low, astrocytic mGluR5 are more efficient and have higher affinity to glutamate when compared to their neuronal equivalents<sup>123</sup>. In addition, expression of mGluR5 in astrocytes was found to be increased in the S1 of rats with neuropathic pain<sup>124</sup>. Overall, the evidence here presented points to a gain of astrocytic function during chronic pain, which is in line with results from **Chapter 2.3**; the extent of the contribution of astrocytes to synaptic transmission, in chronic pain and otherwise, however, is not fully comprehended.

The role of the IL in the affective dimensions of pain should also be taken into account when considering the implications of the present results. One of the best described roles attributed to the IL is the regulation of aversive behavior extinction<sup>89,92,95,125</sup>. Increased activity of the mPFC, and in particular the IL, is highly correlated to the successful extinction of negative emotions<sup>126</sup>; concomitantly, decreased activity correlates with deficits in extinction behavior<sup>127</sup>. This mechanism is of particular interest since the ability to regulate fear extinction also underlies the development of mood-related disorders such as anxiety and depression<sup>128</sup>, which are also common comorbidities of chronic pain<sup>72,116,117</sup>. If we consider that chronic pain consists of a continuous formation of aversive emotional associations, rather than their extinguishing<sup>129</sup>, then the importance of the IL and the circuits it integrates for the processing of pain inputs becomes clearer. To some degree, the manipulation of these affective processes might be the main effect of IL pharmacological modulation and the behavioral alterations we describe an indirect consequence of it. In support of this proposal, overlap between the mechanisms described for pain and other emotional impairments can be found in the existing literature. Of particular interest for our work is the importance of mGluR5 signaling for IL-mediated extinction behaviors: genetic deletion of mGluR5 in mice or pharmacological blockade of mGluR5 in the IL abolishes<sup>115,130</sup>, while enhancing mGluR5 activity in the IL facilitates, fear extinction<sup>131</sup>. However, just as described above regarding pain mechanisms, there are also contrasting reports that indicate increased hyperexcitability in the IL leads to increased anxiety-like behaviors<sup>132</sup>.

### *3.3.3 Descending relays for IL-mediated pronociception*

#### *3.3.3.1 Supraspinal pathways*

The integration of IL inputs into nociceptive pathways is hinted at by anatomical works showing a multitude of connections between the IL and traditional pain modulatory areas<sup>88,133,134</sup>, and by functional imaging studies highlighting the co-occurrence of pain-induced activation of the PFC and brainstem pain modulatory regions, as well as by changes in their functional connectivity<sup>135-137</sup>.

In an attempt to determine the supraspinal outputs of IL mGluR5-induced nociceptive facilitation, the DRt emerged as a potential relay due to its facilitatory influence in dorsal horn neuronal activity as well as upon nociceptive behavior<sup>138,139</sup>. Indeed, in **Chapter 2.4** transient blockade of the DRt prevented behavioral pronociception from the IL in both healthy and K/C animals. However, the inhibition of DRt activity alone, either through general inactivation with lidocaine or through GABA-induced neuronal tone inhibition, was accompanied by antinociception. In accordance with this result, Almeida and colleagues previously reported that lesioning the DRt reduces nociceptive responses evoked by noxious heat in the tail-flick and hot-plate tests<sup>139</sup>. Additionally, hypoalgesia after lidocaine administration in the DRt was also previously observed in monoarthritic rats<sup>140</sup>.

Since we could not determine if the DRt was indeed a relay for IL-mediated pronociception or if the behavioral results were merely the net result of the effects of IL-mGluR5 activation and DRt inactivation, the behavioral results were inconclusive regarding our initial hypothesis. Electrophysiological results, on the other hand, undeniably showed that mGluR5 activation in the IL increased the spontaneous and heat-evoked discharges of nociceptive responding neurons in the DRt; however, the effect was only present in healthy animals, indicating that prolonged inflammatory pain changed the IL-mediated pathway. In addition, the administration of a mGluR5 antagonist in the IL, which is antinociceptive in K/C animals, had no effect upon DRt neuronal discharges. Inversely, the results from RVM recordings from **Chapter 2.5** show mGluR5 activation in the IL affects neuronal activity only in K/C animals. Interestingly, facilitation from the IL relayed through the RVM results from a disengagement from antinociceptive OFF-cells, instead of increased pronociceptive responses from ON-cells.

In **Chapters 2.2 and 2.3** we presented evidence that the IL undergoes plastic changes after prolonged exposure to the K/C model. The results from **Chapter 2.4 and 2.5**, depicting a shift from a DRt to a RVM-dependent behavioral pronociception add to that evidence, pointing to

alterations not only in the expression of mGluR5, but also to major reorganization of descending inputs from the IL. Interestingly, this is not the first study reporting both the RVM and the DRt as relays in the same pathway. Descending nociceptive facilitation from the ACC can be blocked by inhibiting the RVM<sup>141</sup> and the DRt<sup>142</sup>, and the authors propose that the DRt constitutes the final relay for the pathway. However, we observed no alterations in any RVM cell type, including NEUTRAL-cells, in healthy animals, excluding this hypothesis as the explanation for our results. Instead, we propose the PAG, a central region receiving a significant number of projections from cortical and subcortical regions, including the IL<sup>88,143</sup>, and projecting to both the RVM<sup>62,144</sup> and the DRt<sup>133,134</sup>, could be the common relay for IL pronociception in healthy and K/C rats. In fact, the PAG is a complex region that produces and modulates a variety of behavioral and physiological responses in addition to pain, such as vocalization, autonomic responses, reproductive and sexual behaviors and fear reactions<sup>143</sup>. Hence, in addition to evaluating the modulation of motivational/affective responses by the IL, the possible integration of that information by the PAG merits further investigation in future studies.

### *3.3.3.2 Influence of IL mGluR5-mediated pronociception on dorsal horn activity*

In **Chapter 2.4** we investigated the extent of IL mGluR5 pronociceptive inputs upon the activity of nociceptive neurons of the spinal dorsal horn. Electrophysiological recordings show mGluR5 agonist administration in the IL increased the noxious heat-evoked responses of the two neuronal populations recorded, WDR and NS neurons, a result that mirrors the effect of intra-IL CHPG nociceptive facilitation reported in **Chapter 2.2**. Additionally, CHPG also leads to enhanced WDR spontaneous activity in healthy, but not in K/C rats. Both the DRt and the RVM have previously been described to project directly to the spinal cord, resulting in direct modulation of dorsal horn neuronal activity<sup>62,145</sup>. Interestingly, when comparing the effect of IL mGluR5 activation in the spontaneous activity of the DRt and RVM with those in spinal WDR cells, the same pattern of activation is observed in the spinal cord and in the supraspinal regions. Indeed, in healthy animals CHPG in the IL increases the spontaneous and evoked discharges in the pronociceptive DRt<sup>139,146</sup> and in WDR cells. In K/C rats, on the other hand, CHPG in the IL abolishes the evoked but not the spontaneous responses of RVM's antinociceptive OFF-cells, promoting overall facilitation of nociceptive behavior<sup>62,147</sup>; in parallel, in the spinal cord only the evoked responses of WDR neurons are increased, but not the spontaneous ones. Although these results are in accordance with the

reorganization of IL descending pathways proposed in the previous section of this Discussion, further studies, for instance evaluating simultaneously the discharges of DRt/RVM and dorsal horn neurons after IL mGluR5 activation, are required to validate our hypothesis. Such an experiment would allow to discard other possible explanations, such as the existence of a ceiling effect in the activity of WDR neuronal discharges driven by prolonged exposure to the K/C model.

### *3.3.3.3 TRPV1*

Intrathecal administration of TRPV1 antagonist was able to block IL mGluR5 induced facilitation of responses to noxious heat applied to the hind paw in both experimental groups. Remarkably, baseline withdrawal latencies were not affected (**Chapter 2.4**). Contrary to our results, several works have reported the sensitization of peripheral TRPV1 plays an important role in exaggerating pain in inflammatory states and that TRPV1 antagonists are able to block inflammatory hyperalgesia<sup>148,149</sup>. In addition, as a transducer for heat, it seems paradoxical that intrathecal administration of a TRPV1 antagonist had no effect on heat-evoked latencies<sup>150,151</sup>. However, those studies consider TRPV1 is exclusively expressed in primary afferent nerves. Contrarily to that early assumption, however, TRPV1 expression can also be found in postsynaptic interneurons in the spinal cord<sup>152-154</sup> and in various brain regions<sup>155</sup>. Therefore, we propose that our results reflect the activation of TRPV1 in postsynaptic interneurons over presynaptic central terminals of primary afferent nerve fibers. In support of our proposal and in addition to the lack of effect upon basal heat-evoked latencies in K/C rats, we observed no hyperthermia in our animals, a side effect of peripheral TRPV1 activation<sup>156</sup> that is absent when the central receptor is activated<sup>157</sup>.

Because the contribution of TRPV1 to the transmission of pain in spinal circuits is still in the early stages of investigation, there are still many gaps in our understanding of TRPV1 mechanisms<sup>156</sup>. Additionally, our own results are very general and do not allow to further hypothesize on their significance. Hence, more studies are necessary to understand the full potential of TRPV1 in IL mediated pronociception and in pain modulation in general.



### 3.4 References

1. Whiteside, GT, Adedoyin, A, Leventhal, L (2008) Predictive validity of animal pain models? A comparison of the pharmacokinetic-pharmacodynamic relationship for pain drugs in rats and humans. *Neuropharmacology* 54, 767–75.
2. Backonja, M-M, Stacey, B (2004) Neuropathic pain symptoms relative to overall pain rating. *J. Pain* 5, 491–7.
3. Mogil, JS (2009) Animal models of pain: progress and challenges. *Nat. Rev. Neurosci.* 10, 283–94.
4. Adães, S, Mendonça, M, Santos, TN, Castro-Lopes, JM, Ferreira-Gomes, J, Neto, FL (2014) Intra-articular injection of collagenase in the knee of rats as an alternative model to study nociception associated with osteoarthritis. *Arthritis Res. Ther.* 16, R10.
5. Ferreira-Gomes, J, Adães, S, Castro-Lopes, JM (2008) Assessment of movement-evoked pain in osteoarthritis by the knee-bend and CatWalk tests: a clinically relevant study. *J. Pain* 9, 945–54.
6. Hunter, DJ, McDougall, JJ, Keefe, FJ (2008) The symptoms of osteoarthritis and the genesis of pain. *Rheum. Dis. Clin. North Am.* 34, 623–43.
7. Hargreaves, K, Dubner, R, Brown, F, Flores, C, Joris, J (1988) A new and sensitive method for measuring thermal nociception in cutaneous hyperalgesia. *Pain* 32, 77–88.
8. Wall, P. D., McMahon, S. B., & Koltzenburg, M (Elsevier/Churchill Livingstone, 2013). *Wall and Melzack's Textbook of Pain*.
9. Luukko, M, Konttinen, Y, Kempainen, P, Pertovaara, A, Petrovaara, A (1994) Influence of various experimental parameters on the incidence of thermal and mechanical hyperalgesia induced by a constriction mononeuropathy of the sciatic nerve. *Experimental neurology* 128, 143–154.
10. Le Bars, D, Gozariu, M, Cadden, SW (2001) Animal models of nociception. *Pharmacol. Rev.* 53, 597–652.
11. Bijlsma, JWJ, Berenbaum, F, Lefeber, FPJG (2011) Osteoarthritis: an update with relevance for clinical practice. *Lancet* 377, 2115–26.
12. Berenbaum, F (2013) Osteoarthritis as an inflammatory disease (osteoarthritis is not osteoarthrosis!). *Osteoarthr. Cartil.* 21, 16–21.
13. Randall, LO, Selitto, JJ (1957) A method for measurement of analgesic activity on inflamed tissue. *Arch. Int. Pharmacodyn. Ther.* 111, 409–19.

14. Barton, NJ, Strickland, IT, Bond, SM, Brash, HM, Bate, ST, Wilson, AW, Chessell, IP, Reeve, AJ, McQueen, DS (2007) Pressure application measurement (PAM): a novel behavioural technique for measuring hypersensitivity in a rat model of joint pain. *J. Neurosci. Methods* 163, 67–75.
15. Vrinten, DH, Hamers, FFT (2003) ‘CatWalk’ automated quantitative gait analysis as a novel method to assess mechanical allodynia in the rat; a comparison with von Frey testing. *Pain* 102, 203–9.
16. Gabriel, AF, Marcus, MAE, Honig, WMM, Walenkamp, GHIM, Joosten, EAJ (2007) The CatWalk method: a detailed analysis of behavioral changes after acute inflammatory pain in the rat. *J. Neurosci. Methods* 163, 9–16.
17. Pomonis, JD, Boulet, JM, Gottshall, SL, Phillips, S, Sellers, R, Bunton, T, Walker, K (2005) Development and pharmacological characterization of a rat model of osteoarthritis pain. *Pain* 114, 339–46.
18. Ängeby Möller, K, Kinert, S, Størkson, R, Berge, O-G (2012) Gait analysis in rats with single joint inflammation: influence of experimental factors. *PLoS One* 7, e46129.
19. Schmitt, U, Hiemke, C (1998) Combination of open field and elevated plus-maze: a suitable test battery to assess strain as well as treatment differences in rat behavior. *Prog. Neuropsychopharmacol. Biol. Psychiatry* 22, 1197–215.
20. Prut, L, Belzung, C (2003) The open field as a paradigm to measure the effects of drugs on anxiety-like behaviors: a review. *Eur. J. Pharmacol.* 463, 3–33.
21. Campos, AC, Fogaça, M V., Aguiar, DC, Guimarães, FS (2013) Animal models of anxiety disorders and stress. *Rev. Bras. Psiquiatr.* 35 Suppl 2, S101-11.
22. Bailey, KR, Crawley, JN (CRC Press/Taylor & Francis, 2009). in *Methods of Behavior Analysis in Neuroscience* (ed. Buccafusco, J.).
23. Porsolt, RD, Bertin, A, Blavet, N, Deniel, M, Jalfre, M (1979) Immobility induced by forced swimming in rats: effects of agents which modify central catecholamine and serotonin activity. *Eur. J. Pharmacol.* 57, 201–10.
24. Cryan, JF, Valentino, RJ, Lucki, I (2005) Assessing substrates underlying the behavioral effects of antidepressants using the modified rat forced swimming test. *Neurosci. Biobehav. Rev.* 29, 547–69.
25. Cryan, JF, Markou, A, Lucki, I (2002) Assessing antidepressant activity in rodents: recent developments and future needs. *Trends Pharmacol. Sci.* 23, 238–45.

26. Castagné, V, Moser, P, Porsolt, RD (CRC Press/Taylor & Francis, 2009). in *Methods of Behavior Analysis in Neuroscience* (ed. Buccafusco, J. J.).
27. Leknes, S, Tracey, I (2008) A common neurobiology for pain and pleasure. *Nat. Rev. Neurosci.* 9, 314–20.
28. Reynolds, D V. (1969) Surgery in the Rat during Electrical Analgesia Induced by Focal Brain Stimulation. *Science (80- )*. 164, 444–445.
29. Tsuruoka, M, Willis, WD (1996) Bilateral lesions in the area of the nucleus locus coeruleus affect the development of hyperalgesia during carrageenan-induced inflammation. *Brain Res.* 726, 233–6.
30. Almeida, A, Tjølsen, A, Lima, D, Coimbra, A, Hole, K (1996) The medullary dorsal reticular nucleus facilitates acute nociception in the rat. *Brain Res. Bull.* 39, 7–15.
31. Catterall, W a (2002) Molecular mechanisms of gating and drug block of sodium channels. *Novartis Found. Symp.* 241, 206-18-32.
32. Zhuo, M, Gebhart, GF (1997) Biphasic modulation of spinal nociceptive transmission from the medullary raphe nuclei in the rat. *J. Neurophysiol.* 78, 746–58.
33. Dong, X, Wang, Y, Qin, Z (2009) Molecular mechanisms of excitotoxicity and their relevance to pathogenesis of neurodegenerative diseases. *Acta Pharmacol. Sin.* 30, 379–87.
34. Mark, LP, Prost, RW, Ulmer, JL, Smith, MM, Daniels, DL, Strottmann, JM, Brown, WD, Hachein-Bey, L (2001) Pictorial review of glutamate excitotoxicity: fundamental concepts for neuroimaging. *AJNR. Am. J. Neuroradiol.* 22, 1813–24.
35. Deisseroth, K (2011) Optogenetics. *Nat. Methods* 8, 26–29.
36. Bridges, RJ, Hatalski, CG, Shim, SN, Cummings, BJ, Vijayan, V, Kundi, A, Cotman, CW (1992) Gliotoxic actions of excitatory amino acids. *Neuropharmacology* 31, 899–907.
37. Brown, DR, Kretschmar, HA (1998) The gliotoxic mechanism of alpha-amino adipic acid on cultured astrocytes. *J. Neurocytol.* 27, 109–18.
38. Verkhratsky, A, Butt, A (John Wiley & Sons, Ltd, 2013). *Glial Physiology and Pathophysiology*.
39. Olney, JW, de Gubareff, T, Collins, JF (1980) Stereospecificity of the gliotoxic and anti-neurotoxic actions of alpha-amino adipate. *Neurosci. Lett.* 19, 277–82.
40. Huck, S, Grass, F, Hatten, ME (1984) Gliotoxic effects of  $\alpha$ amino adipic acid on monolayer cultures of dissociated postnatal mouse cerebellum. *Neuroscience* 12, 783–791.
41. Lima, A, Sardinha, VM, Oliveira, AF, Reis, M, Mota, C, Silva, M a, Marques, F, Cerqueira,

- JJ, Pinto, L, Sousa, N, Oliveira, JF (2014) Astrocyte pathology in the prefrontal cortex impairs the cognitive function of rats. *Mol. Psychiatry* 19, 834–41.
42. Fonnum, F, Johnsen, A, Hassel, B (1997) Use of fluorocitrate and fluoroacetate in the study of brain metabolism. *Glia* 21, 106–13.
  43. Pascual, O, Casper, KB, Kubera, C, Zhang, J, Revilla-Sanchez, R, Sul, J-Y, Takano, H, Moss, SJ, McCarthy, K, Haydon, PG (2005) Astrocytic purinergic signaling coordinates synaptic networks. *Science* 310, 113–6.
  44. Li, H, Xie, Y, Zhang, N, Yu, Y, Zhang, Q, Ding, S (2015) Disruption of IP<sub>3</sub>R2-mediated Ca<sup>2+</sup> signaling pathway in astrocytes ameliorates neuronal death and brain damage while reducing behavioral deficits after focal ischemic stroke. *Cell Calcium* 58, 565–76.
  45. Petravicz, J, Boyt, KM, McCarthy, KD (2014) Astrocyte IP3R2-dependent Ca(2+) signaling is not a major modulator of neuronal pathways governing behavior. *Front. Behav. Neurosci.* 8, 384.
  46. Shigetomi, E, Patel, S, Khakh, BS (2016) Probing the complexities of astrocyte calcium signaling. *Trends Cell Biol.* 26, 300–12.
  47. Hamilton, NB, Attwell, D (2010) Do astrocytes really exocytose neurotransmitters? *Nat. Rev. Neurosci.* 11, 227–38.
  48. Bennett, GJ (2000) Update on the neurophysiology of pain transmission and modulation: focus on the NMDA-receptor. *J. Pain Symptom Manage.* 19, S2-6.
  49. Seymour, C, Gleed, R (Wiley, 1999). *BSAVA Manual of Small Animal Anaesthesia and Analgesia*.
  50. Baker, NJ, Schofield, JC, Caswell, MD, McLellan, AD (2011) Effects of early atipamezole reversal of medetomidine-ketamine anesthesia in mice. *J. Am. Assoc. Lab. Anim. Sci.* 50, 916–20.
  51. Murrrough, JW (2012) Ketamine as a novel antidepressant: from synapse to behavior. *Clin. Pharmacol. Ther.* 91, 303–9.
  52. Aan Het Rot, M, Zarate, CA, Charney, DS, Mathew, SJ (2012) Ketamine for depression: where do we go from here? *Biol. Psychiatry* 72, 537–47.
  53. Li, N, Lee, B, Liu, R-J, Banasr, M, Dwyer, JM, Iwata, M, Li, X-Y, Aghajanian, G, Duman, RS (2010) mTOR-dependent synapse formation underlies the rapid antidepressant effects of NMDA antagonists. *Science* 329, 959–64.
  54. Homayoun, H, Moghaddam, B (2007) NMDA receptor hypofunction produces opposite

- effects on prefrontal cortex interneurons and pyramidal neurons. *J. Neurosci.* 27, 11496–500.
55. Pinto-Ribeiro, F, Amorim, D, David-Pereira, A, Monteiro, AM, Costa, P, Pertovaara, A, Almeida, A (2013) Pronociception from the dorsomedial nucleus of the hypothalamus is mediated by the rostral ventromedial medulla in healthy controls but is absent in arthritic animals. *Brain Res. Bull.* 99, 100–108.
  56. Amorim, D, David-Pereira, A, Marques, P, Puga, S, Rebelo, P, Costa, P, Pertovaara, A, Almeida, A, Pinto-Ribeiro, F (2014) A role of supraspinal galanin in behavioural hyperalgesia in the rat. *PLoS One* 9, e113077.
  57. Vahle-Hinz, C, Detsch, O (2002) What can in vivo electrophysiology in animal models tell us about mechanisms of anaesthesia? *Br. J. Anaesth.* 89, 123–42.
  58. Steinbach, JH, Akk, G (2001) Modulation of GABA(A) receptor channel gating by pentobarbital. *J. Physiol.* 537, 715–33.
  59. Olsen, RW (1998) The molecular mechanism of action of general anesthetics: structural aspects of interactions with GABA(A) receptors. *Toxicol. Lett.* 100–101, 193–201.
  60. Olivéras, J-L, Martin, G, Montagne-Clavel, J (1991) Drastic changes of ventromedial medulla neuronal properties induced by barbiturate anesthesia. II. Modifications of the single-unit activity produced by Brevital, a short-acting barbiturate in the awake, freely moving rat. *Brain Res.* 563, 251–260.
  61. Olivéras, J-L, Montagne-Clavel, J, Martin, G (1991) Drastic changes of ventromedial medulla neuronal properties induced by barbiturate anesthesia. I. Comparison of the single-unit types in the same awake and pentobarbital-treated rats. *Brain Res.* 563, 241–250.
  62. Heinricher, MM, Tavares, I, Leith, JL, Lumb, BM (2009) Descending control of nociception: Specificity, recruitment and plasticity. *Brain Res. Rev.* 60, 214–225.
  63. Basbaum, AI, Bautista, DM, Scherrer, G, Julius, D (2009) Cellular and molecular mechanisms of pain. *Cell* 139, 267–284.
  64. Wiest, M, Thomson, E, Meloy, J (CRC Press/Taylor & Francis, 2008). *Multielectrode Recordings in the Somatosensory System. Methods for Neural Ensemble Recordings.*
  65. Ghazanfar, AA, Nicolelis, MA (2001) Feature article: the structure and function of dynamic cortical and thalamic receptive fields. *Cereb. Cortex* 11, 183–93.
  66. Oliveira, LMO, Dimitrov, D (2008). *Surgical Techniques for Chronic Implantation of Microwire Arrays in Rodents and Primates. Methods for Neural Ensemble Recordings.*

67. Neugebauer, V, Han, JS, Adwanikar, H, Fu, Y, Ji, G (2007) Techniques for assessing knee joint pain in arthritis. *Mol. Pain* 3, 8.
68. Schmidt, RF, Willis, WD (Springer Berlin Heidelberg, 2007). *Pain, Encyclopedia*.
69. Sluka, KA, Westlund, KN (1993) Behavioral and immunohistochemical changes in an experimental arthritis model in rats. *Pain* 55, 367–377.
70. Radhakrishnan, R, Moore, S a., Sluka, K a. (2003) Unilateral carrageenan injection into muscle or joint induces chronic bilateral hyperalgesia in rats. *Pain* 104, 567–577.
71. Pinto-Ribeiro, F, Ansah, OB, Almeida, A, Pertovaara, A (2008) Influence of arthritis on descending modulation of nociception from the paraventricular nucleus of the hypothalamus. *Brain Res.* 1197, 63–75.
72. Amorim, D, David-Pereira, A, Pertovaara, A, Almeida, A, Pinto-Ribeiro, F (2014) Amitriptyline reverses hyperalgesia and improves associated mood-like disorders in a model of experimental monoarthritis. *Behav. Brain Res.* 265, 12–21.
73. Altman, RD, Gold, GE (2007) Atlas of individual radiographic features in osteoarthritis, revised. *Osteoarthr. Cartil.* 15, A1–A56.
74. Kellgren, JH, Lawrence, JS (1963) Atlas of standard radiographs. The epidemiology of chronic rheumatism.
75. Hochberg, MC, Silman, AJ, Smolen, JS, Weinblatt, ME, Weisman, MH (2015). *Rheumatology*.
76. Hunter, DJ, Guermazi, A, Roemer, F, Zhang, Y, Neogi, T (2013) Structural correlates of pain in joints with osteoarthritis. *Osteoarthr. Cartil.* 21, 1170–8.
77. Haviv, B, Bronak, S, Thein, R (2013) The complexity of pain around the knee in patients with osteoarthritis. *Isr. Med. Assoc. J.* 15, 178–81.
78. Musumeci, G, Szychlinska, MA, Mobasher, A (2015) Age-related degeneration of articular cartilage in the pathogenesis of osteoarthritis: molecular markers of senescent chondrocytes. *Histol. Histopathol.* 30, 1–12.
79. Murphy, LB, Sacks, JJ, Brady, TJ, Hootman, JM, Chapman, DP (2012) Anxiety and depression among US adults with arthritis: prevalence and correlates. *Arthritis Care Res. (Hoboken)*. 64, 968–76.
80. Silverwood, V, Blagojevic-Bucknall, M, Jinks, C, Jordan, JL, Protheroe, J, Jordan, KP (2015) Current evidence on risk factors for knee osteoarthritis in older adults: a systematic review and meta-analysis. *Osteoarthr. Cartil.* 23, 507–15.

81. Rich, EL, Shapiro, ML (2007) Prelimbic/infralimbic inactivation impairs memory for multiple task switches, but not flexible selection of familiar tasks. *J. Neurosci.* 27, 4747–55.
82. Gisquet-Verrier, P, Delatour, B (2006) The role of the rat prefrontal cortex in working memory: not involved in the short-term maintenance but in monitoring and processing functions. *Neuroscience* 141, 585–96.
83. Dias, R, Aggleton, JP (2000) Effects of selective excitotoxic prefrontal lesions on acquisition of nonmatching- and matching-to-place in the T-maze in the rat: differential involvement of the prefrontal and anterior cingulate cortices in providing behavioural flexibility. *Eur. J. Neurosci.* 12, 4457–66.
84. Jinks, AL, McGregor, IS (1997) Modulation of anxiety-related behaviours following lesions of the prefrontal or infralimbic cortex in the rat. *Brain Res.* 772, 181–90.
85. Lebrón, K, Milad, MR, Quirk, GJ (2004) Delayed recall of fear extinction in rats with lesions of ventral medial prefrontal cortex. *Learn. Mem.* 11, 544–8.
86. Euston, DR, Gruber, AJ, McNaughton, BL (2012) The role of medial prefrontal cortex in memory and decision making. *Neuron* 76, 1057–70.
87. Zhang, R, Tomida, M, Katayama, Y, Kawakami, Y (2004) Response durations encode nociceptive stimulus intensity in the rat medial prefrontal cortex. *Neuroscience* 125, 777–785.
88. Vertes, RP (2004) Differential projections of the infralimbic and prefrontal cortex in the rat. *Synapse* 51, 32–58.
89. Laurent, V, Westbrook, RF (2009) Inactivation of the infralimbic but not the prefrontal cortex impairs consolidation and retrieval of fear extinction. *Learn. Mem.* 16, 520–9.
90. Marquis, J-P, Killcross, S, Haddon, JE (2007) Inactivation of the prefrontal, but not infralimbic, prefrontal cortex impairs the contextual control of response conflict in rats. *Eur. J. Neurosci.* 25, 559–66.
91. Oualian, C, Gisquet-Verrier, P (2010) The differential involvement of the prefrontal and infralimbic cortices in response conflict affects behavioral flexibility in rats trained in a new automated strategy-switching task. *Learn. Mem.* 17, 654–68.
92. Vidal-Gonzalez, I, Vidal-Gonzalez, B, Rauch, SL, Quirk, GJ (2006) Microstimulation reveals opposing influences of prefrontal and infralimbic cortex on the expression of conditioned fear. *Learn. Mem.* 13, 728–33.

93. Vertes, RP (2006) Interactions among the medial prefrontal cortex, hippocampus and midline thalamus in emotional and cognitive processing in the rat. *Neuroscience* 142, 1–20.
94. Millecamps, M, Centeno, M V., Berra, HH, Rudick, CN, Lavarello, S, Tkatch, T, Apkarian, VA (2007) d-Cycloserine reduces neuropathic pain behavior through limbic NMDA-mediated circuitry. *Pain* 132, 108–123.
95. Quirk, GJ, Garcia, R, González-Lima, F (2006) Prefrontal mechanisms in extinction of conditioned fear. *Biol. Psychiatry* 60, 337–43.
96. Quirk, GJ, Russo, GK, Barron, JL, Lebron, K (2000) The role of ventromedial prefrontal cortex in the recovery of extinguished fear. *J. Neurosci.* 20, 6225–31.
97. Neugebauer, V, Galhardo, V, Maione, S, Mackey, SC (2009) Forebrain pain mechanisms. *Brain Res. Rev.* 60, 226–242.
98. Vlaeyen, JWS, Linton, SJ (2012) Fear-avoidance model of chronic musculoskeletal pain: 12 years on. *Pain* 153, 1144–7.
99. Vlaeyen, JW, Linton, SJ (2000) Fear-avoidance and its consequences in chronic musculoskeletal pain: a state of the art. *Pain* 85, 317–32.
100. Kulkarni, B, Bentley, DE, Elliott, R, Julyan, PJ, Boger, E, Watson, A, Boyle, Y, El-Deredy, W, Jones, AKP (2007) Arthritic pain is processed in brain areas concerned with emotions and fear. *Arthritis Rheum.* 56, 1345–54.
101. Neugebauer, V, Li, W, Bird, GC, Bhave, G, Gereau, RW (2003) Synaptic plasticity in the amygdala in a model of arthritic pain: differential roles of metabotropic glutamate receptors 1 and 5. *J. Neurosci.* 23, 52–63.
102. Ji, G, Sun, H, Fu, Y, Li, Z, Pais-Vieira, M, Galhardo, V, Neugebauer, V (2010) Cognitive impairment in pain through amygdala-driven prefrontal cortical deactivation. *J. Neurosci.* 30, 5451–5464.
103. Ji, G, Neugebauer, V (2011) Pain-related deactivation of medial prefrontal cortical neurons involves mGluR1 and GABA<sub>A</sub> receptors. *J. Neurophysiol.* 106, 2642–2652.
104. Ji, G, Neugebauer, V (2014) CB1 augments mGluR5 function in medial prefrontal cortical neurons to inhibit amygdala hyperactivity in an arthritis pain model. *Eur. J. Neurosci.* 39, 455–466.
105. Kiritoshi, T, Ji, G, Neugebauer, V (2016) Rescue of impaired mGluR5-driven endocannabinoid signaling restores prefrontal cortical output to inhibit pain in arthritic rats.



- J. Neurosci.* 36, 837–50.
106. Metz, AE, Yau, H-J, Centeno, MV, Apkarian, a V, Martina, M (2009) Morphological and functional reorganization of rat medial prefrontal cortex in neuropathic pain. *Proc. Natl. Acad. Sci. U. S. A.* 106, 2423–2428.
  107. Leite-Almeida, H, Guimarães, MR, Cerqueira, JJ, Ribeiro-Costa, N, Anjos-Martins, H, Sousa, N, Almeida, A (2014) Asymmetric c-fos expression in the ventral orbital cortex is associated with impaired reversal learning in a right-sided neuropathy. *Mol. Pain* 10, 41.
  108. Devoize, L, Alvarez, P, Monconduit, L, Dallel, R (2011) Representation of dynamic mechanical allodynia in the ventral medial prefrontal cortex of trigeminal neuropathic rats. *Eur. J. Pain* 15, 676–82.
  109. Luongo, L, De Novellis, V, Gatta, L, Palazzo, E, Vita, D, Guida, F, Giordano, C, Siniscalco, D, Marabese, I, De Chiaro, M, Boccella, S, Rossi, F, Maione, S (2013) Role of metabotropic glutamate receptor 1 in the basolateral amygdala-driven prefrontal cortical deactivation in inflammatory pain in the rat. *Neuropharmacology* 66, 317–329.
  110. Chu, Z, Hablitz, JJ (1998) Activation of group I mGluRs increases spontaneous IPSC frequency in rat frontal cortex. *J. Neurophysiol.* 80, 621–7.
  111. Marek, GJ, Zhang, C (2008) Activation of metabotropic glutamate 5 (mGlu5) receptors induces spontaneous excitatory synaptic currents in layer V pyramidal cells of the rat prefrontal cortex. *Neurosci. Lett.* 442, 239–43.
  112. Pollard, M, Bartolome, JM, Conn, PJ, Steckler, T, Shaban, H (2014) Modulation of neuronal microcircuit activities within the medial prefrontal cortex by mGluR5 positive allosteric modulator. *J. Psychopharmacol.* 28, 935–46.
  113. Homayoun, H, Moghaddam, B (2006) Bursting of prefrontal cortex neurons in awake rats is regulated by metabotropic glutamate 5 (mGlu5) receptors: rate-dependent influence and interaction with NMDA receptors. *Cereb. Cortex* 16, 93–105.
  114. Homayoun, H, Moghaddam, B (2010) Group 5 metabotropic glutamate receptors: role in modulating cortical activity and relevance to cognition. *Eur. J. Pharmacol.* 639, 33–9.
  115. Fontanez-Nuin, DE, Santini, E, Quirk, GJ, Porter, JT (2011) Memory for fear extinction requires mGluR5-mediated activation of infralimbic neurons. *Cereb. Cortex* 21, 727–735.
  116. Buchner, M, Neubauer, E, Zahlten-Hinguranage, A, Schiltenswolf, M (2007) The influence of the grade of chronicity on the outcome of multidisciplinary therapy for chronic low back pain. *Spine (Phila. Pa. 1976)*. 32, 3060–6.

117. Pais-Vieira, M, Aguiar, P, Lima, D, Galhardo, V (2012) Inflammatory pain disrupts the orbitofrontal neuronal activity and risk-assessment performance in a rodent decision-making task. *Pain* 153, 1625–35.
118. Raghavendra, V, Tanga, FY, DeLeo, JA (2004) Complete Freund's adjuvant-induced peripheral inflammation evokes glial activation and proinflammatory cytokine expression in the CNS. *Eur. J. Neurosci.* 20, 467–73.
119. Chen, F-L, Dong, Y-L, Zhang, Z-J, Cao, D-L, Xu, J, Hui, J, Zhu, L, Gao, Y-J (2012) Activation of astrocytes in the anterior cingulate cortex contributes to the affective component of pain in an inflammatory pain model. *Brain Res. Bull.* 87, 60–6.
120. Kronschläger, MT, Drdla-Schutting, R, Gassner, M, Honsek, SD, Teuchmann, HL, Sandkühler, J (2016) Gliogenic LTP spreads widely in nociceptive pathways. *Science* 354, 1144–1148.
121. Guo, W, Wang, H, Watanabe, M, Shimizu, K, Zou, S, LaGraize, SC, Wei, F, Dubner, R, Ren, K (2007) Glial-cytokine-neuronal interactions underlying the mechanisms of persistent pain. *J. Neurosci.* 27, 6006–18.
122. Lan, L, Yuan, H, Duan, L, Cao, R, Gao, B, Shen, J, Xiong, Y, Chen, L-W, Rao, Z-R (2007) Blocking the glial function suppresses subcutaneous formalin-induced nociceptive behavior in the rat. *Neurosci. Res.* 57, 112–9.
123. Panatier, A, Robitaille, R (2016) Astrocytic mGluR5 and the tripartite synapse. *Neuroscience* 323, 29–34.
124. Kim, SK, Hayashi, H, Ishikawa, T, Shibata, K, Shigetomi, E, Shinozaki, Y, Inada, H, Roh, SE, Kim, SJ, Lee, G, Bae, H, Moorhouse, AJ, Mikoshiba, K, Fukazawa, Y, Koizumi, S, Nabekura, J (2016) Cortical astrocytes rewire somatosensory cortical circuits for peripheral neuropathic pain. *J. Clin. Invest.* 126, 1983–97.
125. Do-Monte, FH, Manzano-Nieves, G, Quiñones-Laracuente, K, Ramos-Medina, L, Quirk, GJ (2015) Revisiting the role of infralimbic cortex in fear extinction with optogenetics. *J. Neurosci.* 35, 3607–15.
126. Sotres-Bayon, F, Quirk, GJ (2010) Prefrontal control of fear: more than just extinction. *Curr. Opin. Neurobiol.* 20, 231–5.
127. Sierra-Mercado, D, Padilla-Coreano, N, Quirk, GJ (2011) Dissociable roles of prelimbic and infralimbic cortices, ventral hippocampus, and basolateral amygdala in the expression and extinction of conditioned fear. *Neuropsychopharmacology* 36, 529–38.

128. Martínez, KG, Quirk, GJ (2009) Extending fear extinction beyond anxiety disorders. *Biol. Psychiatry* 65, 453–4.
129. Apkarian, AV, Baliki, MN, Geha, PY (2009) Towards a theory of chronic pain. *Prog. Neurobiol.* 87, 81–97.
130. Xu, J, Zhu, Y, Contractor, A, Heinemann, SF (2009) mGluR5 has a critical role in inhibitory learning. *J. Neurosci.* 29, 3676–84.
131. Sethna, F, Wang, H (2014) Pharmacological enhancement of mGluR5 facilitates contextual fear memory extinction. *Learn. Mem.* 21, 647–50.
132. Bi, LL, Wang, J, Luo, ZY, Chen, SP, Geng, F, Chen, YH, Li, SJ, Yuan, CH, Lin, S, Gao, TM (2013) Enhanced excitability in the infralimbic cortex produces anxiety-like behaviors. *Neuropharmacology* 72, 148–156.
133. Leite-Almeida, H, Valle-Fernandes, A, Almeida, A (2006) Brain projections from the medullary dorsal reticular nucleus: An anterograde and retrograde tracing study in the rat. *Neuroscience* 140, 577–595.
134. Almeida, A, Cobos, A, Tavares, I, Lima, D (2002) Brain afferents to the medullary dorsal reticular nucleus: a retrograde and anterograde tracing study in the rat. *Eur. J. Neurosci.* 16, 81–95.
135. Baliki, MN, Chang, PC, Baria, AT, Centeno, M V, Apkarian, A V (2014) Resting-state functional reorganization of the rat limbic system following neuropathic injury. *Sci. Rep.* 4, 6186.
136. Apkarian, AV, Bushnell, MC, Treede, R-D, Zubieta, J-K (2005) Human brain mechanisms of pain perception and regulation in health and disease. *Eur. J. Pain* 9, 463–463.
137. Tracey, I, Mantyh, PW (2007) The cerebral signature for pain perception and its modulation. *Neuron* 55, 377–91.
138. Almeida, A, Størkson, R, Lima, D, Hole, K, Tjølsen, A (1999) The medullary dorsal reticular nucleus facilitates pain behaviour induced by formalin in the rat. *Eur. J. Neurosci.* 11, 110–22.
139. Almeida, A, Tjølsen, A, Lima, D, Coimbra, A, Hole, K (1996) The medullary dorsal reticular nucleus facilitates acute nociception in the rat. *Brain Res. Bull.* 39, 7–15.
140. Amorim, D, Viisanen, H, Wei, H, Almeida, A, Pertovaara, A, Pinto-Ribeiro, F (2015) Galanin-mediated behavioural hyperalgesia from the dorsomedial nucleus of the hypothalamus involves two independent descending pronociceptive pathways. *PLoS One* 10, e0142919.

141. Calejesan, AA, Kim, SJ, Zhuo, M (2000) Descending facilitatory modulation of a behavioral nociceptive response by stimulation in the adult rat anterior cingulate cortex. *Eur. J. Pain* 4, 83–96.
142. Zhang, L, Zhang, Y, Zhao, ZQ (2005) Anterior cingulate cortex contributes to the descending facilitatory modulation of pain via dorsal reticular nucleus. *Eur. J. Neurosci.* 22, 1141–1148.
143. Shipley, MT, Ennis, M, Rizvi, TA, Behbehani, MM (Springer US, 1991). in *The Midbrain Periaqueductal Gray Matter* 417–448.
144. Fields, HL, Heinricher, MM, Mason, P (1991) Neurotransmitters in nociceptive modulatory circuits. *Annu. Rev. Neurosci.* 14, 219–245.
145. Almeida, A, Tavares, I, Lima, D (2000) Reciprocal connections between the medullary dorsal reticular nucleus and the spinal dorsal horn in the rat. *Eur. J. Pain* 4, 373–387.
146. Almeida, A, Størkson, R, Lima, D, Hole, K, Tjølsen, A (1999) The medullary dorsal reticular nucleus facilitates pain behaviour induced by formalin in the rat. *Eur. J. Neurosci.* 11, 110–22.
147. Fields, HL, Bry, J, Hentall, I, Zorman, G (1983) The activity of neurons in the rostral medulla of the rat during withdrawal from noxious heat. *J. Neurosci.* 3, 2545–52.
148. Xu, Z-Z, Zhang, L, Liu, T, Park, JY, Berta, T, Yang, R, Serhan, CN, Ji, R-R (2010) Resolvins RvE1 and RvD1 attenuate inflammatory pain via central and peripheral actions. *Nat. Med.* 16, 592–7.
149. Cui, M, Honore, P, Zhong, C, Gauvin, D, Mikusa, J, Hernandez, G, Chandran, P, Gomtsyan, A, Brown, B, Bayburt, EK, Marsh, K, Bianchi, B, McDonald, H, Niforatos, W, Neelands, TR, Moreland, RB, Decker, MW, Lee, C-H, Sullivan, JP, Faltynek, CR (2006) TRPV1 receptors in the CNS play a key role in broad-spectrum analgesia of TRPV1 antagonists. *J. Neurosci.* 26, 9385–93.
150. Caterina, MJ, Schumacher, M a, Tominaga, M, Rosen, T a, Levine, JD, Julius, D (1997) The capsaicin receptor: a heat-activated ion channel in the pain pathway. *Nature* 389, 816–824.
151. Caterina, MJ, Leffler, A, Malmberg, AB, Martin, WJ, Trafton, J, Petersen-Zeitz, KR, Koltzenburg, M, Basbaum, AI, Julius, D (2000) Impaired nociception and pain sensation in mice lacking the capsaicin receptor. *Science* 288, 306–13.
152. Ferrini, F, Salio, C, Lossi, L, Gambino, G, Merighi, A (2010) Modulation of inhibitory

- neurotransmission by the vanilloid receptor type 1 (TRPV1) in organotypically cultured mouse substantia gelatinosa neurons. *Pain* 150, 128–40.
153. Kim, YH, Back, SK, Davies, AJ, Jeong, H, Jo, HJ, Chung, G, Na, HS, Bae, YC, Kim, SJ, Kim, JS, Jung, SJ, Oh, SB (2012) TRPV1 in GABAergic interneurons mediates neuropathic mechanical allodynia and disinhibition of the nociceptive circuitry in the spinal cord. *Neuron* 74, 640–7.
  154. Valtschanoff, JG, Rustioni, A, Guo, A, Hwang, SJ (2001) Vanilloid receptor VR1 is both presynaptic and postsynaptic in the superficial laminae of the rat dorsal horn. *J. Comp. Neurol.* 436, 225–35.
  155. Mezey, E, Tóth, ZE, Cortright, DN, Arzubi, MK, Krause, JE, Elde, R, Guo, A, Blumberg, PM, Szallasi, A (2000) Distribution of mRNA for vanilloid receptor subtype 1 (VR1), and VR1-like immunoreactivity, in the central nervous system of the rat and human. *Proc. Natl. Acad. Sci. U. S. A.* 97, 3655–60.
  156. Choi, S-I, Lim, JY, Yoo, S, Kim, H, Hwang, SW (2016) Emerging role of spinal cord TRPV1 in pain exacerbation. *Neural Plast.*
  157. Gawwa, NR, Bannon, AW, Surapaneni, S, Hovland, DN, Lehto, SG, Gore, A, Juan, T, Deng, H, Han, B, Klionsky, L, Kuang, R, Le, A, Tamir, R, Wang, J, Youngblood, B, Zhu, D, Norman, MH, Magal, E, Treanor, JJS, Louis, J-C (2007) The vanilloid receptor TRPV1 is tonically activated in vivo and involved in body temperature regulation. *J. Neurosci.* 27, 3366–74.









#### **4. Conclusions and Future Perspectives**

The work here presented shows the K/C model is suitable to study the development of chronic inflammatory pain such as observed in patients with OA. Although the onset of the disease lacks translational value when comparing rodents and human patients, the subsequent pathological development presents a better correlation of the disease severity with the time elapsed when compared to other chemically induced models, without requiring such prolonged time periods as spontaneous and genetic models. Future works should focus on further characterizing the K/C model in terms of the immune response.

The characterization of the prolonged pathological progression of the K/C model adds more relevance to the remaining results. Our studies strongly suggest that in addition to the peripheral alterations we observed in K/C rats, the persistence of knee joint pain also drives CNS plastic changes. Specifically, we observe alterations in the mGluR5 function in the IL, a gain of function from IL astrocytes regarding descending modulation of nociception, and broader changes in the pathways relaying IL-mediated pronociception. Future studies should evaluate the motivational, affective and cognitive aspects of IL descending modulation, as we believe it would greatly contribute to our knowledge of pain as a multidimensional experience. In addition, the significance of the switch in IL nociceptive descending pathways should also be addressed. The specific contribution of astrocytes, microglia and oligodendrocytes towards chronic pain should also be addressed; since the study of glial cells is still in its infancy, though, the development of new approaches is necessary to accurately pinpoint their involvement. Particularly for this work, the use of optogenetic tools would allow to study each cellular type while ensuring their functional integrity.



